Secteur des Sciences de la Santé
Institut de neuroscience
Ecole doctorale en Science médicales

Spinal and supraspinal pain-motor interactions and pain-related changes in brain connectivity explored by combining neuroimaging with non-invasive brain stimulation techniques

by

Maxime Algoet, M.D.

Jury:

Prof. Valery LEGRAIN, Président (UCLouvain)
Prof. André MOURAUX, Promoteur (UCLouvain)
Prof. Julie DUQUE (UCLouvain)
Prof. Carsten Dahl MØRCH (Aalborg University)
Prof. Patrice FORGET (University of Aberdeen)
Prof. Josep VALLS SOLÉ (Universitat de Barcelona)

Thèse de doctorat présentée en vue de l'obtention du grade de Docteur en Sciences médicales

Bruxelles, april 2022

Cette thèse s'inscrit dans le projet PROBING PAIN financé par le European Research Council.

Cover figure: (1) Brain responses evoked by TMS of the right DLPFC delivered at 120% of the rMT, (2) the two burts of the withdrawal reflex elicited by intra-epidermal stimulation of the sole of the foot and (3) the percentage of signal change of the MR signal in a line of voxels in front of a TMS coil.

Foreword

La finalisation de ce travail marque la fin d'une aventure enrichissante débutée en 2010 en tant qu'étudiant chercheur au sein du laboratoire d'André Mouraux. Après quatre années à naviguer entre les études et le laboratoire, j'ai eu la chance de découvrir plus en profondeur le monde de la recherche sous sa supervision. Je tiens à lui adresser mes remerciements les plus sincères car sans lui, cette aventure n'aurait pas été possible. L'environnement stimulant du laboratoire, l'entraide, l'écoute, la réflexion et l'exigence ont été essentiels à la finalisation de ce travail. Cette ambiance positive associée à la patience et à la liberté accordée par André ont été bien cruciales dans cette entreprise bien imprévisible qu'est la thèse. En effet, passer du « désarroi » lors de résultats « négatifs » à « l'excitation » lorsqu'un projet est mené à bon port, et ce après des heures de travail et de remise en question, participe selon moi au caractère fécond de cette expérience. Avoir appris à appréhender des domaines variés, parfois éloignés de la pratique clinique neurologique, sera sans aucun doute un atout majeur pour la pratique médicale, et même bien au-delà. Je te remercie donc André, de m'avoir permis de découvrir ce monde passionnant qu'est la recherche scientifique en neurosciences.

Merci également à Cédric Lenoir avec qui j'ai partagé nombre de projets de recherche. Nos nombreuses discussions dans le bureau sur les projets IRM et cTBS ainsi que les moments toujours positifs et constructifs resteront (surtout pour certains) gravés dans nos mémoires.

Je remercie également Julien Lambert pour toute l'aide apportée sans compter et ce tant sur les « set up » que sur les codes Matlab. Je n'aurais jamais pensé, pendant un assistanat de neurologie, discuter autant de méthodes d'interpolation.

Je voudrais également remercier Emanuel van den Broeke qui, outre la bonne humeur qu'il apporte dans l'équipe et de ses remarques/questions toujours pertinentes, a permis la réalisation de l'étude portant sur le réflexe nociceptif présentée au chapitre 4.

Merci à Gan Huang pour m'avoir guidé lors de mes premiers pas avec la TMS. Merci à Laurence Dricot pour l'aide apportée dans la mise au point des séquences IRM. Je tiens également à remercier toute l'équipe du labo pour leurs conseils, leur aide ou pour avoir été volontaires lors de certaines expériences pilotes. Je n'oublierai pas les nombreux moments de détente passés en votre compagnie que ce soit en congrès ou tout simplement sur le campus en fin de semaine. Durant les années passées au labo, j'espère avoir construit des liens d'amitié qui j'en suis persuadé perdureront bien au-delà de la fin de la thèse.

Mener à bien ce travail n'aurait pas été possible sans le soutien sans faille de ma famille, de mes proches ou de mes amis. Merci à ceux qui ont accepté de participer comme sujet à mes expériences parfois douloureuses. Merci à mes parents pour m'avoir continuellement encouragé à finaliser ce travail après mon retour en clinique. Merci à ma sœur et mon frère, Chloé et Louis, de m'avoir permis, à de nombreuses reprises, de stimuler une petite partie de leur cerveau ou de leurs membres par des stimulations en tout genre. Ce

soutien permanent, et ce malgré les trop nombreux moments de détente passés à travailler, m'aura sans aucun doute permis de mener à terme ce travail.

Je tiens finalement à remercier Vanessa qui a dû se dire à plusieurs reprises qu'elle s'était embarquée dans un bien drôle d'histoire. Merci pour le soutien affiché durant les années de retour en clinique et merci d'avoir accepté de dégager ta table de couture afin de la transformer en « bureau de la dernière ligne droite ».

Table of Contents

List of abbreviations

ACC: anterior cingulate cortex

ADM: *abductor digiti minimi*

AMH: A-fiber mechano-heat nociceptors

APB: *abductor pollicis brevis*

B_0: static magnetic field

BA: Brodmann area

BB: *biceps brachialis*

BF: *biceps femoris*

BOLD: blood-oxygen-level dependent

CGRP: calcitonin gene-related peptide

CLBP: chronic low back pain

CMCT: central motor conduction time

cMEPs: cervico-medullary motor-evoked potentials

CMH: C-fiber mechano-heat or polymodal nociceptors

CoG: Center of Gravity

CRPS: complex regional pain syndrome

CSP: cutaneous silent period

DLPFC: dorsolateral prefrontal cortex

DMN: default mode network

dmPFC: dorsomedian prefrontal cortex

ECR: *extensor carpi radialis*

EEG: electroencephalography

EMG: electromyography

EPI: echo-planar imaging

EPSCs: excitatory postsynaptic currents

ERP: event-related potentials

FBSS: failed back surgery syndrome

FCR: *flexor carpi radialis*

FDI: *first dorsal interosseous*

fMRI: functional magnetic resonance imaging

FOV: field-of-view

FRA: flexor reflex afferents

GLM: General Linear Model

GL: *gastrocnemius medialis*

HFS: high frequency electrical stimulation

HRF: hemodynamic response functions

HT: high-threshold

IASP: International Association for the Study of Pain

ICA: independent components analysis

ICF: intracortical facilitation

IES: intra-epidermal stimulation

IFG: inferior frontal gyrus

IHI: interhemispheric inhibition

ILI: *iliopsoas*

ISI: inter-stimulus interval

I-waves: descending indirect volleys

LAI: long-latency afferent inhibition

LTD: long-term depression

LTP: long term potentiation

M1: primary motor cortex

MEPs: Motor-evoked potentials

mPFC: medial prefrontal cortex

MSO: maximum stimulator output

MT: motor threshold

NMDA: N-methyl-D-aspartate

NRS: numerical rating scale

NWR: nociceptive withdrawal reflex

OA: osteoarthritis

PAG: periaqueductal gray

PCC: posterior cingulate cortex

PET: positron emission tomography

PL: *peroneus longus*

QVL: *quadriceps vastus lateralis*

rCBF: regional cerebral blood flow

RF coil: radiofrequency MRI coil

RMS: root-mean-square

rMT: resting motor threshold

RRF: reflex receptive field

RVM: rostral ventro-medial medulla

S1: primary somatosensory cortex

S2: secondary somatosensory cortex

SAI: short-latency afferent inhibition

SCM: *sternocleidomastoid*

SICI: short interval intracortical inhibition

SMA: supplementary motor area

SNR: signal-to-noise ratio

SOL: *soleus*

ST-FFT: short-term Fast Fourier transform

TA: *tibialis anterior*

TB: *triceps brachialis*

TCES: transcranial electrical stimulation

TE: echo time

TES: transcutaneous electrical stimuli

TKEO: Teager-Kaiser Energy Operator

TMS: transcranial magnetic stimulation

TR: repetition time

TTL: Transistor-Transistor logic

VTC: volume time course

WDR: wide-dynamic-range

Chapter 1. Introduction

1. General introduction

The ability to detect, localize and react to the occurrence of salient and potentially threatening sensory events is crucial for survival. Indeed, generating an appropriate reaction allows individuals to promptly adapt their behavior to the changing environment and thus prevents and/or limits tissue damages (Iannetti and Mouraux, 2010). Therefore, generating an adequate protective motor response to potentially threatening sensory events can be considered one of the most important functions of nociception. The term nociception refers to the neural activity in both the peripheral and central nervous systems triggered by the occurrence of a noxious stimulus[1] and thus can be regarded as an "alarm system" aiming to preserve bodily integrity. Nociception and pain have to be distinguished. Indeed, pain is a complex experience currently defined by the International Association for the Study of Pain (IASP; Taxonomy) as "an *unpleasant sensory and emotional experience associated with, or resembling that associated with, actual or potential tissue damage"* (Raja et al., 2020). Pain may emerge from the activation of peripheral high-threshold receptors called nociceptors. Importantly, nociceptors can be activated by stimuli of a wide variety of energy forms (mechanical, thermal and/or chemical) which do not necessarily elicit pain. Therefore, the information coded by the

[1] A noxious stimulus, which can take various forms of energy (e.g. thermal, mechanical or chemical), is a stimulus being capable of inflicting tissue damages and which thus constitutes a potential or real threat to bodily integrity.

nociceptive system, from peripheral nociceptors to central neural structures, are not systematically associated to a conscious experience of pain (e.g. Lee et al. (2009), Mouraux et al. (2010), Mouraux et al. (2014)). Pain can thus be regarded as one of several responses elaborated by the nociceptive system to protect us from potential threats.

In humans, congenital analgesia highlights the dramatic consequences of the inability to adequately respond to noxious stimuli. Indeed, congenital analgesia is characterized by an insensitivity to pain which, a fortiori, implies an absence of appropriate reactions, leading to potentially serious injuries. Therefore, this lack of behavioral adaptation to pain is associated with a reduced life expectancy (Nagasako et al., 2003).

Interactions between nociceptive and motor systems have been reported at multiple levels of the nervous system, involving both spinal and supraspinal structures with sometimes compelling effects on motor excitability (Hodges et al., 2003; Martin et al., 2008). Such interactions are relatively well-documented at spinal level. For instance, high-intensity electrical stimulation of upper or lower extremities can trigger a prompt withdrawal of the stimulated limb (Floeter et al., 1998; Sandrini et al., 2005; Andersen, 2007). Similarly, threatening stimuli can activate spinal inhibitory circuits, inducing a transient suppression of muscle contraction, therefore promoting the interruption of the ongoing movements (Floeter, 2003). Although less understood, phasic pain-evoked changes in supraspinal structures involved in motor function were also reported (Bank et al., 2013). Indeed, spinothalamic projections to brain regions involved in motor function, such as the primary motor cortex (M1) (Frot et al., 2013) or the cingulate areas

(Dum et al., 2009), could underlie the interactions between the two systems. A more detailed analysis of the modulatory effects of a brief nociceptive stimulus on the motor system will be discussed in section 2 of this chapter. You can also refer to the studies of chapters 3 and 4 for a discussion on phasic-evoked changes in motor system excitability.

Although leading to immediate benefits, motor adaptation to pain can have long-term negative consequences when pain persists for months or years. Historically, two main models have been put forward to explain persistent *muscle* pain-related changes in motor function. First, the vicious circle theory proposed a "pain-spasm-pain cycle" as a consequence of a uniform increased muscle activity (Roland, 1986; Johansson and Sojka, 1991). Later, Lund et al. (1991), in the so-called pain adaptation model, proposed that muscular activity recorded from painful muscles or from muscles generating a painful movement was inhibited. This inhibition, in conjunction with a facilitation of antagonist muscles activity, aims at protecting the injured part of the body. However, numerous clinical and experimental reports were inconsistent with both the vicious circle theory and the pain adaptation model. More recently, Hodges and Tucker (2011) proposed that the adaptation of the motor system to pain aims (1) to protect from further injuries and (2) to promote recovery by redistributing muscular activity within and between muscles (Madeleine et al., 2006; Tucker and Hodges, 2009). The resulting changes in mechanical behavior (Tucker and Hodges, 2010) could lead to a protection against further pain. However, this adaptation may have negative consequences in the long term, for instance in chronic pain conditions. Sustained pain-evoked changes in motor system

have been less investigated for pain of cutaneous origin. Moreover, contradictory results were reported, suggesting either a decrease (Farina et al., 2001), an increase (Fierro et al., 2010) or a lack of modulatory effect on motor cortex excitability (Martel et al., 2017; Mavromatis et al., 2017). Similar conflicting results have been reported on processes underlying tonic cutaneous pain-evoked changes in the motor system at spinal level. Indeed, while some studies suggest a lack of sustained changes in spinal pathways (Farina et al., 2001; Traverse et al., 2020), other evidence, notably from animal studies, suggest the implication of motor spinal processes (Woolf, 1983; 1984; Coderre and Melzack, 1985; Gronroos and Pertovaara, 1993). Section 3 of the present chapter is devoted to the modulatory effects of both tonic cutaneous and muscle pain on motor excitability.

Cutaneous tissue injuries can be associated with the development of hyperalgesia at the injured site (primary hyperalgesia) which is characterized by an increased pain sensitivity to both heat and mechanical stimuli (Hardy et al., 1950; LaMotte et al., 1983; Raja et al., 1984). It has been shown that hyperalgesia in the primary zone is due, at least in part, to a sensitization of primary afferents nociceptors (Campbell et al., 1979; Meyer and Campbell, 1981; Thalhammer and LaMotte, 1982; Campbell and Meyer, 1983; LaMotte et al., 1983; Reeh et al., 1987; Campbell et al., 1988), although central mechanisms could also play a part (Randic et al., 1993; Liu and Sandkuhler, 1997; Sandkuhler and Liu, 1998; Ikeda et al., 2003; Ikeda et al., 2006; Sandkuhler, 2009). In addition to primary hyperalgesia, an increased pain sensitivity to punctate stimuli can also be observed in the surrounding uninjured skin (Hardy et al., 1950; Raja et al., 1984; Dahl et al., 1993;

Moiniche et al., 1993). This secondary mechanical hyperalgesia is thought to be mainly mediated by central sensitization (Baumann et al., 1991; LaMotte et al., 1991; Simone et al., 1991; LaMotte et al., 1992; Torebjork et al., 1992), which is considered an *"increased responsiveness of nociceptive neurons in the central nervous system to their normal or subthreshold afferent input"* by IASP (Taxonomy). Long term potentiation (LTP), a physiological model of activity-dependent synaptic plasticity operating in the spinal cord (Bliss and Collingridge, 1993; Cooke and Bliss, 2006), has been proposed as one (of several) underlying mechanisms of central sensitization (Liu and Sandkuhler, 1997; Ikeda et al., 2003; Sandkuhler, 2009). Interestingly, hyperalgesia to mechanical stimuli in the surrounding uninjured skin is a prominent clinical feature in persistent pain conditions, such as postoperative pain (Lavand'homme et al., 2005). It can therefore be assumed that the hyperalgesia reported in patients bears a resemblance to the mechanical hyperalgesia observed in the surrounding uninjured skin and could be a consequence of central sensitization. Secondary mechanical hyperalgesia is discussed in more details in section 4 of chapter 1. Chapter 5 is devoted to an experiment paradigm in which I tried to characterize the changes in motor system following a sustained activation of cutaneous nociceptors generating central sensitization. In this experimental study, high frequency electrical stimulation (HFS) of the skin was used to induce a mechanical hyperalgesia in the secondary zone. Indeed, robust LTP of the synaptic efficiency between C-fiber primary afferents and dorsal horn neurons can be elicited in animals by delivering brief HFS bursts to the afferent nerve (Liu and Sandkuhler, 1995; 1997). By repeating, this time on humans, the HFS

protocol used in animal experiments, Klein et al. (2004) showed that HFS could lead to a long-term enhancement of pain perception to mechanical punctate stimuli outside the skin conditioned by HFS, closely resembling the secondary mechanical hyperalgesia observed in the surrounding uninjured skin (Hardy et al., 1950; Raja et al., 1984; Dahl et al., 1993; Moiniche et al., 1993). Studying changes in motor system excitability in a state of central sensitization of the nociceptive system induced by experimental models such as HFS is of clinical interest in order to improve our understanding of the motor system plasticity underlying the changes in motor behavior in chronic pain patients.

As already stated above, although promoting immediate benefits, changes in motor system evoked by persistent pain can have long-term negative consequences when pain persists for months or even years. Pathological chronic pain represents a major European healthcare issue. Indeed, approximatively 19-35% of European adults suffer from moderate to severe chronic pain (Elliott et al., 1999; Breivik et al., 2006; Breivik et al., 2013). Furthermore, chronic pain conditions markedly impair the quality of life and have severe socioeconomic impacts on our communities. The financial burden associated with persistent pain condition is also considerable and is at least equivalent to that of heart diseases and cancer (Breivik et al., 2013). In consequence, progress in our understanding of the neural representation of chronic pain in humans is essential in order to prevent, diagnose and develop an effective management of chronic pain conditions. However, there is no consensus on a precise definition of chronic pain (Apkarian et al., 2009). Currently, it is commonly admitted that, in chronic pain conditions,

pain extends the healing process after an injury (IASP, Taxonomy). A prolonged activation of nociceptive pathways, induced by injuries and/or inflammation, can cause long-term changes in both peripheral and central structures, leading to a sensitization of the nociceptive system which can contribute to the transition from an acute to a chronic state. A number of studies investigated long-term modifications occurring in chronic conditions, in both the peripheral (e.g. Reinert et al. (1998)) and central nervous systems, mainly at spinal level (e.g. Woolf and Thompson (1991)). Supraspinal activity-dependent changes, alteration of functional connectivity between brain regions as well as structural changes have also been reported in chronic pain conditions. Indeed, both structural and functional changes in various brain areas were observed and could underlie, at least in part, the chronification of pain (Maihofner and Handwerker, 2005; Seifert and Maihofner, 2009; Apkarian et al., 2011; Seifert and Maihofner, 2011). Because the cortical mechanisms underlying the chronification of pain are still poorly understood, I developed an original approach, combining transcranial magnetic stimulation (TMS) and functional magnetic resonance imaging (fMRI), which may be able to isolate activity-dependent changes in nociceptive function and, thereby, provide novel insights into the cortical mechanisms underlying the chronification of pain (see section 6 of chapter 1 and chapter 6). Although not directly under the scope of the present work, section 6.1 of this chapter is devoted to an overview of structural and functional changes in chronic pain. More precisely, I focused the discussion on the changes in cortical excitability and functional connectivity of the dorsolateral prefrontal cortex (DLPFC) in chronic low-back pain (CLBP)

patients. Indeed, such a brain target in this particular chronic pain condition seems to be appropriate to probe the representation of pathological pain in the human brain with the experimental approach I developed (see section 6.1 of chapter 1 and chapter 6).

2. Transient changes in the motor system triggered by the occurrence of a brief nociceptive stimulus

2.1 Phasic pain-evoked changes in spinal pathways activity

Nociception-evoked motor responses have been extensively investigated at spinal level as illustrated by the short-latency electromyographic (EMG) response elicited in various upper and lower limb muscles after noxious electrical stimulation of the skin. This swift motor response allows to move the stimulated limb away from the offending source (Figure 1.1; for reviews, see Andersen (2007), Sandrini et al. (2005) and Skljarevski and Ramadan (2002)).

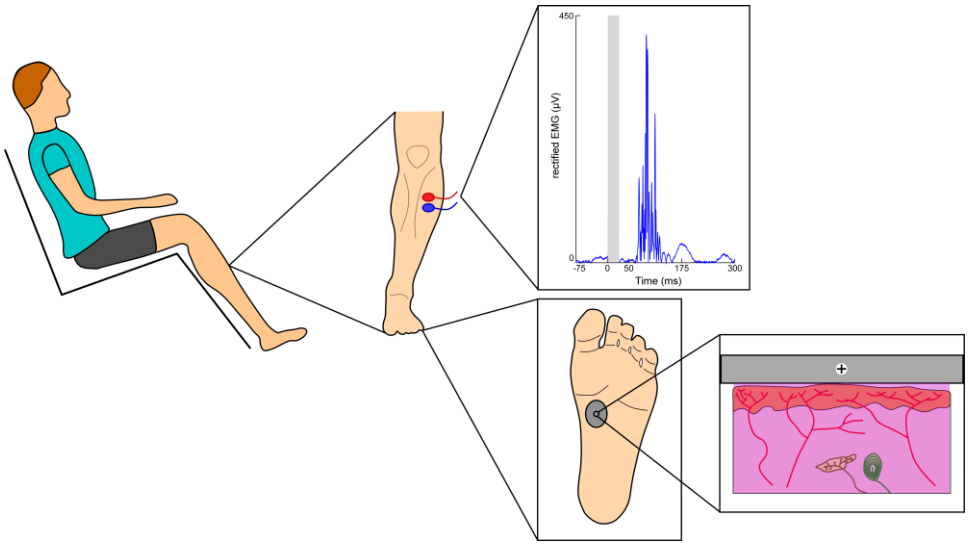

Figure 1.1. Schematic experimental setup to record the withdrawal reflex from the *tibialis anterior* (TA) muscle in humans. Subjects are seated in a comfortable reclining chair. The hip, knee and ankle joints are usually flexed at approximatively 90°. The reflex is usually elicited by high-intensity transcutaneous electrical stimulation by using relatively large skin surface electrodes. Such stimuli allow a synchronized activation of cutaneous afferents, compatible with the recording of time-locked responses such as the withdrawal reflex. However, because large-diameter afferents have a lower electrical activation threshold than small-diameter afferents, at the intensity required to activate small-diameter nociceptive afferents, such stimuli unavoidably also activate large-diameter non-nociceptive afferents. Note the EMG response elicited by electrical stimulation using large surface electrodes represented in the upper right part of the figure (data from the experimental study presented in chapter 4).

The nociceptive withdrawal reflex (NWR) is characterized by a spinal polysynaptic pathway controlled by descending influences (Clarke and Harris, 2004). The reflex was first described by Sherrington (1910) in spinalized cats as a stereotyped flexion of the stimulated limb (i.e. the

activation and relaxation of flexor and extensor muscles, respectively) combined to a crossed extension of joints of the non-stimulated limb. Later, the neuroscientists grouped the afferents fibers capable of generating a flexion reflex under the term *"flexor reflex afferents"* (FRA) (Lundberg, 1979; Schomburg, 1990). This includes group II, III and IV muscle, joint and cutaneous afferents. According to this model, all these afferents converge into common spinal interneurons controlled by descending influences originating from supraspinal structures involved in the current motor task. In case of strong peripheral afferent inputs, especially for nociceptive afferents, a flexion of the limb can be observed, therefore interrupting the current motor program (Eccles and Lundberg, 1959; Schomburg, 1990). Fairly soon, excitatory responses were also reported in cats' extensor muscles, at least for specific stimulation sites. This was observed when the activation of these muscles, regardless of whether they acted as extensor or flexor, produced a movement allowing to move the limb away from the noxious stimulus (e.g. Megirian (1962)). It has to be noted that the withdrawal pattern involving extensor muscles was already recognized in the FRA model as being conveyed by non-FRA pathways (Schomburg, 1990). Schouenborg and Kalliomaki (1990) proposed another model to take into account the reflex elicited in extensor muscles of the stimulated limb. In their experiment, they investigated the organization of the hind limb withdrawal reflex triggered by a noxious mechanical stimulation of the skin by means of single motor unit recordings in anesthetized rats. They found that the majority of hind limb muscles can be activated in response to a noxious stimulation delivered to a restricted skin area. Therefore, they

introduced the notion of reflex receptive field (RRF) which consists of the distribution of the reflex sensitivity on the skin (Schouenborg and Kalliomaki, 1990). In the RRF of a given muscle, both the amplitude and the onset latency of the reflex gradually decrease towards its border while the threshold to elicit the EMG response increases. Importantly, they demonstrated that the RRF of a given muscle corresponds to the skin area withdrawn away from the offending threat when the muscle in question was contracting. The optimal skin location to effectively withdraw the limb corresponded to the locus at which higher motor responses were obtained (Schouenborg and Kalliomaki, 1990; Schouenborg, 2002). Based on these observations, in addition to the similarities in the reflex thresholds and the time course between various agonist muscles, they proposed a functional organization of the withdrawal reflex allowing to generate an appropriate pattern of muscle activation to effectively withdraw the limb from the offending source (Schouenborg and Kalliomaki, 1990). Note that the existence of cutaneous inhibitory RRF, probably subserving an inhibition of inappropriate withdraw responses, has been reported several years later (Weng and Schouenborg, 1996). Therefore, the withdrawal reflex seems to be organized following a modular organization in which a module represents a given muscle, or a small group of synergistic muscles, and its RRF. In this model, the simultaneous activation of several modules results in a mechanically optimal movement driving the limb away from the noxious stimulus (Schouenborg and Weng, 1994). In humans, arguments for a functional organization of the withdrawal reflex also exist (Hagbarth, 1960; Grimby, 1963). For instance, Grimby (1963) delivered noxious electrical

stimuli to various locations on the sole of the foot. He observed that when the stimulus was progressively moved towards the big toe, the pattern of the activated muscles was more and more consistent with a dorsal flexion of the hallux. The reverse was observed when the stimulus was progressively shifted towards the heel. See figure 1.2 for a description of the methodology used to determine the RRF in humans (Andersen, 2007).

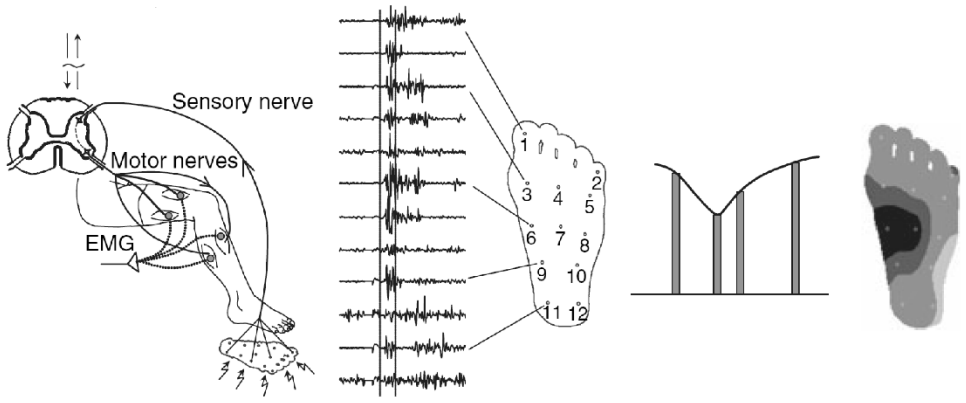

Figure 1.2. Experimental procedure for determining the RRF in humans. High-intensity electrical stimulations are delivered at several locations on the sole of the foot while the surface EMG is recorded from a given muscle. Then, EMG responses are interpolated and extrapolated, resulting in a map of the RRF (Adapted from Figure 4 in Andersen (2007)).

Further evidence of a modular organization of the withdrawal reflex in humans were provided by Andersen et al. (1999). By delivering noxious electrical stimuli at various locations on the sole of the foot, they determined the RRF of several flexor and extensor muscles of the lower limb. Their findings support a functional organization of the withdrawal reflex characterized by a pattern of muscle activation generating an appropriate

protective response (Figure 1.3). For instance, higher EMG responses in TA muscle were recorded when both the distal and medial parts of the sole of the foot were stimulated. This activity correlated well with a dorsal flexion of the ankle, as measured by a goniometer. On the contrary, more consistent responses were recorded in the *gastrocnemius medialis* (GM), an antagonist muscle of the TA, when the stimuli were delivered closer to the heel, thus resulting in a plantar flexion of the foot. Similar results were found for both the *soleus* (SOL) and *peroneus longus* (PL) muscles. The RRFs of more proximal muscles, the *biceps femoris* (BF) and *rectus femoris* (RF), respectively controlling the flexion and the extension of the knee, were larger than those of distal muscles and covered the entire plantar surface. Reflex amplitudes were significantly higher in BF than in RF, suggesting that flexion is the dominant withdrawal pattern for proximal muscles.

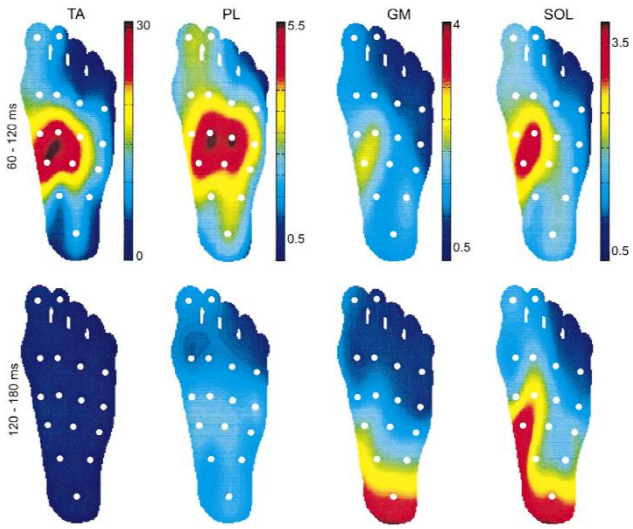

Figure 1.3. RRF for TA, GM, PL and SOL. White dots represent the actual sites of stimulation. The reflex amplitude is expressed according to the size of the

M-wave (10^{-3} × maximum peak-to-peak M-wave) recorded by electrical stimulations delivered on the muscle's motor nerve. Note that two time windows were explored, i.e. 60-120 ms and 120-180 ms (Adapted from Figure 5 in Andersen et al. (1999)).

Based on these observations, the authors proposed that the human withdrawal reflex follows a modular organization as previously shown in animal studies (Andersen et al., 1999). In a second experiment, they showed that increasing the stimulus intensity above the intensity eliciting the maximal RRF area only evoked higher reflexes within that RRF (i.e. enhancement of the volume of the RRF) without further expansion of the RRF area. This suggests that lower limb muscles, at least leg muscles, have a relatively restricted RRF in accordance with the modular theory (Andersen et al., 2001). In this regard, a specific RRF for a given muscle (or for a small group of muscles) was also found when electrical stimulations were applied on the dorsal side of the foot. Indeed, both the withdrawal direction and the pattern of muscle activation were dependent on the stimulated site (Sonnenborg et al., 2001). Interestingly, in rats, the spatial sensitivity of the RRF is not present at birth but progressively appears during the postnatal weeks. Changes in supraspinal influences seem to be involved in this learning process (Holmberg and Schouenborg, 1996; Levinsson et al., 1999; Andersen, 2007). This sensory input-based development of the RRF probably underlies a learning function of pain.

In humans, the withdrawal reflex can easily be obtained by stimulating either the sural nerve in the lateral malleolus space (Willer, 1977; Sandrini et al., 2005) or skin afferent terminals of the sole of the foot by using both

large surface (Figure 1.1; Andersen (2007), Ellrich and Treede (1998)) or transcutaneous needle electrodes (Grimby, 1963; Shahani and Young, 1971). Electrical stimuli are most often used to elicit a well synchronized afferent volley, thereby compatible with the recording of time-locked EMG responses such as the withdrawal reflex. We then obtain reflexes that are more consistent and reproducible than those elicited by more natural stimulations such as radiant heat stimuli (Andersen, 2007). However, if an electrical stimulus is used, a concomitant activation of both non-nociceptive large-diameter afferents and small-diameter nociceptive afferents is unavoidable. Consequently, a number of studies reported two EMG responses (Figure 1.4; Hugon (1973), Shahani and Young (1971)). The fact that the first EMG response, termed RII component, (1) is elicited at latencies (± 40-60 ms after stimulation onset) which are compatible with the conduction velocity (CV) of large diameter afferents and (2) is recorded when low stimulus intensities - i.e. below the pain threshold - are used, leads the researchers to propose that the RII component should be conveyed by non-nociceptive Aβ-fibers (Hugon, 1973; Willer, 1977). The second component, termed RIII or NWR, is thought to be conveyed by nociceptive Aδ-fibers given its longer onset latency (± 80-130 ms after stimulation onset) and the high-intensity stimulation - i.e. above the pain threshold - that is needed to elicit the motor response. There is also a close relationship between the RIII and the pain threshold. Furthermore, a significant correlation between the RIII amplitude and the intensity of pain elicited by the evoking stimulus has been described. These observations were interpreted as arguments in favor of the nociceptive origin of the RIII component (Hugon, 1973; Willer, 1977).

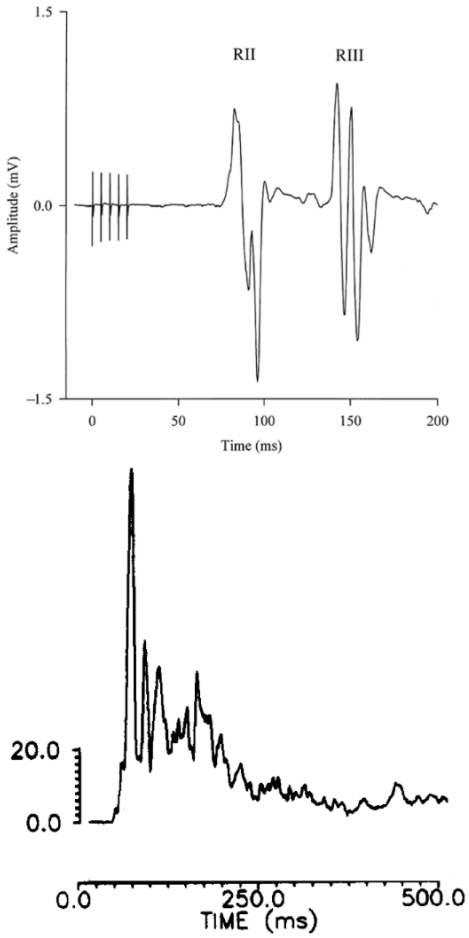

Figure 1.4. *Upper part.* The RII and RIII components elicited by high-intensity electrical stimulation delivered just proximally to the toe in one representative subject. Note that authors specified that the RIII component was observed sporadically in the 11 volunteers that were tested (Adapted from Figure 3 in Ellrich and Treede (1998)). *Lower part.* Rectified withdrawal reflex elicited by electrical stimulation of the sural nerve. Amplitude is expressed in µV. Note that a clear separation of the two components is impossible (Adapted from Figure 3 in Dowman (1991)).

However, it should be emphasized that if a clear separation of the RII and RIII components is often impossible (Figure 1.4), it is probably because the two components overlap each other (Chan and Dallaire, 1989; Dowman, 1991). Therefore, a number of studies estimated the size of the RIII by using a time window which excludes the early-latency responses in order to minimize the contribution of the RII component (e.g. Plaghki et al. (1998), Rhudy and France (2007)). It is important to highlight that several studies reported, in addition to a first component occurring at 60-120 ms - which was considered the RIII - a late EMG response occurring 120-200 ms after the onset of the electric stimulus. This response was not supposed to be of spinal origin and was attributed to a reflex pathway involving supraspinal structures (e.g. Andersen et al. (1999), Sonnenborg et al. (2001)). For a brief comment on supraspinal reflexes, please see Box 1. However, most of these studies did not report any EMG activities at latencies compatible with the RII component, therefore questioning the relative contribution of non-nociceptive afferent pathways in the first responses they observed. While some authors argued that the RII component was labile and highly susceptible to habituation (Hugon, 1973; Willer, 1977), others suggested the reverse (Shahani and Young, 1971; Meinck et al., 1985). For instance, Ellrich and Treede (1998) considered that the responses they observed with an onset latency between 115 ms and 180 ms was the RIII. While this response was not observed at every trial, the earlier response they recorded - characterized by an onset latency <100 ms - was more constant. They thus considered the first EMG response to be the RII (Figure 1.4). Moreover, in the same study, the CV of the afferent pathway involved in the first EMG

response was determined by comparing the onset latency of the EMG burst elicited by stimulation of both the sole of the foot and the medial retromalleolar space. The mean CV was estimated at 49 ± 11 ms, which is compatible with the CV of non-nociceptive Aβ-fibers (Ellrich and Treede, 1998). Note that various ranges of CVs are reported in the literature (Andersen, 2007). For instance, by stimulating the tibial nerve either at the ankle or in the popliteal fossa, Ertekin et al. (1975) estimated the onset latency of the BF reflex at ± 90 ms when the nerve was stimulated at the ankle. They estimated the CVs at 10-25 m/s, therefore compatible with afferent inputs conveyed by nociceptive Aδ-fibers. On the other hand, CVs of the primary afferents, responsible of the first component, were estimated between 35 and 47 m/s by others (Meinck et al., 1981). In addition, 50% of the initial EMG bursts elicited by electrical stimulation of the tibial or deep peroneal nerves at the ankle had an onset latency <50 ms (Meinck et al., 1981). These contradictory observations can be explained, at least in part, by the fact that the responses investigated in these studies were more or less contaminated by non-nociceptive afferent inputs. Consequently, taking into consideration the large range of Aδ-fibers CVs (2-30 m/s), it has been proposed that any EMG activity detected with an onset latency >60 ms may be ascribed to nociceptive Aδ-fibers whereas any EMG activity with an onset latency <60 ms should be considered to be related to the RII (Hugon, 1973; Andersen, 2007). See figure 1.5 for an example of onset latency estimation for reflexes elicited in TA after electrical stimulation of the sole of the foot with large surface electrodes (Andersen, 2007).

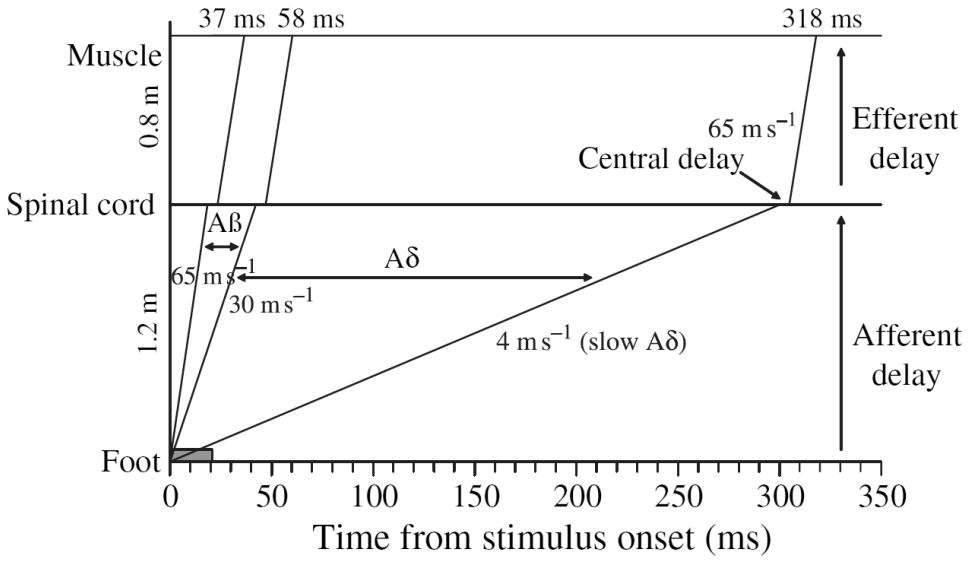

Figure 1.5. Estimation of the onset latency for an EMG response elicited in TA by high-intensity electrical stimulation delivered by large surface electrodes placed on the sole of the foot. Calculations were based on CVs of 30-65 m/s and 4-30 m/s for Aβ- and Aδ-fibers, respectively. The afferent and efferent pathways were estimated at 1.2 m and 0.8 m respectively. A central delay of 5 ms was added. Finally, CVs of 60 m/s were considered to estimate the efferent delay. The grey bar on the x-axis indicates the duration of the stimulus train. Based on this graph, the authors proposed that 60 ms should be an appropriate time point to effectively separate the RII and RIII components. (Adapted from Figure 2 in Andersen (2007)).

Two studies investigated the reflexes evoked by the selective activation of nociceptive fibers by means of CO_2 laser stimuli delivered to the dorsum of the foot on a surface of 2 cm^2 for a duration of 200 ms (Figure 1.6; Morch et al. (2007), Andersen et al. (2006)). Reflexes were recorded at ± 270 ms in TA and BF muscles (Morch et al., 2007) and at ± 350 ms in the *semitendinosus* muscle (Andersen et al., 2006). However, these responses were less

reproducible than when elicited by high-intensity electrical stimulation. Indeed, consistent reflexes were reported in <50% of the trials. A direct comparison between the onset latency of the motor responses elicited by selective activation of nociceptive fibers and the onset latency of the reflexes obtained by transcutaneous electrodes is difficult to draw because of (1) the transduction delay for radiant heat stimuli delivered to the skin (± 40 ms; Bromm and Treede (1984)) and (2) the duration of the laser stimulus needed to record time-locked EMG responses.

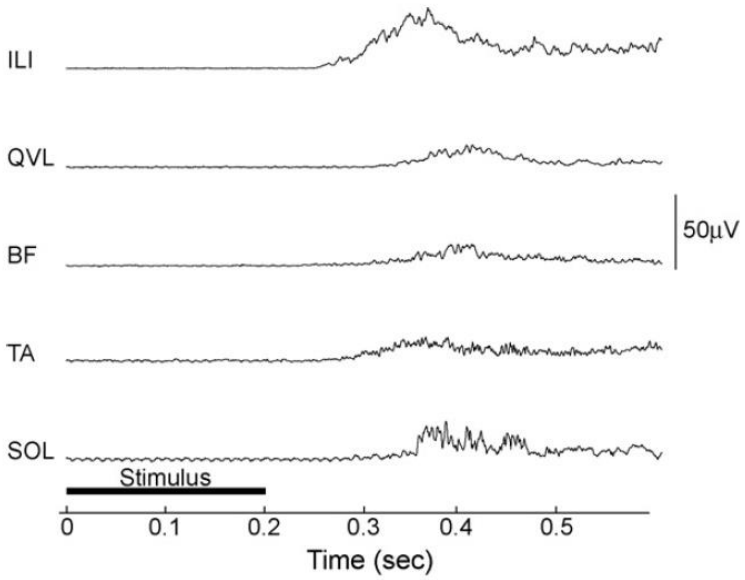

Figure 1.6. Rectified EMG responses evoked by CO_2 laser stimuli delivered to the dorsum of the foot. Responses in *iliopsoas* (ILI), *quadriceps vastus lateralis* (QVL), BF, TA and SOL muscles are shown. Note that the onset latency of the reflex evoked by the selective activation of nociceptive fibers seems consistently delayed relative to the EMG burst elicited by high-intensity electrical stimulation using large surface electrodes, even when

both the transduction time and the duration of laser stimulation are considered (Adapted from Figure 2 in Morch et al. (2007)).

In addition to the withdrawal reflex, high-intensity electrical stimulation of a digital nerve can transiently interrupt the voluntary muscle contraction of the stimulated limb through spinal inhibitory circuits (Figure 1.7; Kranz et al. (1973), Floeter (2003)). This cutaneous silent period (CSP) is particularly robust in intrinsic hand muscles lasting up to 100 ms (Floeter, 2003) but it can also be recorded in lower limb muscles (Uncini et al., 1991).

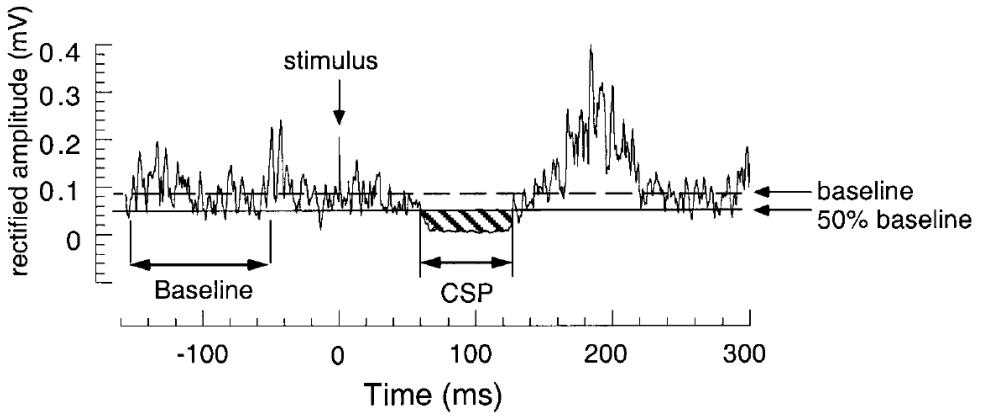

Figure 1.7. Example of the transient suppression of the rectified EMG response. The dashed lines represent the average EMG signal, determined during a 100 ms time window prior to the stimulus onset. The CSP was defined as being the period of time during which the EMG signal was less than 50% of the baseline (Adapted from Figure 2 in Floeter (2003)).

Based on their onset latency (50-80 ms), small-diameter Aδ nociceptive afferents are thought to be the main constituent of the afferent pathway. As for the withdrawal reflex, the CVs of the afferents causing the CSP have been estimated by stimulating two separate points along the afferent pathway or

by subtracting both the estimated efferent time and the central delay from the onset latency. The estimated range of CVs was between 10 and 20 m/s, i.e. consistent with afferent inputs conveyed by nociceptive Aδ-fibers (Kranz et al., 1973; Inghilleri et al., 1997). Moreover, a CSP in intrinsic hand muscles has been observed after laser stimulation delivered on the palm of the hand (Romaniello et al., 2004). However, for the same reasons as for the withdrawal reflex, a contribution of non-nociceptive large-diameter afferent fibers is acknowledged, at least in the early part of the CSP (Floeter, 2003). This is in accordance with the CSP elicited after low-intensity electrical stimulation of the finger (Serrao et al., 2001). It is however generally admitted that, although contributing to the CSP, non-nociceptive Aβ-fibers are not the predominant afferent pathways of this reflex arc, which can therefore be considered an inhibitory part of a defensive behavior able to stop an ongoing movement in response to a sudden threatening event (Inghilleri et al., 1997). The distribution of the CSP across proximal and distal muscles of the upper limb after noxious digit stimulation is compatible with a protective reflex movement serving to retract the hand from the offending source. Indeed, the CSP is of longer duration in intrinsic hand muscles than in more proximal muscles, such as the *biceps brachialis* (BB) and the deltoid, in which no CSP is observed (Inghilleri et al., 1997; Leis et al., 2000).

Comment on supraspinal motor reflexes (Box. 1)

Reflex responses can be defined as a swift automatic and involuntary reaction to a somatosensory stimulus. Although generally mediated by neurophysiological mechanisms operating at spinal level with supraspinal influences (Sandrini et al., 2005; Gilio et al., 2008), motor responses occurring at latencies thought to be too long for a spinal origin were reported. Importantly, the onset latency of such responses seems to be too early to be considered a voluntary reaction. For instance, a startle reflex - involving brainstem structures - can be observed following unexpected sensory stimuli such as sudden sounds (e.g. Gogan (1970)) or unexpected visual or somatosensoriel events (e.g. Bradley et al. (1990), Alvarez-Blanco et al. (2009)). It is important to note that this motor response can be observed in the lower limb at a similar temporal window to the one of the RIII (Dowman, 1992). Given that the startle response is highly sensitive to habituation, some studies investigated spinal reflexes by discarding the first trials (e.g. Kruger et al. (1985), Morch et al. (2007)) or by analyzing motor responses in an arbitrary time window which does not exceed a fixed time point (e.g. Rhudy and France (2007)).

Furthermore, cutaneous transcortical reflexes have been reported in humans, especially after non-nociceptive electrical stimuli of digital nerves during an isometric voluntary contraction of upper limb muscles

(e.g. Deuschl et al. (1991)). This cutaneomuscular reflex is composed of a mixture of inhibitory and facilitatory periods and includes (1) a short-latency excitatory response (E1 component; ± 35 ms) followed by (2) a suppression of the EMG signal (I1 component; ± 50 ms). Most of the time, a long-latency EMG burst (3) - termed E2 - can be observed ± 65 ms after the onset of the electric stimulus, at latencies compatible with a cortical origin (Macefield, 2009). The CSP, detailed above, is elicited by increasing stimulation intensity. The potential "contamination" of the NWR by supraspinal reflexes is discussed in chapter 4.

2.2 Phasic pain-evoked changes in supraspinal structures

Evidence of changes in motor system excitability induced by brief nociceptive stimuli at cortical level have been reported. However, these interactions have not been characterized as extensively as spinal processes. In epileptic patients, Frot et al. (2013) recorded intracortical responses to brief laser stimuli delivered to the hand dorsum by using intracerebral electrodes implanted in the pre- and post-central gyri. Laser-evoked potentials (LEPs), peaking at 170 ms were recorded in M1 (Figure 1.8). Several findings suggested a local origin in M1. Indeed, LEPs with a phase-reversal across the precentral gyrus were obtained. Also, higher LEPs were observed close to the anterior bank of the central sulcus; their amplitudes decreased as the distance from the sulcus increased. The authors proposed that these early-latency responses could reflect, at least in part, inputs from the spinothalamic tract to M1. Indeed, LEPs of similar latencies were observed in the postcentral gyrus, suggesting that these responses, or at

least their early part, were not conveyed by direct projections from the primary somatosensory cortex (S1) to M1 (Frot et al., 2013).

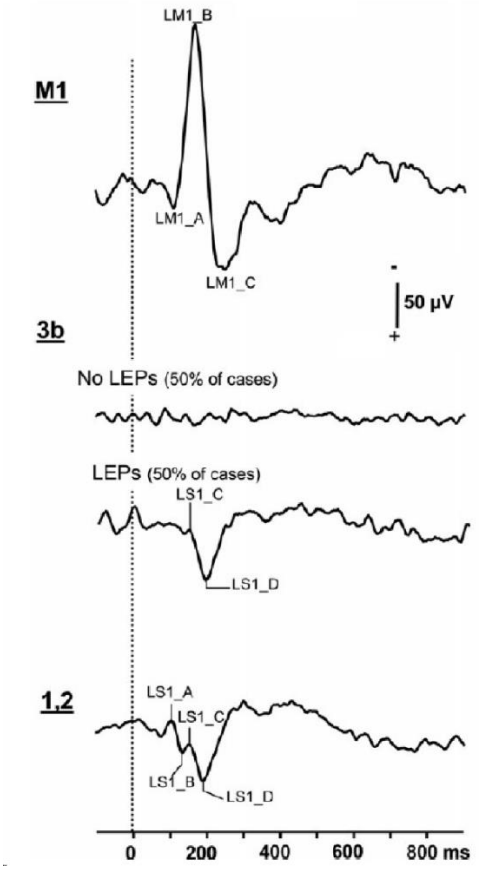

Figure 1.8. Intracortical LEPs recorded in both M1 and areas 1, 2 and 3b of S1. Depth recordings were performed in epileptic patients. LEPs in M1 were elicited by delivering laser stimuli on the hand dorsum. LEPs recorded in M1 started approximately 120 ms after the stimulation onset, and peaked at 170 ms (Adapted from Figure 3 in Frot et al. (2013)).

These findings are supported by the results obtained in anaesthetized cats in which short-latency responses were recorded in motor cortical cells in response to inputs conveyed by the spinothalamic tract. These responses

were also observed when the dorsal part of the spinal cord as well as the somatosensory cortex and the cerebellum were damaged (Padel and Relova, 1991). By using the anterograde transneuronal transport of herpes simplex virus type I injected into lower cervical segments of the spinal cord in monkeys, Dum et al. (2009) identified several cortical targets of the spinothalamic tract such as the granular insular cortex and the secondary somatosensory cortex (S2). Furthermore, neurons in cingulate areas were also labeled by this technique. By using a retrograde transport of a tracer injected into the ventral premotor cortex before injecting the herpes virus in the cervical dorsal horn, motor regions of the cingulate cortex were identified. Thanks to this double labeling approach, they found a strong correspondence between both cingulate areas targeted by the spinothalamic tract and cingulate motor areas. Indeed, each cingulate motor areas significantly overlapped with regions receiving inputs from the spinothalamic tract (Figure 1.9; Dum et al. (2009)). It is interesting to note that cingulate motor areas are known to project to dorsal and ventral premotor areas as well as to M1 (Dum and Strick, 2005).

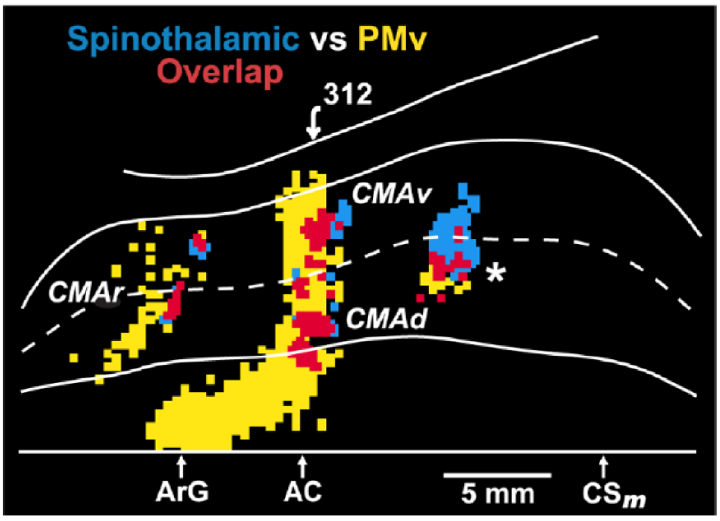

Figure 1.9. Unfolded map of neurons located in the medial wall of the hemisphere, in the direct vicinity of cingulate areas. Cortical regions projecting to the ventral premotor cortex are shown in yellow. Regions receiving inputs from the spinothalamic tract are represented in blue. Overlapping cortical regions are colored in red (Adapted from Figure 9 in Dum et al. (2009)).

In the same study, they performed a meta-analysis of fMRI and positron emission tomography (PET) studies in humans reporting activations in cingulate areas following a noxious stimulation perceived as painful. Their analysis suggests that the cingulate areas found to be activated in humans were similar to the cingulate motor regions targeted by the spinothalamic tract in monkeys. Interestingly, cingulate motor areas and premotor cortex are involved in motor control of the upper limb, including in defensive movements (Turken and Swick, 1999; Cooke and Graziano, 2003; 2004). In humans, a direct approach to characterize modulatory effects of nociception on the motor system is to assess the effect of nociceptive stimuli on the

motor-evoked potentials (MEPs) elicited by TMS of M1 (see Box 2 for a short comment on the single pulse TMS approach).

Comment on the single pulse TMS approach (Box 2).

In humans, non-invasive stimulation of brain regions can be achieved by delivering a short-lasting high-intensity electrical current through a coil of wire, termed TMS coil, generating a strong magnetic field following the electromagnetic induction principle. When placed on the scalp of participants, this changing magnetic field induces an electric field in brain tissues which may depolarize neurons (Figure 1.10; Hallett (2000), Hallett (2007)).

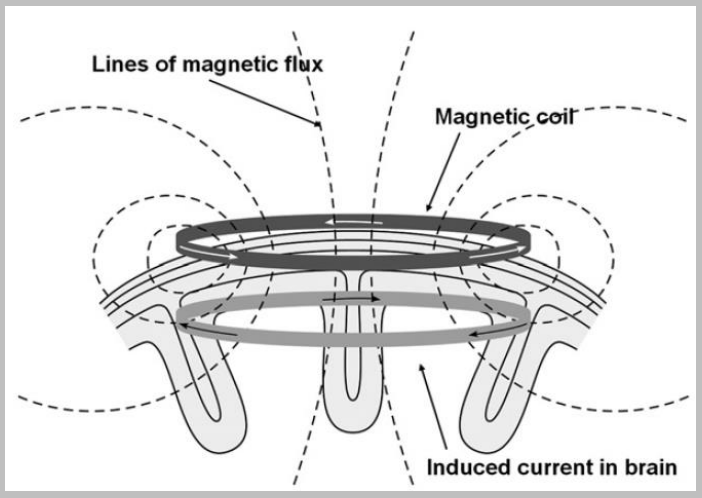

Figure 1.10. Schematic representation of the high-intensity electrical current elicited by the discharge of a capacitor across a TMS coil, made of turns of wire, placed on the scalp. The resulting changing magnetic field induces a current of opposite direction in the brain which may depolarize neurons (Adapted from Figure 1 in Hallett (2007)).

When delivered on M1, single pulses of TMS can induce a motor response, termed MEPs, which can be measured by placing electrodes over the muscle of interest (Barker et al., 1985).

Both the stimulus waveform and the current direction in the TMS coil influence the effect of TMS pulses on the pyramidal tract neurons and their axons (Niehaus et al., 2000). The influence of the current direction on motor thresholds is known from the early days of TMS. Indeed, to stimulate the left M1, a counterclockwise current has to be delivered in a round coil placed on the vertex (Sommer and Paulus, 2008; Di Lazzaro and Ziemann, 2013) due to the orientation of the cortico-spinal neurons and axons (Brasil-Neto et al., 1992). Regarding the pulse configuration, two distinct pulse waveforms can be distinguished according to the mono- or biphasic form of the current pulse delivered through the coil (Figure 1.11). Monophasic pulses induce a magnetic field that increases rapidly from zero to its maximal value, before returning more slowly to zero. The waveform of a biphasic pulse consists of one damped cycle of a sinusoid (Figure 1.11; Ruohonen and Ilmoniemi (2005)).

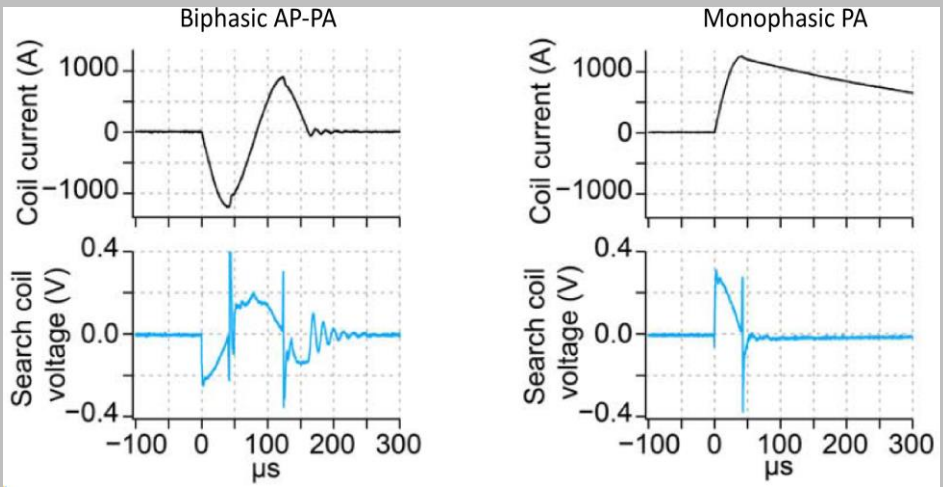

Figure 1.11. Current waveforms in the TMS coil (black lines) and the resulting voltage induced in a search coil (blue lines). In monophasic pulses, the current is stopped after the first quarter cycle. In biphasic pulses, the current consists of a full-sine cycle (Adapted from Figure 2 in Delvendahl et al. (2014)).

When monophasic pulses are used, significant lower resting/active motor thresholds and MEP amplitudes/latencies are observed with an anterior-posterior (AP) current direction in the coil, i.e. a postero-anterior (PA) current direction in the brain (Di Lazzaro et al., 1999; Kammer et al., 2001; Sommer et al., 2006; Sommer et al., 2018). Smaller differences are observed when biphasic pulses are used. However, the most effective stimulation is achieved when the initial current is in the opposite direction from that of a monophasic pulse, i.e. an AP-PA direction in the brain (Kammer et al., 2001; Sommer et al., 2006). Given that the first phase, i.e. the first quarter, is similar concerning both mono- and biphasic pulses, it has been proposed that the second and third quarters mainly contribute to the higher biphasic waveform efficacy (Niehaus et al., 2000; Corthout et al., 2001). By investigating the effect of a given half-segment of the biphasic pulse's alteration on the motor threshold, Delvendahl et al. (2014) found that the half-segment of biphasic pulses inducing a PA current in the brain mainly contributes to the efficiency of the TMS pulse to elicit a lower motor threshold, regardless of whether it is the first or second segment, probably because PA and AP pulse waveforms activate different neuronal structures with different thresholds (Di Lazzaro et al., 2001). They also bring evidence regarding the important role of the middle part of the electric field waveform in biphasic stimulation (Delvendahl et al., 2014; Sommer et al., 2018). It is generally admitted that biphasic pulses with an AP-PA direction in the brain lead to lower motor thresholds than both biphasic PA-AP and monophasic pulses (Niehaus et al., 2000; Kammer et al., 2001; Sommer et al., 2006).

Various types of TMS coils are available for research and/or clinical applications. The first coil to be used was a circular coil placed on the vertex which allows a good penetration of the cortex at the cost of a lack of focality (Epstein, 2008; Deng et al., 2013). A flat figure-of-eight coil can be obtained by placing two round coils side by side. Because the current flows add to each other at the junction, the induced electric field is maximal directly under this junction (Epstein, 2008). This type of coil, allowing a more focal stimulation, is suitable for stimulating superficial cortical targets such as M1 (Deng et al., 2013). A flat figure-of-eight coil was then used in Chapter 3 and 5 to stimulate M1. In Chapter 6, the stimulation of the DLPFC was achieved by using a similar MRI-compatible TMS coil without ferromagnetic materials.

By using a figure-of-eight coil, optimal motor responses are elicited when the coil is at ± 45° from the parasagittal line resulting in an electric field direction perpendicular to the central sulcus (Brasil-Neto et al., 1992; Mills et al., 1992). This is due, at least in part, to an optimal TMS-induced electric field orientation relative to either the cortical columns (Fox et al., 2004) and/or the horizontal fibers in the gyral crown (Mills et al., 1992). Modeling studies have shown that the TMS-induced electric fields are strongest in the gyral crown and within the subcortical white matter, suggesting that TMS of M1 should activate cortical interneurons in the gyral crown or pyramidal neurons in the lip of the sulcus (Salvador et al., 2011; Opitz et al., 2013; Laakso et al., 2014). Direct recording of descending volleys via electrodes implanted in the high cervical spinal cord in humans brought significant insights about the action of single pulses of TMS on M1 (Di Lazzaro et al., 2004).

A short-latency wave (2.4-2.6 ms) can be recorded in the epidural space when anodal stimulation of the motor cortex is delivered using transcranial electrical stimulation (TCES) (Figure 1.12). Given its latency, and because voluntary contraction had no effect on its amplitude, it has been suggested that this early-latency wave was originated from direct stimulation of the cortico-spinal axons (Di Lazzaro et al., 1998; Di Lazzaro et al., 1999), which is similar to the D-waves observed in the cervical spinal cord recordings in animals when the gray matter is removed (Patton and Amassian, 1954). Given their short latency, it is thought that the site of activation is near the cell soma, probably at the junction between the gray and white matters where the axons bent (Amassian et al., 1992). Using monophasic TMS pulse with a PA-induced current in the brain, later volleys - thought to be originated from indirect transsynaptic activation of cortico-spinal neurons - are observed and termed I-waves (I1-, I2- or I3-waves depending on the order in which they appear) (Figure 1.12). The earliest descending volley (I1-wave) occurs 1-1.4 ms after the D-wave observed with TCES (Gibbs et al., 1995; Di Lazzaro et al., 1998). During a voluntary contraction, both the size and the number of I-waves increased while the threshold to elicit a descending activity seems to be less affected compared to rest condition. This suggests a transsynaptic activation of cortico-spinal neurons by magnetic pulses via the stimulation of presynaptic axons (Figure 1.13; Di Lazzaro et al. (1998)). Less consistent descending activities are observed when monophasic pulses with an AP-induced current direction are used (Figure 1.12). This is accompanied by a preferential recruitment of late I3-waves in some subjects while I1- and D-waves are mainly seen in others (Di Lazzaro et al., 2001). Descending volleys evoked by biphasic pulses are

characterized by a more complex pattern because the two phases of the pulse are able to trigger descending activities (Di Lazzaro and Rothwell, 2014) and stimulate different sets of intracortical interneurons (Novotny and Gommert-Novotny, 1988; Delvendahl et al., 2014; Sommer et al., 2018).

Interestingly, when AP-PA biphasic pulses are delivered, in addition to later I-waves, a small short-latency volley that is slightly delayed (± 0.4 ms longer) compared to the D-wave is observed (Figure 1.12), suggesting that such pulse waveforms could stimulate the axon hillock (Di Lazzaro and Rothwell, 2014). These observations highlight that the TMS of M1 activates pyramidal neurons transsynaptically. According to both the current waveform and direction as well as the intensity of the TMS pulse, distinct mono- or polysynaptic pathways can be activated, as shown by the different patterns of descending activities (Di Lazzaro and Rothwell, 2014).

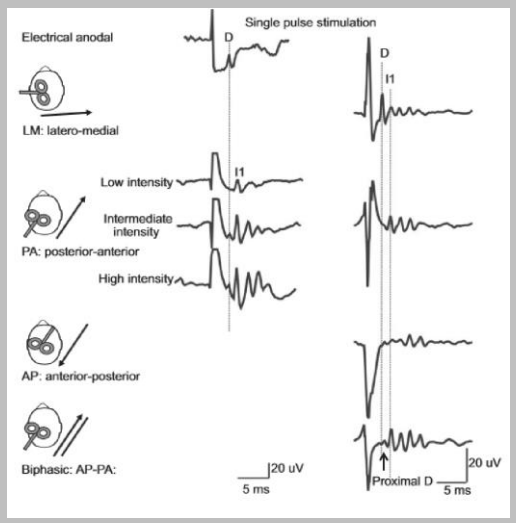

Figure 1.12. Descending volleys evoked by electrical and magnetic stimulation. A short-latency response is elicited by electrical anodal stimulation of M1, termed D-wave. Note that the two columns represent

two different subjects. Monophasic pulses with a PA-induced current in the brain delivered at low intensity evoke a single descending wave with a latency ± 1 ms longer than the D-wave evoked by anodal stimulation. This response was termed I1-wave. By increasing the stimulation intensity, later I-waves can be evoked. When high-intensities are used, a small wave with a similar latency to that of the D-wave elicited by anodal stimulation can be recorded. Note that TMS pulses with a latero-medial-induced current in the brain preferentially evoke D-waves. When biphasic stimulation is used, the earliest volley is slightly delayed (± 0.4 ms longer) with respect to the D-wave evoked by both latero-medial induced current in the TMS coil and electrical anodal stimulation. Therefore, because of its longer latency, it has been proposed that the D-waves evoked by biphasic pulses take their origin closer to the cell body of the cortico-spinal neurons. Then, this D-wave is often termed "proximal D wave" (Adapted from Figure 1 in Di Lazzaro and Rothwell (2014)).

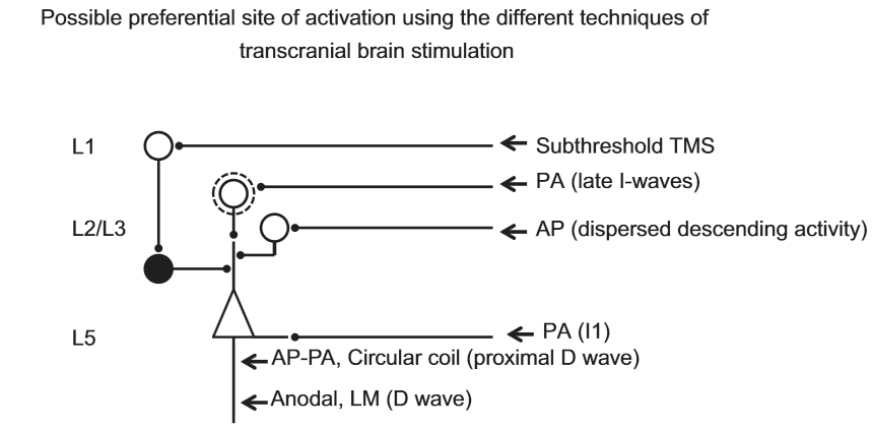

Figure 1.13. Schematic representation of potential sites of activation of anodal electrical stimulation and mono/biphasic pulses of TMS. The open circles represent excitatory neurons while filled circles indicate inhibitory neurons. This model includes (1) a superficial inhibitory circuit composed of layer 1 (L1) neurons that have connections with layer 2 and 3 (L2 and L3) interneurons (filled circle). These interneurons inhibit the distal apical dendrites of layer 5 pyramidal neurons (L5) while L2 and L3 bursting (open circle inside a dotted circle) and non-bursting excitatory

interneurons (2) project upon the distal apical dendrites of L5 pyramidal neurons. Finally, cortico-cortical axons (3) project upon basal dendrites of L5 pyramidal neurons. It has been proposed that anodal electrical stimulation and latero-medial magnetic stimulation could activate directly the cortico-spinal axons of pyramidal tract neurons, resulting in a short latency wave termed D-wave. The waves evoked by low-intensity PA TMS pulses that are delayed by 1–1.4 ms compared to the D-wave evoked by anodal stimulation are thought to be evoked by monosynaptic activation of basal dendrites from pyramidal neurons via cortico-cortical axons activated by the magnetic stimulus. The later I-waves evoked at higher intensities might be produced by a circuit involving cortico-cortical axons that activate L2 and L3 bursting neurons, which activate the apical dendrites of pyramidal neurons. The AP stimulation could involve non-bursting L2 and L3 interneurons via their projections on pyramidal neurons apical dendrites. Biphasic TMS pulses with an AP-PA induced current in the brain are thought to activate the cortico-spinal axons closer to the cell body, at the level of axon hillock. This could explain the longer latency of the D-wave evoked by biphasic stimulation compared to anodal electrical and latero-medial magnetic stimulations. Finally, it is proposed that inhibitory effects produced by a subthreshold conditioning stimulus delivered in paired-pulse paradigms could be explained by a selective enhancement of the excitability of the GABAergic circuit originating from L1 neurons which project on the apical dendrites of the pyramidal neurons (Adapted from Figure 2 in Di Lazzaro and Rothwell (2014)).

By comparing the effects of a noxious heat stimulus (CO_2 laser) delivered to the hand dorsum on EMG responses evoked either by TMS or TCES of M1, Valeriani et al. (1999) found an early (170-270 ms) and transient reduction of the MEPs amplitude recorded from the *first dorsal interosseous* (FDI) muscle of the stimulated limb. For a short comment on radiant heat stimuli

which activate thermonociceptors, see Box 3. In a separate experiment, MEPs elicited by TMS delivered over the ipsilateral M1 relative to the stimulated hand were reduced ± 210 ms after the onset of the nociceptive stimulus. Most importantly, motor responses evoked by TCES were not modulated by nociceptive afferent inputs. Given that anodal stimulation of M1, if not delivered at too high-intensity, activates directly cortico-spinal axons (Di Lazzaro et al., 1998), the authors proposed that the observed reduction in MEPs magnitude should be attributed to a decrease of motor system excitability occurring at cortical level (Valeriani et al., 1999). The lack of changes in MEPs when the TMS pulses were delivered before the peak latency of the N1/P1 LEPs component - i.e. before the nociceptive afferent volley has reached the cortex - subserves this statement. Later, in a second study conducted on only five subjects, the same authors characterized the effect of CO_2 laser stimuli delivered on the hand dorsum on a more proximal muscle which controls the flexion of the forearm, i.e. the BB muscle. Again, a significant reduction of the MEPs size elicited in the stimulated limb was observed 160-200 ms after the onset of the nociceptive stimulus. On the contrary, MEPs elicited by TCES of M1 during a voluntary contraction were not significantly modulated by the laser stimulus, again suggesting a mechanism operating at cortical level (Valeriani et al., 2001). The authors interpreted this motor inhibition as a down-regulation of M1 excitability allowing the spinal motor system to generate a stronger protective reflex movement (Valeriani et al., 1999; Valeriani et al., 2001; Farina et al., 2003). Other evidence suggesting an effective top-down regulation of defensive mechanisms by voluntary actions was brought by Fossataro et al. (2020),

who showed a significantly higher reduction of MEPs during painful stimulus in other-generated compared to self-generated actions. A number of studies also reported a decrease of MEPs amplitude following a brief noxious stimulus. For instance, although they were aiming to study long-term changes in motor cortex induced by paired associative protocol combining repetitive laser stimulations of the hand dorsum with low-frequency TMS of M1, Suppa et al. (2013) obtained similar results. Their protocol consisted of repetitive laser stimulations delivered at 0.1 Hz during 10 minutes, each stimulus being followed by a TMS pulse with an inter-stimulus interval (ISI) corresponding to the peak latency of the N1 component + 50 ms. Though MEPs were increased until 60 minutes after the intervention, a reduction of their amplitudes was seen directly after the onset of the protocol (Suppa et al., 2013). Along these lines, the magnitude of MEPs elicited in both lower and upper limb muscles is decreased during a short-lasting noxious heat stimulation delivered by a thermode (Dube and Mercier, 2011; Mercier et al., 2016; Billot et al., 2018). Similar results were generally observed after high-intensity electrical stimulation of the skin, except for BB and *triceps brachialis* (TB) muscles in which MEPs were enhanced (Kofler et al., 1998; Kofler et al., 2001; Urban et al., 2004). Again, because similar results were obtained for MEPs elicited by both TMS and TCES of M1, in addition to the fact that the time courses of the CSP and the modulatory effects of noxious electrical stimuli on MEPs were similar, it was hypothesized that spinal structures should be mainly involved (Kaneko et al., 1998; Kofler et al., 2001; Kofler et al., 2008). Note that a direct comparison between the modulatory effect of both high-intensity electrical (Kofler et al., 1998; Kofler et al., 2001)

and laser stimulation (Valeriani et al., 1999; Valeriani et al., 2001) is difficult because of the unavoidable concurrent activation of non-nociceptive afferent fibers when electrical stimuli are used. Similarly, the use of a thermode requires a direct contact with the skin, leading to the activation of low threshold mechanosensitive afferent fibers.

Comment on radiant heat stimulus (Box. 3)

The selective activation of Aδ- and C-fibers can be obtained by delivering brief and powerful laser stimuli on the skin. High power infrared laser stimulator, such as a CO_2 laser, is a light source characterized by radiative energy confined to a narrow beam of parallel monochromatic electromagnetic waves, resulting in a high energy density (Plaghki and Mouraux, 2003). Furthermore, the wavelength of a CO_2 laser is in the far infrared (10.6 μm) allowing a nearly complete absorption by the superficial layers of the skin (Plaghki and Mouraux, 2003), where Aδ- and C- free nerve endings are mainly located (Munger and Halata, 1983; Kruger et al., 1985; Novotny and Gommert-Novotny, 1988). Finally, the skin temperature at which nociceptors are activated can be reached within a few milliseconds given the rise rate of the temperature ramp (>10 000°C/s), resulting in a quasi-synchronized activation of the nociceptive afferents (Plaghki and Mouraux, 2003). Therefore, the activation of nociceptive fibers elicited by a laser stimulation of the skin allows to investigate the interactions between the nociceptive and motor system without concomitant activation of non-nociceptive fibers. This seems of importance because (1) non-nociceptive afferents are capable of modulating the spinal transmission of nociceptive information (Nathan et al., 1986) and (2) because the activation of non-nociceptive Aβ-fibers can modulate the motor system excitability at cortical level as

as shown by (1) the so-called cutaneomuscular reflex (Burke et al., 1991; Gibbs et al., 1995) and (2) the suppression of MEPs after non-nociceptive electrical stimulation of both the median nerve and the digits (e.g. Chen et al. (1999), Clouston et al. (1995), Tokimura et al. (2000)).

In addition, laser pulses delivered to the hand dorsum induce a reduction of the sensorimotor mu rhythm over the hemisphere contralateral to the stimulated hand (Raij et al., 2004). Note that a similar decrease was observed before a predictable noxious electrical stimuli delivered to the index finger tip (Babiloni et al., 2003). The mu rhythm level started to decrease at ± 180 ms after the onset of the nociceptive stimulation and lasted, at least for the α-activity, until ± 2 seconds after the stimulus onset (Figure 1.14). In the same experiment, nociceptive stimuli were delivered by using a smaller laser surface area (0.2-0.3 mm^2). This method, by stimulating a tiny skin surface area, allows a (quasi) selective stimulation of non-myelinated nociceptive C-fibers (Bragard et al., 1996), taking advantage of their higher skin innervation density compared to myelinated nociceptive Aδ-fibers (Plaghki and Mouraux, 2002). Again, in the study of Raij et al. (2004), a later depression of the oscillatory activity corresponding to the mu rhythm was observed starting ± 820 ms after the onset of the C-fibers afferent inputs.

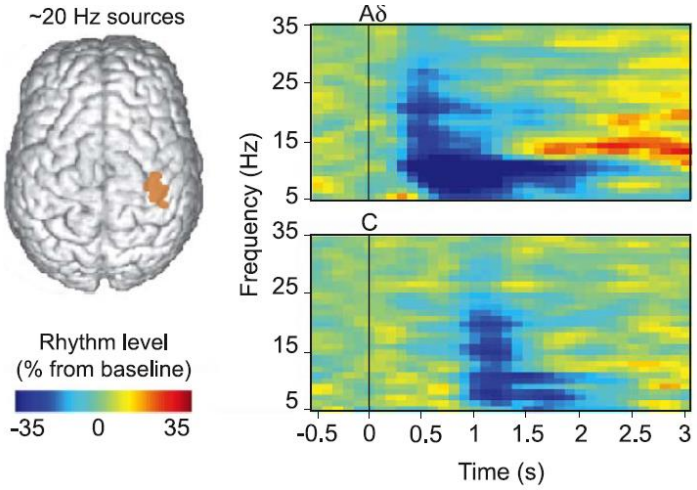

Figure 1.14. Laser stimulus-evoked changes in cortical sensorimotor oscillatory activity. The frequency content of the electroencephalography (EEG) signal is shown as a function of time. Note that the preferential activation of both Aδ- and C-fibers leads to a suppression of the sensorimotor mu rhythm (Adapted from Figure 1 in Raij et al. (2004)).

Again, this decreased oscillatory activity was interpreted as a defensive mechanism serving to withdraw the stimulated limb from an offending source (Ploner et al., 2006; Stancak et al., 2007). Misra et al. (2017) proposed that the suppression of the β-oscillatory activities could underlie a prompter voluntary movement. Indeed, in their study, the reaction times for initiating voluntary movements were shorter during an ongoing painful stimulus delivered via a thermode. In addition, there was no concomitant alteration in the kinematics and the accuracy of the movement. The decrease of the β-band oscillations' power in the contralateral hemisphere relative to the noxious stimuli was significantly correlated with the reaction times, leading the authors to suggest that this suppression could promote a prompter voluntary movement (Misra et al., 2017). Similarly, in a simple reaction time

task in which participants had to press a button with their right index as quickly as possible after having been delivered a laser stimulation on the left hand dorsum, they found an enhancement of γ-band oscillations in the hemisphere contralateral to the stimulation. The γ-activity, which was temporally coupled to the nociceptive stimuli but not to the motor responses, predicted the motor response speed (Schulz et al., 2012). This led the authors to propose that the γ-oscillations they observed were originating from the motor cortex and could reflect a sensorimotor transformation of nociceptive stimuli.

3. Tonic pain-evoked changes in motor system excitability

Ongoing pain sensation can have strong influences on the motor system (Hodges and Tucker, 2011; Bank et al., 2013). This can easily be conceivable by considering both the structural and functional long-term changes in the motor system observed in chronic pain conditions (Parker et al. (2016); Chang et al. (2018), see Box 4 for a brief comment on pain-motor interactions in chronic pain conditions). However, the difficulties to recruit patients within a reasonable period of time as well as the comorbidities often inherent to chronic pain (Graven-Nielsen, 2006) led the researchers to develop experimental models to study both cutaneous and muscle tonic pain in healthy participants (Ali et al., 1996; Arendt-Nielsen and Svensson, 2001). Various experimental models, based on (1) thermal - such as long-duration stimulation delivered via a thermode placed on the skin (Apkarian et al., 2000) or intramuscular injection of cooled/heated isotonic saline (Graven-Nielsen et al., 2002) - (2) electrical - such as long-duration

intramuscular electrical stimulation (Laursen et al., 1997) - or (3) chemical stimulation - such as topical application or intradermal and intramuscular injection of capsaicin (Ali et al., 1996; Witting et al., 2000) - have been used. These experimental models are often referred to as being exogenous methods, in contrast to endogenous methods based on ischemia or exercise (Arendt-Nielsen and Svensson, 2001). A large amount of experimental studies aiming to investigate the mechanisms underlying the interactions between both acute tonic pain and the motor system focused on the effect of tonic muscle pain (Hodges and Tucker, 2011). Intramuscular hypertonic saline injection is the most common method for inducing tonic muscle pain (Arendt-Nielsen and Svensson, 2001). Indeed, the prolonged infusion provokes an increase of intramuscular sodium concentration able to activate nociceptive afferents of the muscular tissues (Graven-Nielsen et al., 1997). Such a sustained stimulation of muscle nociceptive afferents has been shown to reduce the maximal voluntary contraction of both extensor and flexor muscles of the lower limb (Graven-Nielsen et al., 1997; Graven-Nielsen et al., 2002). Such sustained stimulation can also induce functional changes in both muscle activity and coordination during gait (Arendt-Nielsen et al., 1996; Graven-Nielsen et al., 1997; Henriksen et al., 2011) or mastication (Svensson et al., 1996).

Tonic muscle pain induces changes at multiple levels of the motor system (Hodges and Tucker, 2011; Bank et al., 2013), with sometimes compelling effects on motor excitability (Hodges et al., 2003; Martin et al., 2008). Based on clinical and experimental reports, Hodges and Tucker (2011) proposed that the adaptation of the motor system to pain aims to both (1) protect

from further injury and (2) promote recovery by redistributing activity within and between muscles (Madeleine et al., 2006; Tucker and Hodges, 2009). The resulting changes in the mechanical behavior (Tucker and Hodges, 2010) can lead to a protection against further pain. They postulated that, although it can have immediate benefits, long-term negative consequences could result from this motor adaptation to pain. A number of studies have shown that tonic muscle pain has modulatory effects at multiple levels of the motor system (Bank et al., 2013). These changes, which may be complementary, additive or competitive, would aim to protect from further injury and promote recovery (Hodges and Tucker, 2011). Experimental studies suggest that the electrophysiological properties of the muscle fibers are not altered by tonic muscle pain. For instance, the M-wave, a short-latency response elicited by the electrical stimulation of motor axons used to test the peripheral nerve excitability (Knikou, 2008), is not modulated by sustained muscle pain (Svensson et al., 1998; Svensson et al., 2003; Farina et al., 2005a). Similarly, both the contractile properties of the muscle fiber's membranes (Graven-Nielsen et al., 2002) and the CVs of motor units (Farina et al., 2004a; Farina et al., 2005a) do not seem to be affected by acute tonic muscle pain. These observations suggest that interactions between muscle pain and the motor system are mainly centrally mediated (Graven-Nielsen et al., 2002).

At spinal level, animal studies suggest that group III and IV muscle afferents exert opposite effects on flexor and extensor spinal motoneurons (Schomburg et al., 1999; Schomburg and Steffens, 2002). Contradictory results were reported in humans. Indeed, while such a differential

modulatory effect was reported by some authors (Butler et al., 2003; Martin et al., 2006), others instead reported a uniform facilitation of cervico-medullary MEPs (cMEPs) - used to test spinal motoneurons excitability by direct stimulation of the cortico-spinal tract (Taylor, 2006) - during pain (Martin et al., 2008). For instance, MEPs elicited in the TB muscle by direct stimulation of the cortico-spinal tract during a brief maximal voluntary contraction of that muscle were reduced after sustained contraction of both the TB and BB muscles while cMEPs elicited from the BB muscle were enhanced after fatiguing contractions of the elbow extensor muscles (Martin et al., 2006). This differential influence on flexor and extensor motoneurons persisted when muscle ischemia was maintained by using a sphygmomanometer cuff placed around the upper limb inflated to 300 mmHg. In elbow flexors muscles, cMEPs are depressed during fatiguing contraction of the BB muscle but this depression does not seem to be maintained by muscle ischemia (Butler et al., 2003), suggesting that elbow flexor motoneurons are not directly inhibited by group III and IV muscle afferents like those of elbow extensors. However, these results were not replicated in Martin et al. (2008) in which a uniform facilitation of flexor and extensor motoneurons by inputs from group III and IV muscle afferents was observed. In this study, cMEPs from both the TB and BB muscles were facilitated during a constant-EMG contraction performed during an ongoing muscle pain. In their experiment, cMEPs were also evoked during contractions linked to both constant levels of force and EMG background. In constant-force contractions, the voluntary EMG activity decreased while cMEPs were unaltered. On the other hand, the EMG responses were

increased in the constant-EMG condition. In the constant-EMG output, the total synaptic input to the motoneurons pool is unchanged despite of the additional excitatory input from nociceptive muscle afferents, suggesting a reduction of other excitatory inputs, for instance those from descending pathways. Therefore, the facilitation of cMEPs during vs. before pain while the total excitatory input on the motoneurons pool was kept constant suggests that the additional excitatory afferent volleys from nociceptive muscle fibers have a different distribution to the motoneurons pool from that of the supraspinal descending pathways; this excitatory input being more pronounced for the higher-threshold motoneurons recruited into the cMEPs. Findings from constant force condition agree with this hypothesis. Indeed, cMEPs were not reduced during muscle pain despite a reduced EMG background. Therefore, these observations suggest that additional excitatory inputs from group III and IV muscle afferents are greater for large motoneurons than for small ones. This leads to a compression of the range of thresholds across the motoneurons pool (Martin et al., 2008). In addition, assuming that the slope of the EMG–force curve reflects the motor unit recruitment pattern, Wang et al. (2000) showed that hypertonic saline infusion injected in the masseter muscle was able to modulate the motor unit recruitment pattern in jaw-closing muscles. Moreover, it has to be noted that Del Santo et al. (2007) observed an increase of EMG background of the *abductor digiti minimi* (ADM) muscle during pain elicited by injecting ascorbic acid in that muscle. On the contrary, surface EMG recordings from the BB muscle were significantly decreased during pain. Because MEPs elicited from both the ADM and BB muscles were facilitated during pain, the

authors proposed that higher cortico-spinal inputs triggered by the TMS pulses, possibly associated with pain-induced changes in the population of active motor units, could account for the increased MEP amplitude during a painful steady contraction. In addition to direct excitatory inputs from nociceptive muscle afferents on spinal motoneurons, a number of mechanisms implying indirect spinal pathways could account for the interaction between nociceptive muscle afferents and spinal motoneurons (Martin et al., 2006).

First, Rossi et al. (1999) have shown that a sustained discharge in group III and IV afferents from the foot *extensor digitorum brevis* muscle could reduce the excitability of the Ia fibers projecting on the SOL motoneurons, possibly via presynaptic inhibition of these Ia fibres. This is in agreement with an animal study that suggests a presynaptic inhibition of the afferent fibers of the monosynaptic reflex by capsaicin-sensitive group III and IV fibers, directly or via interneurons (Pettorossi et al., 1999).

Second, sustained inputs from nociceptive muscle afferents can influence the spinal Ib inhibitory pathways. Using local injection of levo-ascorbic acid in the body of *extensor digitorum brevis*, Rossi and Decchi (1997) studied the effect of tonic muscle pain on the heteronymous Ib pathways from the GM to the SOL motoneurons. The H-reflex elicited from the SOL was used to test the heteronymous Ib inhibition to SOL motoneurons evoked by the electrical stimulation of the GM. They found that tonic nociceptive stimulation of a dorsal foot muscle (i.e. *extensor digitorum brevis* muscle) decreased both the H-reflex elicited in the SOL muscle and the heteronymous Ib inhibition from GM to SOL motoneurons. Segmental and/or supraspinal pathways

operating at pre and/or post synaptic level could account for interaction between Ib and nociceptive pathways (Rossi and Decchi, 1995; 1997). Indeed, animal studies have shown pre and post synaptic effects of group III and IV cutaneous afferents on the Ib fiber terminals (Harrison and Jankowska, 1985). The presynaptic changes in Ia fibers induced by muscle nociceptive afferents, described above, could decrease the excitability of the spinal Ib inhibitory pathways by projecting on both spinal motoneurons and interneurons mediating the Ib inhibition (Rossi et al., 1999).

Third, alteration in the recurrent inhibition could occur during the discharge of group III and IV muscle fibers. Using a paired H-reflexes method, Rossi et al. (2003) observed that a muscle nociceptive discharge provoked an increase of the homonymous recurrent inhibition during a steady weak voluntary contraction, suggesting that group III-IV muscle afferents can potentiate the facilitation of α-motoneurons and their respective Renshaw cells triggered by the voluntary contraction. This increased excitability of Renshaw cells during a nociceptive muscle discharge could promote recovery of the damaged muscle by limiting its contraction (Rossi et al., 2003). Note that opposite effects on the Renshaw cells excitability have been described in cats (Kalezic et al., 2004).

Finally, nociceptive muscle afferents could have modulatory effects on the fusimotor discharge. For instance, the human SOL stretch reflex is increased during tonic muscle pain induced in both the homonymous muscle and in the TA muscle (Matre et al., 1998; Matre et al., 1999). On the other hand, the H-reflex, the electrical analogue of the stretch reflex, was reported as being either decreased (Rossi and Decchi, 1997; Le Pera et al., 2001) or

unchanged (Matre et al., 1998) by tonic muscle pain. Matre et al. (1998) proposed that tonic muscle pain could increase the dynamic muscle spindle sensitivity, possibly via γ-motoneurons; the lack of H-reflex increase suggesting the absence of α-motoneurons depolarization, possibly via an increased resting discharge of the primary muscle spindle afferents (Matre et al., 1998). This is in agreement with animal studies in which the muscle spindle discharge can be facilitated by nociceptive muscle afferents (Jovanovic et al., 1990; Ro and Capra, 2001; Thunberg et al., 2002). Moreover, a facilitation of the recurrent inhibition by tonic muscle pain could, at least partially, explain the decrease of the motor units' firing rate observed during sustained muscle pain (Sohn et al., 2000; Farina et al., 2004a).

A number of studies aimed to disentangle spinal from supraspinal mechanisms underlying the changes in motor system excitability induced by tonic muscle pain (Burns et al., 2016a). In rats, a decrease of motor cortex excitability, demonstrated by an enhancement of the intracortical microstimulation threshold, was induced by the infusion of glutamate in the right anterior tongue (Adachi et al., 2008). In humans, functional imaging studies found a significant increase of both regional cerebral blood flow (rCBF) (Svensson et al., 1997; Korotkov et al., 2002; Kupers et al., 2004; Thunberg et al., 2005; Owen et al., 2010; Owen et al., 2012) and blood-oxygen-level-dependent (BOLD) responses (Niddam et al., 2002; Macefield . et al., 2007; Nash et al., 2010; Maeda et al., 2011; Takahashi et al., 2011; Uematsu et al., 2011; Loggia et al., 2012) in a number of brain regions such as the contralateral sensorimotor cortex, the lenticular nucleus, the anterior

cingulate and prefrontal cortices. Note that studies investigating the BOLD responses in the contralateral M1 also reported a deactivation in the contralateral M1 relative to the stimulated side (see Burns et al. (2016a)). More insights about cortical mechanisms underlying the changes in the motor system induced by tonic muscle pain were brought by TMS studies. Indeed, it has been shown that tonic muscle pain induced by intramuscular injection of hypertonic saline has an inhibitory effect on MEPs amplitude recorded in various upper limb muscles (Le Pera et al., 2001; Svensson et al., 2003). A reduction of both the H-reflex elicited in the *flexor carpi radialis* (FCR) muscle and cMEPs elicited in the FDI led to suggest the existence of concomitant spinal and supraspinal inhibitory processes (Le Pera et al., 2001; Svensson et al., 2003). However, a slight delay between the changes in MEPs and H-reflexes was observed in Le Pera et al. (2001), therefore suggesting a partial overlap between spinal and supraspinal inhibitory processes. On the other hand, Martin et al. (2008) observed a facilitation of the MEPs elicited by the direct electrical stimulation of the cortico-spinal tract without any concomitant increase of the MEPs elicited by M1 stimulation. This suggests that the inhibitory effect of tonic muscle pain on the motor cortex could be concomitant to an enhancement of spinal motoneurons excitability (Figure 1.15). These contradictory results can be explained, at least in part, by the influence of presynaptic, reciprocal and non-reciprocal inhibitions on the H-reflex (Knikou, 2008) while cMEPs - elicited by direct stimulation of the cortico-spinal tract which has monosynaptic projections with spinal motoneurons (de Noordhout et al., 1999; Petersen et al., 2002) - are not affected by presynaptic inhibition (Nielsen and Petersen, 1994). Schabrun

and Hodges (2012) brought additional insights to the mechanisms underlying the decreased excitability of the cortical motoneurons during tonic muscle pain. They investigated the mechanisms underlying the changes in motor cortex excitability induced by tonic muscle pain by using paired-pulse paradigms with ISIs of 2-3 and 13 ms. This allowed them to investigate the short interval intracortical inhibition (SICI; mediated, at least in part, by gamma-aminobutric acid A receptor ($GABA_AR$) (Kujirai et al., 1993)) and intracortical facilitation (ICF; probably mediated by glutamatergic N-methyl-D-aspartate receptor-(NMDA) (Ziemann et al., 1996; Ziemann et al., 1998)), respectively. ICF was decreased during the infusion of hypertonic saline into the FDI muscle as well as after the cessation of pain while SICI was enhanced only after (and not during) pain. As the reduction of ICF shared a similar time course with the reduction of MEPs amplitude observed during an ongoing muscle pain (Le Pera et al., 2001), they suggest that the changes observed in ICF could contribute to the depression of motor outputs (Schabrun and Hodges, 2012).

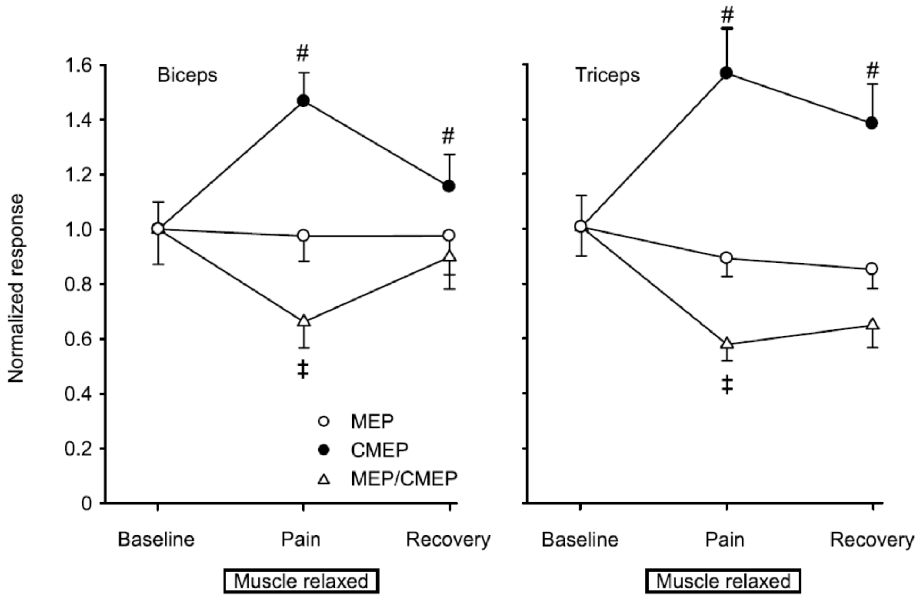

Figure 1.15. EMG responses in the BB and TB muscles before (baseline), during (pain) and after (recovery) the infusion of hypertonic saline in BB. The average area of the EMG responses elicited by cortical (MEPs) and cortico-spinal tract (cMEPs) stimulation is shown. Note that the area was expressed as the proportion of the mean response elicited at baseline. The ratio MEP/cMEP is also represented. cMEPs were significantly increased during the pain condition while MEPs were modulated neither during pain nor in the recovery phase. However, in comparison to cMEPs, MEPs decreased significantly (Adapted from Figure 3 in Martin et al. (2008)).

Additional arguments about supraspinal changes induced by tonic muscle pain in the motor system were brought by studies mapping M1 with TMS (Schabrun et al., 2016; De Martino et al., 2018; De Martino et al., 2019). In this procedure, single pulses of TMS are delivered to different scalp locations in order to generate a map of M1, thanks to the MEPs amplitude elicited at each scalp point (Brasil-Neto et al., 1992; Wassermann et al., 1992; Mortifee et al., 1994; Miranda et al., 1997; Malcolm et al., 2006). This mapping of M1

using TMS is detailed in section 5 of this chapter. By experimentally inducing several days of muscle pain in healthy participants, several studies reported changes in various map parameters such as the map volume, i.e. the sum of the mean MEPs elicited at each point of the map, and the number of discrete peaks (Schabrun et al., 2016; De Martino et al., 2018; De Martino et al., 2019). In these studies, repeated intramuscular injection of nerve growth factor for several days was used as a model to mimic both the time-course and the neural processes involved in the transition from acute to chronic musculoskeletal pain (Hayashi et al., 2013). In the study of Schabrun et al. (2016), opposite effects on both SICI and ICF were observed. Indeed, SICI was decreased while ICF was enhanced. In addition, short- and long-latency interhemispheric inhibition (IHI) between the two M1, assessed by paired-pulse TMS protocols (Ferbert et al., 1992), were decreased. These observations were interpreted as an adaptation to find alternate motor strategies during the transition towards sustained muscle pain (Schabrun et al., 2016).

Though less investigated than the effects of tonic muscle pain, a prolonged painful stimulation of cutaneous tissues is also able to modulate the motor system excitability at both spinal and supraspinal levels. For instance, significant BOLD-responses were induced in the contralateral M1 by long-duration (35 seconds) painful thermal stimuli delivered via a thermode placed on the skin (Apkarian et al., 2000). Farina et al. (2001) observed a decrease of MEPs amplitude recorded in the FDI muscle 20-30 minutes after topical application of capsaicin on the skin overlying the FDI and FCR muscles. In this study, capsaicin-induced pain started 10-20 minutes after

the application of capsaicin and persisted for at least 60-70 minutes. Authors observed a reduction of MEPs only during pain. No suppression was reported 90 minutes after the application of capsaicin, i.e. when the subjects did not report any pain sensation (Figure 1.16). Because the F-, H- and M-waves remained unchanged throughout the experiment, this effect was interpreted as originating from mechanisms operating at cortical level (Farina et al., 2001).

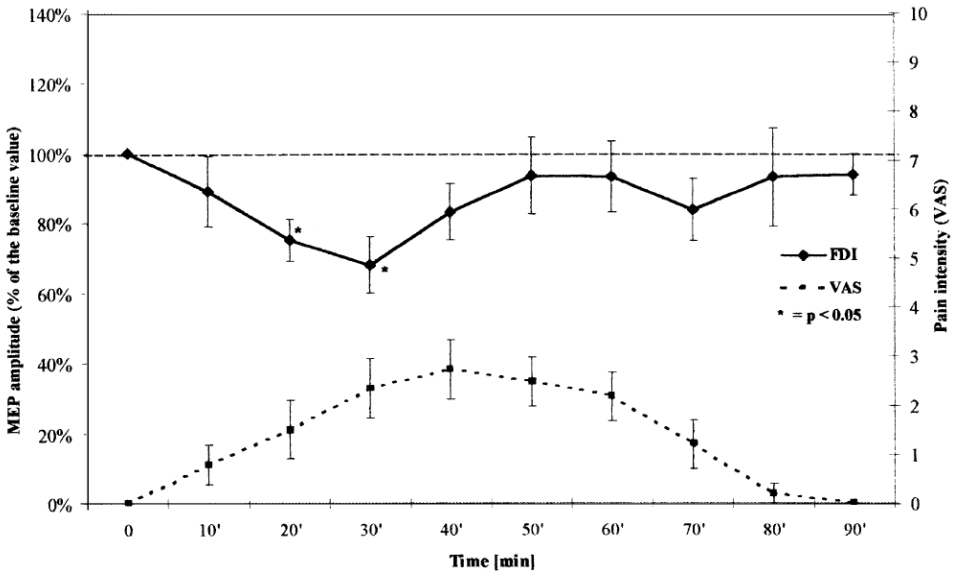

Figure 1.16. MEPs inhibition in the FDI muscle after topical application of capsaicin. Note that MEPs were significantly reduced only during pain sensation, as shown by the asterisks (Adapted from Figure 1 in Farina et al. (2001)).

Fierro et al. (2010) compared the MEPs amplitude, SICI and ICF before vs. after topical application of capsaicin for 60 minutes on the hand dorsum. Similarly to Farina et al. (2001), they observed a significant reduction of both

MEPs amplitude and SICI 20 minutes after the application of capsaicin. No changes were observed for ICF. Though capsaicin-induced pain was not assessed in this experiment, a control experiment revealed that the spontaneous pain evoked by capsaicin became significant 20 minutes after its application, suggesting that the suppression of both MEPs and SICI was concomitant to the ongoing pain (Fierro et al., 2010). However, these observations were not replicated in Mavromatis et al. (2017) who showed no effect of topical capsaicin on both MEPs amplitude and SICI. Furthermore, in another study, neither the TMS recruitment curves, reflecting the strength of the cortico-spinal projections (Devanne et al., 1997; Abbruzzese and Trompetto, 2002), nor the sensorimotor oscillatory activity were affected by capsaicin cream applied on the forearm, although two thirds of the subjects showed a reduced TMS recruitment curve slope associated to an increase sensorimotor oscillatory activity (Martel et al., 2017). Other EEG studies showed a reduction of the sensorimotor mu rhythm over the hemisphere contralateral to the stimulated limb (Giehl et al., 2014; Peng et al., 2014; Huishi Zhang et al., 2016), possibly reflecting functional connectivity between the sensorimotor and medial prefrontal cortices (Nickel et al., 2020). By measuring corrective muscle responses to sensory perturbations, Traverse et al. (2020) showed that a prolonged painful stimulation of the skin can modulate the long-latency motor responses involving supraspinal structures but not the short-latency responses which depend of spinal sensorimotor interactions. Therefore, the authors suggest that, contrary to nociceptive muscle afferents, interactions between both nociceptive cutaneous afferents and the motor system could

mainly operate at cortical level. However, insights from animal studies suggest the implication of spinal processes. Indeed, a reduction of the withdrawal reflex latency was observed in rats with heat tissue injury (Coderre and Melzack, 1985), including in decerebrate rats (Woolf, 1983; 1984). In addition, Gronroos and Pertovaara (1993) found a significant decrease of the lower limb withdrawal reflex threshold after topical application of capsaicin on the human skin.

Importantly, several studies reported persistent changes in motor system excitability at both spinal and supraspinal levels, lasting 20-30 minutes after the cessation of muscle pain (Rossi and Decchi, 1997; Matre et al., 1998; Le Pera et al., 2001; Svensson et al., 2003; Martin et al., 2008; Nash et al., 2010; Schabrun and Hodges, 2012; Schabrun et al., 2013; Rittig-Rasmussen et al., 2014; Burns et al., 2016b). It has been suggested that these long-lasting effects could indirectly result from LTP occurring in the nociceptive system (Svensson et al., 2003; Martin et al., 2008). These observations are congruent with the results of Wall and Woolf (1984) who showed that sustained low-frequency electrical stimulation (20 s, 1Hz) delivered at a strength that preferentially excites C-fibers of muscle afferents - known to generate a progressive increase in action potential discharge (windup) - induced a long-lasting enhancement of the withdrawal reflex in rats (up to 90 minutes) (Wall and Woolf, 1984; Woolf and Wall, 1986; Woolf and Thompson, 1991). Because no changes were observed either in the motoneurons excitability, as tested with the H-reflex, or in the Aδ- fiber terminals excitability located in the lamina I of the dorsal horn (Cook et al., 1986), it has been postulated that the long-lasting enhancement of the

withdrawal reflex could be explained by heterosynaptic mechanisms likely conveyed by C-fiber afferents (Woolf and Wall, 1986). Again, TMS studies brought additional insights to the supraspinal mechanisms underlying the persistent changes in motor excitability when pain had disappeared. Once more, most of our knowledge about persistent changes in motor function induced by the sustained activation of nociceptors come from studies that investigated tonic muscle pain. For instance, it has been shown that SICI was increased after (but not during) pain (Figure 1.17). In addition, ICF was decreased both during and after experimental pain induced by intramuscular infusion of hypertonic saline (Figure 1.17; Schabrun and Hodges (2012)). Similarly, a reduction of short- and long-latency afferent inhibition (SAI and LAI) has been reported both immediately after muscle pain release and 15 minutes later, respectively (Burns et al., 2016b). SAI and LAI can be assessed by pairing a conditioning stimulation, consisting in a non-nociceptive electrical stimulation of a trunk nerve, with a test TMS stimulus. Two phases of MEPs inhibition were described: firstly when the conditioning stimulus preceded the test TMS pulse of 20-50 ms (SAI) and secondly when the ISI was between 200 and 1000 ms (LAI) (Tokimura et al., 2000). The resulting suppression of MEPs recorded from proximal and distal upper limb muscles (Clouston et al., 1995; Manganotti et al., 1997; Bertolasi et al., 1998; Classen et al., 2000; Helmich et al., 2005; Bikmullina et al., 2009) is thought to be mediated by inhibitory processes operating at cortical level. Indeed, while SAI probably results from cortical inhibitory mechanisms conveyed by cholinergic and $GABA_A$ergic pathways (Di Lazzaro et al., 2000; Di Lazzaro et al., 2005), LAI is thought to be mediated by mechanisms involving basal

ganglia, thalamo-cortical (Sailer et al., 2003) and cortico-cortical interactions (Chen et al., 1999; Abbruzzese et al., 2001; Sailer et al., 2002). The functional significance of this reduction of inhibition, i.e. the reduction of both SAI and LAI observed several minutes after pain release, and its interactions with the changes observed in both SICI and ICF observed just after the cessation of pain, is unclear. Burns et al. (2016b) proposed that the enhancement of SICI could be the main mechanism underlying a protective strategy operating directly after pain release while the depression in SAI and LAI could promote recovery by promoting a return to a normal motor output.

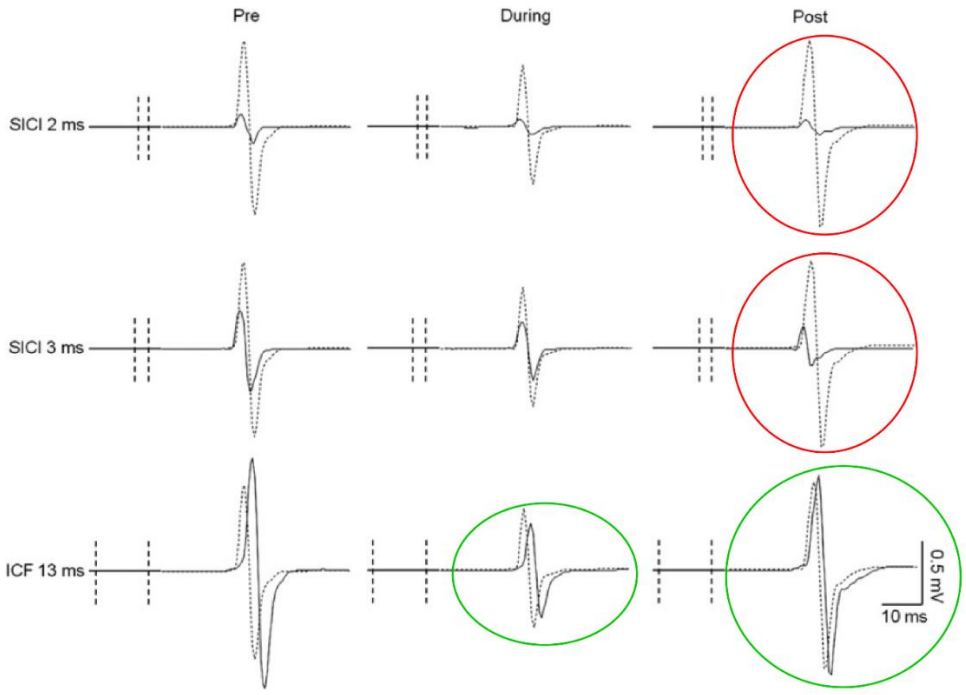

Figure 1.17. MEPs during both SICI (with ISIs of 2 and 3 ms) and ICF protocols of one representative subject in Schabrun and Hodges (2012). EMG responses are shown before, during and after pain release. The two vertical

dashed lines represent the subthreshold conditioning TMS pulse and the suprathreshold unconditioned test TMS pulse. EMG traces represented by solid and dashed lines are elicited by conditioned and unconditioned test stimuli respectively. Both SICI and ICF are calculated by dividing the MEP amplitude of the conditioned test pulse by the MEP amplitude of the unconditioned test pulse. Note that while ICF was decreased during and after pain (green circles), SICI was altered only after pain (red circles) (Adapted from Figure 5 in Schabrun and Hodges (2012)).

Most studies investigating the effect of cutaneous tonic pain on motor function did not investigate persistent changes when pain had disappeared (Farina et al., 2001; Farina et al., 2003; Fierro et al., 2010; Martel et al., 2017). Only Salo et al. (2019) reported a facilitation of SICI several minutes after cold water exposure during 90 seconds. Nonetheless, insights from animal studies suggest that a sustained activation of cutaneous nociceptors is able to elicit long-lasting changes in the motor system excitability (Woolf, 1983; 1984; Woolf and McMahon, 1985; Clarke et al., 1992) although it is admitted that the activation of muscle nociceptive fibers is more robust to generate prolonged excitability changes of spinal motoneurons (Wall and Woolf, 1984; Woolf and Wall, 1986). For instance, heat thermal injury on the foot resulted in prolonged changes of the hindlimb flexor reflex in rats as shown by both the facilitation of its amplitude and the decrease of its mechanical and thermal thresholds. Note that the mechanical threshold of the withdrawal reflex was altered for at least 3 hours (Woolf, 1983). In another study, the decrease in the mechanical threshold of the hindlimb reflex persisted for a period of time of at least 35 days after having injured the skin of the foot by a metal probe for five seconds (Woolf, 1984; Woolf and

McMahon, 1985). Finally, it has been shown that a chemical injury can also induce persistent changes in the reflex threshold for two weeks (Woolf, 1984; Woolf and McMahon, 1985).

Comment on pain-motor interactions in chronic pain conditions (Box. 4)

Abnormalities in the characteristics of movement have been described in patients suffering from various chronic pain conditions. For instance, Heales et al. (2016) reported differences in the synergistic organization of the activation of forearm muscles in patients with chronic lateral elbow pain. Indeed, excessive finger flexion was observed during grip release in patients vs. healthy matched controls. Similarly, the 3D motion analysis of the stance phase of subjects presenting a gluteal tendinopathy during stair ascent revealed a greater hip adduction moment and a more pronounced internal rotation associated to a greater contralateral trunk lean than healthy controls (Allison et al., 2016). Changes in cortico-spinal tract excitability have also been reported. Indeed, an enhancement of the rMT in painful *erector spinae* muscles was observed in CLBP patients and not in pain-free volunteers, suggesting a decrease of cortico-spinal excitability in these patients (Strutton et al., 2005). Similar observations were reported for the active MT in the *infraspinatus* muscle in people with chronic shoulder pain (Bradnam et al., 2016) as well as for the rMT in upper and lower limb muscles in fibromyalgia (Salerno et al., 2000; Mhalla et al., 2010). The lack of changes in the spinal motor system excitability, as tested by the F- and H- waves (Salerno et al., 2000), associated with alterations observed in cortical inhibitory mechanisms such as the cortical silent period, SAI, SICI and ICF (Strutton et al., 2005; Mhalla et al., 2010; Bradnam et al., 2016; Masse-Alarie et al., 2016), led the authors to

propose that these changes could be explained by supraspinal mechanisms. Note that contradictory results were reported by others. Indeed, an increase of the motor system excitability was observed in various chronic pain conditions such as the rotator cuff tears (Berth et al., 2009), osteoarthritis (OA) and the myofascial pain syndrome (Caumo et al., 2016) as well as in chronic knee pain (On et al., 2004). Similarly, ICI was reduced in complex regional pain syndrome (CRPS) patients and after a partial peripheral nerve lesion. In these patients, ICF and the rMT were not modulated (Schwenkreis et al., 2003; Schwenkreis et al., 2010; Schwenkreis et al., 2011). Studies using TMS to map M1 also observed changes in motor excitability in chronic pain. For instance, the volume of the TMS map of both the *transversus abdominis* muscle in CLBP patients and wrist/finger extensor muscles in subjects suffering from persistent elbow pain was higher than in healthy controls (Tsao et al., 2008; Schabrun et al., 2015). On the contrary, the volume was decreased in both CRPS patients (Krause et al., 2006) and in patients with persistent patellofemoral pain (Te et al., 2017). Other studies reported an alteration of the organization of M1, as shown by the decrease of the number of discrete peaks within the TMS map (Schabrun et al., 2017) or by a shift in the center of the TMS map (Elgueta-Cancino et al., 2019). In a systematic review restricted to studies using TMS, Parker et al. (2016) found evidence of a motor cortex disinhibition in various chronic pain populations. On the other hand, a meta-analysis aiming to evaluate evidence underlying alterations in the M1 structure, organization and function revealed that changes in most measures reflecting the motor system excitability were inconsistent between studies (Chang et al., 2018). Therefore, further studies with larger samples are required in

order to understand changes in the motor system in various chronic pain conditions, with possibly different changes between patient groups.

4. Hyperalgesia as a perceptual correlate of LTP in the human nociceptive system

4.1 Increased pain sensitivity at the injured skin location: primary hyperalgesia

After a skin injury, an increased pain sensitivity characterized by changes in both the threshold and the perceived intensity of pain to suprathreshold stimuli is observed at the location of the injury and outside the injured skin area (Figure 1.18).

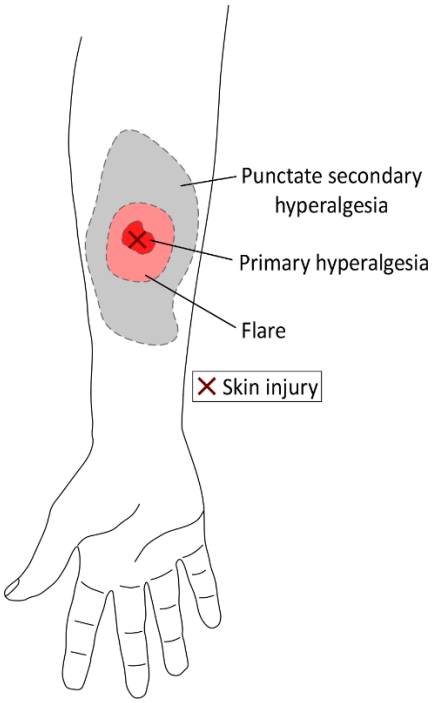

Figure 1.18. Schematic representation of both primary and secondary hyperalgesia which can be observed after a skin lesion. Note that a flare reaction, which is an area of increased skin blood flow, is often observed after cutaneous injuries. The size of the flare area is smaller than that of secondary hyperalgesia.

At the location of a burn or a mechanical injury, *primary hyperalgesia* to both mechanical and heat stimuli is usually observed (Hardy et al., 1950; LaMotte et al., 1983; Raja et al., 1984). Hyperalgesia in the primary zone is thought to be conveyed, at least in part, by peripheral sensitization of primary nociceptive afferents. Indeed, changes in the response properties of both Aδ- and C-fibers, such as C-fiber mechano- and heat-sensitive (CMH) and A-fiber mechano- and heat-sensitive (AMH) nociceptors, to heat (Meyer and Campbell, 1981; Campbell and Meyer, 1983; LaMotte et al., 1983; Campbell et al., 1988) and mechanical (Thalhammer and LaMotte, 1982; Reeh et al., 1987) stimuli were reported after both burn (Campbell et al., 1979; Meyer and Campbell, 1981; Thalhammer and LaMotte, 1982; Campbell and Meyer, 1983; LaMotte et al., 1983) and mechanical injuries (Reeh et al., 1987; Campbell et al., 1988). Central mechanisms can also contribute to the increased pain perception at the injured skin. Indeed, *in vitro* and *in vivo* studies reported LTP, a physiological model of activity-dependent synaptic plasticity (Bliss and Collingridge, 1993; Cooke and Bliss, 2006), in the nociceptive system at synapses between primary C-fiber afferents and neurons located in the dorsal horn of the spinal cord (Liu and Sandkuhler, 1997; Ikeda et al., 2003; Sandkuhler, 2009). For instance, LTP of synaptic transmission between primary C-fiber afferents and spinal dorsal horn neurons have been observed in spinalized rats after intense heat and mechanical stimulation of the skin (Sandkuhler and Liu, 1998). Similar observations were made after HFS of primary afferents in the dorsal root (Randic et al., 1993; Ikeda et al., 2003; Ikeda et al., 2006). These observations suggest that homosynaptic LTP, i.e. occurring at synapses activated by the

conditioning stimulus, within the spinal nociceptive pathways could contribute to the hyperalgesia observed in the primary zone.

4.2 Increased pain sensitivity in the surrounding uninjured skin: Secondary hyperalgesia

Cutaneous tissue injury can also lead to pain amplification in the surrounding uninjured skin (termed *secondary hyperalgesia*; Figure 1.18) (Hardy et al., 1950; Raja et al., 1984; Dahl et al., 1993; Moiniche et al., 1993). This increased pain sensitivity is mainly observed for mechanical punctate stimuli and has been less often reported for heat stimuli. For instance, before and after a burn lesion, Raja et al. (1984) tested both the threshold for pain evoked by mechanical stimuli using a monofilament and the threshold for heat pain and the perceived intensity to suprathreshold heat stimuli by means of a CO_2 laser. Burn lesions were induced at two locations of the palm of the hand separated by 1 cm. While a decrease of pain threshold to mechanical stimuli was observed at both the primary zone (i.e. at the two lesion sites) and in a large area surrounding the injured skin, an increased pain sensitivity to heat stimuli was only observed at the injured skin area. A decrease of pain perception to heat was even observed between the two lesions where a decreased mechanical pain threshold was reported (Figure 1.19).

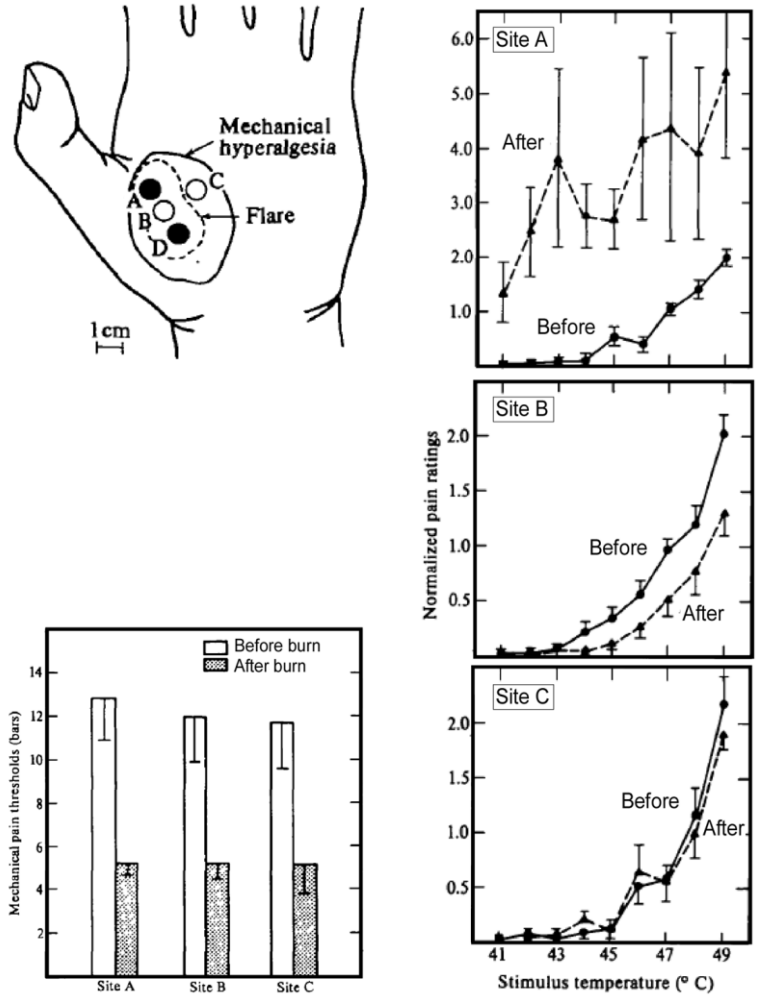

Figure 1.19. Characteristics of both primary and secondary hyperalgesia after burn lesions were made at two locations on the palm of the hand. Left part. Burn lesions were made at both sites A and D. The mechanical pain threshold was determined at site A (injury site) and in uninjured skin locations (sites B and C). Note that the mechanical pain threshold was decreased in both injured and uninjured skin locations. Right part. Pain ratings to heat stimuli at sites A, B and C. Note that heat hyperalgesia was observed only at the site of the lesion (inspired from Figure 1 in Treede et al. (1992), adapted from Figures 2-4 in Raja et al. (1984)).

Significant insights about the mechanisms of secondary mechanical hyperalgesia have been acquired by intradermal injection or topical application of capsaicin, a substance found in hot chili peppers which selectively activates nociceptive afferents through the TRPV1 receptors (Caterina et al., 1997). Indeed, intradermal injection of capsaicin was shown to induce secondary mechanical hyperalgesia to punctate stimuli but not to heat stimuli, closely resembling the phenomenon of secondary mechanical hyperalgesia observed after a skin lesion (Ali et al., 1996). LaMotte et al. (1991) performed a series of psychophysical studies on humans in which they characterized the phenomenon of secondary mechanical hyperalgesia after intradermal injection of capsaicin. These experiments suggest that capsaicin-activated nociceptive afferents can induce central sensitization in dorsal horn neurons of a mechanosensitive pathway, which leads to mechanical hyperalgesia away from the injection site (Baumann et al., 1991; LaMotte et al., 1991; Simone et al., 1991; LaMotte et al., 1992; Torebjork et al., 1992). Central sensitization is defined as an *"increased responsiveness of nociceptive neurons in the central nervous system to their normal or subthreshold afferent input"* (IASP, Taxonomy). Simone et al. (1991) reported that pinprick stimuli delivered to the skin surrounding the site where capsaicin was injected induced a stronger response of both wide-dynamic-range (WDR) and high-threshold (HT) dorsal horn neurons than those elicited before the capsaicin injection. Moreover, peripheral activity of Aδ- and C-fibers in the secondary zone was not enhanced after the

injection of capsaicin (Baumann et al., 1991). Based on these observations, it has been proposed that secondary mechanical hyperalgesia is mainly mediated by central mechanisms (Baumann et al., 1991; LaMotte et al., 1991; Simone et al., 1991; LaMotte et al., 1992; Torebjork et al., 1992), although peripheral mechanisms could also be involved (Treede et al., 1992). Previous studies challenged the idea that secondary hyperalgesia is characterized by an increased perception of mechanical, but not heat stimuli. Indeed, thermal hyperalgesia has been reported in the area surrounding a skin lesion (Hardy et al., 1950; LaMotte et al., 1991; Pedersen and Kehlet, 1998) and a capsaicin-treated zone (Serra et al., 1998). However, this apparent heat hyperalgesia could be explained, at least in part, by the increased skin temperature associated to the flare reaction in the secondary zone (Figure 1.19; Treede et al. (1992), cfr. *infra*).

4.3 High frequency electrical stimulation as a model to elicit activity-dependent plastic synaptic changes

LTP, a physiological model of activity-dependent synaptic plasticity (Bliss and Collingridge, 1993; Cooke and Bliss, 2006), has been proposed as one potential underlying mechanism of central sensitization and could explain some forms of hyperalgesia. Indeed, *in vitro* and *in vivo* studies reported LTP in the nociceptive system at synapses between primary C-fiber afferents and neurons located in the dorsal horn of the spinal cord (Liu and Sandkuhler, 1997; Ikeda et al., 2003; Sandkuhler, 2009). LTP in the nociceptive spinal pathways can be induced by various conditioning stimuli, for instance through subcutaneous injection of capsaicin (Ikeda et al., 2006), nerve injury

(Sandkuhler and Liu, 1998), peripheral lesions leading to inflammatory processes (Sandkuhler and Liu, 1998) or electrical stimulation delivered at low (Ikeda et al., 2006) or high (Liu and Sandkuhler, 1997) frequencies (Figure 1.20). More specifically, robust LTP of the synaptic efficiency between C-fiber primary afferents and dorsal horn neurons can be obtained in rats by brief HFS bursts applied to the afferent nerves (Liu and Sandkuhler, 1995; 1997). For instance, it has been shown that HFS of primary peptidergic C-fiber afferents induced the LTP of C-fiber-evoked excitatory postsynaptic potentials in lamina I neurons that express the NK1 receptors for substance P and that project to the parabrachial area (Ikeda et al., 2003; Ikeda et al., 2006). Dorsal horn neurons expressing the receptor for substance P seem essential for the development and the total expression of some forms of hyperalgesia as illustrated by the reduction of hyperalgesia-related behaviors in rats in which these neurons had been destructed (Mantyh et al., 1997; Nichols et al., 1999; Khasabov et al., 2002).

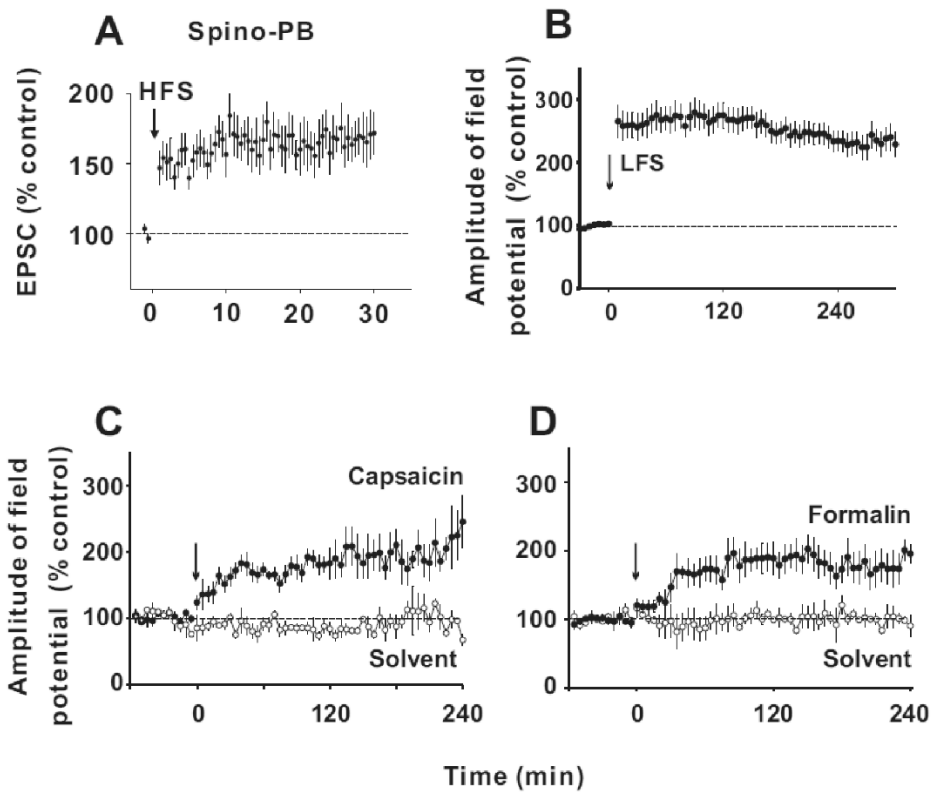

Figure 1.20. LTP of the synaptic strength between C-fiber primary afferents and dorsal horn neurons induced by various conditioning stimuli. **A.** Average of amplitudes ±SD of C-fiber-evoked excitatory postsynaptic currents (EPSCs) in lamina I neurons with a projection to the parabrachial area. **B-D.** LTP can be induced *in vivo* by more natural conditioning stimuli generating a low-frequency afferent barrage. Mean time courses of C-fiber-evoked field potentials recorded extracellulary in the superficial spinal dorsal horn in response to low-frequency electrical stimulation of the sciatic nerve in anaesthetized rats (B). Intradermal injection of capsaicin into the glabrous skin of the ipsilateral hind paw can also induce LTP compared to control condition (solvent) (C). Similar results are shown for formalin (D) (Adapted from Figures 3 and 4 in Ikeda et al. (2006)).

Klein et al. (2004) investigated whether HFS of peptidergic C-fibers - which induced LTP of the synaptic transmission in spinal dorsal horn - could lead to an increased pain perception in humans. This would suggest that the LTP of the spinal synaptic transmission play a role in hyperalgesia in human subjects. To that end, electrical stimuli were delivered by means of small diameter electrodes (punctate electrodes; 200 µm) allowing to achieve high current density at low current intensity, resulting in the preferential activation of nociceptors in the superficial layers of the epidermis. Ten punctate electrodes were mounted in a circular fashion on a plastic frame to increase the spatial summation. The HFS protocol consisted of five trains of 100 Hz for 1-s, repeated in a 10-s interval, at 20x the individual detection threshold applied to the forearm at 10 cm distal to the fossa cubita (Figure 1.21).

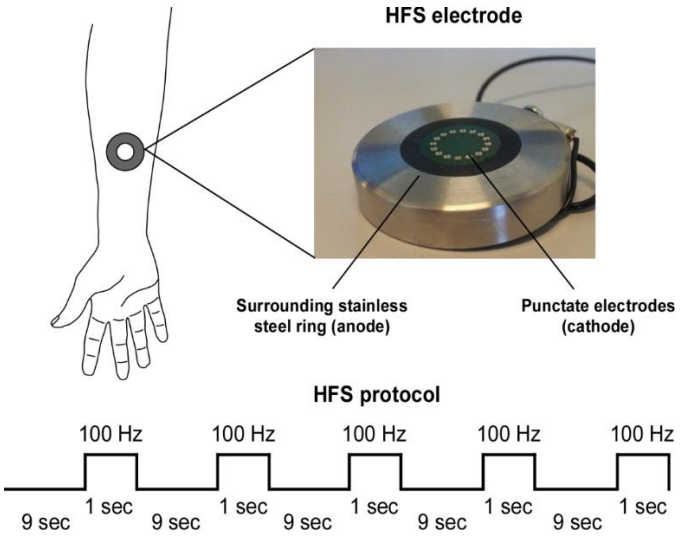

Figure 1.21. HFS electrode and protocol. The cathode consists of 10-16 blunt stainless steel pins with a diameter of 0.2 mm protruding 1mm from the

base. The pins are placed in a circle with a diameter of 10 mm. The anode consists of a surrounding stainless steel ring having an inner diameter of 22 mm and an outer diameter of 40 mm. The HFS protocol consisted of five trains of 100 Hz for 1-s, repeated in a 10-s interval, at 20x the individual detection threshold. HFS is usually applied to the forearm.

In the study of Klein et al. (2004), the successful activation of peptidergic cutaneous afferents was achieved as illustrated by a large area of increased skin blood flow measured with laser doppler imaging in the skin surrounding the area stimulated by HFS. This flare reaction is thought to be mainly conveyed by a subgroup of peptidergic C-fibers, the mechano-insensitive C-fibers, which release neuropeptides such as calcitonin gene-related peptide (CGRP) (Lynn et al., 1996; Schmelz et al., 2000). This neuropeptide release caused a neurogenic inflammation that lead to the vasodilatation of blood vessels (Groetzner and Weidner, 2010). Klein et al. (2004) observed that a single high-intensity electrical test stimulus, delivered through the HFS electrode, was perceived as more painful after HFS (Figure 1.22A). This long-lasting increased pain sensitivity, which they called homotopic hyperalgesia, lasted several hours and had a plateau at ± 30 minutes (Pfau et al., 2011).

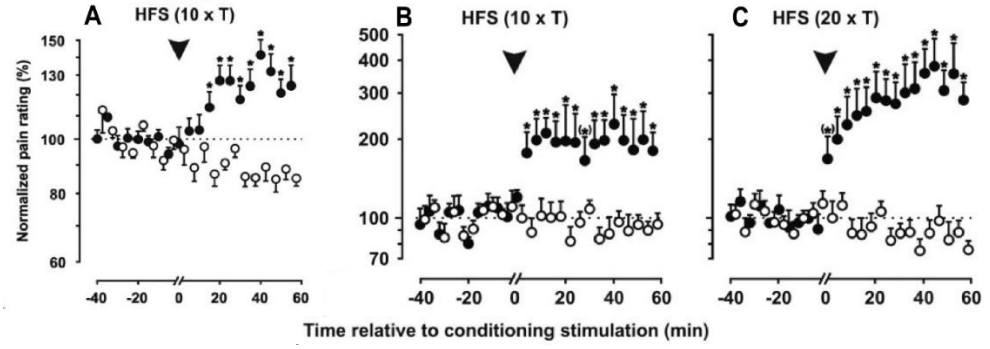

Figure 1.22. Homotopic and heterotopic effects of HFS. **A.** After HFS delivered at 10x individual detection threshold, pain ratings evoked by single electrical test pulses delivered via the HFS electrode (homotopic zone) was significantly increased (black dots) compared to identical stimuli delivered via a remote electrode (white dots). **B and C.** HFS delivered at both 10x and 20x individual detection threshold induced a significant increase of pinprick-evoked pain in the surrounding unstimulated skin (heterotopic zone) (Adapted from Figures 3 and 4 in Klein et al. (2004)).

In a first instance, the authors attributed this long-lasting enhancement of pain perception as a perceptual correlate of homosynaptic LTP, i.e. the long-term changes in the perception of pain mediated by an increased synaptic strength of the conditioned pathway (in this case the peptidergic primary C-fiber afferents) at spinal level. Later, they observed a similar enhancement of pinprick-evoked pain in both the homotopic and heterotopic zone after HFS of the forearm (Lang et al., 2007; Klein et al., 2008). As pinprick stimuli predominantly activate Aδ-fibers, these observations suggest that heterosynaptic mechanisms can also contribute to homotopic hyperalgesia. This is in agreement with the observations of Hansen et al. (2007), who asked subjects to describe, by means of a list of descriptors, the quality of electrical stimuli delivered to the homotopic area after HFS. After HFS,

participants qualified the test electrical stimuli as more “stinging” and “burning” than before HFS, suggesting a facilitation in both Aδ- and C-fiber pathways. Heterosynaptic LTP seems to be the main mechanism that accounts the increased Aδ-fiber-related perception after HFS because animal studies have shown that HFS of Aδ-fibers did not induce homosynaptic LTP but homosynaptic long-term depression (LTD) instead (Cheng and Randic, 2003). This could explain the decreased pain perception of high-intensity electrical stimuli delivered in the conditioned skin site 30 minutes after HFS (van den Broeke et al., 2012). Together, these observations show that the homotopic/primary hyperalgesia induced by HFS comes, at least in part, from both homo- and hetero-synaptic LTP in spinal nociceptive pathways.

In addition, Klein et al. (2004) observed a long-term enhancement of pain perception to mechanical punctate stimuli outside the skin conditioned by HFS, resembling to secondary mechanical hyperalgesia observed in the surrounding uninjured skin. The increased pain sensitivity to mechanical stimuli (heterotopic mechanical hyperalgesia) they observed after HFS was attributed to heterosynaptic LTP in spinal nociceptive pathways. As outlined by Klein et al. (2004), heterotopic hyperalgesia was observed outside the conditioned skin and was elicited by mechanical punctate stimuli which activate different afferent pathways than the conditioned input pathway (i.e. peptidergic C-fibers), such as Aδ-fibers sensitive to mechanical inputs, suggesting a heterosynaptic mechanism. Also, it has been shown that this increased pain sensitivity reached its maximum 60 minutes after HFS and disappeared 25.4h after the cessation of the conditioning stimuli. This

suggests that early-LTP (LTP 1; i.e. depending on post-translational processes and lasting up to ± 24h) can be induced by HFS of the skin in healthy volunteers (Klein et al., 2006). Evidence suggests that different mechanisms underlie heterotopic and homotopic hyperalgesia elicited by HFS. As explained above, homosynaptic and heterosynaptic mechanisms can both contribute to the increased pain sensation elicited by electrical stimuli delivered into the conditioned skin area. The contribution of homosynaptic LTP in the homotopic zone can for instance explain that low-doses of the N-methyl D-aspartate (NMDA)-receptor antagonist ketamine prevented homotopic hyperalgesia, which was tested with electrical stimuli, but not heterotopic hyperalgesia, tested with pinprick stimuli (Klein et al., 2007). This is in agreement with animal studies showing that the pharmacological blockage of NMDA receptors prevented the development of spinal nociceptive LTP by HFS of primary C-fiber afferents (Ikeda et al., 2003) and suggests that the LTP occurring in the conditioned pathway is NMDA-dependent while other NMDA-insensitive mechanisms should, at least in part, underlie the heterosynaptic LTP (Klein et al., 2007).

Secondary mechanical hyperalgesia, as observed after HFS or capsaicin injection, is of particular interest because increased pain sensitivity to mechanical stimuli in the undamaged skin is a prominent clinical feature in persistent pain conditions such as postoperative pain (Stubhaug et al., 1997; Lavand'homme et al., 2005). Moreover, LTP in the nociceptive system is thought to be a key mechanism leading to chronic pain in humans (Rygh et al., 2005; Sandkuhler, 2009).

4.4 Contribution of A- and C- fibers to secondary mechanical hyperalgesia

Previous studies investigated the relative contribution of both A- and C-fibers to the increased pain perception to pinprick stimuli in the area of secondary hyperalgesia. Ziegler et al. (1999) did not observe an enhancement of the punctate stimuli-evoked pain perception in the secondary zone during a complete block of myelinated A-fibers. However, punctate hyperalgesia was observed when the nerve block was released. Because a prolonged pressure nerve block affects the conduction of myelinated primary afferents to a greater extent than the conduction of unmyelinated C-fibers (Torebjork and Hallin, 1973; Nahra and Plaghki, 2003), these results suggest that myelinated A-fibers participate in the increased perception of mechanical punctate stimuli in the secondary zone. Again, because (1) capsaicin-evoked pain was not altered under nerve block (suggesting that capsaicin-induced pain is mainly conveyed by capsaicin-sensitive C-fibers) and (2) myelinated nociceptive afferents significantly contribute to the pain perception evoked by punctate stimuli, these observations suggest that secondary mechanical hyperalgesia is, at least in part, conveyed by spinal heterosynaptic mechanisms given that the facilitated and facilitating pathways consist of different populations of primary afferents fibers (Ziegler et al., 1999). Denervation of capsaicin-sensitive free nerve endings in the epidermal layer can be achieved by topical application of capsaicin (Nolano et al., 1999). This has been used by Magerl et al. (2001) to show that secondary mechanical hyperalgesia is principally mediated by capsaicin-insensitive Aδ-fibers, including HTM

(Szolcsanyi et al., 1988) and AMH type I (Ringkamp et al., 2001). AMH type I nociceptors do not respond to short-lasting heat stimuli but show a delayed response to sustained heat stimuli (Treede et al., 1995; Treede et al., 1998). Therefore, van den Broeke et al. (2016b) delivered long-duration heat stimuli (30s) inside the area of the secondary mechanical hyperalgesia induced by HFS of the skin by means of a CO_2 laser. After HFS, the perception of long-duration heat stimuli was not significantly different compared to before HFS. This suggests that AMH type I nociceptors do not contribute to secondary hyperalgesia to punctate stimuli. Finally, it has to be noted that an increase of heat sensitivity in the area of secondary hyperalgesia has been reported (van den Broeke and Mouraux, 2014a). Quickly responding C-fiber afferents could possibly contribute to this increased heat sensitivity (Lenoir et al., 2018c) via LTP in spinal nociceptive pathways involving glial cells (Kronschlager et al., 2016; Lenoir et al., 2018c).

4.5 Sustained activity-dependent changes induced by HFS at supraspinal level

Supraspinal descending influences from brainstem structures such as the rostral ventromedial medulla (RVM) can contribute to the development and/or maintenance of secondary mechanical hyperalgesia (Urban and Gebhart, 1999; Suzuki et al., 2002). Indeed, animal studies have shown that the reduction of both the supraspinal descending facilitation (Urban and Gebhart, 1999) and inhibition from spinothalamic tract neurons (Lin et al., 1996) could be involved in secondary mechanical hyperalgesia. More specifically, animal studies showed that HFS of primary C-fiber afferents can

induce changes in brain activity. Using PET, Hjornevik et al. (2008) observed metabolic changes in the amygdala and adjacent cortical structures, striatum, RVM and in the periaqueductal gray (PAG) until 150 minutes after HFS of the sciatic nerve. Such structures are known to modulate the spinal nociceptive transmission (Heinricher et al., 2009).

In humans, short-lasting effects of HFS have been reported on brain responses elicited by non-nociceptive stimuli presented in the area of secondary hyperalgesia such as innocuous tactile (van den Broeke and Mouraux, 2014b) or visual stimuli (Torta et al., 2017). This suggests that HFS can trigger supraspinal and multimodal changes, possibly via attentional mechanisms (Torta et al., 2018). Note that it is known that HFS can have long-lasting effects on event-related potentials (ERP) evoked by noxious mechanical stimuli (van den Broeke et al., 2016a; van den Broeke et al., 2017). However, the relative contribution of spinal and supraspinal processes to these changes in ERPs' amplitude, as well as the origin of potential supraspinal mechanisms, is currently unknown (van den Broeke et al., 2010).

5. Non-invasive mapping of M1 using single pulses of TMS

Single pulses of TMS can be applied at different scalp locations to generate a map of the scalp points at which consistent MEPs, above a given threshold, are recorded (Figure 1.23). Thanks to the MEPs amplitude elicited at each location, it is possible to elicit a map of the cortical representation of a given muscle in humans (Brasil-Neto et al., 1992; Wassermann et al., 1992; Mortifee et al., 1994; Malcolm et al., 2006). Neuronavigation data are often

used to visualize the TMS map online; the position markers being an accurate and instantaneous feedback about the TMS stimulus position.

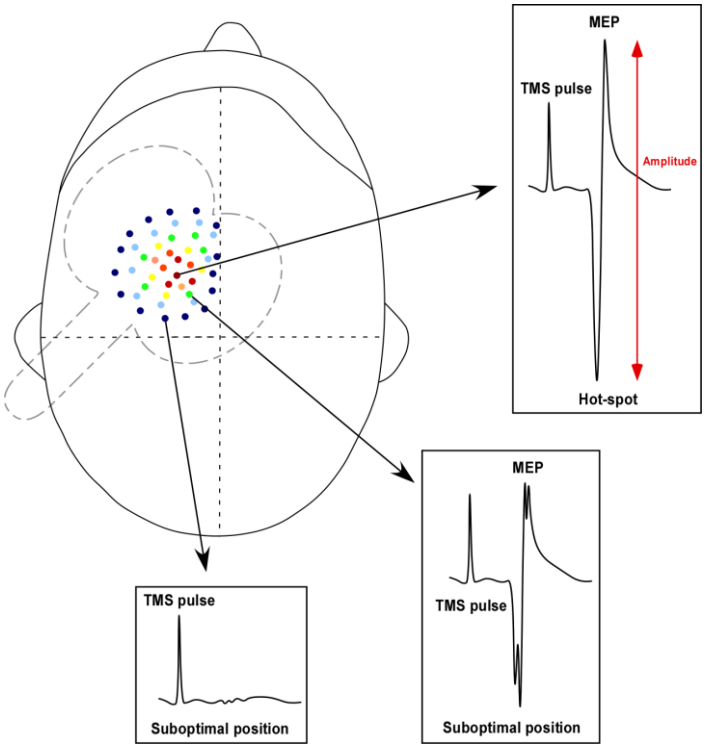

Figure 1.23. Schematic representation of the TMS map procedure. Single TMS pulses are delivered at different scalp locations. Thanks to the MEPs amplitude, a map of a given muscle can be obtained.

Then the MEPs are interpolated, resulting in a color-scaled 3D map of the investigated muscle (Figure 1.24; Borghetti et al. (2008)). Several measures can be extracted from this TMS-estimated map (Figure 1.24). First, the optimal site representing the location at which the MEPs with the maximal amplitude can be recorded. This represents the zone containing cortico-spinal neurons with the lowest threshold (Wassermann et al., 1992). Second,

the extent of the map area (expressed in cm^2) from which consistent MEPs, above a given amplitude, can be recorded. Obviously, the area of the TMS map is larger than the actual neural representation of a given muscle due to the current spread. Indeed, the fall-off of MEPs amplitude when the TMS coil is moved away from the center of the map (i.e. the hotspot) can be attributed to a decrease of the efficacy of the TMS pulse to stimulate a constant cortical region. Thus, this does not represent additional recruitment of cortico-spinal neurons projecting to a given muscle (Thickbroom et al., 1998). Nevertheless, when the excitability of cortico-spinal neurons is enhanced, they are more easily excitable, even when the TMS coil is not directly located at the optimal position (Najib et al., 2011). Modifications of the motor map area after a given intervention can result from changes in motor system excitability. Importantly, this does not mean that these changes result from changes in M1. Indeed, the TMS-mapped representation of a given muscle can also be dependent of changes in both remote brain structures sending inputs to M1 and/or spinal motor pathways (Ridding and Rothwell, 1997; Najib et al., 2011). The third parameter which can be extracted from the TMS map is its volume. This represents the sum of the mean MEPs amplitude elicited at each point of the map, providing a measure of the total excitability of the TMS-mapped representation of a given muscle. The center of gravity (CoG) of the TMS map, which is a position representing the amplitude-weighted center of the map area, can also be computed. This depicts the Ant-Post and Med-Lat coordinates of the central point around which the motor map is evenly distributed. The following

mathematical formula can be used for the calculation of its x- and y-coordinates:

$$\text{CoGx} = \frac{\sum(\text{MEP}xi \times \text{X}i)}{\sum \text{MEP}i}$$

$$\text{CoGy} = \frac{\sum(\text{MEP}yi \times \text{Y}i)}{\sum \text{MEP}i}$$

MEP_i represents the average amplitude of MEPs at each target point. The amplitude-weighted of MEPs at each scalp location represents the contribution of that position to the total amplitude of the map (i.e. the map volume) (Wassermann et al., 1992). The CoG is used to determine the position of the map center and can be used to differentiate the spatial location of adjacent muscles (Wassermann et al., 1992; Wilson et al., 1993; Miranda et al., 1997). Indeed, the CoG is considered an accurate estimation of the cortical location of a given muscle. For instance, it has been shown that the CoG of a TMS motor map is generally spatially congruent with the CoG of the activation area related to hand movements observed in fMRI (Boroojerdi et al., 1999; Herwig et al., 2002) and PET (Wassermann et al., 1996; Classen et al., 1998). The CoG can also be used to identify a shift in the cortical representation of a given muscle after an intervention. Such shifts could result from intracortical functional changes (Wassermann et al., 1992; Wilson et al., 1993; Uy et al., 2002). Finally, the number of discrete peaks inside the map (Figure 1.24) has been used to characterize functional

changes in M1. Indeed, multiple areas of greater excitability inside the TMS map were observed in a number of TMS studies (Tsao et al., 2011; Schabrun et al., 2016; Masse-Alarie et al., 2017; Schabrun et al., 2017). The significance of such discrete peaks within a TMS-mapped representation is currently unknown. However, this is in agreement with the fact that several sites within M1 can participate in the control of a single muscle (Donoghue et al., 1992; Schieber, 2001; Schneider et al., 2001). It has been proposed that they could participate in (1) the elaboration of motor synergies between adjacent cortical motor representations and/or (2) the coordination between both muscles and joints (Schabrun et al., 2015). Note that a smaller number of peaks was observed in chronic pain patients (Schabrun et al., 2015; Schabrun et al., 2017). This leads the authors to draw a parallel with the loss of motor control observed in chronic pain conditions (Hodges and Tucker, 2011).

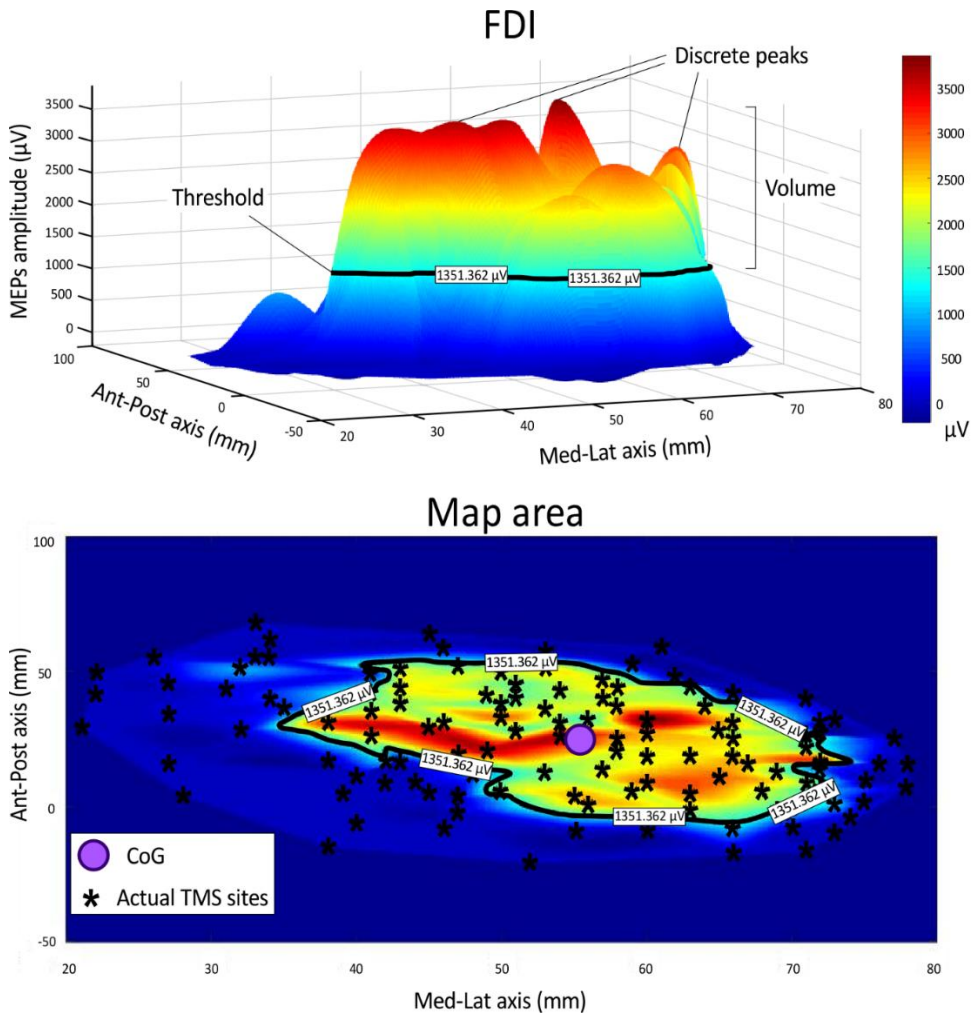

Figure 1.24. TMS-mapped representation of the right FDI muscle in a representative subject (personal data). The map area consists in the size of the map, considering MEPs ≥ a given threshold (black line; in this case 1351.362 µV). The volume is computed by adding the interpolated MEPs amplitude exceeding or equal to the threshold. The CoG, which is the center of the excitable map, and three examples of discrete peaks, two parameters used to explore functional changes in M1, are also represented.

Several studies suggested that mapping the motor cortex using TMS can be used to differentiate the cortical representation of proximal and distal muscles of the upper limb (Figure 1.25). It has been shown that the map area volume was greater for distal muscles, such as FCR or *abductor pollicis brevis* (APB) muscles, than for proximal muscles, such as BB or deltoid muscles (Wassermann et al., 1992; Metman et al., 1993; Miranda et al., 1997). Moreover, despite significant overlaps, their map area can be distinguished (Figure 1.25). Indeed, the TMS-mapped representation of distal muscles is more lateral than the TMS-mapped representation of more proximal muscles (Wassermann et al., 1992; Metman et al., 1993). Furthermore, by using TMS mapping techniques, the map representation of intrinsic hand muscles (APB and *abductor digiti minimi* muscles; ADM) can also be distinguished, the TMS map of the APB muscle being more lateral than that of the ADM muscle (Wilson et al., 1993).

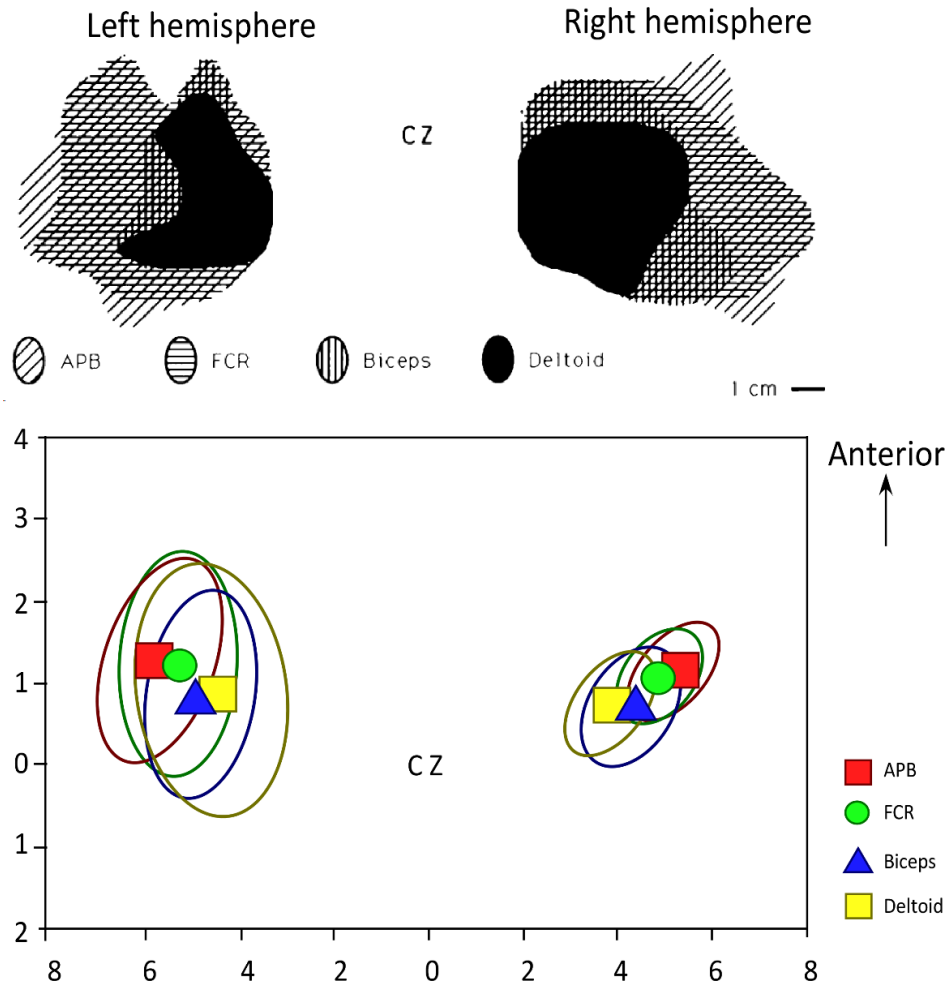

Figure 1.25. Upper part. Superimposed TMS-mapped representation of the APB, FCR, BB and deltoid muscles. Lower part. Averaged position of the CoGs with their respective 95% confidence intervals. Note that, although the TMS maps overlap each other, distal muscles are more lateral than proximal muscles (Adapted from Figures 4 and 5 in Wassermann et al. (1992)).

In healthy subjects, rapid changes in the TMS cortical motor map have been reported. For instance, an enhancement of the TMS map of upper limb muscles proximal to an ischemic nerve block was observed ten minutes after

the beginning of the intervention (Brasil-Neto et al., 1993; Ridding and Rothwell, 1997). Similarly, Pascual-Leone et al. (1995) compared the TMS-mapped representation of both flexor and extensor finger muscles before vs. after a motor skill acquisition. The fine motor skill consisted in a sequence of finger movements performed on a piano keyboard and was practiced for two hours daily during five days. The TMS motor cortex map was assessed before the exercise and every day 20-30 minutes after it. Over the course of the five days, they observed an enhancement of the TMS map which was not observed in control conditions. Moreover, this increase was already present the first day, i.e. after one session of motor skill learning (Pascual-Leone et al., 1995). Similar observations were reported by comparing the TMS-mapped representation of the FDI of the reading hand in blind subjects before (in the morning) vs. after (in the evening) a working day in which they were reading Braille for at least six hours. Such an enhancement was not observed in non-working days (Pascual-Leone et al., 1995). Finally, cortical reorganization in pathological conditions such as stroke (Liepert et al., 1998; Liepert et al., 2000) and dystonia (Thickbroom et al., 2003) or after brain surgery (Kastrup et al., 2000) has been assessed with TMS motor cortical brain mapping.

6. Changes in brain connectivity explored by concurrent transcranial magnetic stimulation and functional magnetic resonance imaging

6.1 Abnormal structure and function of the DLPFC in CLBP patients

Pathological chronic pain represents a major European healthcare issue. Indeed, it has been estimated that 19-35% of adult Europeans suffer from moderate to severe chronic pain (Elliott et al., 1999; Breivik et al., 2006; Breivik et al., 2013). Furthermore, chronic pain conditions noticeably impair the quality of life of individuals and have severe socioeconomic impacts upon communities. The financial burden associated with persistent pain conditions is similar to that of heart diseases and cancer (Breivik et al., 2013). Low back pain constitutes a common problem as up to 75% of the population will present at least one episode during their live (Deyo and Weinstein, 2001; Atkinson, 2004). Though most acute episodes are resolved themselves in a few months, a number of patients will develop chronic low back pain (i.e. recurrent episodes for more than 6 months) reaching up to 5% of the population (Deyo and Weinstein, 2001; Atkinson, 2004). Consequently, furthering our understanding of the neural representation of various chronic pain conditions in humans is essential to prevent, diagnose and develop an effective management of chronic pain.

Physiopathologic mechanisms associated with chronic pain states, derived either from long-term changes due to tissue injuries or from neuronal injuries (neuropathic pain), take place at different levels of the nervous system, from peripheral afferents terminals (e.g. Devor et al. (1994), Reinert

et al. (1998)) to spinal cord neurons (e.g. Woolf and Thompson (1991)) or via the alteration in descending controls (e.g. Bouhassira et al. (2003)). At cortical level, abnormalities in brain chemistry were reported by Grachev et al. (2000) in CLBP patients, especially in the DLPFC which showed a consistent depletion in N-acetyl aspartate and glucose while an opposite pattern was observed in the thalamus. No changes were observed in the cingulate, sensorimotor, orbitofrontal and insular cortices. Moreover, the chemical interrelationship across brain regions was altered in CLBP patients, suggesting abnormal chemistry connectivity in such patients. Other studies reported abnormalities in brain biochemistry in various chronic pain states such as CRPS (Grachev et al., 2002) or neuropathic pain after a spinal cord injury (Pattany et al., 2002). Morphometric changes in various brain structures, such as the DLPFC, the thalamus and the somatosensory cortex were also reported (for reviews see May (2008), May (2011)). Changes in brain connectivity in chronic pain patients have been extensively studied, mainly via resting state functional connectivity (Kucyi and Davis, 2015). Resting state functional connectivity is based on the identification of remote brain regions which show synchronous BOLD responses when the subjects are laying on the scanner bed without performing any task. Therefore, by selecting a seed voxel corresponding to a starting point to perform the analysis of brain connectivity, or by using data exploration techniques such as independent components analysis (ICA), it is possible to identify brain regions for which the spontaneous brain activity time courses, i.e. the BOLD time courses, are correlated across fMRI scans. By analyzing resting-state data, a certain number of brain regions which show a coherent activity have

been identified, *inter alia*, in brain networks involved in visual (Lowe et al., 1998), auditory (Cordes et al., 2000), somato-motor (Biswal et al., 1995) and attentional (Fox et al., 2006) processes. In chapter 6, I present an original and relatively simple approach which aims to record TMS-evoked responses by using concurrent TMS-fMRI to characterize changes in the cortical excitability and functional connectivity within different brain areas. Our objective was to investigate changes in brain connectivity related to chronic pain. Specifically, I aimed to validate the recording of BOLD responses elicited by TMS over the DLPFC. I chose the DLPFC as a target because (1) DLPFC is a superficial structure easily reached with a figure-of-eight coil (2) in which consistent structural changes were reported in chronic pain. Furthermore (3), despite the structural modifications, changes in the functional connectivity between the DLPFC and remote brain areas is rarely reported in the literature (Seminowicz and Moayedi, 2017). This can be explained, at least in part, by the fact that the DLPFC is not easily identifiable by using the resting-state approach. Consequently, the first part of this section is dedicated to an overview of changes in brain morphometry and connectivity with an emphasis on the DLPFC in CLBP patients, which represents one of the most frequent chronic pain state in our societies (Andersson, 1999). In the second part, I will develop some technical and methodological considerations about concurrent TMS-fMRI.

6.1.1 Anatomy and function of the DLPFC - an overview

The DLPFC is a heterogeneous brain region. Using tractography-based parcellation to identify voxels with a similar connectivity profile in humans,

Sallet et al. (2013) identified six distinct areas in the lateral frontal cortex (Figure 1.26). From these regions, clusters 5, 6, 8 and 10 are typically referred as being the DLPFC in human studies (Figure 1.27; Seminowicz and Moayedi (2017)). The DLPFC encompasses the Brodmann areas (BA) 9, 8a, 8b and the dorsal part of the BA 46. This includes most of the middle frontal gyrus, the superior frontal sulcus, and the lateral part of the superior frontal gyrus. The precentral gyrus and the anterior prefrontal cortex (BA 10) represent its posterior and anterior boundaries, respectively (Seminowicz and Moayedi, 2017).

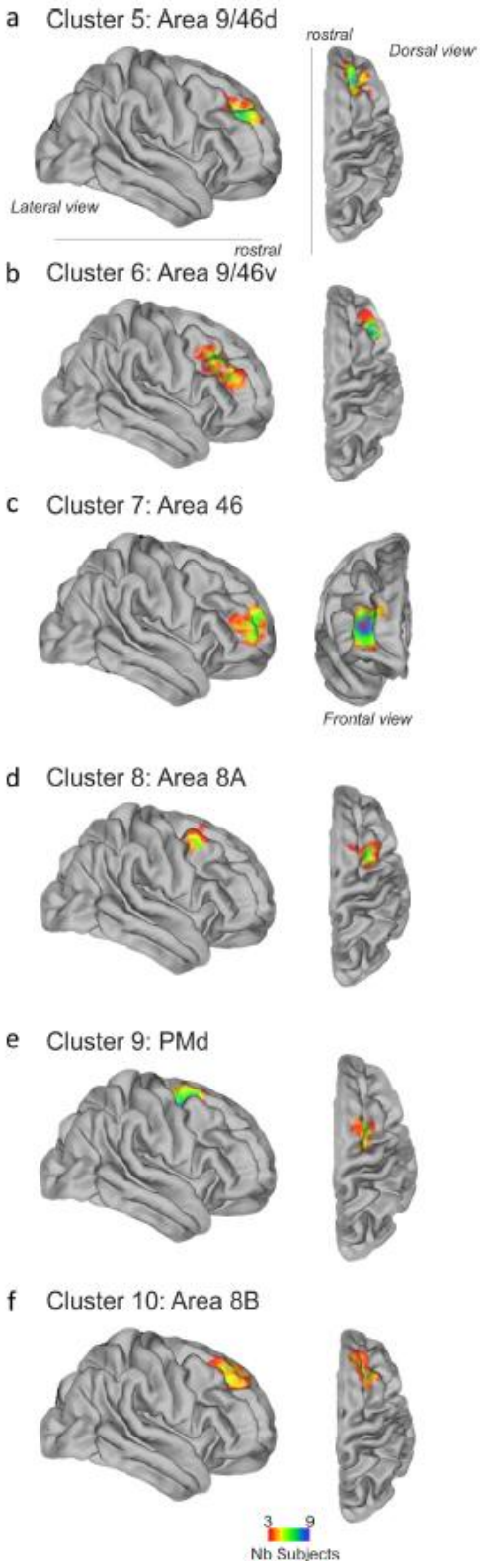

Figure 1.26. Tractography-based parcellation revealed six clusters in the human lateral frontal cortex. The inter-regional BOLD coupling patterns associated with cluster 5 in humans suggest that this cluster may resemble to the area 9/46d in macaque. Similarly, cluster 6 was associated to area 9/46v, cluster 7 with area 46, cluster 8 with area 8A, cluster 9 with the anterior dorsal premotor cortex and cluster 10 with area 8B (Adapted from Figure 9 in Sallet et al. (2013)).

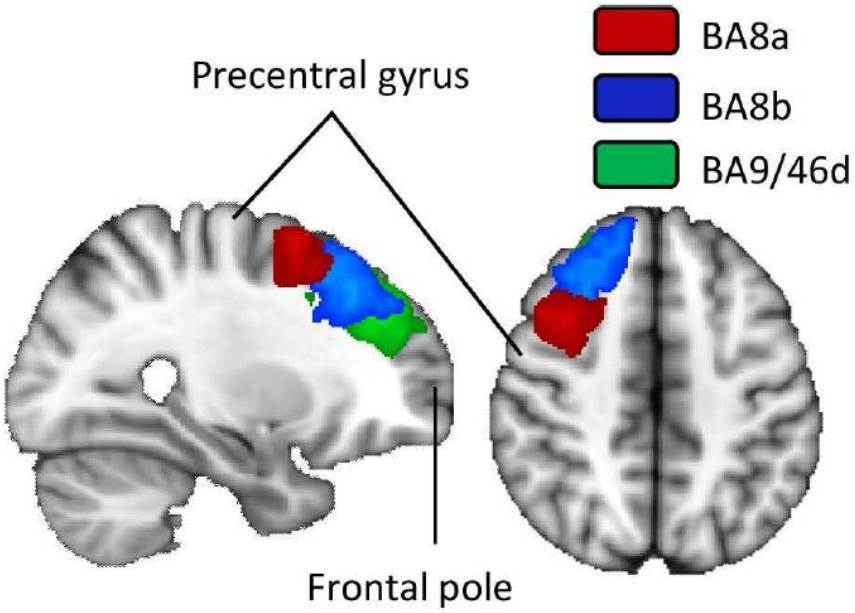

Figure 1.27. BAs 8, 9 and the dorsal part of BA 46 referred as the DLPFC in humans. The three clusters shown are consistent with the sub-regions of the DLPFC based on the tractography-based parcellation in Sallet et al. (2013) (Adapted from Figure 1 in Seminowicz and Moayedi (2017)).

The DLPFC is hypothesized to be involved in multiple cognitive processes such as working memory (Petrides, 2005), decision-making (Philiastides et al., 2011), emotion (Buhle et al., 2014) and visual attention (Amiez et al., 2006). Although not directly within the scope of the present work, activation of the DLPFC has been reported by neuroimaging techniques such as fMRI or PET after the deliverance of an acute nociceptive stimulus perceived as painful (Apkarian et al., 2005). Briefly, the DLPFC is usually included in the "medial pain system" thought to be involved in the affective and motivational aspects of pain processing (Treede et al., 1999). This region could be involved in the "pain modulatory pathways", for instance via top-

down influences on other brain regions such as the insula, the anterior cingulate cortex (ACC) and the thalamus (Nakamura et al., 2002; Brascher et al., 2016). The DLPFC is also thought to be a key region in the placebo analgesia, i.e. the expectation of pain relief (Krummenacher et al., 2010). Furthermore, this region shows structural and functional changes in various chronic pain conditions (Seminowicz and Moayedi, 2017). Therefore, as our aim was to study the changes in both the cortical excitability and functional connectivity of the DLPFC in CLBP patients, the following sections focus on structural and functional changes in the DLPFC in chronic pain.

6.1.2 Structural changes in the DLPFC associated with CLBP

Apkarian et al. (2004) were the first to report differences in brain morphometry of patients suffering from chronic pain (> 1 year) compared to matched healthy subjects. The whole-brain cortical gray matter volume was significantly lower in CLBP patients compared to matched controls (Figure 1.28). After correcting for age and gender, CLBP patients showed a decrease of gray matter volume of 11% compared to controls. This decreased volume was significantly correlated with pain duration, at least for CLBP of neuropathic origin (Figure 1.28). Using voxel-based morphometry, they found a decrease of regional gray matter density mainly in both the left and right DLPFC and in a lesser extent in the right anterior thalamus (Figure 1.28). Pain characteristics, such as the pain duration/intensity and the negative-affective dimensions associated to CLBP, as evaluated by the McGill pain questionnaire, were strongly related to the DLPFC structural changes while minimal relationships were found for anxiety and depression, evaluated by

the Beck questionnaire. This led the authors to suggest that the changes they observed could be involved in the pathophysiology of chronic pain, possibly via alterations of descending controls (Apkarian et al., 2004).

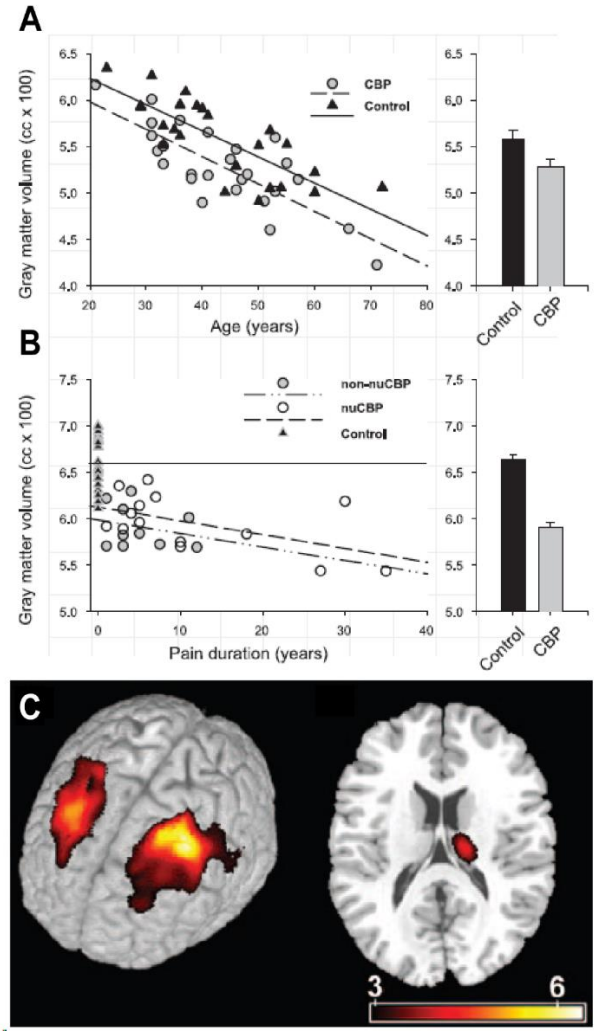

Figure 1.28. A. Gray matter volume as a function of age for CLBP patients and healthy controls. The average decrease in gray matter volume was more pronounced in CLBP patients compared to healthy matched controls (30 cm^3 difference corresponding to a 5.4% decrease). **B.** Gray matter volume as a

function of pain duration, after correcting for age and gender. The right parts of A and B show the group-level average ±SD of gray matter volumes before (A) and after (B) correcting for age and gender. **C.** The regional gray matter density decreases in CLBP patients in both the left and right DLPFC and in the right anterior thalamus. Color positive values show regions where the gray matter density was decreased in CLBP subjects compared to healthy controls (Adapted from Figures 1 and 2 in Apkarian et al. (2004)).

These results were partially replicated by Schmidt-Wilcke et al. (2006) who found a significant reduction of gray matter in the somatosensory cortex, the right DLPFC and the right temporal lobe. Furthermore, an enhancement of gray matter density was reported bilaterally in the putamen and in the left posterior thalamus. They suggested that this pattern of structural changes could contribute - in addition to peripheral and other central mechanisms - to the chronification of pain. This hypothesis was based on correlational analysis showing significant relationships between both the intensity and unpleasantness of pain (evaluated on the day of the imaging) and brain structural changes while no significant correlation was found with pain duration (Schmidt-Wilcke et al., 2006). Other studies reported a decrease of the thickeness of the gray matter in various brain regions such as the medial prefrontal cortex (mPFC), the bilateral operculo-insular cortex, the ACC, the amygdala and the posterior parietal cortex (Buckalew et al., 2008; Seminowicz et al., 2011; Ivo et al., 2013; Mao and Yang, 2015; Fritz et al., 2016). In CLBP patients, Seminowicz et al. (2011) found that, from all brain regions which show a reduction of the cortical thickness compared to controls, only the left DLPFC showed an increased cortical thickness six months after an efficient surgical intervention, i.e. in patients having lower

scores either on the McGill pain or on the Oswestry Disability index questionnaires. This recovery of the cortical thickness was independent of depression but was significantly correlated with the reduction of both pain intensity and pain-related disabilities. Similarly, activity in the left DLPFC elicited by an attention-demanding cognitive task was normalized after an efficient treatment. These observations suggest that structural and functional brain abnormalities in the DLPFC may be reversible after an efficient surgical treatment (Seminowicz et al., 2011). Note that, though some reports suggest that DLPFC structural changes could be lateralized to the right hemisphere (Seminowicz and Moayedi, 2017), consistent changes in the left (Seminowicz et al., 2011) and right DLPFC (Schmidt-Wilcke et al., 2006; Ivo et al., 2013) have been described. Apkarian et al. (2004) and Fritz et al. (2016) found structural modifications in both the left and right DLPFC. Furthermore, others reported an increased gray matter density in the DLPFC of CLBP patients (Ung et al., 2014). On the contrary, some studies did not observe any change either in the cortical thickness or in the whole brain volume (Dolman et al., 2014; Mansour et al., 2017). Several factors can explain, at least in part, these discrepancies. For instance, the small sample size of some studies, the inclusion of patients suffering of CLBP of various etiologies (e.g. neuropathic vs. non-neuropathic) as well as the severity of symptoms could play a role. Furthermore other confounding factors such as the medications (e.g. use of opioids or benzodiazepine), the age or other associated comorbidities such as depression have to be considered before making assumption on chronic pain-related changes (Dolman et al., 2014). For instance, by selecting a homogeneous sample including 14 patients

suffering from CLBP of discogenic origin without depression traits and medications such as benzodiazepines and opioids, Dolman et al. (2014) found a cortical thickening in the right DLPFC. However, this increased thickness was not significant when age was included as a covariate. Therefore, the heterogeneity of CLBP patients regarding their etiologies, their associated comorbidities or their drugs consumption highlights the importance of controlling for confounding factors, by selecting homogeneous samples for example. However, this approach will inevitably limit the generalizability of the results. Moreover, although contradicting results were reported, morphological alterations of the cortical gray matter have been reported in CLBP patients. At least some of the structural changes observed in the DLPFC could be a consequence of chronic pain and may participate to the chronification of pain. These modifications could add up to the long-term changes observed in chronic pain occurring at both the nociceptor and spinal levels and in the descending pathways (Woolf and Salter, 2000).

6.1.3 Functional changes in the DLPFC associated with CLBP

A few studies reported functional changes in the DLPFC associated to chronic pain. For instance, Seminowicz et al. (2011) observed that CLBP patients have abnormal activations in the left DLPFC during a cognitive demanding task compared to healthy controls. By using two arterial spin labeling sessions, Wasan et al. (2011) found that the exacerbation of the ongoing back pain in CLBP patients by clinical maneuvers was associated, *inter alia*, with an increased activity in the DLPFC. This was not observed in control

matched healthy subjects. Regarding the functional connectivity, though several studies investigated the brain connectivity in various chronic pain conditions, only a small number reported abnormal patterns of connectivity involving the DLPFC. However, by using the resting-state fMRI approach, abnormal activities have been observed in various networks, mainly in the default mode network (DMN) but also in regions corresponding to the so-called salience network (Figure 1.29; Kucyi and Davis (2015)). The DMN, including the mPFC, the posterior cingulate cortex (PCC), the medial and lateral parietal cortex and the medial temporal lobe, is typically more activated when subjects do not perform any engaging task, i.e. when subjects are at rest (Raichle et al., 2001). On the other hand, the salience/ventral attention network which includes the left and right DLPFC, the anterior insula, the temporoparietal junction and the mild cingulate cortex (Seeley et al., 2007; Kucyi et al., 2012) is consistent with regions involved in the detection of salient sensory events (Downar et al., 2002; Mouraux et al., 2011). Finally, the functional connectivity of brain regions which play a role in the descending modulation of the spinal nociceptive transmission - often called the antinociceptive system - and which include the PAG, the RVM and the mPFC, has also been investigated (Kucyi and Davis, 2015).

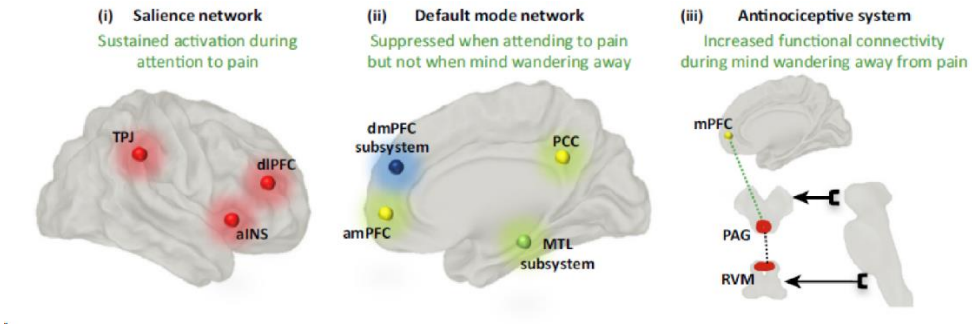

Figure 1.29. Schematic representation of the salience network, the DMN and the antinociceptive system network (Adapted from Figure 2 in Kucyi and Davis (2015)).

Aberrant activities in the DMN of CLBP patients have been observed in a number of studies (Baliki et al., 2008; Tagliazucchi et al., 2010; Baliki et al., 2011; Yu et al., 2014) and in other chronic pain conditions (Baliki et al., 2014). Baliki et al. (2008) were the first to observe that CLBP patients exhibited less deactivation in brain regions corresponding to the DMN while they performed a visual attention task. Loggia et al. (2013) showed that the DMN connectivity was stronger with the right insula, the pregenual part of the ACC and the left parietal lobule in CLBP patients compared to controls. A greater pain perception at the time of the scan was positively correlated with the DMN-right insula connectivity while a negative correlation was found for the DMN-mPFC (pregenual ACC) connectivity. Furthermore, an increased back pain induced by physical maneuvers was also associated with a greater connectivity of the insula (Loggia et al., 2013). Similar results were reported in the study of Baliki et al. (2014) in which patients suffering from chronic pain, in particular CLBP patients, exhibited both a decreased connectivity between the mPFC and the precuneus and an increased

connectivity between the mPFC and the insular cortices, bilaterally. They observed a decreased connectivity between the mPFC and other parts of the DMN; this reduction was inversely proportional to the increased connectivity with the insular cortex. Again, the strength of the mPFC-insula connectivity correlated positively with pain ratings. CLBP patients exhibited also a higher connectivity between the PAG and the left mPFC compared to healthy controls as well (Yu et al., 2014). Moreover, in the study of Baliki et al. (2014), alterations of oscillatory activities characterizing the BOLD signal in the DMN were also observed in chronic pain patients. Indeed, they observed an enhancement of the high-frequency activities (0.12-0.2 Hz)[2] in the mPFC. More importantly, by exploring the phase properties between the DMN and other brain regions, they found changes in phase-locking in patients (vs. controls) between the DMN and multiple brain regions including the DLPFC (Baliki et al., 2014). In failed back surgery syndrome (FBSS), while a reduction of the functional connectivity within the DMN was found, an increased functional connectivity with other brain regions including the right DLPFC has been reported (Kornelsen et al., 2013). After a spinal surgical intervention (vs. before), widespread changes in the functional connectivity of the left and right DLPFC were found with multiple regions such as the sensorimotor cortex, the cingulate areas and the insular cortex (Ceko et al., 2015). In other chronic conditions than CLBP, a reduced connectivity between the PAG and the DLPFC, the insular, the cingulate and

[2] Resting state connectivity is often studied in the slow ranges of frequencies observed in the BOLD signal (0.01-0.2 Hz). In their study, Baliki et al. defined three frequency bands: low (0.01-0.05 Hz), middle (0.05-0.12 Hz) and high (0.12-0.2 Hz).

prefrontal cortices was found in subjects developing cephalic or extracephalic allodynia during a migraine attack (Mainero et al., 2011). Alterations of the PCC-DLPFC connectivity have also been reported in these patients (Hubbard et al., 2014). In people suffering of fibromyalgia, Schmidt-Wilcke et al. (2014) explored the patterns of functional connectivity of multiple brain regions known to be involved in the descending pain modulatory system ("the antinociceptive system") including the PAG, ACC, DLPFC and the amygdala. Among other results, they found that, compared to placebo, the right DLPFC-left inferior parietal lobule functional connectivity at baseline could predict the treatment response to a serotonin–norepinephrine reuptake inhibitors (milnacipran).

Taking these observations into consideration, i.e. (1) the fact that the mPFC-DMN and mPFC-insula connectivity is significantly correlated with the individual pain perception at the time of the scan (Loggia et al., 2013; Baliki et al., 2014) and because (2) both the mPFC-PCC (precuneus) functional connectivity - enhanced in patients with temporomandibular disorders (vs. controls) - and the mPFC-PAG connectivity were significantly associated with pain rumination[3] in patients (Kucyi et al., 2014), it has been proposed that the mPFC could be a key point of pain-attention interactions in chronic pain patients (Figure 1.30; Kucyi and Davis (2015)).

[3] A form of sustained thoughts focused on pain.

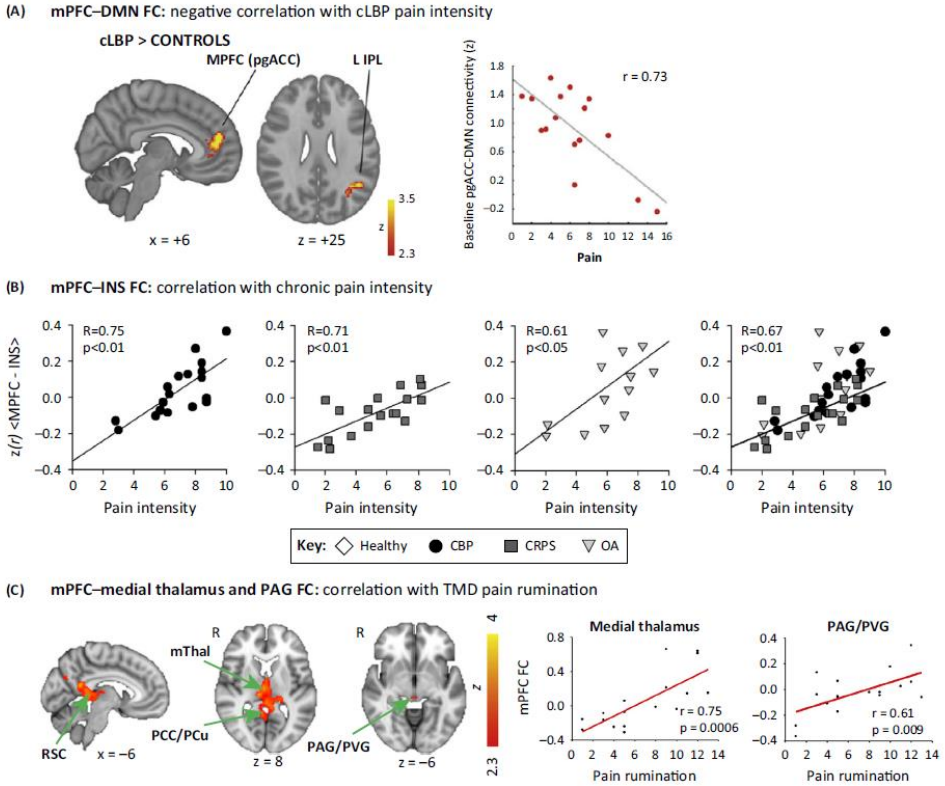

Figure 1.30. Relation of the mPFC connectivity with the DMN (A), the insular cortex (B) and the medial thalamus and PAG (C). **A.** Negative correlation between both the resting state connectivity of the mPFC and the DMN with pain intensity in CLBP patients. **B.** Positive correlation between the resting state connectivity of the mPFC and the insula with pain intensity in CLBP, CRPS and OA. **C.** Positive correlation between the resting state connectivity of the mPFC and regions of the DMN and antinociceptive system with pain rumination in temporomandibular disorder (Adapted from Figure 3 in Kucyi and Davis (2015)).

On the other hand, several studies showed that the activity in the mPFC is inversely proportional to that in the DLPFC (Mayberg et al., 1999; Northoff et al., 2000). In CLBP patients, Baliki et al. (2006) have exhibited a negative

correlation between the activity observed in the left and right DLPFC and the mPFC (Figure 1.31). In their study, they asked patients to continuously rate their spontaneous pain while they were in the scanner. The periods of time during which patients reported highly sustained pain resulted in an increased activity in the mPFC. The periods of time including the increasing phase of spontaneous pain were, in contrast, characterized by an activation of the insular cortex as well as of the S1-M1, S2 and ACC, i.e. brain regions often activated by brief noxious stimuli. At coordinates at which maximal structural changes were found in the DLPFC in their previous study (Apkarian et al., 2004), they found a negative correlation with the activity in the mPFC during periods of sustained spontaneous pain (Figure 1.31). In fact, when spontaneous pain was rated as high, the examination of the time course of the BOLD signal revealed that, though the activity in the DLPFC preceded that of the mPFC, this activity was suppressed for the period in which the mPFC showed a sustained signal, suggesting that both the mPFC and the DLPFC are able to inhibit each other. This led the authors to propose the hypothesis that the sustained activity recorded in the mPFC when the ongoing pain was high could be promoted by structural and/or functional changes in the DLPFC. Importantly, the correlational analysis performed in their study does not imply that the connectivity between both the mPFC and the DLPC are altered in CLBP patients given that the activity, inversely proportional, of both regions was studied during periods of high sustained pain in CLBP patients. Whether a similar relationship also exists in healthy volunteers, for instance during a sustained thermal stimuli, is unknown.

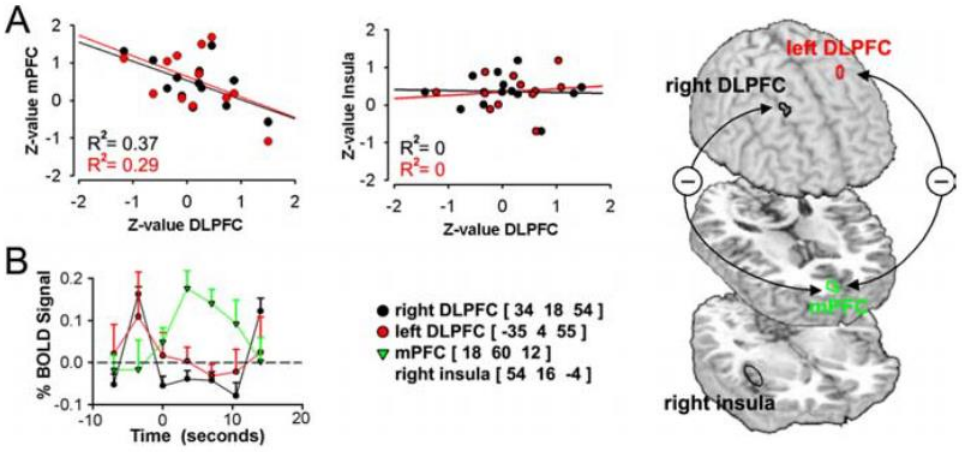

Figure 1.31. A. Inverse relationship between the activity in the mPFC and DLPFC when spontaneous pain was high (at coordinates of the peak atrophy observed in Apkarian et al. (2004)). This was not observed for the insula. **B.** Group-level ±SD of the BOLD responses in the left and right DLPFC and the mPFC. Note that in the DLPFC, the BOLD responses are characterized by an early and transient increase. A reduced activation was observed during the mPFC activation. The right part of the figure shows these correlations. These observations suggest that the mPFC and the DLPFC are able to inhibit each other (Adapted from Figure 4 in Baliki et al. (2006)).

Consequently, chronic pain seems to be associated to structural changes in various brain regions. Though contradicting results are reported in the literature, the DLPFC is one of the most frequent regions in which morphometric changes are reported. In addition, chronic pain-related alterations in the functional connectivity of various brain regions have been explored mainly by the resting state approach. Among others, the connectivity of the mPFC, the insular cortex or the PAG seems to differ in patients suffering from chronic pain. Particularly, the mPFC is thought to play a prominent role in the sustained attention to pain in chronic conditions

(Kucyi and Davis, 2015). On the other hand, despite the structural alterations often observed, reports of changes in the DLPFC functional connectivity are sparse in the literature for both CLBP/FBSS (Hashmi et al., 2012; Kornelsen et al., 2013; Baliki et al., 2014; Ceko et al., 2015) and other chronic pain states (Mainero et al., 2011; Hubbard et al., 2014; Schmidt-Wilcke et al., 2014). However, evidence suggests that the DLPFC and the mPFC inhibit each other and that structural changes in the DLPFC could, at least in part, promote the enhanced activity observed in the mPFC (Baliki et al., 2006). However, there are no strong evidence of alteration in the mPFC-DLPFC connectivity in chronic pain. Interestingly, studies delivering short-bursts of TMS over the DLPFC concomitantly to fMRI recordings observed a significant deactivation in the mPFC, opening the possibility to investigate the mPFC-DLPFC reciprocal connectivity by using concurrent TMS-fMRI (Li et al., 2004; Hanlon et al., 2016). Consequently, I developed an approach using concurrent TMS-fMRI to record BOLD responses elicited by TMS delivered over the DLPFC. Sections 6.3 and 6.4 of the present chapter are devoted to technical considerations about concurrent TMS-fMRI. An original approach to deliver TMS over the DLPFC during fMRI acquisition is presented in chapter 6.

6.2 TMS paradigms for studying the effective connectivity - an overview

The study of the *structural connectivity* of the human brain refers to the investigation of the structural properties of white matter tracts underlying anatomical connections between brain regions (Paus, 2008). Although our

anatomical knowledge of the structural connections between brain structures provides valuable insights about neural connectivity, this does not allow to study how the information flows between different brain regions and how this flow is dependent of the functional state of a given network (Paus, 2008). Several neuroimaging techniques can be used to explore *functional connectivity* such as EEG, fMRI or PET (Friston et al., 1993; Biswal et al., 1995). Functional connectivity can be defined as a temporal correlation or a covariation in brain activity recorded in spatially remote brain regions. This reflects direct and/or indirect functional relationships among these regions (Friston et al., 1993; Paus, 2008). For instance, studies investigating resting-state connectivity, which is the most popular of the correlational techniques to probe functional connectivity, identified several brain regions in which synchronous spontaneous fluctuations in the BOLD signal are observed. Resting state studies do not require an external stimulus, the subjects are at rest into the scanner bed without performing any experimental task (Biswal et al., 1995; Raichle, 2015). Interestingly, the regions that are similarly co-activated during a given task (such as a visual, auditory or motor task) tend to have coherent spontaneous BOLD signal fluctuations at rest while spontaneous activities of brain regions which show opposite functionality are anticorrelated (Fox and Raichle, 2007). By using resting state connectivity, several sets of brain regions showing a coherent activation have been found. For instance, visual (Lowe et al., 1998; Cordes et al., 2000), auditory (Cordes et al., 2000), somato-motor (Biswal et al., 1995), dorsal/ventral attention (Fox et al., 2006), memory (Vincent et al., 2006) and default mode (Raichle, 2015) networks have been described by

resting state analyses. The study of spontaneous BOLD activity at rest is one of the main technique used to study functional connectivity and has several advantages such as a high SNR and a high patient compliance leading to the possibility to study a large cohort of patients suffering from neurologic or psychiatric disorders (Fox et al., 2012). However, the resting state analysis is based on the level of co-activation of various connected brain regions over time. There is no information on both the causality and the direction of the effect of a given structure to another distant structure (i.e. *effective connectivity*).

On the other hand, the brain connectivity can be explored by TMS (Hampson and Hoffman, 2010; Hallett et al., 2017). *Per se*, MEPs elicited by a single TMS pulse delivered on M1 represent a connectivity measure of the motor system. Indeed, the efferent volley has to cross through a polysynaptic pathway to induce a contraction of the contralateral muscle (Paus, 2008; Fox et al., 2012). Moreover, the connectivity between distant brain regions can be inferred using single TMS pulse paradigms. For instance, an enhancement of MEPs amplitude recorded from hand muscles contralateral to the dominant hemisphere has been observed as the subjects were reading aloud (Tokimura et al., 1996; Seyal et al., 1999; Meister et al., 2003), suggesting a functional connectivity between the hand representation of M1 and the language areas. Similarly, the modulation of MEPs by brief non-nociceptive and nociceptive stimulations of the skin in both healthy subjects and patients with neurological disorders can be used to infer on the functional interplay between distinct brain networks (Chen et al., 1999; Valeriani et al., 1999; Abbruzzese et al., 2001; Sailer et al., 2003; Algoet et al., 2018).

However, although providing significant insights into the temporal profile and/or the specificity of the changes evoked in the motor system, these studies give indirect evidence about the cortical interactions underlying the observed effects. Again, insights about causal effects exerted by one given region to another one is speculative and based on *a priori* knowledge of the structural and/or functional connections between brain networks. By using TMS, effective connectivity studies have been conducted on interhemispheric interactions between both the left and right M1. For instance, a single pulse delivered on the ipsilateral M1 relative to a tonic voluntary contraction of an upper limb muscle can induce a short-lasting suppression of the EMG response. This ipsilateral silent period is thought to represent transcallosal interactions between the left and right M1 given that its latency is 12-15 ms longer than that of the MEPs recorded from the contralateral limb (Ferbert et al., 1992). Furthermore, this silent period is altered in patients with lesions of the trunk of the *corpus callosum*, in particular in its posterior half (Meyer et al., 1995; Meyer et al., 1998). On the other hand, this silent period is not observed in children <5years in which transcallosal fibers do not yet reach their maturation (Heinen et al., 1998). Taking these observations in consideration, the ipsilateral silent period has been used to assess the alterations in the interhemispheric functional/effective connectivity in neurodegenerative disorders such as corticobasal degeneration (Trompetto et al., 2003) or multiple sclerosis (Schmierer et al., 2000).

A more direct approach to explore effective connectivity between anatomically remote regions in the human brain is the paired-pulse TMS

paradigms (Hallett et al., 2017). Indeed, by varying ISIs in paired-pulse paradigms - in which the conditioning and the test stimuli are delivered on a given brain region of interest and on M1, respectively - it is possible to characterize the effects of the first stimulus on the motor system. Ferbert et al. (1992) were the first to investigate the interhemispheric cortico-cortical interactions by using TMS delivered on both the left and right M1 (Figure 1.32). Several ISIs were tested, ranging from 3 to 25 ms. When the TMS pulses were delivered at the same intensity, a suppression of the MEPs elicited by the second TMS pulse was observed with a minimum ISI of 6-7 ms. The inhibitory effect of the conditioning TMS pulse on the test MEP was attributed to interhemispheric cortico-cortical interactions operating via transcallosal connections and was termed IHI. Indeed, by using epidural recordings, it has been shown that the descending cortico-spinal volleys (the I2- and I3-waves) elicited by the second stimulus were decreased by the conditioning stimulus (Di Lazzaro et al., 1999). Moreover, the IHI was normal in patients with a subcortical stroke sparing the transcallosal motor fibers but destroying the cortico-spinal tract (Boroojerdi et al., 1996). Similarly, by adapting both the current direction in the coil and the ISI between the conditioning and the test pulses, facilitatory interactions between the left and right M1 have also been reported (Ugawa et al., 1993; Hanajima et al., 2001).

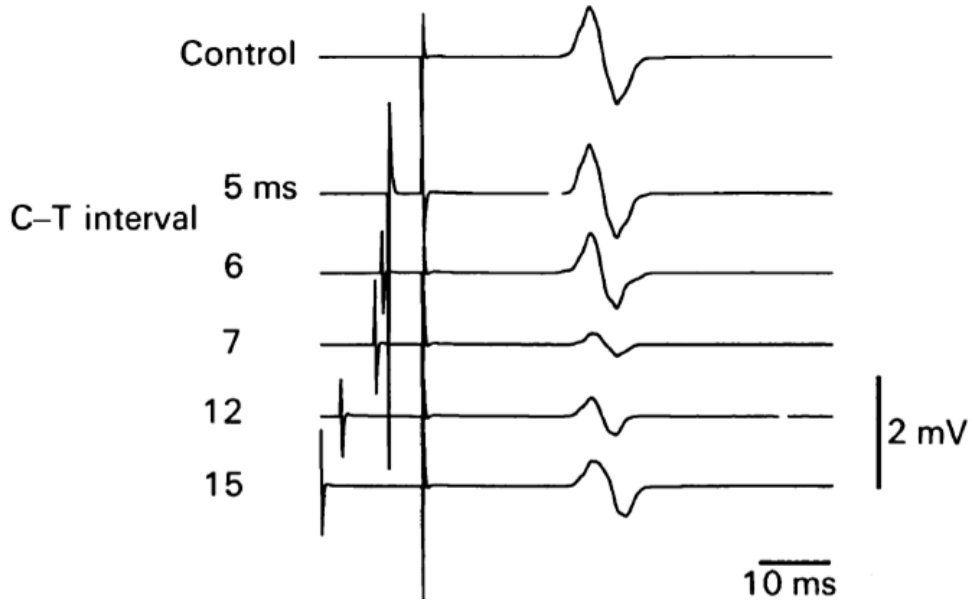

Figure 1.32. IHI. The effect of a conditioning TMS pulse delivered over the left M1 on MEPs recorded in the left FDI produced by a second TMS pulse delivered on the right M1. ISIs of 5, 6, 7, 12 and 15 ms are shown (Adapted from Figure 1 in Ferbert et al. (1992)).

Though fundamental in order to study interhemispheric interactions that precede or that are concomitant to a voluntary movement in both healthy volunteers (Murase et al., 2004) and patients with deficits in motor control (Murase et al., 2004; Duque et al., 2005), this dual TMS paradigm was initially limited to the interhemispheric interactions between the left and right M1. Later, a number of studies used paired-pulse paradigms to study interhemispheric interactions between primary and non-primary motor regions. For instance, both interhemispheric facilitations and inhibitions have been observed between M1 and the dorsal/ventral premotor cortex (Mochizuki et al., 2004; Baumer et al., 2006; Koch et al., 2006; Fiori et al.,

2017), the posterior parietal cortex (Koch et al., 2009), the DLPFC, S1, and the supplementary motor area (SMA) (Ni et al., 2009; Iwata Y. et al., 2016; Fiori et al., 2017). Similarly, cerebro-cerebellar interactions have also been assessed by applying electrical or magnetic stimulations on a cerebellar hemisphere 5-6 ms before a test magnetic pulse delivered on M1. Again, it has been shown that the conditioning cerebellar stimulation could modulate the excitability of the contralateral M1 (Ugawa et al., 1991; Saito et al., 1995; Ugawa et al., 1995; Pinto and Chen, 2001; Iwata et al., 2004). The study of ataxic patients with lesions located either in one cerebellar hemisphere (Di Lazzaro et al., 1994) or in cerebellar efferent pathways (Ugawa et al., 1994; Ugawa et al., 1997) suggests that this modulation could be mediated by inputs from Purkinje cells via the dentate-thalamo-cortical pathway projecting to M1 (Iwata and Ugawa, 2005). Finally, paired-pulse paradigms can also be used to explore intrahemispheric connections from various brain regions to M1. Indeed, the functional connectivity between M1 and several ipsilateral brain regions such as the premotor cortex (Civardi et al., 2001; Cattaneo and Barchiesi, 2011), the parietal cortex (Koch et al., 2007; Cattaneo and Barchiesi, 2011; Karabanov et al., 2013), the DLPFC (Hasan et al., 2013) and the pre-SMA (Civardi et al., 2001; Fiori et al., 2016) have been studied.

Whether or not the dual TMS protocol is used to study inter-, intra- or cerebello-cortical interactions, the effect of the conditioning stimulus on the test response has been used to examine the state-dependent changes of the functional connectivity between a given brain region and M1, for instance relative to the current or upcoming motor context (Pinto and Chen, 2001;

Koch et al., 2006; Davare et al., 2008; Koch et al., 2008; Davare et al., 2009). Although some studies, using a triple TMS coils approach, investigated the functional interplay between non-primary motor areas during or before a given motor task (Davare et al., 2010; Koch et al., 2010; Shields et al., 2016), most studies that have investigated functional connectivity using paired-pulse TMS focused on the motor or visual (e.g. Silvanto et al. (2006)) systems in which an overt response can be observed. Moreover, the connectivity between deep brain structures is difficult to investigate with dual paradigms, because the TMS coils which are designed to reach deeper regions - such as the double-cone coil - stimulate large area of both superficial and deep cortices (Deng et al., 2014).

6.3 Combining TMS with functional neuroimaging techniques

Another approach to investigate the human brain connectivity is to combine TMS with online functional neuroimaging techniques (Figure 1.33) such as EEG (Ilmoniemi et al., 1997), PET (Fox P. et al., 1997; Paus et al., 1997) or fMRI (Bohning et al., 1997).

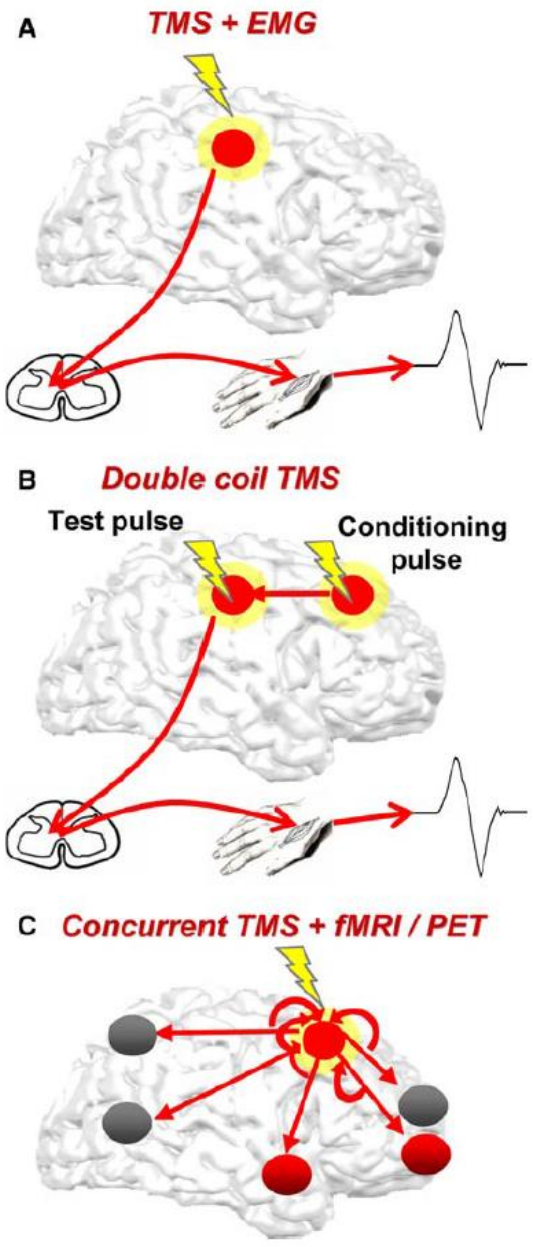

Figure 1.33. TMS as a tool to probe effective connectivity in the central nervous system. **A.** The recording of MEPs after delivering single pulses of TMS on M1 represents a measure of the connectivity across the motor system. **B.** Paired-pulse paradigms are able to test whether the stimulation of a given cortical target may exert a causal influence on M1. This is quantified by MEPs recorded in contralateral muscles. Note that, thanks to the high temporal resolution of TMS, this procedure enables the study of the time-course of such causal interactions. **C.** The concomitant use of TMS and functional neuroimaging techniques opens the possibility to characterize the impact of a stimulation delivered to a given brain region on a multitude of cortical (red circles) and subcortical (grey circles) sites, for many potential targets other than M1 (Adapted from Figure 1 in Bestmann et al. (2008c)).

Chapter 6 of this work is dedicated to a procedure I developed to combine online TMS with fMRI. Our specific aim was to validate the recording of BOLD responses elicited by TMS over the DLPFC. Therefore, the two following sections (sections 6.4 and 6.5) focus on MR signal generation, image formation and TMS-fMRI combination. The combination of these two techniques allows the recording of the brain activity at the stimulated site as well as in distant interconnected regions (Figure 1.33). Usually, short bursts of TMS pulses are delivered to facilitate the detection of the BOLD signal (Bergmann et al., 2016). This online approach can be used to quantify both the excitability of the stimulated brain region and its functional/effective connectivity with distinct anatomical regions (Bergmann et al., 2016). The target site is used as an "entry point" to assess the connectivity of a given brain network. Importantly, remote activations elicited by short bursts of TMS can be explained by two distinct phenomena. First, the direct propagation of the impulses generated at the target via axonal propagation can induce a transsynaptic activation of remote neurons populations similarly to the motor responses investigated by single and paired-pulse paradigms. Secondly, short bursts of TMS delivered at one point of a given network also interfere with the ongoing neural activity at this specific target, which could trigger an indirect perturbation of distant zones not directly connected (Siebner et al., 2009b). This can be explained either by compensatory mechanisms triggered by the changes in activity at the stimulated point or via a polysynaptic propagation of the nerve impulse. Therefore, the so-called "perturb and measure" approach (Paus, 2005), in which short bursts of TMS are delivered during an fMRI acquisition can be

used to (1) interfere with the ongoing neuronal activity at the target site and to (2) measure its immediate impact on the whole brain activity (Bergmann et al., 2016) allowing to visualize a given network via its response to a TMS pulse.

The changes in network activity observed by combining single pulses or short bursts of TMS with neuroimaging techniques are probably not due to long-term plasticity changes, contrary to those evoked by offline repetitive TMS (Bestmann and Feredoes, 2013). Indeed, concurrent TMS-EEG studies showed that the activity elicited by both single pulses (Komssi et al., 2002; Bonato et al., 2006) and short bursts of TMS (Taylor et al., 2007a; 2007b) at the target propagates rapidly (a few tenths of a millisecond) towards distant brain regions. Moreover, the spread of this activity is dose-dependent when both TMS-evoked BOLD signals (Bohning et al., 1999; Hanakawa et al., 2009) or TMS-evoked potentials (Komssi et al., 2004) are recorded in remote regions. Therefore, by using the so-called “perturb and measure” approach (Paus, 2005), short bursts of TMS delivered during an fMRI acquisition can be used to (1) interfere with the ongoing neuronal activity at the target site and (2) measure its immediate impact on the whole brain activity (Bergmann et al., 2016). The hemodynamic changes in network activity triggered by short bursts of TMS thus reflect a spread of this activity in remote anatomical interconnected brain regions and can be used to study the brain connectivity.

6.4 MRI scanners and basic principles of both MR signal generation and image formation

The goal of this section is to provide a general overview of how a MRI scanner works. This is also an introduction on the basic principles of both MR signal generation and image formation. Although beyond the scope of the present work, basic knowledge on this topic is necessary for a comprehensive approach of the following section dedicated to concurrent TMS-fMRI. For more advanced discussion, lectors are invited to consult textbooks such as *Functional Magnetic Resonance Imaging*, third edition (Huettel et al., 2014) and websites such as *MRIquestions.com* of Allen D. Elster (http://mriquestions.com/index.html). Note that the present section is consistently inspired from these two supports.

MRI scanners are characterized by three main components. The first component is the main static magnetic field described in section 6.4.1. Secondly, radiofrequency (RF) coils generate and receive electromagnetic fields of the atomic nuclei placed inside the main static magnetic field. This process will be presented in section 6.4.2. Finally, MRI scanners contain gradient coils generating spatial gradients along the z-, x- and y- directions of the main static magnetic field. This represents the final step for image formation, a process presented in section 6.4.3.

6.4.1 The main static magnetic field and its effect on atomic nuclei

The main static magnetic field, termed B_0, provides the “magnetic” term in MRI. This strong magnetic field is used to align certain nuclei, most often

hydrogen given its abundance in the human body. Importantly, the B_0 magnetic field has to be as homogeneous as possible to avoid that the signal measured from a given part of the object being scanned depends on its location within the magnetic field. Most MRI scanners used a solenoid to elicit a uniform magnetic field (Figure 1.34).

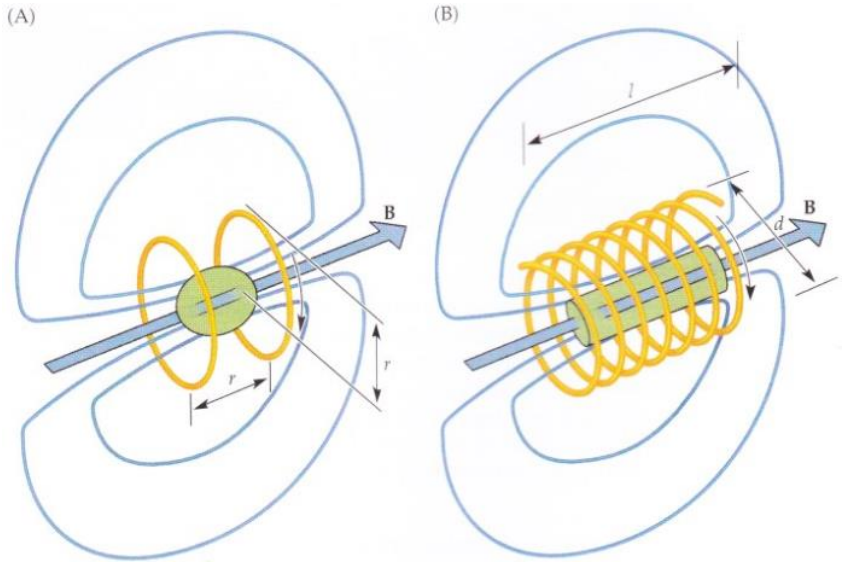

Figure 1.34. Generation of the B_0 field in MRI scanners. The left part of this figure **(A)** depicts a Helmholtz pair which is a pair of circular wire loops of identical size separated by a distance equal to their radius. An identical current is carried by the two loops. The right part of the figure **(B)** shows a solenoid, a design used by most MRI scanners to elicit a strong and homogenous magnetic field. A solenoid is characterized by a winding of wires around a cylindrical frame. If the length (*l*) of the solenoid is high enough compared to its cross-sectional diameter (*d*), the resulting magnetic field can be highly homogenous at the center of the solenoid. In MRI scanners, the density of wires and the electrical current are optimized to generate a homogeneous static magnetic field. The green surfaces in the

figure indicate the area of maximum uniformity (Adapted from Figure 2.3 in Huettel et al. (2014)).

Another characteristic of the static magnetic field is its field strength, usually between 1.5 and 3 Tesla. This large magnetic field can be achieved by using superconducting electromagnets cooled by helium liquid to a temperature near the absolute zero. By doing that, the resistance in the wires disappears. A proton of hydrogen is characterized by an intrinsic property called *spin*. The spin motion can be viewed as a rotating movement of protons on their axes (Figure 1.35A).

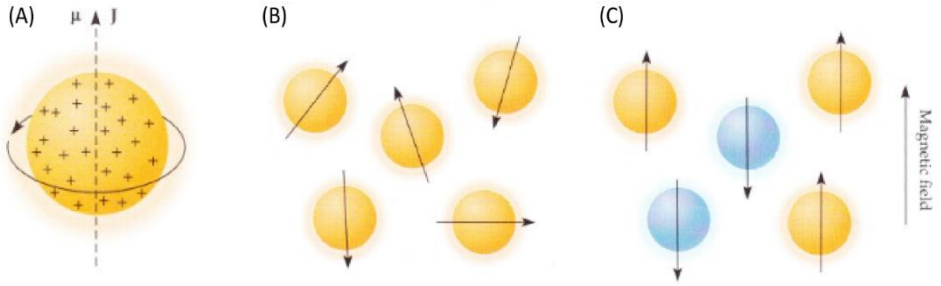

Figure 1.35. (A) A single proton of hydrogen possesses a spin. Protons are spinning on their axes. This rotational motion has two consequences. First, protons are a magnetic source as they carry a positive charge which generates an electrical current on their surface. Therefore, a torque is generated when protons are placed in an external magnetic field such as in MRI scanners. This torque is called magnetic moment *(μ)*. In addition, the spin of the protons results in an angular momentum *(J)* due to its odd-numbered atomic mass. **(B)** In the absence of external magnetic fields, the spin axes will be aligned randomly. They therefore cancel each other resulting in a net magnetization infinitesimally small. **(C)** Inside an external magnetic field, the spin axis of each proton will be aligned either in the parallel (low energy; orange) or antiparallel (high energy; blue) states. A greater proportion of the spin is in the parallel state resulting in a net

magnetization parallel to the B_0 magnetic field (Adapted from Figures 3.2 and 3.3 in Huettel et al. (2014)).

Because protons consist of a positive charge in motion, their spins create an electrical current on their surface, thus generating both a magnetic source and a rotational force (a torque) when placed inside an external magnetic field (Figure 1.35). The strength of this magnetic source is described by the *magnetic moment (μ)* which is the torque exerted on a moving electrical charge when placed in a magnetic field. Furthermore, because hydrogen has an odd-numbered atomic mass, its spin motion provokes an *angular momentum (J)*. Both the magnetic moment and the angular momentum can be represented by a vector pointing in the same direction. To possess nuclear magnetic resonance property, atomic nuclei have to possess both a magnetic moment and an angular momentum. Indeed, if the number of protons is equal to the number of neutrons, the magnetic moment will be cancelled. In the absence of an external magnetic field, the spin axes of each proton are oriented randomly and thus cancel each other (Figure 1.35B). In this condition, the sum of the totalty of magnetic moments, termed *net magnetization (M)* is near zero. When placed within a strong external magnetic field such as the main static magnetic field generated by MRI scanners (B_0), each spin axes will be aligned to the magnetic field in a parallel or antiparallel state (Figure 1.35C). More precisely, the spinning protons will initiate a gyroscopic motion termed *precession* (Figure 1.36A). This motion can be viewed as if protons precess around an axis parallel to the main magnetic field. The precession frequency depends on the type atomic

nucleus and is therefore the same for all protons placed in the same external magnetic field. This frequency is termed the Larmor frequency.

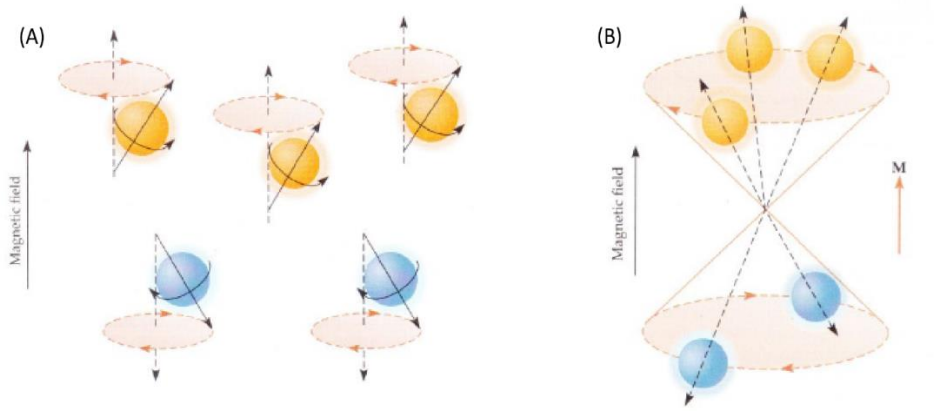

Figure 1.36. (A) When placed inside an external magnetic field such as the B_0 field, protons initiate a gyroscopic motion in which the axis of the spin rotates around a central axis. All protons precess at the same frequency when placed in the same magnetic field. This is the Larmor frequency which determines the frequency of electromagnetic radiation needed during the excitation process. **(B)** In a spin system, the net magnetization *(M)* is determined by the proportion of spins in the parallel (orange) vs. antiparallel (blue) states (Adapted from Figures 3.6 and 3.8 in Huettel et al. (2014)).

There are two states for protons which are precessing, one parallel state which is the low energy state in which the spin precesses around an axis parallel to the main magnetic field. Protons that precesses in the antiparallel state have a higher energy than protons in the parallel state. Because the low energy state is more stable, there are always more protons in the parallel state in the absence of energy delivered from an external source. The rapport of protons in the parallel and antiparallel states depends on both the temperature and the strength of the magnetic field. The difference in energy between the two states corresponds to the energy possessed by

an electromagnetic wave delivered at the Larmor frequency. Importantly, MR techniques measure the net magnetization of all nuclei in a given volume. As for the magnetic moment of a single proton, the net magnetization of a spin system can be viewed as a vector with two components: (1) a longitudinal component that is parallel or antiparallel to the B_0 field and (2) a transverse component perpendicular to the main magnetic field. It is admitted that, given the great number of spins in a given volume, the transverse components cancel each other. This results in the absence of a net magnetization perpendicular to the B_0 field. Therefore, the net magnetization is a vector oriented in the longitudinal direction with an amplitude proportional to the number of spins in the parallel or antiparallel states (Figure 1.36B). Note that the net magnetization precesses at the same frequency that individual spin, i.e. at the Larmor frequency. By increasing the strength of the main static magnetic field, it is possible to increase the proportion of parallel spins leading to an enhancement of the net magnetization. Therefore, by placing the human body in a very strong static magnetic field, it is possible to increase the net magnetization of the sample to be imaged. The net magnetization of a spin system represents the fundamental basis to generate a MR signal. However, the net magnetization cannot be measured in equilibrium conditions. The general idea is to perturb the equilibrium state of the spins and then observe the reaction of the spin system to this perturbation. This can be achieved by a process called *excitation* in which electromagnetic energy is send to the imaged sample at the resonant frequency by using radiofrequency coils. The excitation process will be discussed in the following section.

6.4.2 RF coils and the excitation process

MRI scanners contain RF coils that generate and receive electromagnetic fields that resonate at a particular frequency (the Larmor frequency) depending of the atomic nucleus of interest located within the main static magnetic field. This particular resonant frequency is dependent of the strength of the main static magnetic field. RF coils are needed to produce MR signals and give the "resonance" term in MRI. Most atomic nuclei of interest in MRI, e.g. hydrogen, have resonant frequencies in the RF portion of the electromagnetic spectrum when protons are placed in a magnetic field with a strength corresponding to that used in a MRI scanner. This process is termed *excitation*. When excited, atomic nuclei such as hydrogen absorb the energy of the RF pulse. When the RF pulse is switched off, the release of this energy by protons allows a return to the equilibrium state. The energy which is released can be detected by the same RF coils in a process termed *reception*. This energy detected by the RF coils constitutes the MR signal. In MRI, the RF coils are placed closed to the object which is imaged. Surface coils, volumes coils or phased array coils can be used as RF coils. Surface coils are placed directly on the object to be imaged. Their circuits consist on a single loop inductor-capacitor in which the rapid discharge of electricity between both the inductor and the capacitor induces an oscillating current that can be adapted to the frequency of interest. Because surface coils are closed to the imaged sample, they provide a high imaging sensitivity and are therefore used in fMRI studies aiming to investigate one particular brain target. However, they provide a poor coverage of the brain. Therefore, brain regions located far from the surface

coil contribute less to the MR signal than regions located closer to the coil. Volume coils are composed of the same single loop inductor-capacitor circuit than surface coils. However, this circuit is replicated around a cylindrical surface. Though such a coil provides a uniform coverage of the entire brain, volume coils are placed further from the head and are therefore less sensitive to the MR signal. Phased array coils are a mix of both surface and volume coils. Such a coil uses a volume coil for the excitation process and a set of surface coils for the reception of the MR signal. This allows to increase the spatial coverage without affecting the sensitivity.

RF coils bombard spins in the B_0 field with electromagnetic waves that oscillate at the resonant frequency of a given nucleus, in this case hydrogen. The deliverance of this energy, which is equivalent to the energy difference between the parallel and antiparallel states of the spins, favors the transition from the low to high energy spin states (Figure 1.37B). The amount of electromagnetic energy needed to generate an equal number of hydrogen nuclei in the two states is known as the 90° excitation pulse. This is equivalent to tipping the net magnetization from the longitudinal to the transverse plane. The excitation process is stopped when the RF pulse is turned off. Then, the spin system tends to return to the equilibrium state. The excess of spins at the high energy level will fall back to the low energy level so that the equilibrium state can be restored (Figure 1.37C). This transition from high to low energy state is accompanied by the emission of electromagnetic waves which contain a quantity of energy equal to the energy difference between the two states. The process of measuring electromagnetic energy emitted by a sample via a receiver coil is known as

reception. Given that the frequencies of both excitation and reception are the same, identical RF coils can be used for the two processes. The induced current in the RF coils during the reception process constitutes the MR signal.

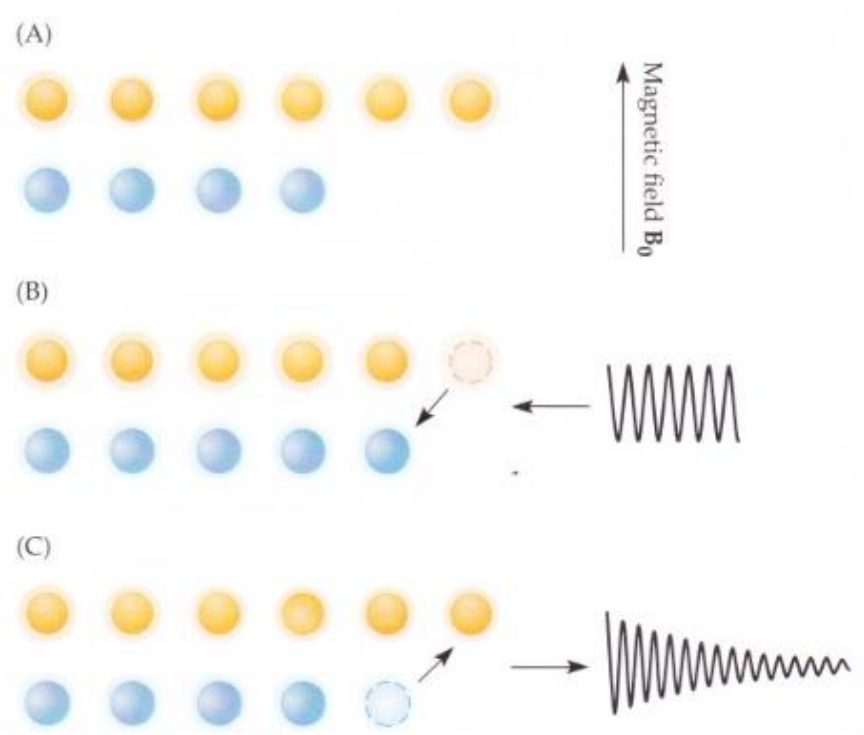

Figure 1.37. (A) When placed in an external magnetic field, more spins are at the low energy (orange) than at the high energy state (blue). **(B)** When an excitation pulse is delivered with the correct amount of energy, some of the spins absorb its energy and switch towards the high-energy state. **(C)** When the excitation pulse is turned off, some of the high energy spins release this energy in the form of a RF wave to return in the low energy state. This RF wave has the same frequency than the excitation pulse. The amount of the released energy decreases over time (Adapted from Figure 3.10 in Huettel et al. (2014)).

This MR signal does not stay stable for long. Indeed, it changes according two mechanisms during the reception process. First the transverse magnetization rapidly loses coherence (Figure 1.38A). Second, the longitudinal magnetization progressively recovers (Figure 1.38B). This change in net magnetization over time, and the resulting changes in MR signal, are termed *relaxation*. The transverse relaxation refers to the decay of transverse magnetization while the longitudinal relaxation consists on the longitudinal recovery (Figure 1.38A and B). Given that the net magnetization is the vector sum of all the individual spins, its magnitude is higher when spins precess at both the same phase and frequency. However, spins loss coherence over time due to spatial interactions between spins close to each other. This difference in the frequency of precession induces a loss of phase which leads to an exponential decay in the MR signal described by a time constant termed T2. T2 is therefore a time constant characterizing the decay of the transverse magnetization caused by the accumulated phase difference. The T2* decay also takes in consideration the effect of spatial inhomogeneities in the static magnetic field, which will cause some nuclei to precess at different frequencies than others. As the spin system loses energy in the form of radiofrequency waves detected by receiver coils, the system returns progressively towards an identical state as it was before the excitation process, i.e. with the net magnetization along the longitudinal axis (Figure 1.38B). This longitudinal recovery, relatively short (a few milliseconds to a few seconds), is described by the time constant T1.

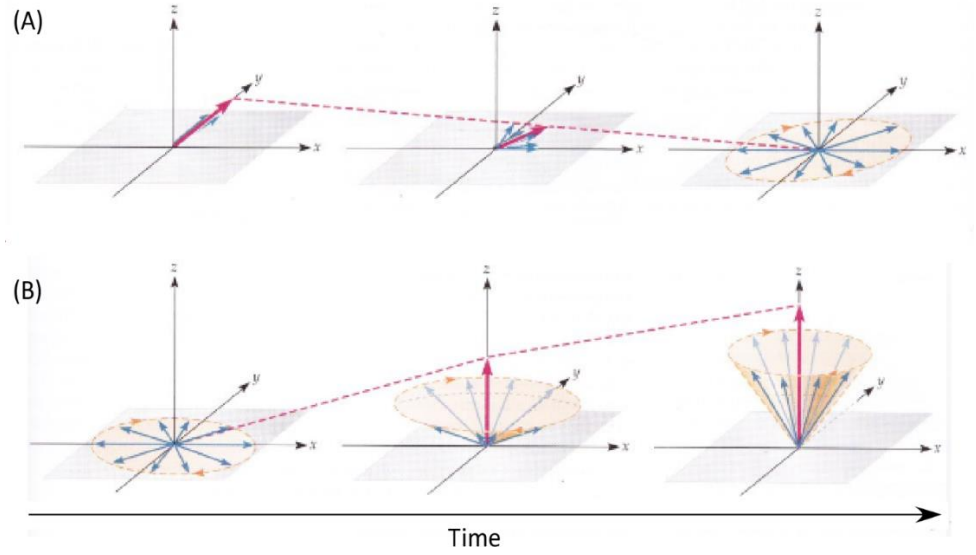

Figure 1.38. (A) Conceptual representation of the T2 decay. After being tipped in the transverse plane by the RF excitation pulse, the net magnetization in the transverse plane rapidly decays due to the loss of phase coherence of the spins. The net magnetization which participates in the MR signal reaches zero within a few milliseconds. **(B**) Conceptual representation of the T1 recovery. When the excitation pulse is turned off, the spins release the energy back. This leads to the recovering of the net magnetization along the longitudinal axis. This return to the equilibrium state takes a few seconds (Adapted from Figure 3.11 and 3.12 in Huettel et al. (2014)).

6.4.3 Gradient coils and MR image formation

The process of image formation requires the alteration of the main static magnetic field over space in a predictable manner by using gradient coils. This gives the "imaging" term in MRI. Indeed, the current detected in the RF coils during the reception process, i.e. the raw MR signal, does not possess any spatial information and is thus insufficient to obtain an image. Gradients coils allow to generate a magnetic gradient superimposed on the main

magnetic field. By doing that, the MR signal becomes spatially dependent in a predictable manner. Indeed, different locations in space will contribute differentially to the MR signal over time. Three gradients coils are used to modify the strength of the main magnetic field along the z-, x- and y-directions relative to the static magnetic field. The z-axis represents the direction parallel to the main magnetic field, the x- and y-directions are perpendicular to the main field and to each other. The coil arrangements to create the spatial gradients are depicted on Figure 1.39.

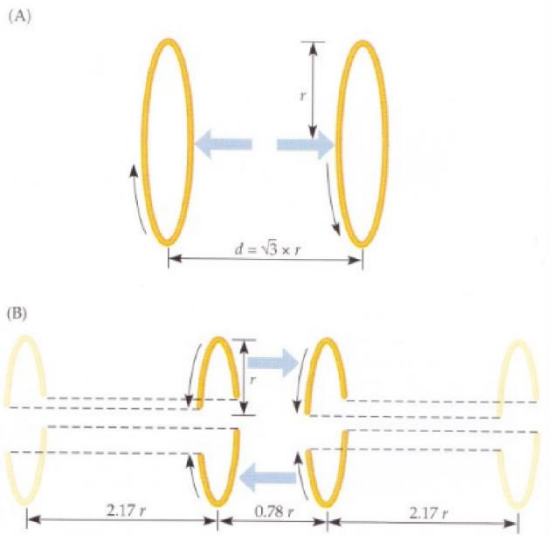

Figure 1.39. (A) Coils arrangement for generating spatial gradients. A pair of loops with opposite currents, known as a Maxwell pair, is used to generate magnetic field gradients along the z-direction (along the main magnetic field). **(B)** The Golay pair used to generate magnetic field gradients along the x- and y-directions, perpendicular to the main magnetic field (Adapted from Figure 2.6 in Huettel et al. (2014)).

Importantly, the transverse gradients (Gx and Gy) do not produce smaller magnetic fields along the x- or y-directions but instead, they change the strength of the main static magnetic field along the z-direction (Figure 1.40).

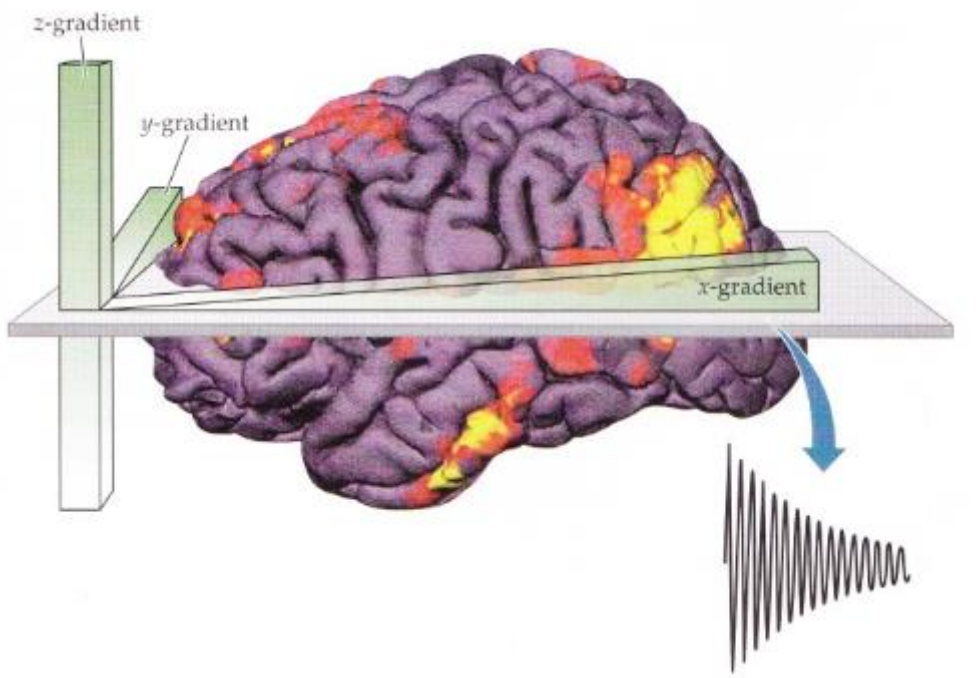

Figure 1.40. Transverse gradients (Gx and Gy) do not produce smaller magnetic fields along the x- or y-directions. They introduce a spatial gradient which changes the strength of the main static magnetic field along the z-direction (Adapted from Figure 4.8 in Huettel et al. (2014)).

A large number of MRI scanners construct the 3D-image of the brain by using a set of 2D-slices, therefore restricting the MR signal to one 2D-slice at a time in a process called *slice selection*. This step requires, in addition to spatial magnetic field gradients, the use of a RF pulse which excites spins within a given slice. Spins from other adjacent slices have to be excited as little as possible. Matching the precession frequency within the desired slice with

the frequency of the RF excitation pulse is the major step of this process (Figure 1.41). For instance, if a spatial gradient is applied along the z-direction (Gz) leading to a higher magnetic field towards the back of the scanner vs. at its front, then spins located at the front of the scanner will precess more slowly than those at the back. Therefore, in order to select a slice in the middle of the brain, the frequency of the RF excitation pulse has to match the precession frequency of the spins located in the middle slice (Figure 1.41). By doing that, the spins of the middle slice will be on resonance with the RF excitation pulse and will change from the low to high energy state by absorbing the energy of the RF excitation pulse. The MR signal will be emitted by the spins of this middle slice after the RF excitation pulse cessation. In practice, delivering a magnetic gradient such that spins within a given slice are excited without the participation of spins located in other adjacent slices is impossible. Indeed, the spatial gradient fields continuously alter the main magnetic field. Therefore, the RF excitation pulse contains a range of frequencies which will match with the frequency range of a band in the gradient field (Figure 1.41). The bandwidth of the RF excitation pulse can be adapted according to the desired slice thickness.

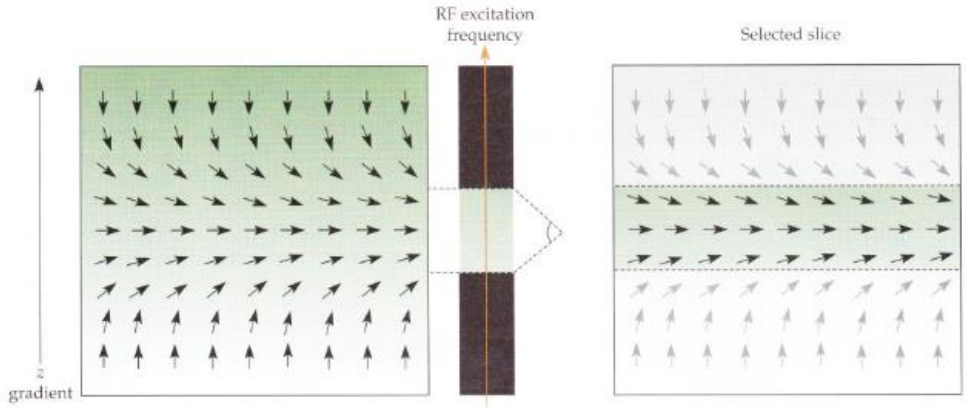

Figure 1.41. Schematic representation of the slice selection process. Before the RF excitation pulse, a spatial gradient is introduced along the z-direction leading to differences in the precession frequencies of spins along that gradient. The RF excitation pulse frequency has to be matched to the precession frequency of the spin located in the desired slice. Note that a RF pulse contains a band of frequencies (Adapted from Figure 4.3 in Huettel et al. (2014)).

Directly after the cessation of the RF excitation pulse, both T1 and T2 relaxation processes begin, leading to a decay of the MR signal. Therefore, the slice selection has to be immediately followed by other gradients which provides information about the spins within the slice of interest. The *pulse sequence* used to create an image is the pattern of RF pulse and magnetic gradients necessary for generating an MR image. The pulse sequence is usually depicted as a diagram composed of horizontal lines representing how a given component of the MR scanner changes over time (see Figure 1.50).

When the slice is selected, all protons excited within that slice similarly contribute to the MR signal. There is therefore no spatial information at this moment of the pulse sequence. Additional gradients, termed *frequency-*

encoding and *phase-encoding* gradients, are needed to make that spins at different spatial locations precess at different frequencies in a controlled manner. The frequency-encoding of a spatial position within a slice is achieved by using a magnetic field gradient called by convention Gx. This gradient distorts the B_0 magnetic field in a predictable manner. Therefore, the resonance frequency will change as a function of position within the slice (Figure 1.42). On the pulse sequence, the frequency-encoding gradient is usually indicated by Gx (Figure 1.50).

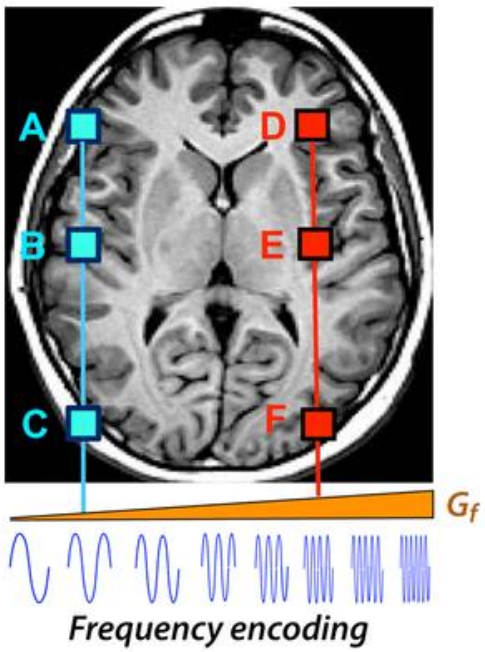

Figure 1.42. Encoding spatial localization within a slice by using a frequency-encoding gradient (Gf in the figure). The frequency-encoding gradient begins on the left of the image and increases linearly towards the right part. The narrow band of precession frequency is similar for a given column (e.g. ABC). Inversely, in distinct columns (for instance ABC vs. DEF), spins precess at different frequencies. Note that, though necessary for image generation, the

frequency-encoding gradient does not allow to discriminate between pixels within a given column (e.g. A vs. B vs. C) because of their similar frequency (Adapted from Elster (2021a)).

Though the frequency-encoding gradient resolves the spatial information in the x-direction, a second gradient in the y-direction, termed phase-encoding gradient is necessary to resolve the 2D-spatial information. For instance, if the phase-encoding gradient is turned on before the frequency-encoding gradient, spins will differ in their phase when the frequency-encoding gradient will be initiated. Indeed, depending on their spatial location, spins will precess at different rates during the phase-encoding gradient. These spins thus differ in their phases when the frequency-encoding gradient is initiated (Figure 1.43).

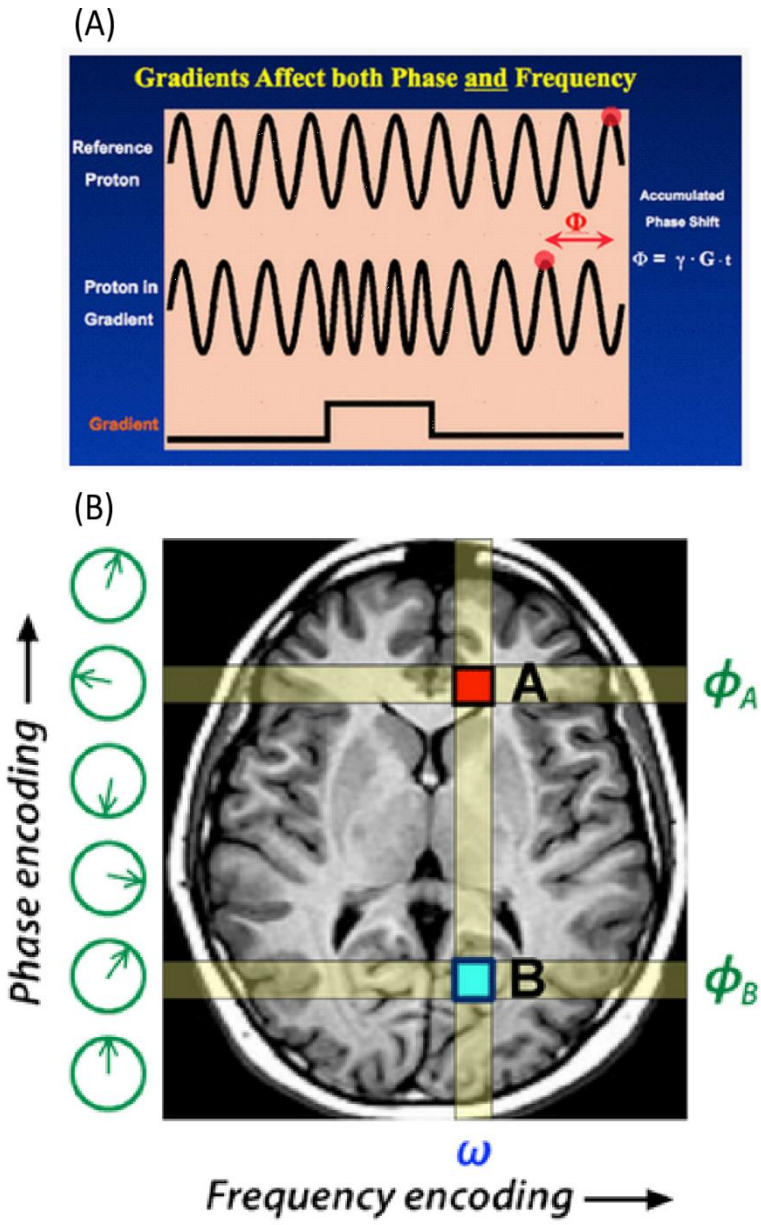

Figure 1.43. (A) All gradients temporarily change the resonant frequencies (ω) of the spins during their application. At the cessation of the gradient, spins go back to their original precession frequencies. However, there is either a gain or a loss of phase compared to their reference state. Therefore,

there is a phase shift (Φ). **(B)** Pixels A and B are in the same column, they therefore precess at the same frequency. Thanks to the phase-encoding gradient, they precess with a different gradient-induced phase shift. (Adapted from Elster (2021b) and Elster (2021c)).

Note that the MR signal which is measured is a sine wave representing the sum of the signal from all pixels. By considering the two pixels example of Figure 1.43, it is impossible to determine the phase contribution for pixels A and B from a single measurement. Multiple phase-encoding steps are therefore needed to sort out spatial information in the phase-encoding direction (Figure 1.44).

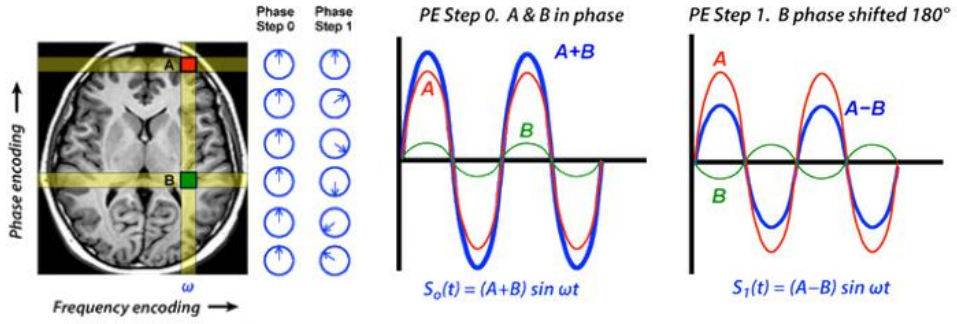

Figure 1.44. The addition of two sine waves (A and B) with the same frequency (ω) but with different phases is equal to another sine wave with the same frequency but a different phase. When the phases of the sine waves are close together, they constructively interfere and inversely. Therefore, their sum consists on another sine wave of a certain frequency and phase. It is thus impossible from this single observation to sort out the individual contribution of sine waves A and B. However, determining the relative contribution of both A and B is possible with two observations shifted by a difference in their phases. For simplicity, let's say that pixel A is in the zero position of the phase-encoding gradient and does not change its phase. Pixel B, at the contrary, is in a higher portion of the gradient and gains exactly 180° of phase relative to pixel A. At Step 0, i.e. the baseline before

the phase-encoding gradient, the total signal from pixels A and B can be written: $S_o(t)$ = A sin ωt + B sin ωt = (A+B) sin ωt. At Step 1, the phase-encoding gradient causes a phase shift of their spins along the vertical axis. While the signal from pixel A is unchanged, the signal from pixel B is inverted (−B sin ωt). The total signal from both A and B pixels is therefore $S_1(t)$ = A sin ωt − B sin ωt = (A−B) sin ωt. Knowing the difference in amplitude of signals A and B (A−B), computing the unique signal contribution of pixels A and B by simple algebra is now possible (Adapted from Elster (2021d)).

Next, a Fourier transformation is needed to sort out overlapping signal contributions in 2D-dimension, i.e. within a given slice. Figure 1.45 depicts the image formation process by using a Fourier transformation. Note that the process shown in Figure 1.45 is a six pixels example. For high-resolution images such as anatomical images of 256 × 256 pixels, there are 65 536 pixels in a single slice. Therefore, hundreds of phase-encoding steps are needed to finalize the image formation process (Figure 1.46).

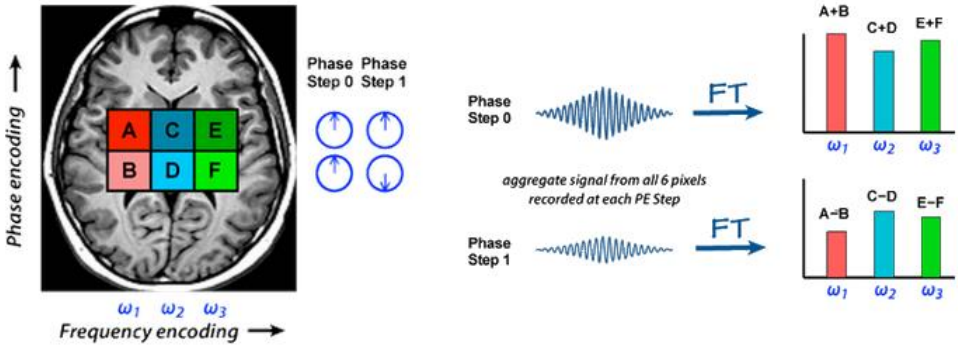

Figure 1.45. Image formation using a Fourier transform. The figure depicts a 2 x 3 array of pixels (A-F) located at the center of the brain. At step 0, the phase-encoding gradient is off and the spins are in phase. The frequency-encoding gradient leads pixels from different columns (AB vs. DC vs. EF) to precess at different frequencies (ω1, ω2 and ω3). At step 2, pixels in the

second row (BDF) all acquire a phase shift of 180° relative to the first row. After each phase-encoding step, a MR signal is recorded which reflects the contribution from each pixel. Therefore, with only two phase-encoding gradients, two MR signals are recorded from the same slice. At step 0, the MR signal is recorded without phase shift between the two rows. The spectrum generated by the Fourier transformation of this MR signal generates three frequencies (ω1, ω2, and ω3). At this stage we only know the sums (A+B), (C+D), and (E+F) of the pixel values for each frequency column. The individual value for a given pixel is unknown. The MR signal recorded from the whole sample after step 1, in which the second row (BDF) has been phase-shifted by 180°, is different. Again, the Fourier spectrum generates three frequencies with a magnitudes equal to A−B, C−D, and E−F. Now, for each frequency column, the differences in the pixel values are known. At this step, it is possible to deduct the phase change information. As for the two pixels example of Figure 1.44, an algebraic manipulation allows to compute A, B, C, D, E, and F. In reality, a MR image have hundreds of pixels in each dimension. Therefore, hundreds of phase-encoding gradients are needed to finish the MR image formation. However, the basic principle is the same as for this six pixels example (Adapted from Elster (2021e)).

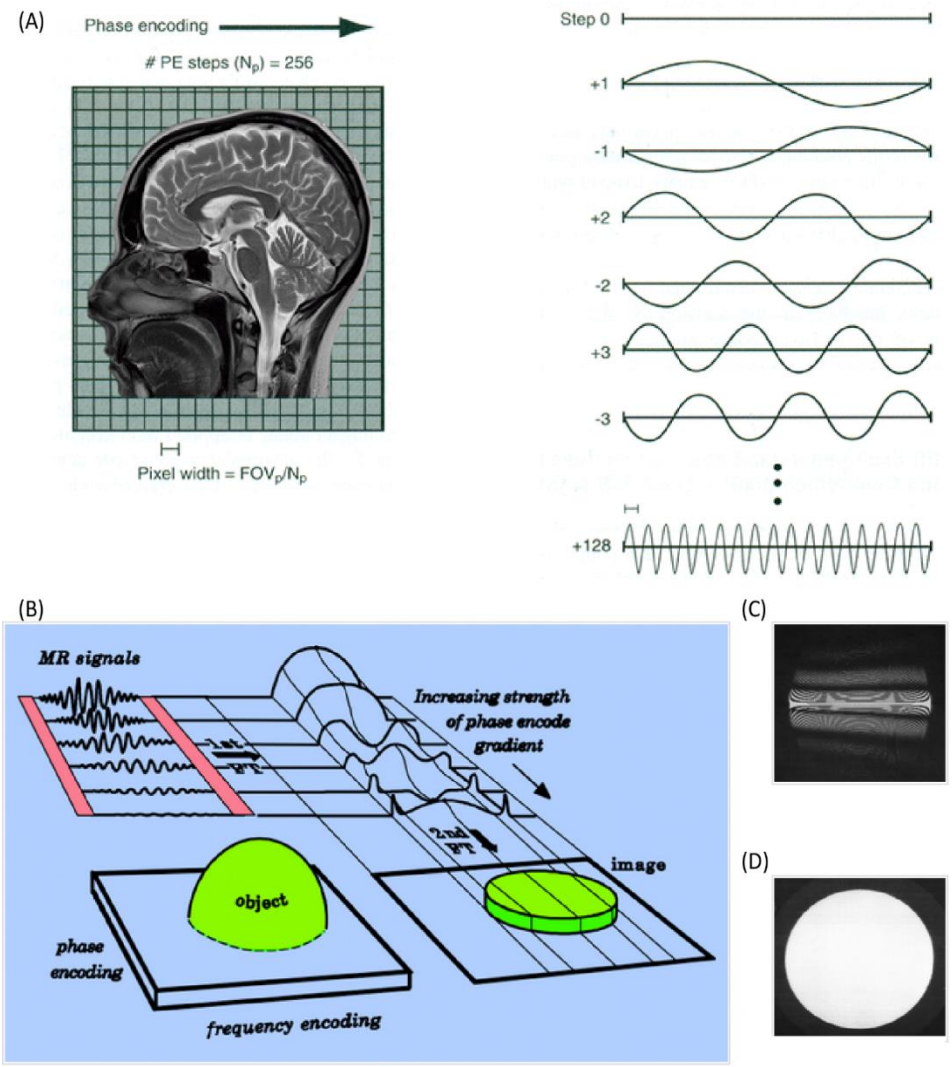

Figure 1.46. (A) For high-resolution images of 256 x 256 pixels, 256 phase-encoding gradients are needed. Advanced mathematical techniques are required to simultaneous resolve multiple equations. For real MR images, the basic principles for images formation are the same as for the six pixels example in Figure 1.45. However, there are several differences. First, typical MR images use 256 “columns” in the frequency-encoding gradient direction. The first Fourier transform spectrum will be thus constituted of 256 frequency "bars" rather than three in the six pixels example of Figure 1.45.

Second, as already stated, the number of echo signals acquired equals the number of phase encoding steps. Third, the phase shifts between the rows are not only multiples of 180°, they vary from echo to echo according to the size of the phase-encoding gradient. Finally, the spectral amplitudes for each echo cannot simply be added or subtracted to calculate individual pixel value because each echo has been acquired using a different set of inter-row phase shifts. Therefore, a second Fourier transform has to be performed. **(B**) Illustration of the 2D-Fourier transform process. Multiple phase-encoding steps are used to elicit an array of different MR signals from a given slice of a spherical object. A frequency projection of this object is elicited by the first Fourier transform of each of the MR signal. Each frequency projection is changed by the phase shifts of each step. For low order phase-encoding gradients, the MR signal is strong and gives an approximation of the shape of the object with few details about the edges. Inversely, higher order phase-encoding gradients are characterized by smaller MR signals and provide information about spatial details, such as the location of the edges. Image shown in **(C)** represents the image processing when it was interrupted after the first Fourier transform. In **(D)** is shown the desired slice of the phantom after the second Fourier transform (Adapted from Elster (2021e) and Elster (2021f)).

Importantly, the appropriate choice of the phase- and frequency-encoding gradients direction is a key element for reducing artifacts. Indeed, the phase-encoding direction is associated with two major artifacts. First, *aliasing* can be observed when the size of the sample to be imaged exceeds the defined field-of-view (FOV)[4] in the phase-encoding direction. This causes the anatomy outside the FOV to be folded in over the main part of the image. This will lead to a "wrap-around" artifact where the parts of the brain outside the FOV will be folded in over the main part of the image. Therefore,

[4] The total extent of an image along a spatial direction.

to avoid aliasing, the phase-encoding direction is usually chosen to be along the shortest anatomic dimension. *Susceptibility artifacts* due to the presence of an external object such as a TMS coil can produce image distortions. It can be difficult to predict in advance the optimal direction for both phase- and frequency-encoding gradients. It is often necessary to work by trial and error. Simply changing the phase- and frequency-encoding directions can significantly decrease the susceptibility artifacts or move it away from the area of interest. The optimal choice of phase- and frequency-encoding directions when a TMS coil is placed within a MRI scanner will be discussed in more details in section 6.5 of this chapter.

The total MR signal recorded from a given slice depends of the net magnetization at all points' coordinates (x and y) within that slice. In addition, the phase of each pixel is dependent of the strength of the gradient fields at that location. In order to facilitate the comprehension of the link between the MR signal and the sample which is imaged, a notation scheme, termed *k-space*, is used. The *k*-space can be viewed as an array of numbers representing the spatial frequencies constituting the MR image. The brightness of each point of the *k*-space is proportional to the relative contribution of the spatial frequency of that point to the final image. The *k*-space is usually shown on a rectangular grid with its principal axes k_x and k_y. These axes represent the spatial frequencies in the x- and y-directions. They do not represent a position in space. Importantly, a given point (k_x;k_y) in the *k*-space does not correspond one-to-one with an individual pixel (x;y) in the image. At the contrary, each *k*-space point contains both the spatial frequency and the phase information about every locations in the final

image (Figure 1.47). In consequence, each pixel of the image maps to every points in the *k*-space. The *k*-space is in fact the Fourier transformation of the MR image (Figure 1.47).

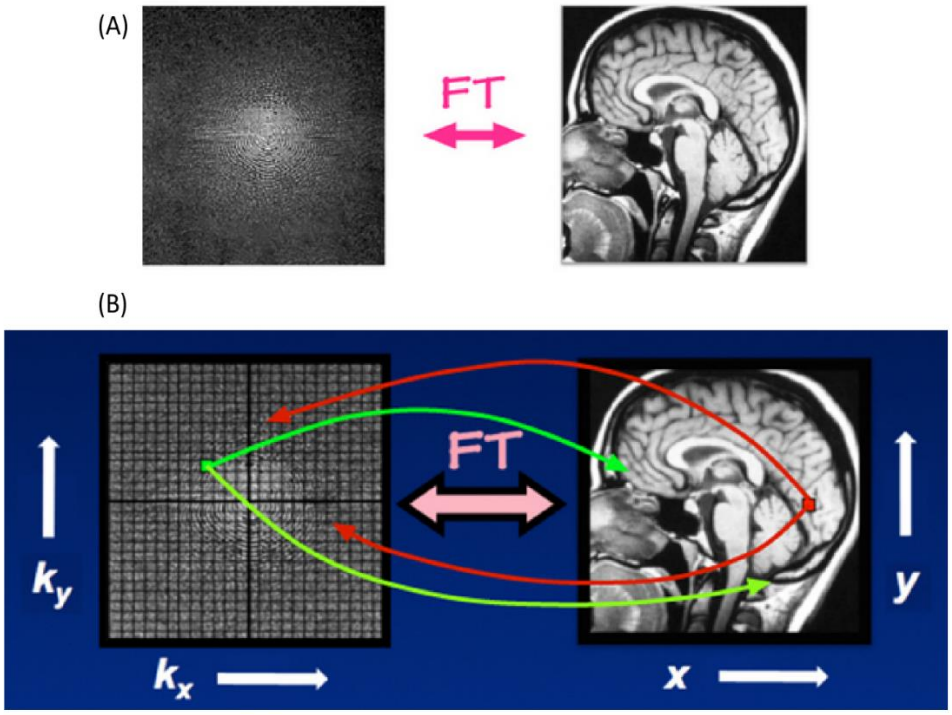

Figure 1.47. (A) The *k*-space is the Fourier transformation of the MR image and vice-versa. **(B)** Each data point in the *k*-space consists of the sum of the MR signal from all pixels in the image space (Adapted from Elster (2021g)).

Distinct parts of the *k*-space correspond to different spatial frequencies in the MR image. Any image can be represented with an assembly of spatial-frequency components. The *k*-space is brightest in its center than near its edges (Figure 1.48). Figures 1.48 and 1.49 illustrate that low spatial frequency data (grating patterns with thick lines; i.e. shapes and contours) are represented near the center of the *k*-space. Inversely, data from the

periphery of the *k*-space are related to high spatial frequencies (grating patterns with thin lines; i.e. edges and details).

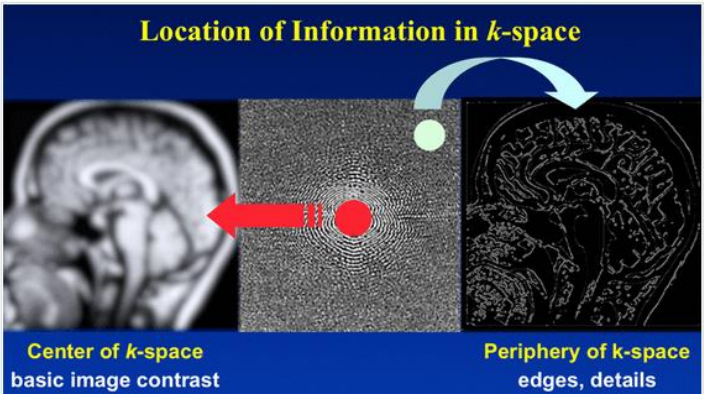

Figure 1.48. Low spatial frequency data are represented near the center of the *k*-space while data from the periphery are related to high spatial frequencies (Adapted from Elster (2021h)).

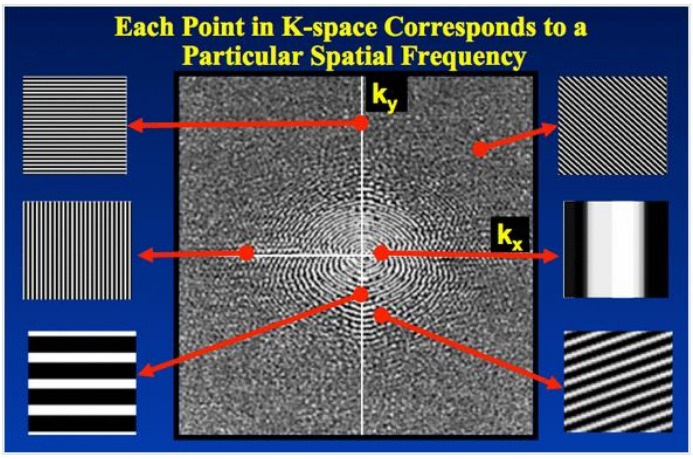

Figure 1.49. The k_x coordinates represent the frequency components along the x-direction of the image. Inversely, the K_y coordinates are related to the frequency components along the y-direction of the image. MR images have frequency components in all directions. A bright point in the *k*-space shows

that the spatial frequency of this particular point significantly contributes to the final image (Adapted from Elster (2021i)).

Note that, in order to decrease the time needed to acquire MR images, echo-planar imaging (EPI) sequences are usually used. In EPI sequences, the collection of an entire 2D-image is achieved by changing spatial gradients quickly after a single RF excitation pulse. To rapidly fill the *k*-space after one single excitation pulse, EPI sequences use a pattern in which alternating lines are scanned in opposite directions as shown on Figure 1.50.

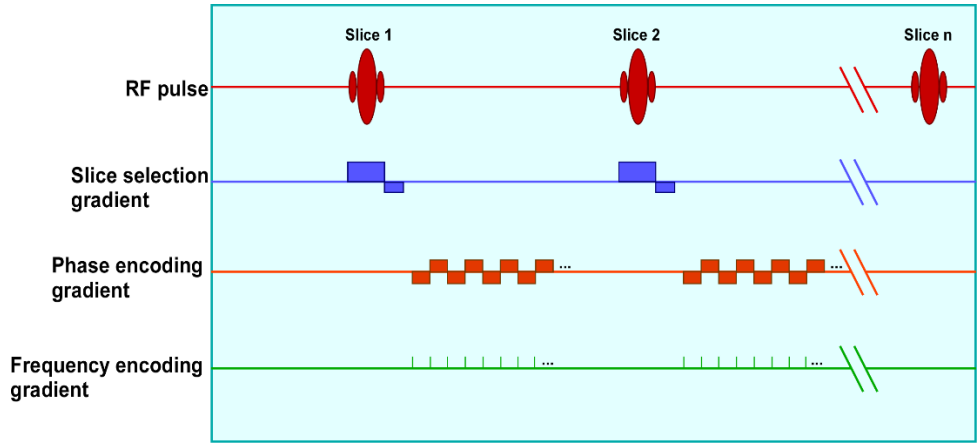

Figure 1.50. An EPI pulse sequence. Pulse sequence is a series of changing magnetic field gradients and RF pulses used for generating an image sensitive to a particular physical property. The RF pulse is usually represented by three ovals to highlight that it is composed of a band of frequencies of a sinc function. The time interval separating two excitation pulses is termed repetition time (TR). The slice selection gradient consists on a first positive gradient followed by a negative gradient whose the goal is to counteract the dephasing effect of the first positive gradient, thus limiting the loss of phase coherence in the transverse plane. In EPI sequences, the collection of an entire 2D-image is achieved by changing the phase- and frequency-encoding gradients rapidly after a single RF excitation pulse. The

way in which they are represented conveys the idea that they are quickly changed over time to rapidly fill the *k*-space by using a back- and forth-trajectory through the *k*-space. Note that data acquisition is typically done simultaneously to the phase- and frequency-encoding gradients. The time interval which separates the excitation pulse and the data acquisition (the time when the signal from the center of the *k*-space is recorded) is termed echo time (TE).

6.5 Concurrent TMS-fMRI

6.5.1 Technical aspects of concurrent TMS-fMRI

The combination of TMS and fMRI is methodologically challenging due to the strong magnetic fields used by the two methods. Indeed, for human use, the static magnetic field (B_0) generated by a MRI scanner is usually between 1.5 and 3 Tesla while the short-lasting magnetic field generated by a TMS coil can reach 1-2 Tesla for 100-200 µs (George et al., 1999). Bohning et al. (1997) were the first to implement TMS with online fMRI. Their initial aim was to produce a map of the magnetic field generated by a TMS coil. To safely insert the TMS coil inside the scanner, they used an MRI compatible TMS coil without ferromagnetic materials (Figure 1.51) in order to avoid projectile effects (Bohning et al., 1997; Bohning et al., 1998). The TMS stimulator, which contains ferrite elements, was placed outside the scanner room and was connected to the TMS coil by a long cable. However, due to inhomogeneities in the surrounding B_0, static artifacts can be induced in T2*-weighted EPI sequences by the mere presence of the non-ferromagnetic TMS coil (Baudewig et al., 2000). Indeed, on T2*-weighted EPI images of a

phantom, Baudewig et al. (2000) observed both signal loss in the vicinity of the TMS coil and geometrical distortions at further distance.

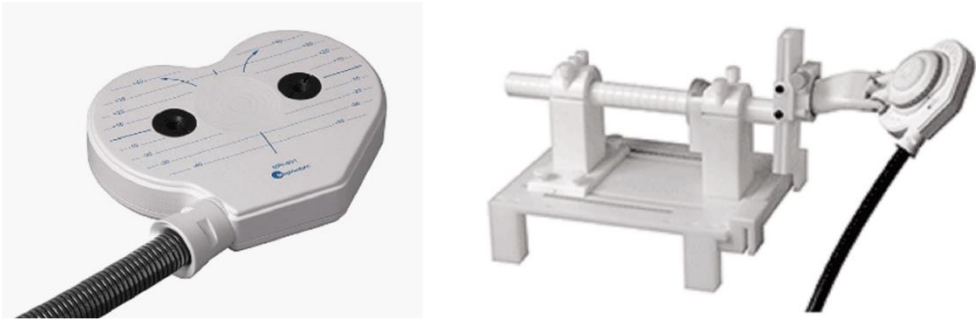

Figure 1.51. MRI-compatible TMS coil and TMS coil holder without ferromagnetic elements.

6.5.1.1 Imaging artifacts induced by the mere presence of the TMS coil

Static imaging artifacts can be reduced by adapting the sequence parameters. For instance, shorter TE by using stronger gradients can reduce the distortions and the signal losses because the data are recorded before a consistent loss of phase of transverse magnetization (Bestmann et al., 2008c). Concurrent TMS-fMRI can also benefit of a parallel acquisition in which undistorted EPI images can be obtained by using an optimal orientation of all the three gradients, i.e. the slice selection, the frequency- and phase-encoding gradients (Figure 1.52).

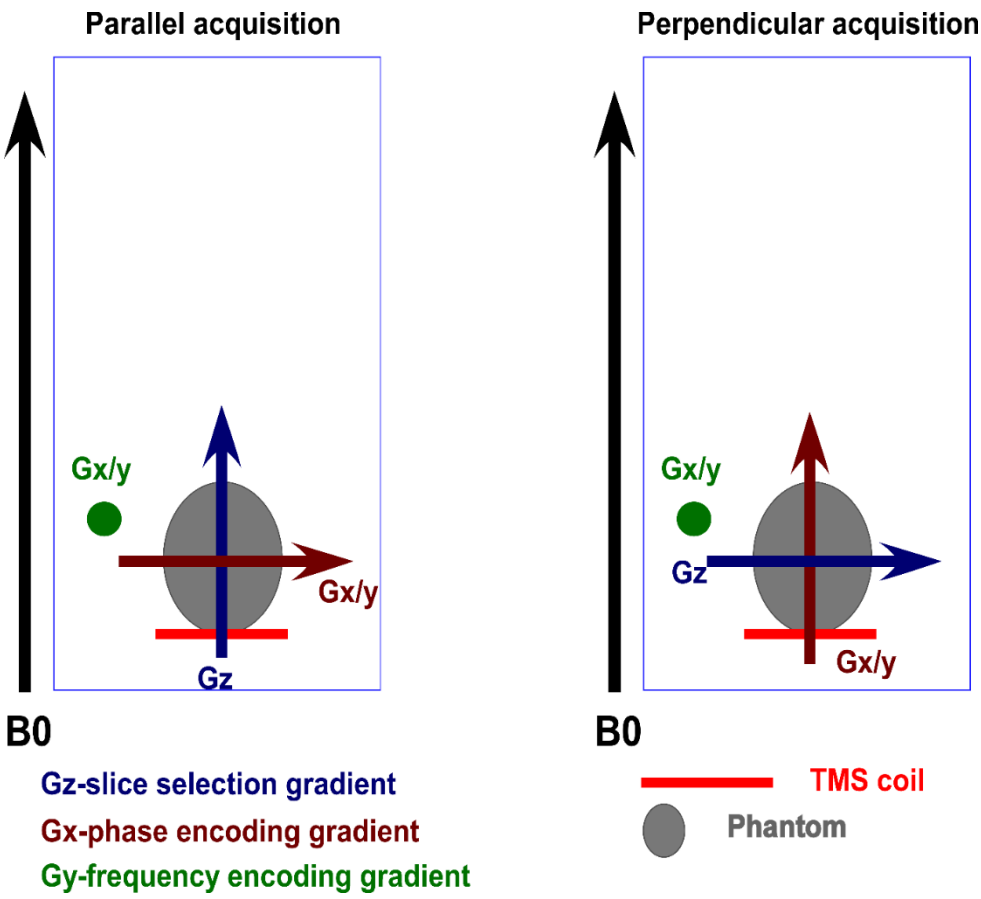

Figure 1.52. Schematic representation of both perpendicular and parallel EPI acquisitions. The black arrow represents the main static magnetic field, B_0, which is stable during the acquisition. Gx, Gy and Gz represent the gradient magnetic fields. The magnetic field inhomogeneities induced by the TMS coil can have distinct influences on the three imaging gradients. In perpendicular acquisition, the phase- or the frequency-encoding gradient have to cross the plane of the TMS coil resulting in distortions in various locations of the image. In contrast, during a parallel acquisition relative to the TMS coil, only the slice selection gradient crosses the TMS coil essentially resulting in signal loss without geometrical distortions.

Indeed, Baudewig et al. (2000) suggest that for perpendicular EPI acquisition, i.e. when the slice selection gradient is parallel to the TMS coil, inhomogeneities in either the phase- or the frequency-encoding gradients, which cross the plane of the coil, result in a perturbation of the *k*-space trajectory, which induce distortions in the EPI image (Figure 1.53). On the other hand, in parallel EPI acquisition, the slice selection gradient crosses the coil plane resulting in signal losses due to perturbations of the transverse magnetization. Therefore, to record undistorted images, concurrent TMS-fMRI benefits of a parallel acquisition in which the phase- and frequency-encoding gradients do not cross the TMS coil. Note that the parallel and perpendicular acquisitions refer to the choice of the phase- and frequency-encoding gradient directions. This should not be confused with the parallel imaging technique which uses multiple surface coils receiving the MR signal to shorten the imaging time. Importantly, in humans, due to the scalp-cortex distance, the signal loss observed with parallel acquisition does not reach the cortex (Figure 1.54; Baudewig et al. (2000)). Although depending on the coil orientation inside the scanner bore, stronger static artifacts are usually observed when the frequency-encoding gradient crosses the plane of the TMS coil and best EPI images can usually be obtained when both the section orientation and the frequency-encoding gradient are parallel to the plane of the TMS coil (Figure 1.55; Bestmann et al. (2003a)). Also, ghost artifacts due to perturbations of the phase-encoding gradient can be alleviated by over-sampling the image in the phase-encoding direction (Bestmann et al., 2008c; Feredoes et al., 2011). According to our personal experience it is often necessary to work by trial and error by simply changing the phase- and

frequency-encoding directions to find the best compromise for reducing the artifacts according to the orientation of the TMS coil.

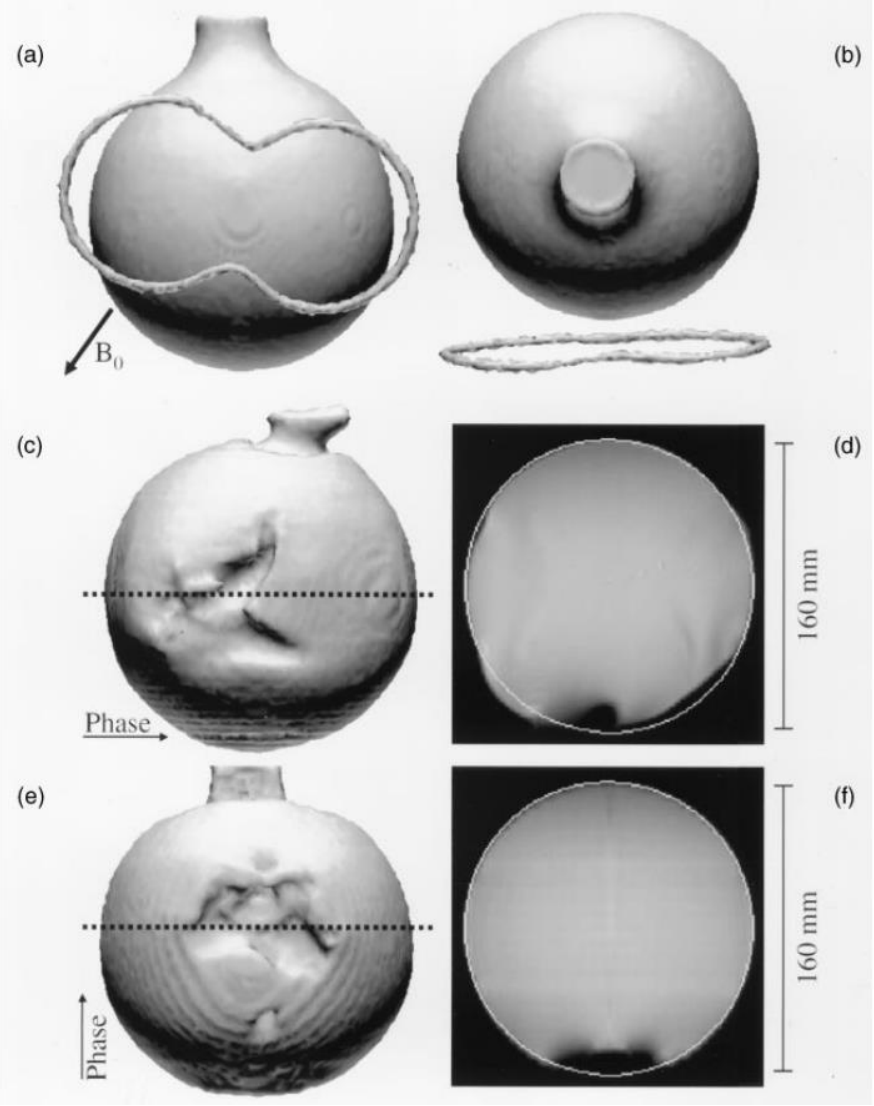

Figure 1.53. A and B. Frontal and top views of a spherical phantom in the presence of a TMS coil. The arrow indicates the direction of B_0. **C.** Frontal view of a 3D-reconstruction of contiguous T2*-weighted EPI scans in which the EPI acquisition was perpendicular to the TMS coil. The arrow indicates

the orientation of the phase-encoding gradient. The dashed line shows the location of the cross-sectional image represented in **D.** Note that in EPI acquisition, both significant distortions and signal losses can be observed in perpendicular acquisition. **E and F**. are the same views as in C and D except that the EPI acquisition was parallel to the TMS coil. Therefore, by using proper orientation of the different gradients, it is possible to reduce static artifacts. Indeed, for EPI acquisitions perpendicular to the TMS coil plane, the images are affected by a regional signal loss in the direct vicinity of the TMS coil. In addition, the images also show consistent distortions at rather far distances (as far as 140 mm in this study). These effects can be significantly reduced by using EPI sections acquired parallel to the TMS coil. However, a more restricted signal loss can still be observed in regions as deep as 25 mm from the TMS coil plane. Note that the distortions seem to have disappeared (Adapted from Figure 1 in Baudewig et al. (2000)).

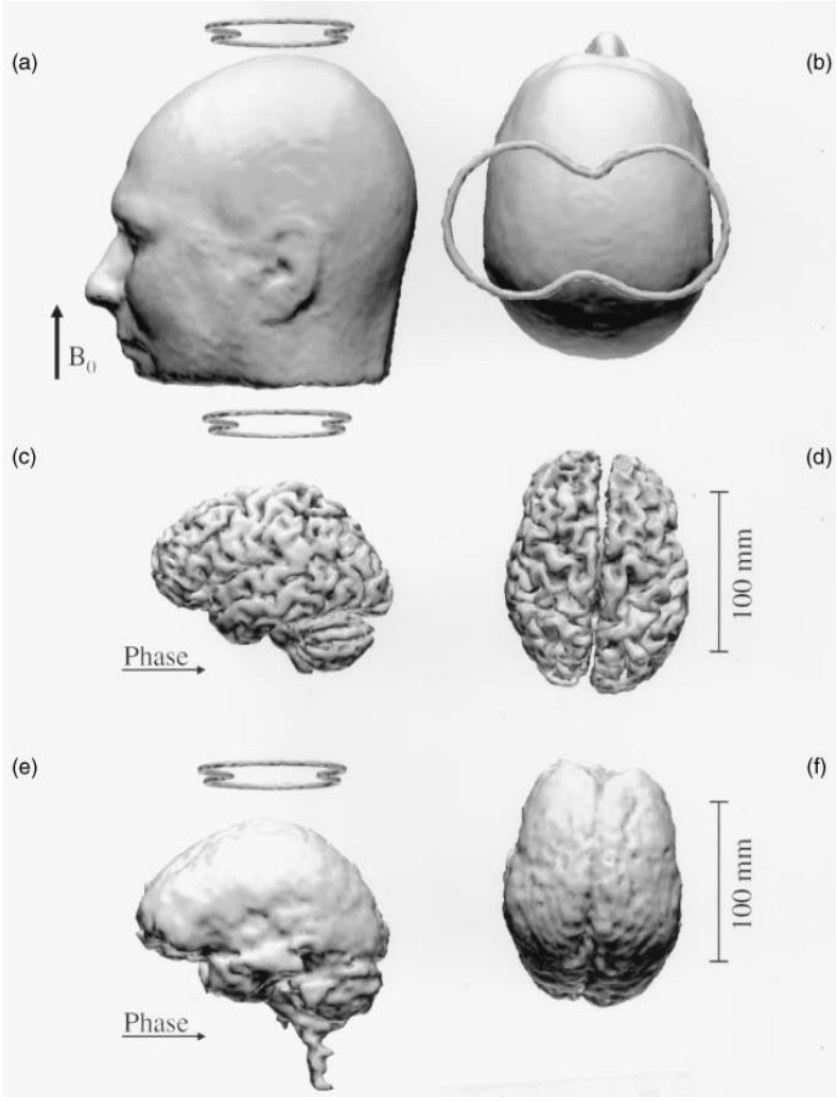

Figure 1.54. A and B. Side and top views of a 3D-head reconstruction of a subject with a TMS coil positioned over the vertex. The same is represented in **C and D** for the cortical surface. In **E and F** the brain surface from a T2*-weighted EPI sequence with a transverse orientation parallel to the TMS coil is represented. Note that in humans, thanks to the scalp-cortex distance, the signal loss observed with parallel acquisition in phantom does not reach the cortex (Adapted from Figure 2 in Baudewig et al. (2000)).

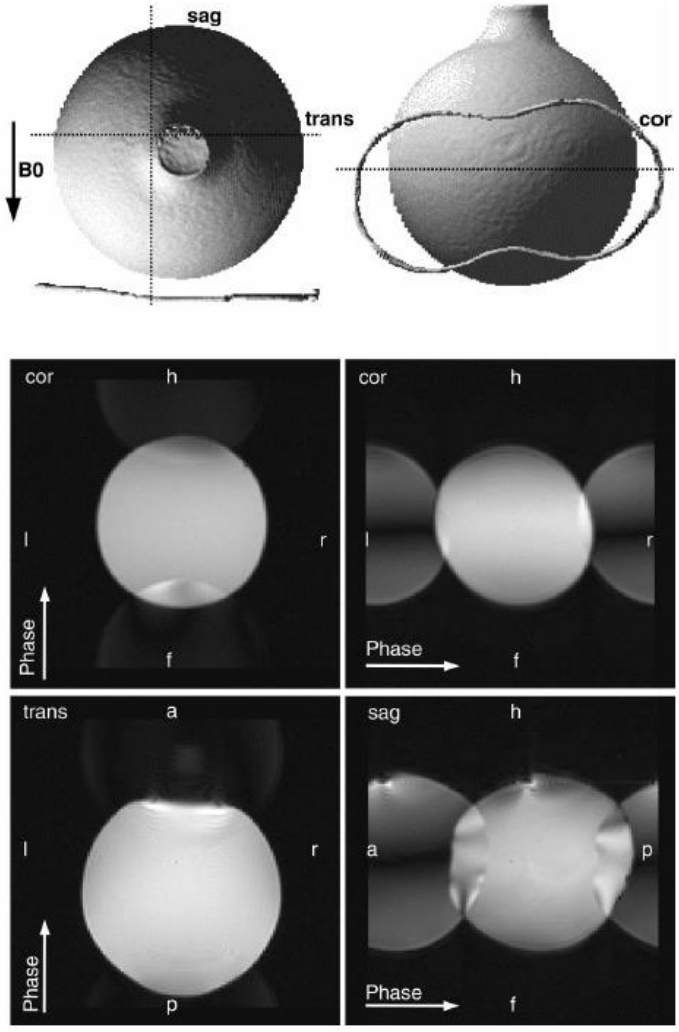

Figure 1.55. EPI effects produced by the presence of a TMS coil with a transverse orientation relative to B_0. In coronal sections (middle), a switch of the frequency- and phase-encoding gradients allows to reduce ghosting artifacts. Similarly, the transverse sections with phase-encoding gradients in a posterior-anterior direction, showed only negligible distortions. Therefore, best results can be elicited when both the section orientation and the frequency-encoding gradient were parallel to the plane of the TMS coil (Adapted from Figure 1 in Bestmann et al. (2003a)).

The transmission of the RF noise into the scanner, via the TMS cable, can alter the SNR in functional images in an extent depending on the specific MR resonance frequency (i.e. the Larmor frequency which depends of the strength of the B_0) (Bestmann et al., 2008c). The alterations of the MR image can be limited by preventing the RF noise to propagate inside the scanner (Bungert et al., 2012a). For instance, in-line filters can prevent the RF noise to be transmitted from the TMS stimulator to the TMS coil (Moisa et al., 2009; Heinen et al., 2011; Bungert et al., 2012a). Others placed the stimulator into a shielded piece or in a shielded cabinet inside the scanner room (Feredoes et al., 2011), thus decreasing external RF influences (Bohning et al., 1999; Heinen et al., 2011). To further attenuate RF perturbations, the TMS cable can be surrounded by ferrite sleeves (Ruff et al., 2008; Feredoes et al., 2011; Heinen et al., 2011). However, Bungert et al. (2012a) showed that any method filtering RF interferences originated only from the environment caused an incomplete RF attenuation. Indeed, RF noise caused by the stimulator itself can have a significant impact on the image quality. Leakage currents in the TMS coil caused by the high-voltage capacitor used by the TMS stimulator can distort the MRI images (Weiskopf et al., 2009). This source of artifacts can be attenuated by the insertion, in the TMS circuit, of a bypass high-voltage diode relay in parallel to the TMS coil, together with two high-voltage diodes in series to the coil (Weiskopf et al., 2009; Feredoes et al., 2011). Closing this remote-controlled relay when the coil is not discharging allows the current to flow through the relay and not through the TMS coil, thus reducing leakage currents in the TMS coil. Finally, Bungert et al. (2012b) showed that passive shimming of both sides

of the TMS coil using thin pieces of austenitic stainless steel can reduce inhomogeneities in the static magnetic field by ± 85 % up to 90 mm under the TMS coil, reducing the signal loss in the direct vicinity of the TMS coil.

6.5.1.2 Imaging artifacts induced by the discharge of the TMS coil

The main technical issue to combine TMS and fMRI acquisition is the dynamic artifacts generated by the discharge of the TMS coil (Figure 1.56). Depending on when the TMS pulses are delivered during the pulse sequence, different dynamic artifacts can be observed (Bestmann et al., 2008a). First TMS pulses delivered prior to the slice acquisition may alter the signal intensity when the time interval between the TMS pulse and the RF pulse is too short. Although this waiting period depends of, *inter alia*, the orientation of the TMS coil and the stimulus intensities, Bestmann et al. (2003a) estimated that 100 ms were required between the pulse and the onset of slice acquisition to avoid consequent artifacts (Figure 1.57). This signal fluctuation can probably be explained by eddy currents in the TMS coil induced by mechanical vibrations (Bestmann et al., 2003a; Bestmann et al., 2008a). Later, by improving the fixation of the TMS coil and thus reducing currents induced by vibrations, Bestmann et al. (2004) succeeded to record functional images free of artifacts with a waiting period of ~ 70ms.

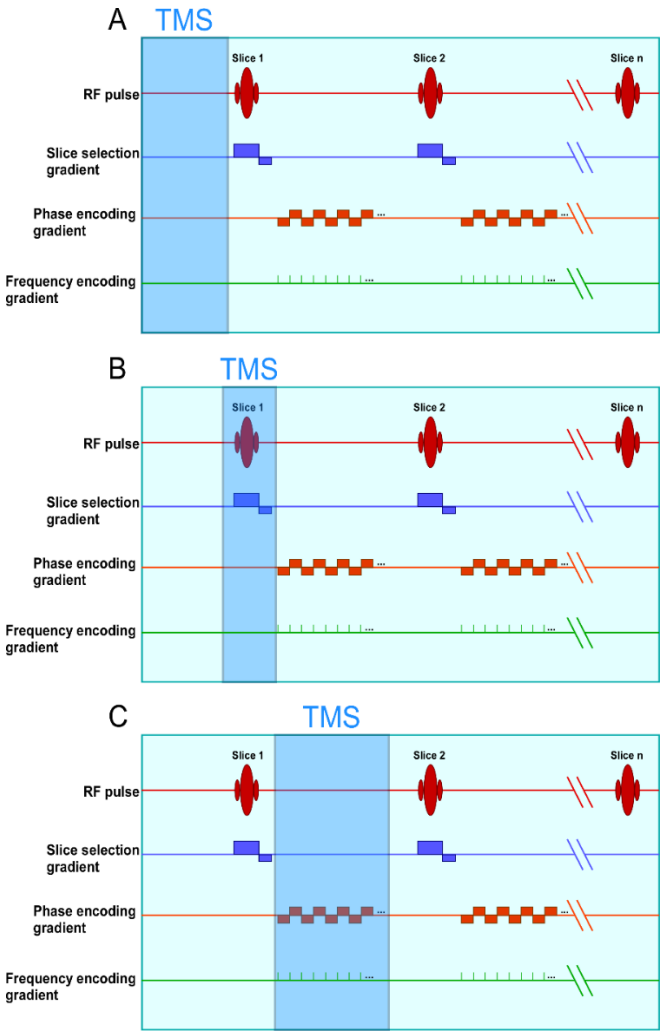

Figure 1.56. Time periods in which TMS can be delivered during an fMRI acquisition. **A.** TMS pulses delivered prior to the slice acquisition. **B.** TMS pulses delivered during the RF pulse. **C.** TMS pulses delivered during the data acquisition.

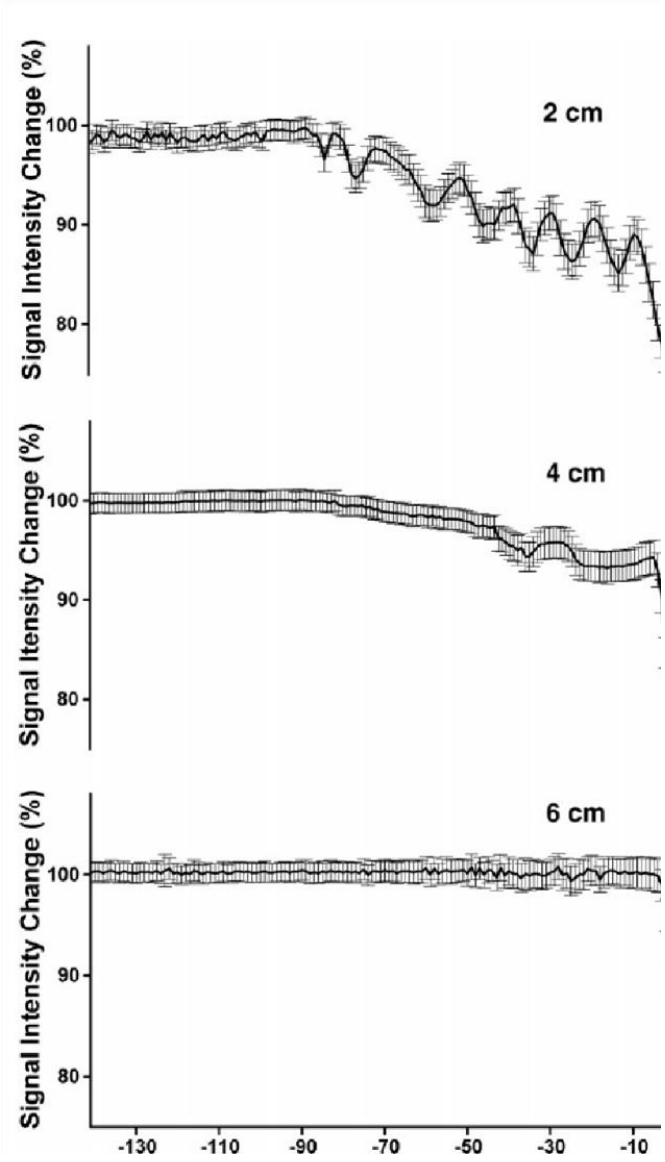

Figure 1.57. EPI signal intensity changes (mean ±SD) from a region-of-interest located at 2 cm, 4 cm, and 6 cm from the TMS coil. The x-axis represents the time separating the TMS pulse (100% MSO) and the RF excitation pulse. Note the signal alteration for waiting periods after the TMS pulse of less than about 100 ms (Adapted from Figure 3 in Bestmann et al. (2003a)).

Secondly, if TMS pulses are delivered at the same time that the RF excitation pulse, the pulse will alter the specificity of the RF pulse for protons. This will cause persistent changes of the signal in spatially adjacent slices (Bestmann

et al., 2008a) which can result in false-positive activations (Figure 1.58; Bestmann et al. (2003a)).

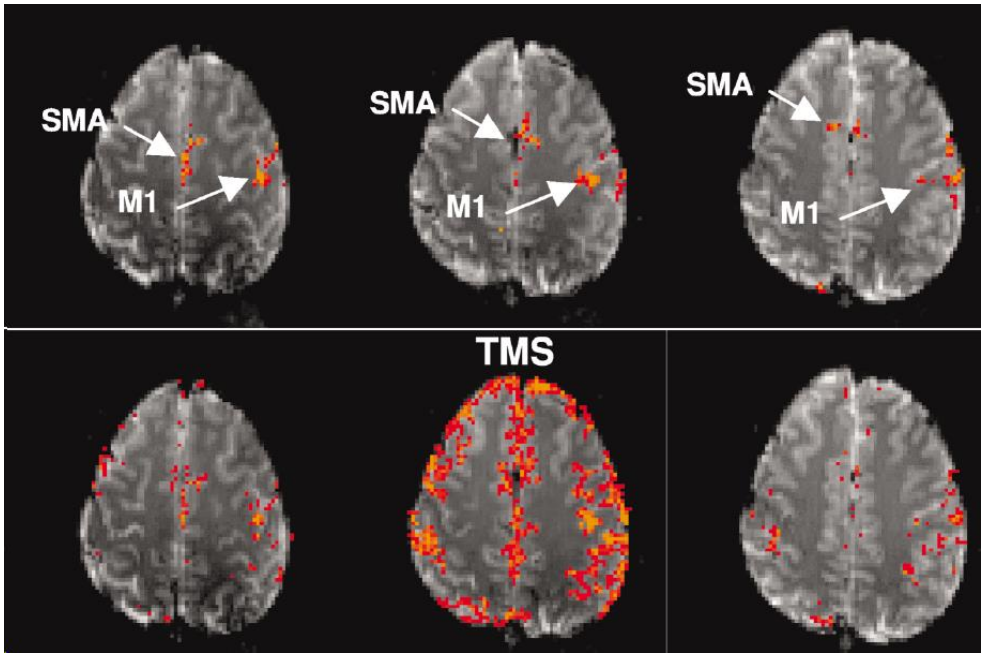

Figure 1.58. Functional activation maps during a sequential finger-to-thumb opposition task obtained without (top) and with (bottom) TMS pulses delivered during the RF pulse. The interference between both the TMS pulses and the RF pulse not only alters the affected image, but also increases the signal intensity in subsequent acquisitions (Adapted from Figure 6 in Bestmann et al. (2003a)).

Finally, TMS pulses delivered during the data acquisition act as spoiler gradients perturbing the transverse magnetization, which results in severe signal losses (Figure 1.59). The MR signal perturbation depends of which part of the *k*-space is affected. Indeed, the later a TMS pulse is delivered during the image acquisition, the fewer signal loss will be observed (Bestmann et al., 2003a).

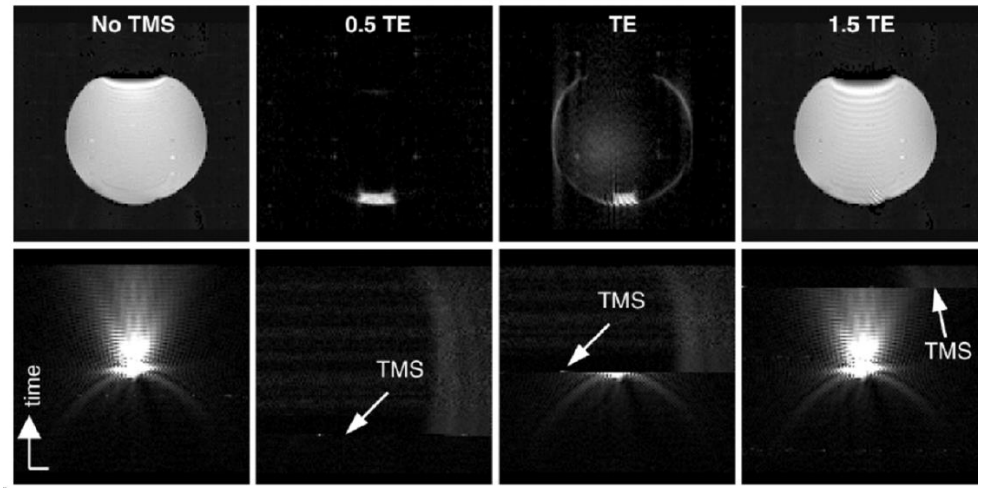

Figure 1.59. The application of a TMS pulse during the first half of data acquisition can induce a complete loss of signal. By increasing the waiting period after the onset of data acquisition, it is possible to obtain images with quality recovering to that elicited without a TMS pulse. The first raw represents EPI data, the second raw represents the different times at which the TMS pulse is delivered during data acquisition in the *k*-space (Adapted from Figure 4 in Bestmann et al. (2003a)).

6.5.2 Synchronization strategies for concurrent TMS-fMRI

6.5.2.1 Time gaps between successive volumes

In order to separate the TMS pulses from the image acquisition, several studies introduced a temporal window between successive volumes in which TMS pulses can be delivered (Bestmann et al., 2008a). This synchronization strategy, although leading to a decrease of the temporal resolution, allows to deliver TMS pulses at a relatively high-frequency (Figure 1.60). For instance, short bursts of TMS were delivered at ~10 Hz during temporal gaps of ~500 ms between successive volumes to investigate top-

down influences of the frontal or parietal cortex to visual areas (Ruff et al., 2006; Ruff et al., 2008; Ruff et al., 2009; Blankenburg et al., 2010; de Weijer et al., 2014).

6.5.2.2 Time gaps between successive slices

The insertion of time windows between successive slices allows to interleave TMS pulses and the EPI fMRI sequence (Bestmann et al., 2008a). If the temporal gap is of sufficient length, a TMS pulse can be delivered without affecting the next slice (Figure 1.60). For instance, Bohning et al. (1999) controlled the timing of TMS by counting, using a computer, the RF excitation pulses and triggered the TMS stimulator using a transistor-transistor logic (TTL) pulse when appropriated. Note that, by using the interleaved TMS-fMRI strategy, the frequency at which the TMS pulses are delivered is limited due to the waiting period needed before the onset of the acquisition of the subsequent slice.

6.5.2.3 Voluntary perturbation of a single slice

TMS can be applied at any time during data acquisition (Figure 1.60). The TMS pulse could corrupt all slices equally, the perturbed slice can be replaced offline by interpolation, using the same slice in the preceding and subsequent volumes (Bestmann et al., 2008a; Feredoes et al., 2011; Hawco et al., 2017). This strategy allows to deliver pulses at random ISIs (e.g. jittered single pulses). Nevertheless, if the TMS pulse perturbs the RF pulse, spatially adjacent slices can be corrupted as well. This perturbation can be attenuated by the introduction of a spatial gap between adjacent slices (Bestmann et al., 2008a).

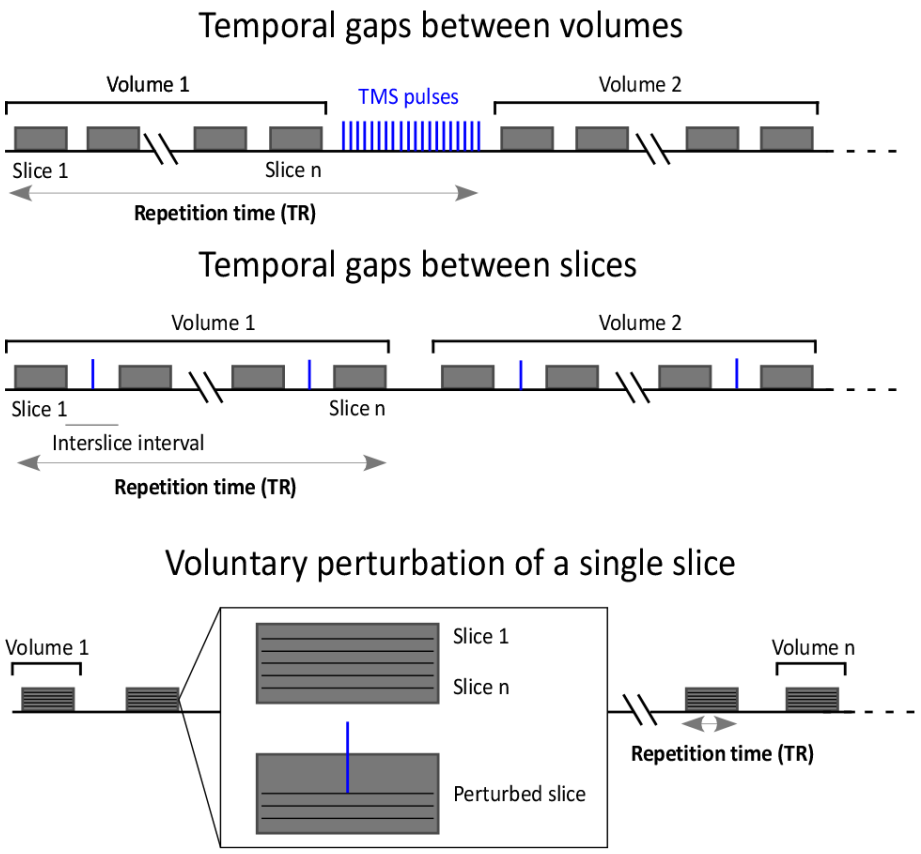

Figure 1.60. Synchronization strategies for concurrent TMS-fMRI.

6.5.3 Practical considerations

A major practical issue in concurrent TMS-fMRI is the stable and fix positioning of the coil on a predefined brain target inside the scanner bore. Therefore, TMS coil holders have been developed allowing a large coverage of the head in order to stimulate a number of cortical targets while being compact enough to enter inside the scanner bore (Figure 1.51; Bohning et al. (2003a)). This kind of device includes several joints allowing to determine the orientation of the TMS coil relative to the selected target.

For stimulating M1, the optimal target can be easily located when subjects are laying in the scanner by adjusting the position of the coil in order to observe consistent motor responses in the contralateral upper limb. However, except for M1 and the visual cortex for which motor responses and phosphenes can be evoked by single pulses of TMS, the functional localization of the selected target is not always possible. Number of studies used either probabilistic atlases (Pascual-Leone et al., 1996) in which the distance between the target and M1 is measured or the international 10-20 EEG system to position the TMS coil on a given brain region (Herwig et al., 2003). Although easy, using probabilistic atlases to position the TMS coil on the desired brain target seems relatively inaccurate (Herwig et al., 2001). On the other hand, the international 10-20 EEG system seems to be more precise and suitable to reach the selected target on a larger scale level (Herwig et al., 2003). Alternatively, anatomical location of the target can be determined using the individual 3D T1-weighted structural MRI data of the whole head of each subject using a neuronavigation system. By doing a mark on the scalp of the subject, the TMS coil can be correctly repositioned on the target when the subject is returned in the MRI scanner. Although more precise than the placement of the coil using the 10-20 EEG system, this method can be time consuming given that the neuronavigation system and the MRI scanner are usually not in the same room. Moreover, difficulties can be encountered to replace the TMS coil on the correct position previously determined on the scalp because the marks can be hidden by the TMS coil. Therefore, several groups developed hardware/software systems which allow to position the TMS coil. For instance, the software developed by

Bohning et al. (2003a) can be used in two modes. First, the experimenters can determine a target on the structural MRI data. Then, their software computes the holder settings to reach that region. Alternatively, the operators can enter the holder parameters in the software which places a mark on the brain images at the corresponding area. Denslow et al. (2005) demonstrated the effectiveness and the accuracy of such image-guided coil placement techniques. However, when targeting M1, this procedure seems to have a low benefit compared to the function-guided method. By using a neuronavigation system, Moisa et al. (2009) described a similar approach in which the coil position is determined on a T1-weighted structural MRI data of the whole head before the experiment. During the TMS-fMRI session, the position of the head in the scanner is determined by a fast structural image which is then coregistered to the high-definition structural image recorded previously. This allows to determine the transformation to be applied to the target position (defined on the high-definition MRI image) to obtain its coordinates in the scanner space. Then, their software determines the parameters needed to be applied at each joints of the coil holder to reach this particular target. Although allowing a robust and precise positioning of the TMS coil, these methods require specific software systems. Therefore, most of studies labeled the TMS coil with markers visible on the MR images (Bohning et al., 2000; Kemna and Gembris, 2003; Bestmann et al., 2003b). These markers can be used for offline validation of the TMS coil position. Similarly, Yau et al. (2013) used a V-shaped marker filled with Gadolinium. The top of the V-shaped marker coincided with the center of the TMS coil. This allowed to check both the coil placement and orientation during the

recording session. This method also enables to visualize the TMS coil on the functional images in order to determine the brain area crossing a line orthogonal to the TMS coil (and passing by its center). The coordinates of the targeted cortical surface can then be projected in a standard space, i.e. a probabilistic atlas, to check the selected brain region. Similarly, de Weijer et al. (2014) developed a point-based registration method allowing to estimate, during scanning, the region which is stimulated.

In addition to correctly positioning the TMS coil inside the scanner bore, it has been shown that the magnetic field induced by the TMS coil can be altered by the static magnetic field generated by the scanner (Figure 1.61; Yau et al. (2014)). Specifically, the influence of the static magnetic field depends of both the coil location and orientation relative to the static field. Indeed, stronger alterations have been observed near the gantry of the scanner where the magnetic field induced by the TMS coil seems to be lower than that induced inside the scanner for identic coil orientations and stimulator outputs (i.e. TMS intensity). This can be explained by an electromagnetic coupling between the TMS and one or more MRI coils such as the superconducting solenoid coil generating the static magnetic field, the gradient or RF coils (Peterchev, 2014). The coupling between the TMS coil and the MRI coils is dependent on the coils location and orientation. Indeed, except for perfect symmetric positions of the TMS coil relative to the scanner coils for which the flux generated by one of the TMS coil loop in the MRI coils cancelled the flux generated by the other one, different coupling for each of the two loops will induced a TMS field reduction (Peterchev, 2014). Practically, these observations are of importance for TMS intensity

calibration and suggest that the intensity of stimulation should be determined inside the scanner bore (Peterchev, 2014).

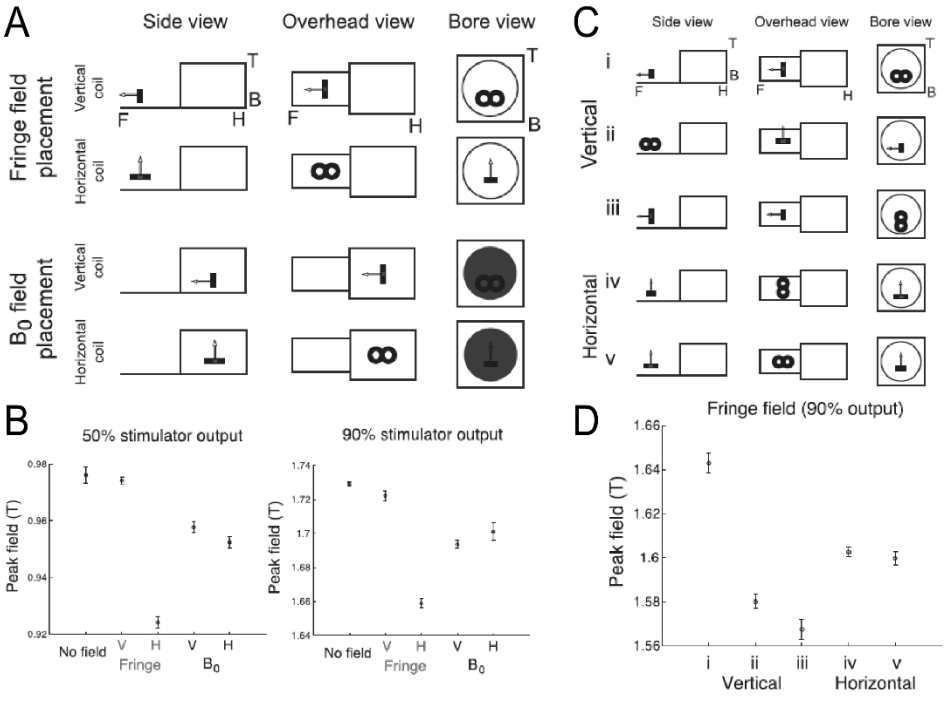

Figure 1.61. A and C. Location (B_0 vs. fringe field) and orientation (vertical vs. horizontal) of the TMS coil in the scanner**. B and D.** TMS field strength measurements in Tesla. While the TMS strength did not differ between horizontal and vertical orientations when the TMS coil was placed within the scanner bore, the orientation of the coil induced consistent alterations of the TMS-induced magnetic field in the fringe field. Indeed, the TMS fields were weaker at horizontal vs. vertical orientations. This is an important observation given that the threshold of TMS is usually determined at this location (Adapted from Figures 2 and 3 in Yau et al. (2014)).

Most TMS-fMRI studies use standard imaging head coils such as a birdcage MR coil which provides a uniform spatial coverage throughout a large

volume, the TMS coil is placed inside the MRI coil (Baudewig et al., 2000; Bestmann et al., 2006; Sack et al., 2007; Peters et al., 2013). The disadvantage of using a volume coil is the difficulty to position the TMS coil inside. Therefore certain cortical targets can be difficult to reach despite the removal of the TMS coil handle. Others, investigating top-down influences over the visual cortex, placed a surface coil over the visual areas while stimulating either the frontal eye-field or the intraparietal sulcus, taking advantage of the high imaging sensitivity provided by the close spatial proximity between the surface coil and the region of interest (Ruff et al., 2006; Ruff et al., 2008; Ruff et al., 2009). However, this solution does not provide a uniform spatial coverage of the whole brain. More recently, a TMS setup was proposed in which the position of both the coil and the head of the subject can be adapted in a space delimited by two RF surface coils positioned at the left and right sides of the head of subjects (de Weijer et al., 2014). However, the SNR was lower and the MR signal was less stable compared to the temporal SNR of the MR signal acquired with a standard head coil, probably because of the distance between the receiver coil and the scalp of the subject (de Weijer et al., 2014). However, they were able to elicit TMS-evoked BOLD responses of similar magnitude and locations than the TMS-evoked activity recorded using a standard head coil in both local and remote regions. Moreover, they did not observe either signal drop out or geometric distortion in the vicinity of the TMS coil. However, for their M1 session, 2 out of 6 subjects moved significantly during the data acquisition probably because their heads were not sufficiently fixed by the setup. Recently, a multichannel receiver MR coil array has been developed

(Navarro de Lara et al., 2015) which can be placed between the TMS coil and the head of the participants. This MR coil can be attached to the TMS coil. Its spherical curvature allows to position the setup over a large variety of head shapes. Moreover, the magnitude of the magnetic field delivered by the TMS coil is moderately attenuated (TMS efficiency loss of ± 15%) thanks to the low thickness of the MR coil (4.5 mm in the center of the coil). In addition, because the coil is placed adjacent to the surface of the scalp, this coil array improves significantly the SNR in the specific region under the coil (Navarro de Lara et al., 2015).

6.5.4 TMS-evoked BOLD responses in stimulated and remote brain regions

The first investigations combining online TMS and fMRI acquisition focused mainly on the motor system, especially on M1, due to the possibility to position the TMS coil and determine the intensity of stimulation according to the elicited muscular response. Bohning et al. (1998), by delivering 1 Hz TMS at 110% of the rMT, were the first to show TMS-evoked BOLD responses in M1, illustrating the feasibility to measure neural activity elicited by TMS pulses with online fMRI acquisition. TMS-evoked hemodynamic changes were dose-dependent as the magnitude of the response, at both the stimulated and non-stimulated areas, increased for higher intensities of stimulation (Bohning et al., 1999; Hanakawa et al., 2009) and for longer train lengths (Bohning et al., 2003b) with both linear and non-linear components in the stimulus-response relationship. Note however that Dowdle et al. (2018) did not find a significant relationship between the intensity of DLPFC-

TMS and the magnitude of BOLD activation. Moreover, the location, the magnitude and the time course of the BOLD responses elicited by short trains of TMS delivered at suprathreshold intensities are concordant with those elicited by a voluntary movement, suggesting that cortical mechanisms underlying these hemodynamic changes are, at least in part, similar (Bohning et al., 2000; Denslow et al., 2004; Shitara et al., 2011; Yau et al., 2013). In agreement, Baudewig et al. (2001) observed a similar pattern of activations in remote regions such as the SMA for both voluntary movement and suprathreshold TMS of M1. However, subthreshold TMS of M1, i.e. below the rMT, was not able to elicit hemodynamic responses either in the stimulated region or in remote brain areas (Baudewig et al., 2001). Similarly, no significant BOLD responses were evoked by TMS of the premotor cortex at suprathreshold intensities (Baudewig et al., 2001; Moisa et al., 2012), including when TMS was delivered at 150% of the rMT (Kemna and Gembris, 2003). Similar observations were reported when the parietal cortex was stimulated (Blankenburg et al., 2008). Given that the stimulation of both non-primary motor areas such as the prefrontal and parietal cortices and M1 at subthreshold intensities do not evoke a muscle twitch, these observations suggest that the cerebral processing related to sensory afferent feedbacks could underlie, at least in part, the BOLD responses evoked by suprathreshold TMS delivered over M1. However, further studies observed that short trains of TMS delivered on M1 at subthreshold intensities were able to induce hemodynamic changes in remote cortical areas such as the SMA, the bilateral premotor cortices, the cingulate motor areas and the contralateral M1 as well as in subcortical structures such as

the putamen, the left and right ventrolateral thalami without inducing consistent responses in the stimulated M1 (Bestmann et al., 2003b; 2004). A parallel can be drawn between (1) the hemodynamic response evoked by subthreshold TMS in remote interconnected regions observed when concurrent TMS-fMRI is used and (2) the changes in cortical excitability in a given brain region observed when a single pulse of TMS is delivered at subthreshold intensity on a distant connected brain area (Ferbert et al., 1992; Civardi et al., 2001; Koch et al., 2006). On the other hand, the lack of activation in the brain region directly under the coil (in this case M1) when subthreshold TMS are used suggests that the BOLD response evoked in M1 by TMS delivered at suprathreshold intensities reflects, to a certain extent, the reafferent feedback processing in the sensorimotor cortex. In agreement, Shitara et al. (2011) investigated the spatial distribution of the BOLD response in motor regions evoked by muscle afferents. They contrasted the pattern of activity elicited by median nerve stimulation above the MT inducing a muscle twitch vs. the activation evoked by median nerve stimulation below the MT, i.e. which does not evoke a muscle contraction. They recorded significant activities in M1, SMA and basal ganglia. The close location of the activity evoked by both suprathreshold TMS (relative to subthreshold TMS) and supra-MT median nerve stimulation (relative to subthreshold median nerve stimulation) suggests that proprioceptive afferents can partially account for the BOLD responses evoked by suprathreshold TMS of M1 not only in local but also in remote interconnected brain regions (Shitara et al., 2011). Similarly, Hanakawa et al. (2009) showed that the stimulus-response profile of the TMS-evoked BOLD

responses included both linear and non-linear components in both the stimulated region and distant brain regions. The non-linear component represented a sharp rise in signal magnitude when the TMS pulses were delivered around the rMT. Because this dose response profile was observed in both the stimulated and non-stimulated regions such as S2, they suggest that the non-linear component reflected, at least in part, cortical processing related to reafferent feedbacks in addition to a nonlinear recruitment of excitatory neurons. On the other hand, given that median nerve stimulation led to a stronger EMG activity than suprathreshold TMS, the same authors, by correcting for the movement size, estimated that muscle afferents-evoked activity could take account for ± 10 % of the signal evoked by suprathreshold TMS in M1 (Shitara et al., 2013).

The lack of significant hemodynamic changes after subthreshold TMS of M1 is surprising. Indeed, although unable to generate descending volleys sufficient to elicit a motor response, TMS pulses delivered at subthreshold intensity over M1 can induce changes in intracortical excitability as shown by paired-pulse techniques (Kujirai et al., 1993). Several hypothesis were put forward to account for the lack of activation in the target directly under the coil (Siebner et al., 2003). First, several studies reported a reduction in signal intensity in slices located in the direct vicinity of the TMS coil which could obscure subtle hemodynamic changes (Bohning et al., 1998; Bohning et al., 1999). Secondly, pulses of TMS could activate both excitatory and inhibitory neurons which could lead to a net synaptic activity insufficient to be translated in a significant BOLD response (Siebner et al., 2003; Bestmann et al., 2004). Differences in excitatory and inhibitory processes in both the

stimulated and remote regions could explain why BOLD responses evoked by subthreshold TMS are detectable only in remote interconnected regions (Hanakawa et al., 2009; Shitara et al., 2011). Moreover, the activation of the target by an electrical currents could lead to an axonal activation which requires less energy than the synaptic activation elicited in remote regions (Attwell and Laughlin, 2001). Therefore, more hemodynamic changes are observed in distant areas (synaptic activation) than in the target (axonal activation) (Hallett et al., 2017). Finally, the time course of the BOLD response elicited by TMS at the target and/or at distant sites could differ from the standard hemodynamic response functions (HRF) (Siebner et al., 2003). However, it has been shown that the standard HRF gives an adequate estimation of the TMS-evoked BOLD responses in both the stimulated M1 as well as in remote interconnected regions (Shitara et al., 2011). It has to be noted that consistent hemodynamic changes were evoked by short trains of TMS delivered at 100% of the rMT over the prefrontal cortex (Li et al., 2004; Hanlon et al., 2013). Although Nahas et al. (2001) and Bestmann et al. (2005) observed BOLD responses in the stimulated prefrontal cortex only for stimulus intensities above the rMT, TMS delivered at MT (Nahas et al., 2001) or below (Bestmann et al., 2005), while sufficient to elicit activity in distant regions including subcortical and contralateral regions, did not evoke hemodynamic activities at the stimulated site. These observations suggest the importance of several factors to elicit consistent responses directly under the coil such as the intensity of stimulation, the train length as well as the frequency of stimulation. For instance, Kemna and Gembris (2003) and Baudewig et al. (2001) used short-trains of 4 and 10 Hz for 1 s respectively

while other studies, which reported local activity, used longer trains, i.e. 1Hz-rTMS during 21 s (Nahas et al., 2001; Li et al., 2004) or 3 Hz-rTMS during 10 s (Bestmann et al., 2005). Several studies succeeded to obtain consistent responses with a small number of TMS pulses delivered either to the DLPFC or to the mPFC at a low frequency of stimulation (Hanlon et al., 2013; Hanlon et al., 2016), suggesting that different patterns of stimulation can be adequate to elicit a local response in different regions.

Most of earlier investigations using concurrent TMS-fMRI delivered short bursts of TMS at rest to induce changes in excitability in a given region while the activity changes in remote areas were assessed by neuroimaging techniques (Bestmann and Feredoes, 2013), according to the perturb and measure approach (Paus, 2005). Importantly, previous studies showed that the local and distant effects of TMS delivered on a specific region were dependent of the cortical excitability when pulses of TMS were delivered. For instance, the TMS intensities required to elicit a facilitation of the H-reflex, i.e. the threshold to evoke descending volleys in the cortico-spinal tract, is lower during a voluntary contraction than at rest (Mazzocchio et al., 1994). Furthermore, changes in both intra-cortical circuits (Ridding et al., 1995; Fujiwara and Rothwell, 2004; Ortu et al., 2008) and interhemispheric interactions (Ferbert et al., 1992) were reported during a tonic contraction (vs. at rest). Moreover, distinct patterns of TMS-evoked potentials were recorded in different phases of sleep (Massimini et al., 2005). By using concurrent TMS-fMRI, Bestmann et al. (2008b) showed that the functional interactions between various motor brain regions were dependent of the excitability of the motor system. Indeed, they observed that TMS of the left

premotor cortex induced an increased activity in both the contralateral dorsal premotor and M1 during an isometric voluntary contraction while a decreased activity was seen at rest. Later, Moisa et al. (2012) reported that, during a visuomotor task, the effect of TMS of the left premotor cortex on the right hemispheric motor areas was dependent of the mode of movement selection, i.e. freely selected movements vs. sequential movements according to a visuomotor association. In addition, by using concurrent TMS-fMRI, Blankenburg et al. (2008) showed that interhemispheric interactions between the right parietal cortex and the left S1 were dependent on the sensory context, i.e. whether or not the median nerve stimulation was delivered to the right hand. Bestmann et al. (2010), in chronic stroke patients, observed a stronger effect of contra-lesional premotor TMS on the BOLD responses evoked in the ipsi-lesional sensorimotor cortex during an active motor task (vs. at rest) in patients with more clinical motor impairments. Similarly, concurrent TMS-fMRI can also be used to investigate state-dependent top-down influences between brain regions. For example, distinct top-down influences of both parietal and frontal cortices on visual regions were identified by concurrent TMS-fMRI (Ruff et al., 2006; Ruff et al., 2008; Ruff et al., 2009). Moreover, by varying the baseline activity of the visual cortex, by using visual inputs at the time of parietal TMS deliverance, they obtained a pattern of activity changes in visual areas which were dependent of the visual context. Indeed, increasing TMS intensities delivered to the parietal cortex induced a decrease of the hemodynamic activity in the visual area V5. This was only observed when moving stimuli were presented. The opposite was shown for visual areas V1-V4, i.e. that

increasing parietal TMS led to an increase of BOLD signal in V1-V4 areas only when no visual inputs were presented (Ruff et al., 2008). Similar state-dependent top-down interactions were highlighted by concomitant TMS-fMRI in various domains such as multisensory integration (Leitao et al., 2013), visuospatial attention (Blankenburg et al., 2010; Heinen et al., 2011) and working memory (Feredoes et al., 2011). Together, these observations illustrate that, by delivering TMS pulses over a given brain region and by concomitantly recording the activity elicited by the TMS pulse in other brain areas by using concurrent fMRI, it can be possible to obtain an index of the cortical excitability and the effective connectivity between the stimulated and recorded brain regions. Moreover, this suggests that concurrent TMS-fMRI can be used to probe changes in functional connectivity related to distinct functional state of a given network of interconnected areas (Ruff et al., 2009). Finally, the concomitant use of TMS and fMRI can give insights in the functional significance of a given region inside a cortical network, opening the possibility to probe the functional interplay between brain areas (Bestmann et al., 2008c; Ruff et al., 2009).

Concurrent TMS-fMRI can also be used in a clinical context to investigate changes in brain activity and connectivity related to neurological/psychiatric disorders or to study the effects of pharmacologically active substances. Li et al. (2004) used interleaved TMS-fMRI in depressed patients to investigate whether TMS of the DLPFC produced hemodynamic changes in limbic regions. They recorded TMS-evoked BOLD responses in remote regions such as the bilateral prefrontal cortices, the right orbitofrontal cortex and the left hippocampus. However, their study did not include a control group,

preventing thus to compare the pattern of activation observed in depressed patients with that of healthy subjects. However, Hanlon et al. (2016) compared, by using concurrent TMS-fMRI, the connectivity of both the medial and lateral fronto-striatal circuits in healthy subjects vs. cocaine users. They observed that cocaine users showed less activation in the ventral striatal circuit in response to TMS of the mPFC while cocaine users did not show the decrease of BOLD response in the DLPFC observed in the control group (Hanlon et al., 2016). Furthermore, concurrent TMS-fMRI has been used to study the effect of psychoactive substances on brain excitability and connectivity. Several studies investigated the TMS-evoked activity patterns before vs. after the administration of both lamotrigine and valproic acid (Li et al., 2004; Li et al., 2010; Li et al., 2011). They observed that when TMS was applied to M1, the administration of both lamotrigine and valproic acid decreased the TMS-evoked hemodynamic responses in the stimulated M1 as well as in the premotor cortex and SMA. On the other hand, when the prefrontal cortex was stimulated, an increase of TMS-evoked BOLD responses in the ACC was observed after the administration of lamotrigine but not after taking valproic acid (Li et al., 2011). Again, these studies illustrate that TMS-fMRI can be a valuable tool to compare the effective connectivity in health and disease, or before vs. after taking neuroactive compounds.

6.5.5 Limitations of concurrent TMS-fMRI: non-specific hemodynamic effects of TMS

In addition to the neural activity evoked by the pulses of TMS at the target as well as in remote interconnected regions, TMS provokes both auditory and somatosensory sensations leading to hemodynamic activities in auditory and somatosensory regions (Bestmann et al., 2008c). For instance, TMS-evoked hemodynamic activities were evoked in superior and transverse temporal gyrus of both hemispheres extending up the *planum temporale* and the inferior frontal gyrus as well as at subcortical level where the inferior colliculi and the medial geniculate nuclei were activated bilaterally (Bestmann et al., 2004). The reason for that is the Lorentz forces in the coil winding which provoke small vibrations leading to the "click" sound (Bestmann et al., 2008c). Moreover, a startle-like response can be observed, especially at the beginning of the session. To control these unspecific effects, various strategies have been used. For example, some studies placed a plastic piece between the TMS coil and the scalp (Leitao et al., 2015; Leitao et al., 2017). Alternatively, the vertex can be used as a control site (Ricci et al., 2012) even though it has been shown that TMS delivered to the vertex induced a widespread decrease of hemodynamic activity (Jung et al., 2016). Recently, it has been shown that placing 3 cm of foam between the TMS coil and the scalp, which preserves the sensory aspects of TMS but decreases the strength of the TMS-induced magnetic field, also produced consistent hemodynamic responses in many of the same brain areas than active TMS (Dowdle et al., 2018). Indeed, TMS-evoked BOLD responses were found in the cingulate, the thalamus, the insula, and the

middle frontal gyri during both active and control conditions, when TMS was delivered to the left DLPFC. However, active TMS provoked higher BOLD responses in the anterior cingulate, caudate and thalamus compared to the control condition. This suggests that, to a certain extent, the TMS-evoked BOLD responses may be related to unspecific effects such as sensory or attentional aspects of TMS. This highlights the importance of control conditions.

Chapter 2. Overall objectives

The first part of the present work (chapters 3-5; Table 2.1) mainly focuses on characterizing pain-motor interactions in healthy individuals. The general objective was, by combining TMS of M1 with both brief and sustained nociceptive stimulation, to characterize the changes in motor excitability induced by various experimental pain models. In a first study (chapter 3), I combined laser stimulation with single pulses of TMS delivered over M1 to explore the limb specificity and the time course of the effects of a transient nociceptive stimulus on motor excitability. I hypothesized that a transient nociceptive stimulus could modulate motor system excitability, potentially differentially (1) within the muscles of the ipsilateral vs. contralateral limb relative to where the nociceptive stimulus was applied and (2) within muscles involved vs. not involved in the withdrawal of the stimulated limb. This was assessed by using TMS of the left and right M1 to elicit MEPs in proximal and distal flexor and extensor muscles of both arms. To assess the time-course of nociception-motor interactions, the TMS pulses were triggered 50-2000 ms after delivering short-lasting nociceptive stimuli, generated by an infrared CO_2 laser stimulator, to the left or right hand dorsum.

In a second study (chapter 4), the onset latency of the motor responses elicited by the preferential activation of nociceptors using intra-epidermal electrical stimulation (IES) of the sole of the foot were compared to the reflex responses elicited by a more conventional technique using high-intensity transcutaneous electrical stimulation (TES) which activates

preferentially non-nociceptive afferents. The NWR constitutes an effective mean to quickly withdraw the lower limb from potentially tissue-damaging threats. In most studies, high-intensity TES delivered by large surface electrodes are used to elicit the NWR. Due to the unavoidable activation of non-nociceptive afferents by such a stimulus, the resulting motor response is composed of two electromyographic (EMG) bursts, the RII and RIII components, conveyed respectively by non-nociceptive and nociceptive fibers. Most of the time, these two components overlap each other, leading the researchers to use time windows aiming to minimize the contribution of the RII component. In chapter 4, I wanted to characterize the EMG responses recorded from lower limb muscles elicited by the *preferential* activation of nociceptors by using IES of the sole of the foot. Responses elicited by IES in a number of neck and upper limb muscles were also recorded in order to investigate whether the IES-evoked responses could be contaminated by a muscle activity of supraspinal origin, such as the startle reaction. I hypothesized that the IES-elicited motor responses would be preferentially related to nociceptive inputs and, hence, should be delayed with respect to the responses elicited by TES.

In a third study (chapter 5), by using a similar approach to the one in chapter 3, I characterized the changes in the TMS-mapped representation of several muscles following the induction of secondary mechanical hyperalgesia by HFS of the skin. Here, our aim was to characterize changes in the motor system induced by a sustained nociceptive stimulus generating central sensitization. Experimentally, it is possible to induce a mechanical hyperalgesia in the secondary zone by HFS of the human skin (Klein et al.,

2004). I therefore determined the effects of HFS of the skin on the cortical motor map generated by TMS. I hypothesized that, in addition to inducing central sensitization of nociceptive pathways at the level of the spinal cord, HFS of human skin may also induce sustained activity-dependent changes at the supraspinal level. Moreover, because of consistent pain-motor interactions in chronic pain patients (Parker et al., 2016; Chang et al., 2018), I made the assumption that this sustained activation also provokes changes outside the nociceptive system, i.e. in the motor system.

Finally, the general objective of the second part of this dissertation (chapter 6; Table 2.1) was the development of a novel approach based on the recording of TMS-evoked BOLD responses sampled by means of concurrent TMS-fMRI. This approach could subsequently be used to study chronic pain-related changes in brain function. Recently, the recording of fMRI-BOLD responses elicited by TMS applied over a given brain region has been proposed as a potential non-invasive tool to measure directly, at a given moment in time, the functional connectivity between brain regions. In chapter 6, I present the method that I developed to combine online TMS with fMRI to study changes in brain connectivity. Our specific aim was to validate the recording of BOLD responses elicited by TMS over the DLPFC. The combination of TMS and fMRI is methodologically challenging due to the strong magnetic fields generated by the two methods. Practically, the limited space provided by birdcage MRI coils, most often used in concurrent TMS-fMRI studies, can be an obstacle to place the TMS coil over lateral or frontal brain regions. Therefore, to place the TMS coil over the DLPFC, the MRI data were collected using two flexible surface MRI coils rather than a

rigid birdcage coil. Our specific aim was to validate the recording of BOLD responses elicited by TMS over the DLPFC by delivering pulses of TMS inside a flexible MRI coil. A second identical MRI coil was placed at the other side of the head to collect MRI data of the entire brain.

Section 6.3 and 6.4 of chapter 1 is dedicated to methodological considerations about concurrent TMS-fMRI. A comment about structural and functional changes of the DLPFC in various chronic pain conditions is provided in section 6.1 of the same chapter. Chapter 6 presents the method I developed to combine TMS delivered over the DLPFC with fMRI by using flexible surface MRI coils.

Table 2.1

	Objectives and hypotheses
Chapter 3.	**Objective:** characterize the temporal profile of the modulatory effect of transient nociceptive stimulation on the excitability of the motor system. **Hypothesis:** phasic pain delivered to the hand dorsum should facilitate a purposeful defensive reaction in the stimulated limb, which would be reflected in a limb-specific and time-dependent modulation of motor excitability within the flexor muscles involved in the withdrawal of the stimulated limb.
Chapter 4.	**Objective:** characterize the reflex elicited by preferential activation of nociceptors by using IES of the sole of the foot. **Hypothesis:** IES-elicited motor responses would be preferentially related to nociceptive inputs and, hence, should be delayed with respect to the responses elicited by TES.
Chapter 5.	**Objective:** characterize changes in motor function induced by a sustained nociceptive stimulus generating central sensitization (HFS). **Hypothesis:** in addition to inducing central sensitization of the nociceptive pathways at the level of the spinal cord, the intense activation of nociceptors may also induce sustained activity-dependent changes at supraspinal level.
Chapter 6.	**Objective:** validate the recording of BOLD responses elicited by TMS over the DLPFC by delivering pulses of TMS inside a flexible MRI coil. **Hypothesis:** this original approach to conduct concurrent TMS-fMRI studies could overcomes some practical issues encountered when usual birdcage MRI coils are used, i.e. the restricted space to place the TMS coil, especially when frontal or lateral regions are targeted.

Table 2.1. Objectives and hypotheses of chapters 3-6.

Chapter 3. Temporal profile and limb-specificity of phasic pain-evoked changes in motor excitability

Algoet M., Duque J., Iannetti G., Mouraux A. Temporal profile and limb-specificity of phasic pain-evoked changes in motor excitability. Neuroscience 2018; 386: 240-255

Abstract

A fundamental function of nociception is to trigger defensive motor responses to threatening events. Here, we explored the effects of phasic pain on the motor excitability of ipsilateral and contralateral arms. We reasoned that the occurrence of a short-lasting nociceptive stimulus should result in a specific modulation of motor excitability for muscles involved in the withdrawal of the stimulated limb. This was assessed using transcranial magnetic stimulation (TMS) of the left and right primary motor cortex to elicit motor-evoked potentials (MEPs) in three flexor and two extensor muscles of both arms. To assess the time-course of nociception-motor interactions, the TMS pulses were triggered 50-2000 ms after delivering short-lasting nociceptive laser stimuli to the left or right hand. We made three main observations. First, nociceptive stimuli induced an early-latency (100 ms) enhancement of MEPs in flexor muscles of the stimulated hand. Considering its latency, this modulation is likely consequent to nociceptive-motor interactions at spinal level. This early and lateralized enhancement was followed by a later (150-400 ms) MEP reduction in extensor muscles of the stimulated hand and flexor muscles of both hands, predominant at the

stimulated hand. Finally, we observed a long-lasting (600-2000 ms) MEP enhancement in muscles of the non-stimulated hand. These later effects of the nociceptive stimulus could reflect nociception-motor interactions occurring at cortical level.

1. Introduction

Because of its intrinsic aversive nature, pain strongly influences behavior. For example, following a lesion, pain-related changes in motor behavior can protect from further injury and promote recovery (Hodges and Tucker, 2011; Burns et al., 2016b). Most importantly, the ability to generate swift motor responses to the detection of a sudden noxious stimulus is crucial to prevent or limit injury, and is thus essential for survival (Iannetti and Mouraux, 2010). Nociception-evoked motor responses imply the existence of strong interactions between nociceptive and motor systems (Bank et al., 2013). Such interactions have been clearly demonstrated at spinal level. For example, nociceptive stimulation of the foot elicits a spinal nociceptive withdrawal reflex (NWR) resulting in a simultaneous activation of flexor muscles and inhibition of extensor muscles of the stimulated limb (Sandrini et al., 2005). Interestingly, this nociceptive response could encompass several reflex modules, each having a characteristic reflex-evoking receptive field, and controlling one or more synergistic muscles (Schouenborg and Kalliomaki, 1990; Andersen et al., 1999). The elicited muscular response would thereby be dependent on the location of the nociceptive stimulus (Andersen, 2007). Similarly, it was shown that high-intensity electrical stimulation of the nociceptive afferents of a digital nerve can transiently interrupt the voluntary muscle contraction of the stimulated limb through spinal inhibitory circuits (Merton, 1951; Caccia et al., 1973; Kranz et al., 1973; McLellan, 1973; Uncini et al., 1991; Inghilleri et al., 1997; Floeter, 2003; Kofler, 2003).

There is also evidence supporting the existence of nociception-motor interactions at cortical level, but these interactions have not been characterized as extensively. For example, Frot et al. (2013) found, using depth electrodes implanted in the pre- and post-central gyri of epileptic patients, that brief nociceptive stimuli delivered to the hand dorsum elicit early-latency responses in the contralateral primary motor cortex (M1), peaking approximately 170 ms after stimulus onset.

A more direct approach to characterize *modulatory* effects of nociception on the motor system at cortical level is to assess the effect of nociceptive stimuli on the motor-evoked potentials (MEPs) elicited by transcranial magnetic stimulation (TMS) of M1 (Hallett, 2000; Bestmann and Duque, 2015). Using this approach, Valeriani et al. (1999; 2001) found, in studies performed in five healthy volunteers, that noxious heat stimuli delivered to the hand dorsum exert an early (170-270 ms) and transient inhibition of MEPs recorded from the *first dorsal interosseous* muscle (FDI) (Valeriani et al., 1999) and *biceps brachialis* (BB) (Valeriani et al., 2001) of the stimulated limb. This inhibition was interpreted as resulting from a change in excitability at cortical level, because MEPs evoked by anodal electrical stimulation of M1, which is thought to directly activate the cortico-spinal tract, were unaffected by the nociceptive stimulus.

Here, we aimed to characterize the temporal profile of the modulatory effect of transient nociceptive stimulation of the hand dorsum skin on the excitability of the motor system controlling a number of muscles of the hand and upper limb ipsilateral and contralateral to the stimulated hand. We hypothesized that phasic pain delivered to the hand dorsum facilitates a

purposeful defensive reaction in the stimulated limb, which would be reflected in a limb-specific and time-dependent modulation of motor excitability within the flexor muscles involved in the withdrawal of the stimulated limb.

2. Experimental procedures

2.1 Participants and experimental design

Ten subjects took part in the experiment (5 men), aged 20-24 years (22 ±1; mean ± standard deviation). None of the participants had a history of neurological or psychiatric disorder, and all were naive to the purpose of the study. All participants gave written informed consent and received a financial compensation for their participation. The protocol was approved by the institutional ethics committee of the Université catholique de Louvain in accordance to the Declaration of Helsinki.

The experimental design is detailed in Figure 3.1. We examined the effect of a nociceptive stimulus delivered to the left or right hand dorsum on the MEPs elicited in flexor (FDI, *flexor carpi radialis*; FCR) and extensor (*extensor carpi radialis*; ECR) muscles of the left and right hand.

The time course of the possible modulatory effects of the laser stimulus on motor excitability was characterized by varying the delay between the onset of the laser stimulus and the onset of the TMS pulses delivered over the left and right M1.

We also conducted a supplementary experiment in which we aimed to assess the effects of nociceptive stimulation on two proximal muscles of the

upper limb controlling the flexion (BB) and extension (*triceps brachialis*, TB) of the forearm. The design of this experiment was almost the same as that of the main experiment (see below).

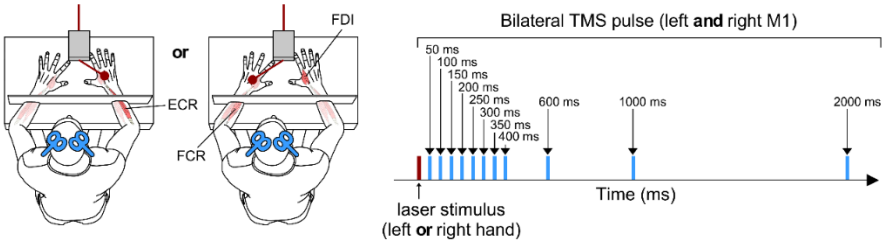

Figure 3.1. Experimental design. MEPs were recorded from intrinsic and extrinsic muscles of both hands (flexors: FDI, FCR; extensor: ECR) using quasi-concomitant stimulation of the left and right M1 (TMS inter-pulse interval: 1 ms). Intrinsic (FDI) and extrinsic (FCR, hatched in the figure, anatomically more anterior than ECR) muscles of the hand are schematically shown. TMS pulses were systematically preceded by a nociceptive laser stimulus delivered either to the left or to the right hand. The time-interval between the laser stimulus (shown in red) and the TMS pulse (shown in blue) was 50, 100, 150, 200, 250, 300, 350, 400, 600, 1000 or 2000 ms (Adapted from Figure 1 in Algoet et al. (2018)).

2.2 Nociceptive stimulation

Participants were seated in a comfortable chair in a dimly-lit room with their arms placed on a cushion and their hand palms resting on a table (Figure 3.1). A small curtain occluded vision of the hands and laser stimulus. Therefore, participants were not aware of which hand was going to be stimulated. High-intensity nociceptive stimuli were 50 ms pulses of radiant

heat generated by an infrared CO_2 laser stimulator (wavelength 10.6 µm; Université catholique de Louvain; Plaghki L. et al. (1994)). The target of the laser stimulator was visualized by a coaxial He-Ne laser beam, and controlled using two mirrors mounted on a computer-controlled 2-axis galvanometer (LSST-10.6-12-105-8062-3A, Sintec Optronics, Singapore). The stimuli were delivered to the left or right hand dorsum, in random order. Beam surface area at target site was 80 mm^2. To avoid skin overheating and nociceptor fatigue or sensitization, the target of the laser beam was displaced to a random position on the hand dorsum after each pulse. The minimum distance between two consecutive pulses on the same hand was set to 20 mm. In a preliminary session, laser stimuli of variable energy were delivered to the hand dorsum such as to determine the energy at which the stimuli elicited a clear painful pinprick sensation, detected with reaction times compatible with the conduction velocity of Aδ-fibers (<650 ms; Mouraux et al. (2003)). The same intensity was used on the two hands and kept constant throughout the whole experimental session.

2.3 Transcranial Magnetic Stimulation and MEP recording

Participants were asked to relax their muscles. Motor responses were obtained simultaneously from the left and right hand, using two figure-of-eight coils (wing internal diameter: 35 mm) positioned over the hand representation of the right and left M1. We chose to record MEPs simultaneously from three different muscles to decrease the total number of TMS pulses required to conduct the experiment, a factor known to induce changes in motor cortex excitability (Pellicciari et al., 2016); and the total

number of laser stimuli, a factor that can lead to nociceptor habituation or sensitization (Bromm and Treede, 1987; Raij et al., 2003). Moreover, it ensured that the responses from all three muscles were recorded in the same state of vigilance and attentiveness (Derosiere et al., 2015).

Monophasic TMS pulses (approx. 0.1 ms rise time and 1 ms total duration) were generated using two Magstim 200 magnetic stimulators (Magstim, Whitland; UK). A 1-ms inter-pulse interval separated the onset of the two pulses, and the order of the two pulses was randomized across trials. The two pulses of TMS were not simultaneous to reduce physical interactions between the electrical fields induced by each of the two coils (Cincotta et al., 2005). A 1-ms inter-pulse interval was chosen as this interval is sufficiently short to avoid inhibitory (Ferbert et al., 1992) or facilitatory (Hanajima et al., 2001) interactions between the two hemispheres. This double-coil TMS approach using a 1-ms inter-pulse interval has been recently validated by Grandjean et al. (2018), in a study showing that MEPs obtained using the double-coil approach to stimulate the left and right M1 are similar to those elicited by single-coil stimulation of the left or right M1. It was also shown to be an effective approach to study cortico-spinal excitability within the context of a motor task (Vassiliadis et al., 2018).

After fitting the participant with an elastic fabric head cap (Electro-cap International, USA), the coils were positioned tangentially to the scalp, with the handle pointing toward the back of the head 45° away from the midline, approximately perpendicular to the central sulcus.

Electromyographic (EMG) signals were recorded using surface electrodes (Ambu, BlueSensor NF-50-K/12/EU, Ballerup, Denmark) placed over the FDI,

FCR and ECR muscles of both hands. The signals were amplified and bandpass filtered on-line (4-1500 Hz) using a Neurolog signal conditioner (Digitimer; Hertfordshire, UK), and digitized at 5000 Hz using a CED 1401 (Cambridge Electronics Design; UK).

For each hemisphere, we first identified the optimal coil location to obtain MEPs simultaneously in the contralateral FDI, FCR and ECR muscles. This location was marked on the cap to provide a reference point throughout the experiment. We then determined the minimum intensity required to elicit a measurable MEP in the FCR muscle (peak-to-peak MEP amplitudes >50 μV) in 5 out of 10 trials. For both left and right FCR muscles, the mean resting motor threshold (rMT) amounted to 43 ±4% and 43 ±5% of maximum stimulator output, respectively. The intensity of TMS used for the experiment was then set to 120% of this value.

2.4 Recording of MEPs following nociceptive stimulation

Each trial started by the delivery of a nociceptive laser stimulus to a random position on the left or right hand dorsum. The laser stimulus was always followed by a TMS pulse delivered with a variable interval.

The time intervals between the onset of the laser stimulus and the delivery of the TMS pulses (inter-stimulus interval; ISI) were 50, 100, 150, 200, 250, 300, 350, 400, 600, 1000 or 2000 ms (Figure 3.1). The trials were presented in five blocks. Within each block, each trial type was repeated two times, resulting in 44 trials per block (2 x 11 time intervals x 2 laser stimulus locations). The order of the trials was pseudo-randomized across blocks. At the end of each trial (3-4 s after the onset of the laser stimulus), a warning

tone prompted the participant to report the intensity of the percept elicited by the laser stimulus using a numerical rating scale (NRS) extending between 0 (no sensation) to 10 (most intense sensation). The inter-trial interval was 6-7 seconds.

2.5 Statistical analyses

2.5.1 Effect of the nociceptive laser stimulus on MEP amplitudes

For each muscle, MEP amplitudes were estimated by measuring the maximum peak-to-peak amplitude of the TMS-evoked EMG response (Figure 3.2). MEP amplitudes were expressed as the percentage of change relative to the average amplitude of the MEPs obtained in both limbs at ISI=50 ms, which served as control (Figure 3.3). The rationale for this approach is that 50 ms after the onset of the rise in skin temperature generated by the laser stimulus, the afferent volley generated by the activation of heat-sensitive nociceptors has not yet reached the spinal cord (because of the time required to reach the thermal activation threshold of these nociceptors, the time required for neural transduction, and the peripheral conduction time) (Bromm and Treede, 1984). Therefore, at ISI=50 ms, the nociceptive afferent volley cannot interact with the descending motor volley generating the MEPs.

If the laser stimulus has no time-dependent effect on motor excitability, the average amplitude of the MEPs elicited 100-2000 ms after the laser stimulus should tend towards the average amplitude of the MEPs elicited at ISI=50 ms of the corresponding side. Therefore, for each limb and for each muscle,

MEP amplitudes obtained at ISIs 100-2000 ms were compared using paired sample t-tests to the MEP amplitudes obtained at ISI=50 ms to assess the time-intervals at which they were either increased or decreased. The results of this first-step analysis was then used to cluster ISIs in four categories prior to comparing changes in motor excitability at the stimulated and non-stimulated limbs. Cluster 1 corresponded to the average MEP amplitude at ISI=50 ms, serving as control. As detailed in the Results section, cluster 2 corresponded to an early-latency increase of MEPs observed in FDI and FCR muscles at ISI=100 ms. Cluster 3 corresponded to a later reduction of MEPs observed in all three muscles at ISIs=150-400 ms. Finally, cluster 4 corresponded to a late and prolonged MEP facilitation observed in ECR and FDI muscles at ISIs=600-2000 ms. Using the average amplitude of the MEPs obtained at the ISIs belonging to each cluster, the differential effect of the laser stimulus on motor excitability at the laser-stimulated limb and at the contralateral non-laser-stimulated limb was assessed separately for each muscle (FDI, FCR, ECR), using a two-way repeated-measures ANOVA with the factors *'ISI cluster'* (four levels: clusters 1-4) and *'side'* of the limb onto which the nociceptive stimulus was applied (two levels: stimulated and non-stimulated limbs). In this analysis, a main effect of *'ISI cluster'* on MEP amplitudes would indicate a global non-limb-specific effect of the nociceptive stimulus on motor excitability, whereas the presence of an interaction between the factors *'ISI cluster'* and *'side'* would indicate a limb-specific effect of the nociceptive stimulus on motor excitability.

The Kolmogorov-Smirnov test was used to assess the assumption of normality. For some measures (4/24), the assumption of normality was

violated according to this test. Importantly, simulation studies have shown that F-tests control well the false positive rate under conditions of non-normality (Glass et al., 1972; Harwell et al., 1992; Lix et al., 1996), suggesting that F-tests remain robust under conditions of non-normality, especially when group sizes are equal (Donaldson, 1968). A Greenhouse-Geisser correction for violations of sphericity was used when appropriate. When justified, post-hoc comparisons of the responses were performed using paired sample t-tests, as follows. For each cluster, MEP amplitudes obtained at the stimulated limb were compared to the MEP amplitudes obtained at the non-stimulated limb to assess the time-intervals at which the laser stimulus differentially affected excitability in the two limbs. Reported p-values were not corrected for multiple comparisons (Rothman, 1990; Feise, 2002). Significance threshold was set at $p<0.05$.

2.5.2 Relationship with background EMG activity

Variations in EMG background activity could have contributed, at least in part, to differences in MEP amplitudes. Therefore, the background EMG activity was estimated by computing the root-mean-square (RMS) amplitude from -100 ms to the onset of each TMS pulse. For each muscle, the average RMS amplitudes obtained at the different ISIs were compared using a two-way repeated-measures ANOVA with the factors *'ISI cluster'* (four levels: clusters 1-4) and *'side'*.

2.5.3 Relationship with intensity of perception

We also examined whether the effect of the nociceptive stimulus on MEP amplitudes was dependent on the reported intensity of perception. For this purpose, a median split was used to separate the trials of each participant in two categories of equal size (low vs. high-intensity of perception). For each muscle, the average MEP amplitudes obtained across the different conditions were then compared using a three-way repeated-measures ANOVA with the factors *'ISI cluster'* (four levels: clusters 1-4), *'side'* and *'perception'* (low vs. high-intensity of perception). In this analysis, a main effect of *'perception'*, or an interaction between the factors *'perception'* and the factors *'ISI cluster'* or *'side'* would indicate that nociceptive stimuli perceived as more or less intense do not exert the same effect on motor excitability.

2.5.4 Baseline MEPs recording

A baseline recording of MEPs was performed at the beginning and at the end of the experiment (20 TMS pulses delivered using a constant 6-7 s inter-trial interval), to assess potential inter-block cumulative effects of the repeated TMS pulses (Pellicciari et al., 2016) and/or differences related to hand dominance (Triggs et al., 1994). The average amplitude of the MEPs obtained at the two baseline measurements were compared using a two-way repeated-measures ANOVA with the factors *'time'* (beginning vs. end of the experiment) and *'dominance'* (MEPs recorded from the dominant vs. non-dominant limb).

2.5.5 Supplemental experiment

In order to assess the effect of a nociceptive stimulus delivered to the hand dorsum on more proximal muscles controlling the flexion (BB) and extension (TB) of the forearm, we conducted a supplemental experiment on seven healthy participants (4 men), aged 22-24 years (23 ± 1). Such as in the main experiment, the laser stimuli were delivered to the left or right hand dorsum, in random order. Because it was not possible to position two coils over the more medial M1 representation of proximal upper-limb muscles, only one hemisphere was stimulated, using a single figure-of-eight coil (wing internal diameter: 45 mm) over the right or left M1. EMG signals were recorded using surface electrodes placed over the BB and TB muscles of either the dominant hand (3 participants) or the non-dominant hand (4 participants). After having identified the optimal coil location to obtain MEPs in both muscles, the minimum intensity required to elicit measurable MEPs in the BB muscles was determined (peak-to-peak MEP amplitudes >20 µV in 5 out of 10 trials). The mean rMT of the left and right BB muscle amounted to 64 ±7% and 68 ±3% of maximum stimulator output, respectively. The intensity of TMS used for the experiment was then set to 120% of this value. On the basis of the results of the main experiment, the time intervals between the laser stimulus and the TMS pulse were 50, 100, 250, 300 or 1000 ms. Trials were presented in five blocks. Within each block, each trial combination was repeated four times, resulting in 40 trials per block (4 x 5 time intervals x 2 laser stimulus locations). Maximum peak-to-peak MEP amplitudes were measured and expressed as the percentage of change relative to the average amplitude of the MEPs obtained at both limbs at ISI=50 ms. For each muscle,

the average amplitude of the MEPs was compared using a two-way repeated-measures ANOVA with the factors *'ISI'* (50, 100, 250, 300, and 1000 ms) and *'side'* of the limb onto which the nociceptive stimulus was applied (stimulated vs. non-stimulated hand).

3. Results

3.1 Nociception-motor interactions in flexor and extensor muscles of the hand

3.1.1 Effect of the nociceptive laser stimulus on MEP amplitudes

Consistent MEPs were recorded from all three muscles controlling flexion and extension of the hands (Figure 3.2). The nociceptive stimulus appeared to induce a consistent sequence of changes in MEP amplitude in all three muscles (Figure 3.3). The paired-sample comparison of the MEP amplitudes obtained at ISI=50 ms with the MEP amplitudes at ISIs 100-2000 ms in each muscle led us to group the different ISIs in four separate clusters (Table 3.1). Cluster 1 consisted in the MEPs obtained at ISI=50 ms, serving as control. Cluster 2 consisted in the MEPs obtained at ISI=100 ms. At this early-latency ISI, an increase in amplitude was observed in the FDI and FCR muscles. Cluster 3 consisted in the MEPs obtained at ISIs 150-400 ms. At these ISIs, a reduction of amplitude was observed in all three muscles. Finally, cluster 4 consisted in the MEPs obtained at ISIs 600-2000 ms. At these ISIs, a late and prolonged increase was observed in ECR and FDI muscles of the non-laser-stimulated hand.

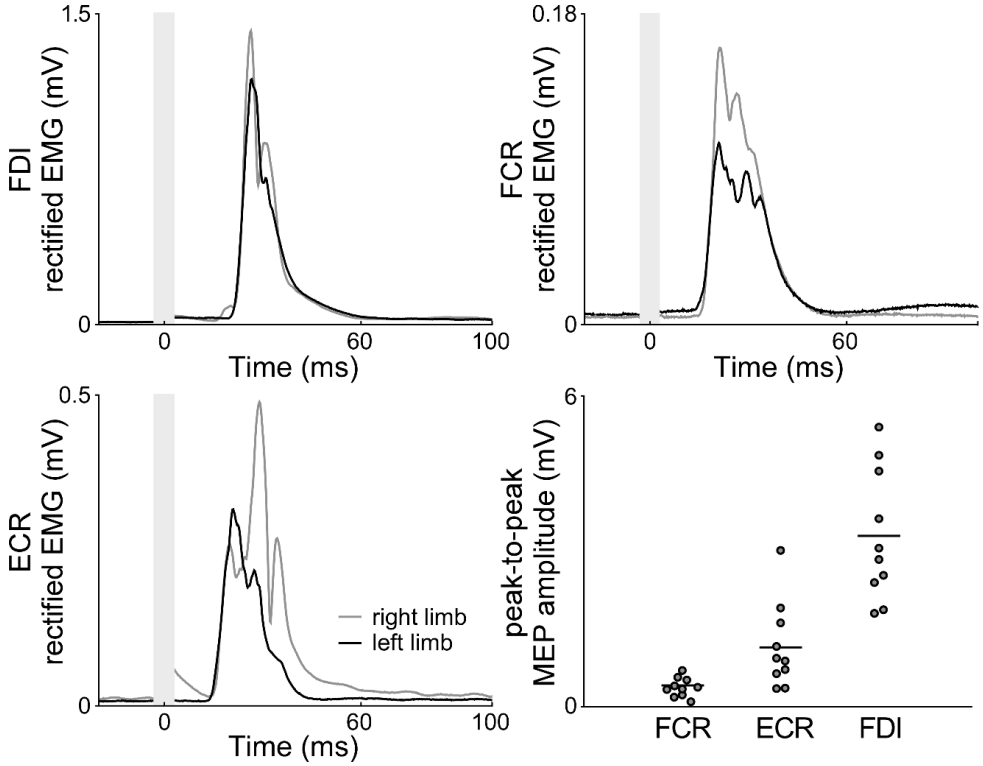

Figure 3.2. Group-level average rectified EMG time courses of the MEPs recorded at ISI=50 ms from left and right FDI, FCR and ECR muscles. Subject- and group-level average ±SD peak-to-peak amplitude of the MEPs recorded from the different muscles. Note that consistent MEPs were recorded from all muscles, but that their magnitude varied greatly across muscles (Adapted from Figure 2 in (Algoet et al. (2018))).

Table 3.1.

ISI (ms)	100	150	200	250	300	350	400	600	1000	2000
Laser-stimulated hand										
FDI	**.006***	**.004****	**.002****	.198	.159	.258	.054	.884	.135	**.042***
FCR	**.023***	**.028***	**.007***	**.026***	.056	.093	**.013***	.921	.1	.128
ECR	.05	.083	.052	.151	.072	.212	**.019***	.339	.453	.06
Non-laser-stimulated hand										
FDI	.354	**.037***	.169	.675	.777	.399	.319	.068	**.012***	**.023***
FCR	.596	.128	.077	.304	.182	.889	.663	.271	.056	.128
ECR	.344	.196	.86	.313	.498	.107	.173	**.017***	**.004****	**<.001****

Table 3.1. Nociception-motor interactions in flexor and extensor muscles of the hand. Time course of the effects of the nociceptive stimulus on the MEPs elicited in the FDI, FCR and ECR muscles of the laser-stimulated and non-laser-stimulated hands. For each limb, MEP amplitudes obtained at ISIs 100-2000 ms were compared to the MEP amplitudes obtained at ISI=50 ms using paired-sample t-tests. Significant increases and decreases in MEP amplitudes are shown in red and blue, respectively. The degrees of freedom are equal to nine for all paired-sample t-tests. * $p<0.05$; ** $p<0.005$

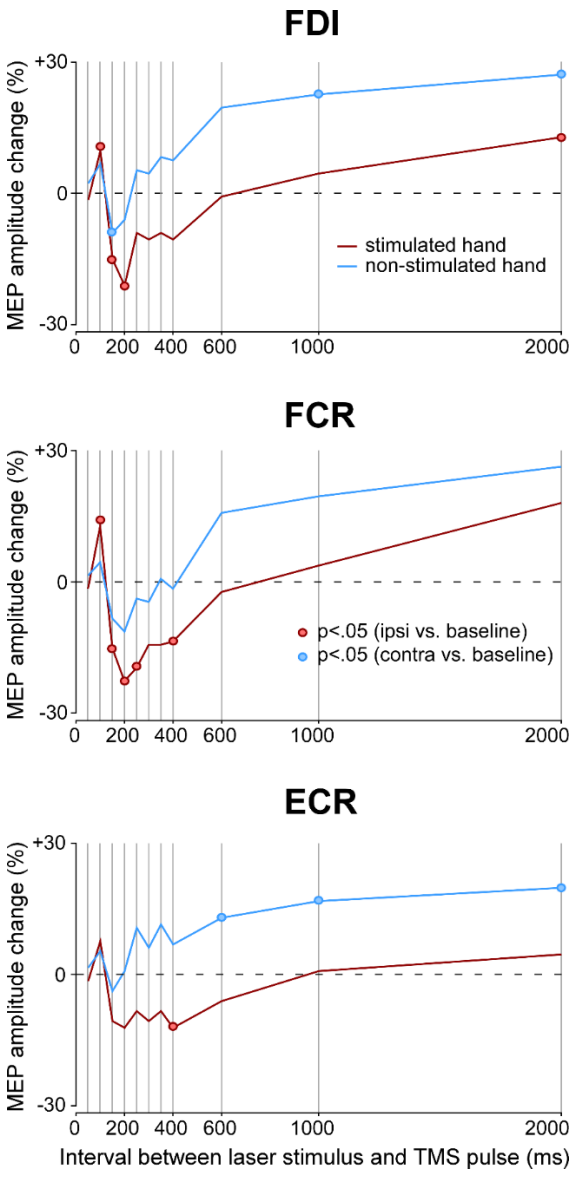

Figure 3.3. Effect of the nociceptive laser stimulus delivered to the hand dorsum on the magnitude of the MEPs elicited in flexor (FDI, FCR) and extensor (ECR) muscles of the laser-stimulated hand (red) and non-laser-stimulated hands (blue). X-axis: time-interval between the onset of the nociceptive laser stimulus and the onset of the TMS pulse. Y-axis: MEP amplitude, expressed as the percentage of change relative to the MEPs obtained at ISI=50 ms. The red and blue dots show the time points at which the change in MEP amplitudes was significantly different from MEPs recorded at ISI=50 ms (Adapted from Figure 3 in Algoet et al. (2018)).

For each of the three muscles, the repeated-measures ANOVA showed a significant interaction between the factors *'ISI cluster'* and *'side'* (laser-stimulated limb vs. non-laser-stimulated limb), indicating that the nociceptive stimulus had a differential effect on the magnitude of the MEPs recorded from muscles of the laser-stimulated limb as compared to the non-laser-stimulated limb (Table 3.2).

Table 3.2.

Factors		FDI			FCR			ECR	
ISI cluster	$F_{3,27}$=6.84	**p=.001****	η^2=.432	$F_{1.5,13.5}$=7.61	**p=.009***	η^2=.458	$F_{3,27}$=5.81	**p=.003****	η^2=.392
side	$F_{1,9}$=10.92	**p=.009***	η^2=.548	$F_{1,9}$=7.7	**p=.022***	η^2=.461	$F_{1,9}$=26.32	**p=.001****	η^2=.745
ISI x side	$F_{3,27}$=9.5	**P<.001****	η^2=.513	$F_{1.27,11.4}$=5.1	**p=.039***	η^2=.36	$F_{1.4,12.8}$=9.9	**p=.005***	η^2=.523

Table 3.2. Two-way repeated-measures ANOVA comparing, for each flexor/extensor muscle of the hand (FDI, FCR, ECR), the MEPs elicited by TMS pulses delivered 50 ms (ISI cluster 1), 100 ms (ISI cluster 2), 150-400 ms (ISI cluster 3) and 600-2000 ms (ISI cluster 4) after the onset of the nociceptive stimulus (factor 'ISI cluster'), and recorded from muscles of the laser-stimulated and non-laser-stimulated hands (factor 'side'). * $p < 0.05$; ** $p < 0.005$

For cluster 2 (ISI=100 ms), post-hoc comparisons of the MEPs obtained at the laser-stimulated and non-laser-stimulated limbs showed that the early-latency enhancement of MEPs was significantly greater in the FCR muscle of the laser-stimulated hand as compared to the non-laser-stimulated hand (Table 3.3 and Figure 3.4). For cluster 3 (ISIs 150-400 ms), the mid-latency reduction of MEPs was significantly stronger in all three muscles of the laser-stimulated limb as compared to the non-laser stimulated limb. Finally, for cluster 4 (ISIs 600-2000 ms), the amplitudes of the MEPs obtained from the FDI and ECR muscles of the non-laser-stimulated limb were significantly greater as compared to the same muscles of the laser-stimulated limb.

Table 3.3.

	FDI	FCR	ECR
Cluster 2 ISI=100 ms	.369	**.049***	.629
Cluster 3 ISI=150-400 ms	**<.001****	**.001****	**<.001****
Cluster 4 ISI=600-2000 ms	**.012***	.081	**<.001****

Table 3.3. Post-hoc comparisons (paired-sample t-tests) of the MEPs elicited in the FDI, FCR and ECR muscles of the laser-stimulated and non-laser-stimulated hands, at ISI=100 ms (cluster 2), ISI=150-400 ms (cluster 3) and ISI=600-2000 ms (cluster 4). The degrees of freedom are equal to nine for all paired-sample t-tests. * $p<0.05$; ** $p<0.005$

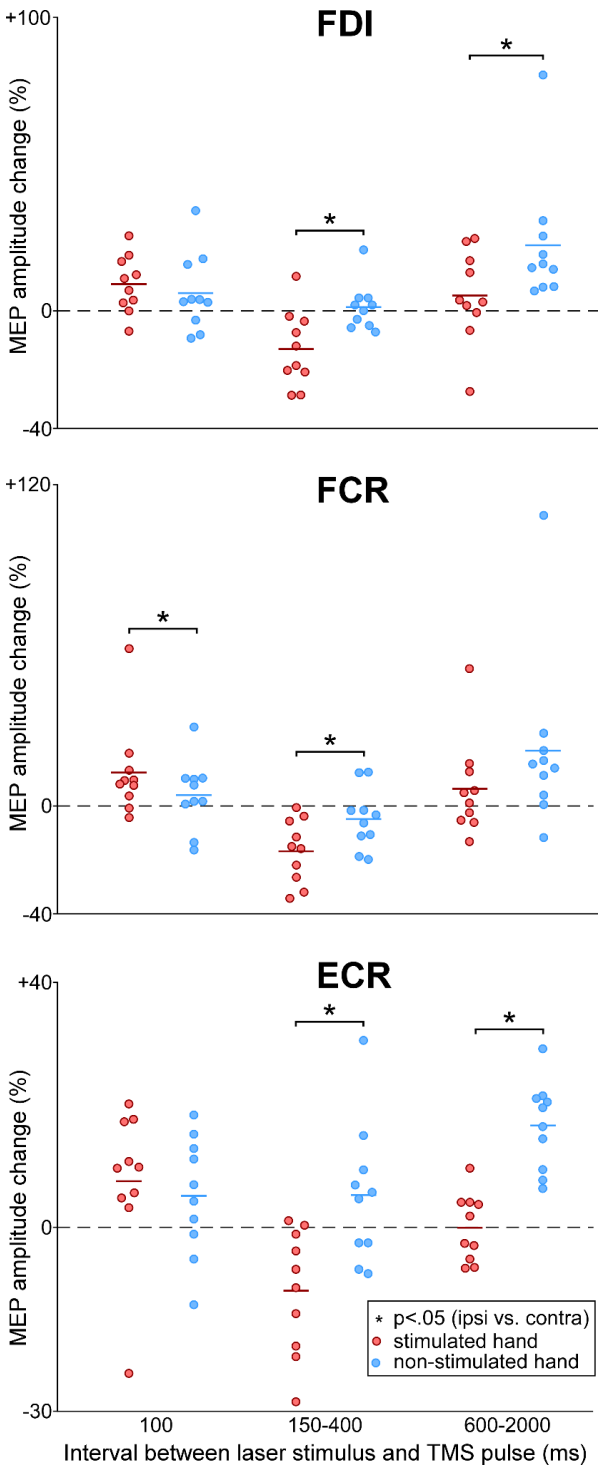

Figure 3.4. Subject- and group-level average ±SD of the MEPs expressed as the percentage of change in MEP amplitude in the FDI, FCR and ECR muscles of the laser-stimulated and non-laser-stimulated limb at ISI=100 ms (cluster 2), ISI=150-400 ms (cluster 3) and ISI=600-2000 ms (cluster 4), relative to the MEPs obtained at ISI=50 ms (cluster 1). The asterisks indicate the clusters at which the magnitude of the MEPs obtained at the laser-stimulated and non-laser-stimulated limbs were significantly different from one another (paired-sample t-tests) (Adapted from Figure 4 in Algoet et al. (2018)).

3.1.2 Background EMG activity

In all muscles, the two-way repeated-measures ANOVA conducted on the measures of background EMG activity showed no main effect of *'side'* (FDI: $F_{(1,9)}$=0.33, p=0.578, η^2=0.036; FCR: $F_{(1,9)}$=0.36, p=0.566, η^2=0.038; ECR: $F_{(1,9)}$=0.14, p=0.718, η^2=0.015), no main effect of *'ISI cluster'* (FDI: $F_{(3,27)}$=2.38, p=0.092, η^2=0.209; FCR: $F_{(1.4,12.1)}$=3.81, p=0.065, η^2=0.297; ECR: $F_{(1.4,12.5)}$=0.51, p=0.546, η^2=0.054), and no interaction between the two factors (FDI: $F_{(3,27)}$=0.28, p=0.841, η^2=0.03; FCR: $F_{(1.3,12)}$=1.87, p=0.199, η^2=0.172; ECR: $F_{(3,27)}$=0.28, p=0.841, η^2=0.03).

3.1.3 Intensity of pain perception

The three-way repeated-measures ANOVA assessing whether the effect of the nociceptive stimulus on motor excitability was dependent on the intensity of the elicited percept showed no significant main effect of *'perception'* (FDI: $F_{(1,9)}$=2.98, p=0.118, η^2=0.249; FCR: $F_{(1,9)}$=0.71, p=0.422, η^2=0.073; ECR: $F_{(1,9)}$=4.56, p=0.062, η^2=0.336) and no significant *'perception'* x *'side'* interaction (FDI: $F_{(1,9)}$=1.59, p=0.239, η^2=0.15; FCR: $F_{(1,9)}$=0.56, p=0.474, η^2=0.058; ECR: $F_{(1,9)}$=0.81, p=0.391, η^2=0.083) or *'perception'* x *'ISI cluster'* interaction (FDI: $F_{(1.9,17.2)}$=0.81, p=0.458, η^2=0.082; FCR: $F_{(3,27)}$=0.41, p=0.745, η^2=0.044; ECR: $F_{(1.5,13.8)}$=1.29, p=0.297, η^2=0.125). There was also no three-way interaction (FDI: $F_{(3,27)}$=0.18, p=0.908, η^2=0.02; FCR: $F_{(3,27)}$=1.8, p=0.172, η^2=0.166; ECR: $F_{(3,27)}$=1.78, p=0.174, η^2=0.165).

3.1.4 Baseline MEPs

Consistent MEPs were recorded from the FDI, FCR and ECR muscles of both hands, both before the TMS-laser session (FDI: 3.4±2.0 mV, FCR: 0.3±0.2 mV, ECR: 0.8±0.4 mV) and after the TMS-laser session (FDI: 2.9±2.2 mV, FCR: 0.3±0.2 mV, ECR: 0.9±1.0 mV). In all three muscles, the two-way repeated-measures ANOVA showed no significant main effects of *'time'* (FDI: $F_{(1,9)}$=1.82, p=0.21, η^2=0.168; FCR: $F_{(1,9)}$=0.61, p=0.457, η^2=0.063; ECR: $F_{(1,9)}$=0.37, p=0.558, η^2=0.04), and *'dominance'* (FDI: $F_{(1,9)}$=0.96, p=0.354, η^2=0.096; FCR: $F_{(1,9)}$=0.57, p=0.470, η^2=0.06; ECR: $F_{(1,9)}$=1.63, p=0.234, η^2=0.153), as well as no interaction between the two factors (FDI: $F_{(1,9)}$=1.40, p=0.266, η^2=0.135; FCR: $F_{(1,9)}$=1.29, p=0.286, η^2=0.125; ECR: $F_{(1,9)}$=0.02, p=0.88, η^2=0.003).

3.2 Nociception-motor interactions in flexor and extensor muscles of the forearm (supplemental experiment)

Consistent MEPs were recorded from the BB and TB muscles of the two forearms. However, interpretation of potential nociception-motor interactions in these muscles was limited by the fact that the magnitude of MEPs recorded in these muscles was markedly lower than the magnitude of MEPs obtained from hand muscles in the main experiment (Figure 3.5). Subject-and group-level averages of the change in MEP amplitude relative to baseline are shown in Figure 3.5. The repeated-measures ANOVA with the factors *'ISI'* (50, 100, 250, 300, and 1000 ms) and *'side'* (stimulated vs. non-stimulated hand) showed no significant main effects of *'ISI'* (BB: $F_{(4,24)}$=1.27, p=0.311, η^2=0.174; TB: $F_{(12,11.7)}$=0.71, p=0.509, η^2=0.106), *'side'* (BB:

$F_{(1,6)}$=0.63, p=0.457, η^2=0.095; TB: $F_{(1,6)}$=5.14, p=0.064, η^2=0.462) and no significant two-way *'side'* x *'ISI'* interaction (BB: $F_{(4,24)}$=1.89, p=0.145, η^2=0.24; TB: $F_{(4,24)}$=1.59, p=0.21, η^2=0.209). No significant modulatory effect of the nociceptive stimulus was thus observed in either muscles (Figure 3.6). In all muscles, there was also no significant change of the background EMG activity. The two-way repeated-measures ANOVA showed no main effect of *'side'* (BB: $F_{(1,6)}$=0.01, p=0.91, η^2=0.002; TB: $F_{(1,6)}$=2.68, p=0.153, η^2=0.309), no main effect of *'ISI'* (BB: $F_{(1.92,11.49)}$=0.91, p=0.425, η^2=0.132; TB: $F_{(4,24)}$=2.21, p=0.099, η^2=0.269), and no interaction between the two factors (BB: $F_{(1.4,8.37)}$=1.43, p=0.279, η^2=0.193; TB: $F_{(1.25,7.5)}$=1.17, p=0.33, η^2=0.163).

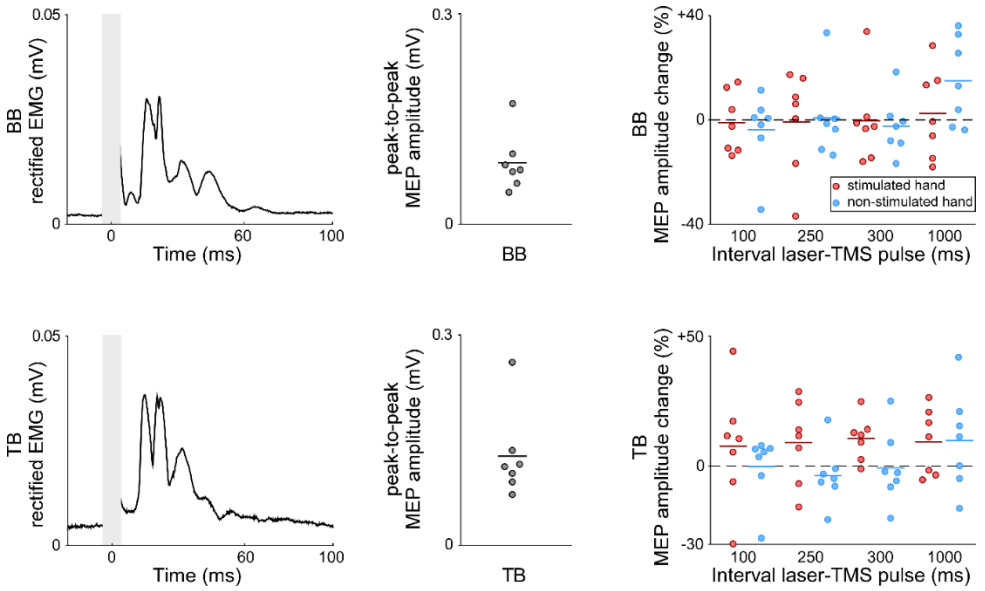

Figure 3.5. Left panel. Group-level average rectified EMG time courses of the MEPs recorded at ISI=50 ms from forearm flexor (BB) and extensor (TB) muscles in the supplemental experiment. Middle panel. Subject-and group-level average ±SD peak-to-peak amplitude of the MEPs recorded from the different muscles. Note that consistent MEPs were recorded from all

muscles, but that their magnitudes were, on average, of much smaller magnitude than the MEPs recorded from distal muscles in the main experiment. Right panel. Subject-and group-level average ±SD of the MEPs obtained at ISI=100-1000 ms, expressed as the percentage of change relative to the MEPs obtained at ISI=50 ms. The x-axis represents the time-interval between the onset of the laser stimulus and the onset of the TMS pulse (Adapted from Figure 5 in Algoet et al. (2018)).

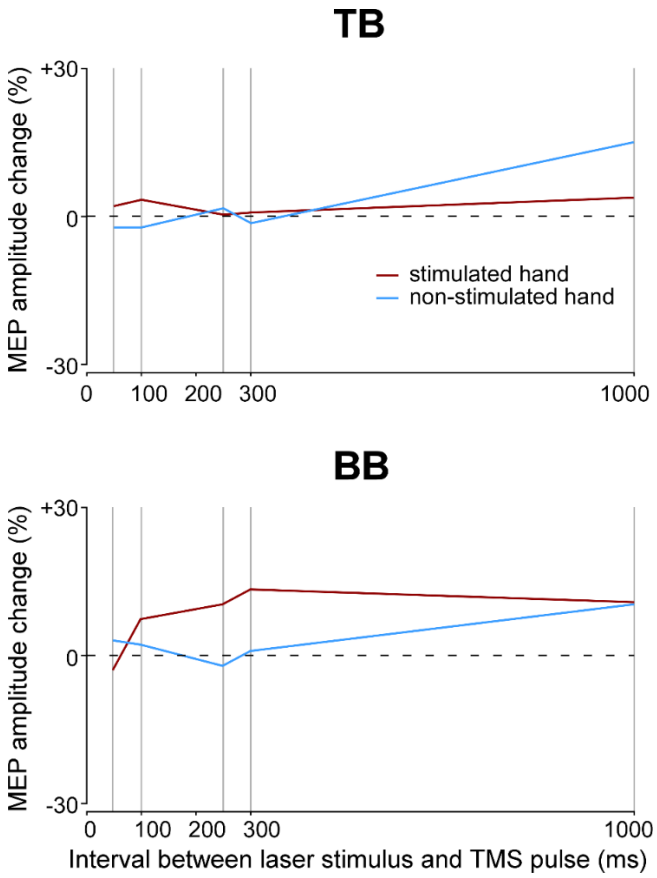

Figure 3.6. Group-level average amplitude of the MEPs elicited in BB and TB muscles of the laser-stimulated and non-laser stimulated hands in the supplemental experiment. X-axis: time-interval between the onset of the

laser stimulus and the onset of the TMS pulse. Y-axis: MEP amplitude, expressed as the percentage of change relative to the MEPs obtained at ISI=50 ms. No significant changes were observed (Adapted from Figure 6 in Algoet et al. (2018)).

4. Discussion

In this study, we characterized the temporal profile of the effects of a transient nociceptive stimulus delivered to the hand dorsum on the motor excitability of extensor and flexor muscles of the stimulated and non-stimulated arm. We hypothesized that the occurrence of phasic pain delivered to one hand would modulate motor excitability in a limb-specific (stimulated vs. non-stimulated limb) and possibly muscle-specific (flexor muscles involved in the withdrawal of the stimulated limb vs. other muscles) manner, with a time-specific profile.

Our results can be summarized as follows. First, 100 ms after the onset of the nociceptive stimulus, the responses in flexor muscles of the stimulated hand (FDI and FCR) were significantly increased. This enhancement was observed at both hands, but was significantly more pronounced at the hand which received the nociceptive stimulus, at least for the FCR muscle. A trend towards an MEP enhancement at ISI=100 ms was also observed in the extensor muscle of the stimulated hand (ECR). Previous studies have suggested that, at ISI=100 ms, the nociceptive afferent volley has not yet reached its cortical projection sites (Xu et al., 1995; Spiegel et al., 1996; Valentini et al., 2012a). Therefore, it is likely that the enhancement observed at ISI=100 ms results from nociceptive-motor interactions occurring at spinal level. Second, this initial enhancement was followed by a reduction of MEP

amplitudes extending between 150 to 400 ms after the presentation of the nociceptive stimulus. This reduction was significantly more pronounced at the stimulated hand, and observed in both flexor and extensor hand muscles. Third, between 600 and 2000 ms we observed a sustained enhancement of the MEPs obtained from the non-laser-stimulated limb as compared to the laser-stimulated limb. Importantly, these changes in MEP amplitude were not the consequence of changes in background EMG activity, which remained similar at all ISI clusters, and at both limbs.

4.1 Early-latency increase of motor excitability at the stimulated hand

At an ISI of 50 ms between the onset of the laser stimulus and the onset of the TMS pulse, the nociceptive afferent volley does not have enough time to reach spinal projection sites and exert an effect on the motor volley generated by the TMS pulse. Indeed, considering the time required for the laser stimulus to bring skin temperature above the thermal activation threshold of heat-sensitive nociceptors and the time required for the transduction of the stimulus into a neural impulse (Bromm and Treede, 1984), the delay between the onset of the laser stimulus and receptor activation should be at least 40 ms. To this delay, one must then add the peripheral conduction time of the nociceptive afferent volley (Kakigi et al., 1991; Tran et al., 2001). Bromm and Treede (1987) estimated the mean conduction velocity of Aδ fibers activated by brief pulses of radiant heat to be approximatively 14 m/s. The peripheral conduction distance separating the hand dorsum from the cervical spinal cord is in the range of 90 cm. Thus,

approximately 60 ms is required for the nociceptive afferent volley to reach the spinal cord. Therefore, considering (1) the time required for receptor activation and (2) the peripheral conduction distance, the afferent volley elicited by the laser pulse can be expected to reach the spinal cord approximately 100 ms after stimulation onset (Tarkka et al., 1992). This latency must then be compared to the central motor conduction time (CMCT), i.e. the time required for the descending motor volley generated by the TMS pulse to reach spinal motoneurons. In healthy subjects, normal values of CMCT are in the range of 4-8 ms (Rossini et al., 1987; Claus et al., 1988; Homberg et al., 1991). Similarly, descending indirect volleys (I-waves) have been recorded in humans with cervical epidural electrodes with latencies of up to ±10 ms after delivering TMS over M1 (Di Lazzaro et al., 1998; Di Lazzaro et al., 2004). Moreover, excitatory postsynaptic potentials generated in spinal motoneurons can last as long as 10-20 ms (Curtis and Eccles, 1959; Landgren et al., 1962; Rall et al., 1967). Taking this into account, when the time-interval between the onset of the laser stimulus and the onset of the TMS pulse was 50 ms, the descending motor volley has already been fully transmitted to peripheral efferents at the time the nociceptive input reaches the spinal cord.

In contrast, when the laser stimulus was delivered 100 ms before the TMS pulse, the nociceptive input conveyed by myelinated Aδ fibers has enough time to interact with the descending motor volley at spinal level, but it does not have enough time to interact at cortical level. Indeed, studies have shown that the first cortical response to laser stimuli delivered to the hand dorsum occurs approximately 140-180 ms after onset (Xu et al., 1995;

Spiegel et al., 1996; Valentini et al., 2012a; Lenoir et al., 2017). Moreover, depth recordings performed in epileptic patients have shown that laser stimuli delivered to the hand dorsum can elicit responses in M1 starting approximately 120 ms after stimulation onset, and peaking 170 ms after stimulation onset (Frot et al., 2013). For these reasons, the early-latency enhancement of motor excitability observed at ISI=100 ms was most probably related to a segmental effect of Aδ fiber nociceptive input on the excitability of spinal motoneurons. Although less investigated than in the lower limb, upper limb nociceptive reflex activities can be recorded following noxious electrical stimulation of the ulnar nerve as well as the fingers (Cambier et al., 1974; Bromm and Treede, 1980; Campbell et al., 1991; Bouhassira et al., 1993; Floeter et al., 1998; Serrao et al., 2006; Serrao et al., 2012; Eckert and Riley, 2013). Such as for the lower limbs, this reflex activity could constitute a protective withdrawal response (Serrao et al., 2006; Peterson et al., 2014). Whether a parallel can be drawn between our observation and the NWR remains an open question. The early latency of our effect (100 ms) is compatible with the fact that the NWR can be observed 60-120 ms after noxious electrical stimulation of the ulnar nerve (Cambier et al., 1974). The relatively early onset of this reflex activity can be explained by the overlap of RII and RIII components, respectively conveyed by non-nociceptive and nociceptive inputs (Floeter et al., 1998). Notably, our results suggest that the laser stimulus affects similarly the MEP amplitudes recorded from flexor and extensor hand muscles (Figures 3.3 and 3.4), whereas it could have been expected that noxious stimulation would induce a differential modulation of motor excitability in muscles involved vs. not

involved in limb withdrawal, i.e. flexor vs. extensor muscles. Supporting our results, several studies have observed simultaneous reflex activity in flexor and extensor muscles, both at the upper and lower limbs (Grimby, 1963; Floeter et al., 1998; Peterson et al., 2014), the activation pattern depending on the location of the nociceptive stimulus and the position of the limbs (Andersen et al., 1999; Andersen, 2007). Considering the biomechanical function of the muscles investigated in the present study, it can be argued that the limb posture (hand palms resting on a table) and the location of the nociceptive stimulus (hand dorsum) would prevent us from observing a withdrawal response in intrinsic (FDI) and extrinsic (FCR) flexor muscles of the hand. Nevertheless, a NWR in the FCR muscle has been described at rest in a semi-flexed position similar to that used in our study (Serrao et al., 2006) and has been recorded from the FDI muscle after delivering noxious electrical stimuli to different fingers (index, middle and fifth finger) (Floeter et al., 1998). Also, the "cutaneous silent period" (CSP), which is thought to be an inhibitory component of a defensive reflex (Inghilleri et al., 1997), can be evoked in the FDI muscle after noxious electrical stimulation of both the index (Floeter et al., 1998) and the hand dorsum (Romaniello et al., 2004; Kahya et al., 2010). Moreover, while the influence of limb position is well established for the lower limb (Andersen, 2007), few studies have investigated this for the upper-limb withdrawal reflex and have found inconsistent results (Eckert and Riley, 2013; Peterson et al., 2014).

4.2 Mid-latency decrease of motor excitability at the stimulated hand

Following the transient early-latency enhancement of the responses recorded in flexor hand muscles, there was a longer-lasting decrease of MEP amplitudes extending between 150 and 400 ms after the onset of the nociceptive stimulus. This decrease was significantly more pronounced at the hand which received the nociceptive stimulus. It was present in flexor and extensor hand muscles. This observation is in agreement with reports of a decreased motor excitability in hand muscles after noxious electrical stimulation (Inghilleri et al., 1995; Kofler et al., 1998; Kofler et al., 2001; Tamburin et al., 2001; Urban et al., 2004; Kofler et al., 2008) or during phasic painful heat stimulation (Dube and Mercier, 2011). Similarly, Valeriani et al. (1999) found a significant reduction of MEP amplitudes in the FDI muscle 170-270 ms after the delivery of a thermal nociceptive stimulus on the stimulated hand dorsum.

At these latencies, the nociceptive input conveyed by Aδ fibers has enough time to reach M1 before the onset of the TMS pulse (Frot et al., 2013). Therefore, this effect could be related to nociception-motor interactions occurring at cortical level (exerting an effect on the excitability of M1) and/or spinal level. Several studies have shown that nociceptive laser stimuli can induce a significant reduction of the sensorimotor mu rhythm, maximal over the hemisphere contralateral to the stimulated hand (Raij et al., 2004; Ploner et al., 2006). Considering that these stimulus-evoked changes in mu rhythm magnitude have been shown to index context-dependent changes in the level of activation of sensorimotor cortices (Valentini et al., 2012b), and

considering the latency of the effect of nociceptive stimulation on mu rhythm magnitude (180-570 ms; Raij et al. 2004), the decrease of MEP amplitudes we observed at 150-400 ms could be related to stimulus-evoked changes in cortical sensorimotor oscillatory activity. Mechanisms underlying theses changes in cortical activity are still poorly understood. Nociceptive inputs could act through spinothalamic projections to brain region involved in motor function such as M1 (Frot et al., 2013) or cingulate areas (Dum et al., 2009) involved in motor control of the upper limb (Turken and Swick, 1999) including defensive movements (Cooke and Graziano, 2003; 2004; Moayedi et al., 2015). Furthermore, interactions between brain regions underlying the processing of nociceptive inputs and those supporting motor control could also be involved (Suppa et al., 2013). In agreement, hemodynamic changes following acute pain have been observed in several motor structures including the cerebellum, the supplementary motor area, and the lenticular and caudate nuclei (Peyron et al., 2000). In parallel, the decrease in MEP amplitudes that we observed could be related to changes in top-down influences on the spinal sensorimotor system (Eccles and Lundberg, 1959; Schomburg, 1990). Indeed, several cortical (Lundberg and Voorhoeve, 1962) and brainstem (Engberg et al., 1968; 1968; Carstens and Campell, 1992) structures can modulate the strength of synaptic transmission within spinal reflex circuits including those underlying the NWR.

Importantly, such sensori-motor interactions (i.e. the reduction of MEPs in flexor and extensor muscles of the stimulated hand) are probably not specific for nociception. Non-nociceptive electrical stimulation of both the

median nerve and the digits provokes, 20-50 ms after stimulation, a suppression of MEPs recorded from proximal and distal upper limb muscles (Clouston et al., 1995; Manganotti et al., 1997; Bertolasi et al., 1998; Classen et al., 2000; Helmich et al., 2005; Tamburin et al., 2005; Bikmullina et al., 2009; Fischer and Orth, 2011). This afferent inhibition is thought to mainly result from cortical inhibitory mechanisms in the sensorimotor cortex (Tokimura et al., 2000; Bikmullina et al., 2009; Ferreri et al., 2012; Tsang et al., 2014; Kojima et al., 2015; Bailey et al., 2016; Noda et al., 2016) conveyed by cholinergic (Di Lazzaro et al., 2000; Di Lazzaro et al., 2002) and $GABA_A$ergic pathways (Di Lazzaro et al., 2005; Di Lazzaro et al., 2007). This short-latency inhibition is followed by a later inhibitory period (200-1000 ms) which could result from mechanisms involving basal ganglia, thalamo-cortical (Sailer et al., 2003) and cortico-cortical interactions (Chen et al., 1999; Abbruzzese et al., 2001; Sailer et al., 2002). Whether the decrease in motor excitability we observed in the current study 150-400 ms after nociceptive stimulation can be explained by similar mechanisms remains an open question that cannot be answered with our experimental protocol.

4.3 Late-latency enhancement of motor excitability in the contralateral hand

Nociceptive stimuli delivered to the hand also induced a late-latency and long-lasting enhancement of the magnitude of the MEPs recorded from the non-laser-stimulated hand, extending 600 ms onwards after stimulus onset, at least for the FDI and ECR muscles.

Again, one can only speculate on the nature of this late effect, which could result from interhemispheric interactions (Terada et al., 2012) and/or crossed interactions occurring at spinal level (Sherrington, 1910; Andersen et al., 2003; Emborg et al., 2009). It has also to be noted that such an enhancement might not be limited to the non-stimulated limb as it was also observed in the FDI muscle of the stimulated hand. Furthermore, considering the late latency of this effect, it could reflect changes induced by nociceptive input conveyed by slow-conducting unmyelinated C fibers.

Using a similar experimental design, Chen et al. (1999) characterized the temporal profile of the changes in motor excitability induced by non-nociceptive electrical stimulation of the median nerve at the level of the wrist. Such as in the present study, they observed an early-latency enhancement of MEPs recorded from hand muscles of the stimulated hand, followed by a later attenuation of MEPs closely resembling the attenuation observed in the present study. The latency at which electrical stimulation of the median nerve exerted effects on motor excitability was shorter than the latency of the effects induced by laser stimulation. As discussed previously, this is easily explained by the time required for skin heating, heat transduction and nerve conduction of heat-evoked responses conveyed by thinly-myelinated Aδ fibers as compared to the responses elicited by direct electrical activation of large-diameter Aβ fibers.

However, contrasting with our results, non-nociceptive electrical stimulation did not appear to induce a late asymmetry of the MEPs elicited within hand muscles of the stimulated and non-stimulated limb (Chen et al., 1999), suggesting that the late asymmetric effect of the laser stimulus on motor

excitability observed in the present study reflects sensori-motor interactions that are specific for nociception. This interpretation is consistent with the observations of Pereon and Guiheneuc (1995). In their experiment, MEPs were recorded from the right *abductor digiti minimi* muscle 200-700 ms after electrical stimulation of the left median nerve. Especially for high stimulation intensities, i.e. when the electrical stimulus was likely to activate small-diameter nociceptive afferents, they observed a late-latency enhancement of MEPs similar to the enhancement observed in the present study.

4.4 Spinal vs. cortical nociception-motor interactions

In the present study, we did not test directly the excitability of spinal motoneurons. Therefore, we cannot determine with certainty whether the late effects of the nociceptive stimulus on motor excitability are due to interactions occurring at the level of the spinal cord, or interactions occurring at the level of the cortex. Valeriani et al. (1999; 2001) attempted to do so by comparing the effects of laser stimulation on the EMG responses elicited by TMS and anodal electrical stimulation of M1, assuming that anodal stimulation generates responses exclusively related to a direct activation of the cortico-spinal tract. However, several studies have suggested that this assumption might not always be true (Di Lazzaro et al., 1998). Other techniques to test spinal excitability suffer from other limitations. H-waves recorded by electrical stimulation of a nerve trunk, in addition to being influenced by presynaptic, reciprocal and non-reciprocal inhibition (Knikou, 2008), are difficult to evoke at rest (Mazzocchio et al.,

1995) and can be insensitive to changes, depending on the test reflex size (Crone et al., 1990). F-waves test only a fraction of the motoneurons pool (Espiritu et al., 2003). The recording of MEPs elicited by transcutaneous electrical stimulation of the cortico-spinal tract at cervico-medullary level could be an interesting mean (Taylor, 2006). However, cervico-medullary MEPs are difficult to obtain in relaxed subjects (Matsumoto et al., 2008). We attempted to record these responses in pilot experiments, but failed to obtain consistent responses compatible with the objective of assessing how they are modulated by a preceding laser stimulus. Further experiments relying on other techniques to disentangle changes in spinal and supraspinal motor excitability are thus needed.

4.5 Phasic vs. tonic pain

A number of studies investigated changes in motor excitability induced by tonic cutaneous pain (Romaniello et al., 2000; Farina et al., 2001; Fierro et al., 2010; Martel et al., 2017) or muscle pain (Romaniello et al., 2000; Le Pera et al., 2001; Svensson et al., 2003; Martin et al., 2008; Schabrun and Hodges, 2012; Schabrun et al., 2013; Burns et al., 2016b). Changes in motor excitability induced by tonic pain and phasic pain could have different functions and reflect different mechanisms. For example, changes induced by phasic pain might be expected to prompt swift protective withdrawal responses, whereas changes induced by tonic pain may induce changes in motor behavior promoting healing and recovery (Farina et al., 2003).

Farina et al. (2001) showed that MEPs recorded from several muscles of the upper limb are reduced up to 20-30 minutes after the topical application of

capsaicin on the skin overlying the FDI and FCR muscles. This inhibitory effect was interpreted as originating from a modulation at cortical level, because measures of peripheral and spinal excitability (F-, H- and M-waves) remained unchanged throughout the experiment. Using paired-pulse measures of MEPs, Fierro et al. (2010) brought additional evidence of changes in cortical motor excitability induced by tonic cutaneous pain. A similar decrease in MEPs was observed after inducing tonic muscle pain (Le Pera et al., 2001; Svensson et al., 2003; Martin et al., 2008). The suppression was explained by a reduction of excitability of both cortical and spinal motoneurons. Tonic muscle pain reduced not only the amplitude of MEPs elicited by M1 stimulation, but also the amplitude of the H-reflex (Le Pera et al., 2001), as well as the MEPs elicited by direct stimulation of descending motor tracts at the level of the foramen magnum (Svensson et al., 2003), indicating a reduction of spinal motoneuron excitability. Conversely, Martin et al. (2008) observed a facilitation of the MEPs elicited by direct stimulation of the cortico-spinal tract using cervico-medullary electrical stimulation without any concomitant increase of the MEPs elicited by cortical M1 stimulation, suggesting a facilitation of spinal motoneurons and a concomitant inhibition of cortical motoneurons. Inhibition at cortical level related to phasic and tonic pain might constitute a mean to induce a *"motor decerebration"* allowing the spinal motor system to generate stronger protective reflex movements (Farina et al., 2003).

4.6 Study limitations

4.6.1 Lack of changes in forearm flexion and extensor muscles

In the supplemental experiment, we attempted to assess the effect of a laser stimulus on more proximal muscles controlling the flexion (BB) and extension (TB) of the forearm. In contrast with the clear modulation of the MEPs recorded from flexor and extensor muscles of the hand, we did not observe any significant effect of the nociceptive stimulus on the MEPs recorded from flexor and extensor muscles of the forearm. This lack of effect contrasts with the results of Valeriani et al. (2001), showing a significant decrease of MEPs in the BB muscle 170-220 ms after the onset of the laser stimulus. However, both results should be interpreted with caution, as the MEPs recorded from forearm muscles were of low amplitude (Figure 3.5). This is related to the fact that activation of the motor representation of these muscles is more difficult than activation of the large motor representation of hand muscles (Wassermann et al., 1992; Metman et al., 1993). The non-linear stimulus-response curve characterizing the relationship between TMS intensity and MEP amplitudes suggests that changes in these motor responses are dependent on the baseline amplitude of MEPs (Devanne et al., 1997). Therefore, further experiments investigating, for example, changes in the stimulus-response curve using a range of TMS stimulation intensities could be more appropriate to assess nociception-evoked changes in the motor excitability of proximal upper limb muscles.

4.6.2 Large-amplitude MEP amplitudes recorded from the FDI muscles

Because the intensity of TMS was set such as to obtain reliable MEPs in FDI, FCR and ECR muscles, the MEPs obtained from the FDI muscle had a large average amplitude, suggesting that for this muscle, the stimulation was probably in the upper part of the sigmoidal input-output curve (Devanne et al., 1997). Importantly, this did not prevent us from observing a time-dependent change in amplitude of the MEPs recorded from the FDI muscle, including a significant increase at ISI=100 ms.

4.6.3 Effect of experimental context

Our experimental design required participants to rest both volar forearms against a table, and to refrain from moving the stimulated hand, in order to allow the recording of reliable MEPs. Future studies should examine whether limb position, location of the nociceptive stimulus, and the instruction to avoid stimulus-evoked movements (Bestmann and Duque, 2016; Duque et al., 2017) could have contributed to the results of the present study as well as the results of previous studies (Valeriani et al., 1999; Farina et al., 2001; Valeriani et al., 2001). Furthermore, at the end of each trial, participants were asked to verbally report the intensity of the percept elicited by the laser stimulus. Performing this task required to evaluate the stimulus, maintain information in working memory, and await a warning tone. Whether these could have influenced our results should thus be considered. An enhancement of MEPs recorded from the tongue has been described before the onset of speech. However, this was observed only

shortly before speech onset (260 ms) (Neef et al., 2015) and, in the present study, the minimum time between the TMS pulse and the verbal report was 1-2 s. Furthermore, an effect of speech on MEPs recorded from upper-limb muscles has, to the best of our knowledge, never been reported. Nevertheless, several studies have suggested that working memory tasks can induce changes in M1 excitability (Honey et al., 2000; Cairo et al., 2004). Most of these studies used protocols requiring the subject to press a button (Tomasino and Gremese, 2016). Because participants did not perform any manual task, it seems unlikely that such an effect of working memory would differentially affect the MEPs elicited in the hand receiving vs. not receiving the laser stimulus.

In conclusion, the present study shows that phasic pain delivered to one of the two hand dorsum induces an early excitatory effect on muscles of the stimulated hand, possibly related to the spinal nociceptive withdrawal reflex. Following this initial enhancement, the nociceptive stimulus induces an inhibitory effect in flexor and extensor muscles of both hands, but maximal at flexor muscles of the stimulated hand. This later effect may be related to nociceptive-motor interactions occurring at cortical level, although late interactions at spinal level cannot be ruled out. Finally, we show that nociceptive stimuli induce a very late and long-lasting facilitation in the flexor and extensor muscles of the non-stimulated hand. This long-lasting effect, which was not previously observed following non-nociceptive stimulation of the median nerve, could be specific for nociception.

Chapter 7. Conclusion, further considerations and perspectives

1. Transient nociceptive stimuli induce a time-dependent modulation of motor excitability: disentangling nociception-motor interactions at spinal and supraspinal levels

Acute pain, because of its intrinsic aversive nature, is an advantage for survival. The nociceptive system, from which this perception may emerge, conveys the processes allowing to detect and warn any situation that could affect bodily integrity. One of the most important function of nociception is to trigger an adequate protective response to a threatening event. Importantly, generating a prompt motor response in reaction to a sudden noxious stimulus is essential for preventing and limiting injury (Iannetti and Mouraux, 2010). I showed that short-lasting nociceptive stimuli delivered to the hand dorsum was able to trigger a time-dependent modulation of motor excitability within flexor and extensor muscles of both the stimulated and non-stimulated limb (chapter 3). Indeed, nociceptive stimuli induced an early-latency (100 ms) enhancement of MEPs in flexor muscles of the stimulated hand. This was followed by a later (150–400 ms) MEP reduction in extensor muscles of the stimulated hand and flexor muscles of both hands, predominant at the stimulated hand. Finally, a long-lasting (600–2000 ms) MEP enhancement in muscles of the non-stimulated hand was observed. Disentangle spinal from supraspinal mechanisms underlying the interactions between pain and the motor system represents a great

challenge. Various techniques used to test spinal excitability suffer from significant limitations. Motor responses elicited by anodal stimulation of M1 is often considered as to be related to a direct activation of the cortico-spinal tract. However, several studies have suggested that this assumption might not always be true (Di Lazzaro et al., 1998). The H-waves, one of the most popular techniques for testing spinal motoneurons excitability, is influenced by presynaptic, reciprocal and non-reciprocal inhibition (Knikou, 2008). In addition, these responses can be difficult to evoke at rest (Mazzocchio et al., 1995) and can be insensitive to changes, depending of the test reflex size (Crone et al., 1990). The F-waves test only a fraction of the motoneurons pool. Furthermore, there is not always a concordance between changes observed in the H- and F-waves (Espiritu et al., 2003). An attractive technique for testing spinal excitability is the recording of cMEPs elicited either by transcutaneous electrical or magnetic stimulation of the cortico-spinal tract at the cervico-medullary level (Taylor, 2006), though these responses can be difficult to record at rest (Matsumoto et al., 2008). Interestingly, cMEPs do not seem to be affected by presynaptic inhibition (Nielsen and Petersen, 1994). One original approach could be to record cMEPs elicited by magnetic stimulation of the cortico-spinal tract at the cervico-medullary level while concomitantly recording brain responses by using EEG. Indeed, the simultaneous recording of brain and spinal responses to a magnetic pulse delivered at the cervico-medullary level could be an interesting mean to disentangle spinal from supraspinal mechanisms underlying pain-motor interactions. Complementary, investigating the effects of a brief nociceptive stimulus on SICI, ICF, IHI or the cortical silent

period could bring new insights about the contribution of spinal vs. supraspinal mechanisms involved in nociception-evoked motor responses. Similarly, a complementary approach to investigate phasic pain-evoked changes in brain connectivity could be to combine TMS with online functional neuroimaging techniques such as EEG (Ilmoniemi et al., 1997).

2. Assessing nociceptive processing at spinal level using the nociceptive withdrawal reflex

Nociception-evoked motor responses have been extensively investigated at spinal level as illustrated by the NWR elicited in various upper and lower limb muscles after noxious electrical stimulation of the skin. This short-latency response constitutes a first line of defense against potentially tissue damaging threats. In most studies, the NWR is elicited either by high-intensity TES using large surface electrodes or by electrical stimulation of the sural nerve in the lateral malleolus space (Sandrini et al., 2005; Andersen, 2007). Electrical stimuli have the advantage of generating a well synchronized afferent volley compatible with the recording of time-locked EMG responses such as the withdrawal reflex. Therefore, more consistent and reproducible reflexes can then be obtained in comparison to those elicited by a purely nociceptive stimulation such as a radiant heat stimulus (Andersen, 2007). Because electrical stimuli unavoidably also activate non-nociceptive afferents, the EMG response evoked by TES consists in one EMG burst including two distinct components (Chan and Dallaire, 1989; Dowman, 1991), referred to as the RII and RIII, and conveyed by non-nociceptive and nociceptive fibers, respectively. This incited the researchers to use time

windows to minimize the contribution of the RII component (e.g. Plaghki et al. (1998), Rhudy and France (2007)). In chapter 4, I characterized the EMG responses recorded from lower limb muscles elicited by the preferential activation of nociceptors by using IES of the sole of the foot. This study showed that the motor responses elicited by IES were significantly delayed compared to those elicited by TES of the same skin area. Furthermore, the EMG responses obtained by IES consist of two separate EMG bursts. Importantly, the early-latency activity elicited by IES appeared significantly later than the muscular response elicited by TES, suggesting that these two responses are conveyed by distinct populations of fibers conducting impulses at different CVs. Based on these observations, I proposed that this early-latency activity elicited by IES could represent a "purer" measure of the RIII than the EMG responses elicited by more classical techniques such as TES. Several studies attempt to elicit the NWR by selectively activating heat-sensitive nociceptors by means of high-intensity radiant heat stimuli (Hardy, 1953; Willer et al., 1979; Campbell et al., 1991; Andersen et al., 2006; Morch et al., 2007). However, in these studies, reflexes were observed in less than half of the trials (Andersen et al., 2006; Morch et al., 2007). In our study, I recorded motor responses in 80% of trials. However, to elicit consistent and reliable IES-evoked responses, pilot experiments were needed to improve the placement of the electrode on the sole of the foot. Therefore, further investigations should consider increasing the spatial summation by using a set of punctate electrodes similar to that used in the multi-pin electrode designed to preferentially activate nociceptive afferents (and used to deliver HFS in chapter 5). Such electrodes could achieve a high

current density at low current intensity allowing the preferential activation of nociceptors in the superficial layers of the epidermis.

3. Pain-motor interactions in the context of central sensitization

Though pain-related changes in motor behaviors can lead to immediate benefices, motor adaptation to pain can have long-term negative consequences when pain persists for months or years (Hodges and Tucker, 2011). Cutaneous tissue injuries can be associated with the development of hyperalgesia at the site of injury, a phenomenon known as primary hyperalgesia. Furthermore, an increased pain sensitivity to mechanical stimuli is also observed in the surrounding uninjured skin and is termed secondary hyperalgesia (Hardy et al., 1950; LaMotte et al., 1983; Raja et al., 1984; Dahl et al., 1993). This secondary hyperalgesia is thought to be conveyed by central sensitization via, at least in part, a LTP in the spinal cord. Interestingly, a prominent clinical feature of central sensitization in persistent pain conditions, such as postoperative pain, is hyperalgesia to mechanical stimuli in the surrounding uninjured skin (Lavand'homme et al., 2005). Therefore, I tried in chapter 5 to determine whether the intense activation of nociceptors could lead to changes in motor system excitability. The effects of HFS of primary nociceptive afferents on the cortical motor map generated by TMS were therefore investigated. Surprisingly, HFS of the skin does not induce sustained changes in the TMS-mapped representation of both intrinsic hand muscle and flexor/extensor muscles of the forearm. Importantly, this does not allow to conclude to the absence of HFS-evoked

changes in motor system at both spinal and supraspinal levels. Further studies, investigating intracortical networks and/or cortico-cortical interactions by combining TMS with neuroimaging techniques could help to assess possible HFS-related changes in the motor cortex organization. Methodological considerations must be also considered. Indeed, in the study of chapter 5, a standard MRI provided by the neuronavigation system was used to generate a 3D-reconstruction of the scalp allowing an instantaneous feedback about the TMS stimulus position. A fixed coil orientation of 45° relative to the mid-sagittal line was then used. This procedure does not take into account the individual anatomy of the central gyrus which shows a characteristic bending in the motor cortex representation of hand muscles, the so-called hand-knob (Yousry et al., 1997). Therefore, neither the TMS coil position relative to the central gyrus nor the coil orientation relative to the shape of the central sulcus were adjusted during the TMS map procedure. By adapting the TMS coil position and its orientation relative to the sulcal shape during the map procedure, which could allow to generate a current perpendicular to the central sulcus at all mapping sites, I could improve the resolution of the motor mapping procedure (Raffin et al., 2015) and decrease the inter-subject variability of the TMS map (Kraus and Gharabaghi, 2015). Furthermore, a fixed TMS coil orientation at 45° away from the midline could not be the optimal TMS coil orientation for all the three muscles investigated in the present study (Bashir et al., 2013). More importantly, most studies that investigated the effects of the sustained activation of cutaneous nociceptors on motor function used experimental models inducing, unlike HFS of the skin, an ongoing pain

sensation during the assessment of motor excitability. Therefore, these studies do not allow to distinguish the ongoing pain- vs. central sensitization-induced changes in the motor system. Further studies are thus needed to explore the modulation of the motor system excitability in a situation of central sensitization without a concomitant ongoing pain sensation.

Allodynia - a condition in which a stimulus that does not normally evoke pain provokes an unexpectedly painful response (Treede et al., 1992; Jensen and Finnerup, 2014) – is, as secondary mechanical hyperalgesia, a prominent clinical feature in persistent postoperative pain (Jensen and Finnerup, 2014). Further studies could try to disentangle spinal vs supraspinal mechanisms underlying allodynia by combining the TMS map procedure I used in chapter 5 with techniques exploring spinal pathways excitability, such as IES and TES used in chapter 4. Interestingly, the spinal convergence of non-nociceptive and nociceptive inputs could play a role in the pathophysiology of allodynia (Ellrich and Treede, 1998). Therefore, combining IES (used as a "purer" measure of the nociceptive part of the spinal reflex) with techniques which preferentially evoke the RII could help to study the mechanisms underlying the clinical phenomenon of allodynia.

Finally, future TMS studies, by means of a TMS map procedure such as in chapter 5 or by combining TMS with neuroimaging techniques, could help to explore central mechanisms of the opioid-induced hyperalgesia, a state of sensitization of the nociceptive system caused by exposure to opioids (Lee M. et al., 2011; Yi and Pryzbylkowski, 2015).

4. Changes in brain connectivity related to chronic pain

Recently, the recording of fMRI-BOLD responses elicited by TMS applied over a given brain region has been proposed as a potential non-invasive tool to measure directly, and at a given moment in time, the functional connectivity between brain regions (Bestmann et al., 2008c). In the last part of this dissertation (chapter 6), I presented a method that I developed to combine online TMS with fMRI to study changes in brain connectivity related to chronic pain. Our aim was to investigate the feasibility of delivering TMS concomitantly to fMRI acquisition by using two flexible surface MRI coils placed on both sides of the head rather than a more classical birdcage MRI coil. Indeed, the limited space provided by birdcage MRI coils can be an obstacle to place the TMS coil over lateral or frontal brain regions. To not be restricted by any spatial consideration, I placed the TMS coil at the center of the right MRI coil. My specific aim was to validate the recording of BOLD responses elicited by TMS of the DLPFC. In further investigations, the recording of TMS-evoked BOLD responses could be used to characterize the supraspinal activity-dependent changes underlying the chronification of pain. More specifically, the DLPFC seems to be an appropriate target in CLBP patients for such a project. Indeed, the DLPFC is a superficial structure easily reached with a figure-of-eight coil. In addition, consistent structural changes were reported in various chronic pain conditions. However, despite these structural alterations, changes in the functional connectivity between the DLPFC and remote brain areas are rarely reported in the literature (Seminowicz and Moayedi, 2017). This can be explained, at least in part, by

the fact that the DLPFC is not easily identifiable by the resting-state approach. On the other hand, CLBP patients represent one of the most frequent chronic pain state in our societies (Andersson, 1999). The variability in fMRI data across subjects (i.e. intersubject variability) and from a single subject (i.e. intrasubject variability) should be a point of interest because of the heterogeneity of CLBP patients regarding their etiologies, their associated comorbidities or their drugs consumption (Dolman et al., 2014). The concurrent TMS-fMRI approach could also be used to explore the changes in functional connectivity induced by experimental acute pain in patients suffering from chronic pain in comparison to healthy subjects. Indeed, cerebral processes which underlie acute pain seem to differ in healthy subjects vs chronic pain patients (Apkarian et al., 2009).

Appendices

A. Report of one confirmed generalized seizure and one suspected partial seizure induced by deep continuous theta burst stimulation of the right operculo-insular cortex

Lenoir C.[#], Algoet M.[#], Vanderclausen C., Peeters A., Ferrao Santos S. and Mouraux A. Report of one confirmed generalized seizure and one suspected partial seizure induced by deep continuous theta burst stimulation of the right operculo-insular cortex. Brain stimul. 2018; 11(5):1187-1188

[#] Both authors contributed equally

Dear Editor,

We report one confirmed generalized epileptic seizure and one suspected partial epileptic seizure that occurred during short (20s) continuous theta burst stimulation (cTBS) over the right operculo-insular cortex. Combined with psychophysics performed before and after cTBS, the aim of the procedure was to test whether modulation of the operculo-insular cortex affects the perception of thermal, nociceptive and tactile stimuli delivered to the ipsilateral and contralateral hands.

Our report is the second describing epileptic seizures triggered by cTBS (Oberman and Pascual-Leone, 2009). Case 1 was a 25-year-old healthy woman with no medical history other than the fact that, two days before the event, she took 150 mg fluconazole and 3x500 mg ornidazole to treat a benign, acute and local non-neurological infection. Case 2 was a 23-year-old healthy man with no medical history. He was not under any medication. The

two participants had no risk factor for epilepsy and no contraindication to cTBS (Rossi et al., 2009).

The study was approved by the ethical committee of UCLouvain (B403201316436). All participants provided written informed consent. In both cases, cTBS was delivered with a MagPro X100 stimulator. Biphasic pulses – with an anterior-posterior eddy current direction – were delivered using a 70-mm double-cone coil (Model D-B80) designed for deep stimulation. The coil was positioned tangentially over the scalp covering the right Sylvian fissure with the handle pointing occipitally. The exact position of the coil over the dorsal-posterior operculo-insular cortex was achieved by means of a MRI-guided neuronavigation system. The stimulation intensity was set to 80% of the average of the left and right tibialis anterior resting motor thresholds (rMT; 52% of the maximal stimulator output (MSO) in case 1 and 39% MSO in case 2). This intensity of stimulation was chosen based on a report of repetitive TMS (rTMS) of the insula (Ciampi de Andrade et al., 2012). The rMT was determined following the guidelines of the International Federation of Clinical Neurophysiology (Rossini et al., 1994). A short cTBS protocol was used, comprised of 100 trains of 3 biphasic pulses delivered at 50Hz with a 200ms inter-train interval (total of 300 pulses). The experiments took place in the Université catholique de Louvain (Brussels, Belgium) under the supervision of a neurologist. During stimulation, the participants were comfortably positioned in left lateral decubitus. To reduce the scalp discomfort associated with the delivery of cTBS, 45 minutes before cTBS, the skin area located under the TMS coil was treated with 2.5 g of topical lidocaine/prilocaine cream (EMLA, AstraZeneca). The participants were

provided with earplugs and a mouth-guard to reduce discomfort due to the sound and the peripheral muscular activation induced by TMS.

Case 1. The event occurred approximately 15 seconds after the beginning of cTBS. The stimulation was interrupted during the 93rd train of pulses. During the first 10 seconds of cTBS the participant had euphoric thoughts immediately followed by mild bilateral paraesthesias at the fingertips, which progressively increased in the left (contralateral to cTBS) upper limb. A dystonic attitude started in the left hemibody followed by clonic movements of the upper and lower limbs and eyes rotation. The participant then tried to sit with a feeling of panic. She recovered within one minute after the onset of the episode. The participant reported afterward that she was not able to speak or move especially the left upper and lower limbs during the incident. She also described dyspnea associated with sensations of laryngeal constriction and thoracic oppression. The neurologist and experimenters confirmed these manifestations (dyspnea, dysarthria and tonic contraction with a striking facial asymmetry). The participant remained conscious. She had no post-ictal confusion. Within 20 minutes, she was admitted to the Department of Neurology of Saint-Luc University Hospital where an electroencephalogram (EEG) examination was performed and did not reveal any epileptic activity nor post-ictal signs. Neurological examination was normal. A T1 structural MRI did not reveal any lesion or structural abnormality. A 24-hours EEG performed a few weeks after the event was normal.

Case 2. The event occurred approximately 10 seconds after the beginning of cTBS. The stimulation was stopped during the 65th train of pulses. As in case 1, during the first seconds of cTBS the participant had euphoric thoughts immediately followed by grunts and a dystonic attitude predominantly of the right (ipsilateral) hemibody, which tended to become bilateral and followed by generalized clonic movements during approximately 2 minutes. TMS was interrupted as soon as the experimenters noted the change in behavior. The participant became unresponsive and presented a stertorous respiration. He had post-ictal confusion during approximately 30 minutes. He was admitted to the Emergency Department of Saint-Luc University Hospital. Neurological examination was normal. A T1 structural MRI did not reveal any lesion or structural abnormality. Both subjects recovered fully.

Our observations suggest that deep cTBS of the operculo-insular cortex triggered two epileptic seizures with an operculo-insular onset. In case 1, the seizure was very short lasting and remained focal. In case 2, the seizure was also short lasting, initially focal, but with secondary generalization. Supporting an operculo-insular onset is the fact that the clinical manifestations and their sequence are highly like the manifestations of insular lobe seizures (Isnard et al., 2004; Wynford-Thomas and Powell, 2017).

In healthy volunteers, the seizure risk associated with TBS appears to be extremely low. Seizure occurrences after TBS and other high-frequency rTMS protocols are respectively estimated to 0.02% and less than 0.1% (Rossi et al., 2009; Oberman et al., 2011). The fact that deep cTBS of the operculo-insular cortex triggered two seizures out of only 18 participants

suggests that this specific protocol is associated with a higher risk of TMS-induced seizures. Two potential factors could have contributed to this increased risk. First, as compared to standard figure-of-eight coils, the double-cone coil can achieve significantly deeper field penetration, but at the expense of more intense and widespread electrical fields (Deng et al., 2014). Therefore, the volume of cortex that is synchronously stimulated by each TMS pulse is probably markedly increased as well as the electric field affecting the superficial cortex. These two factors potentially increase the risk of TMS-induced seizures. Current safety guidelines for rTMS have been proposed only for standard figure-of-eight coils (Rossi et al., 2009; Oberman et al., 2011) and may not be fully applicable to other coil designs (Deng et al., 2014). Nevertheless, it is important to stress that numerous previous studies have delivered deep rTMS using double cone coils at comparable or even higher intensities to what was delivered here without any report of TMS-induced seizure (Benito et al., 2012; Kreuzer et al., 2015). This suggests that deep cTBS of the operculo-insular cortex could be associated with a higher seizure risk than deep cTBS of other deep regions, e.g. cingulate or lower limb motor cortices.

B. Deep continuous theta burst stimulation of the operculo-insular cortex selectively affects Aδ-fiber heat pain

Lenoir C.[#], Algoet M.[#] and Mouraux A. Deep continuous theta burst stimulation of the operculo-insular cortex selectively affects Aδ-fiber heat pain. J Physiol 2018; 596, 4767-4787

[#] Both authors contributed equally

Abstract

Previous studies have suggested a pivotal role of the insular cortex in nociception and pain perception. Using a double-cone coil designed for deep transcranial magnetic stimulation, our objective was to assess (1) whether continuous theta burst stimulation (cTBS) of the operculo-insular cortex affects differentially the perception of different types of thermal and mechanical somatosensory inputs, (2) whether the induced after-effects are lateralized relative to the stimulated hemisphere, and (3) whether the after-effects are due to neuromodulation of the insula or neuromodulation of the more superficial opercular cortex. Seventeen participants took part in two experiments. In Experiment 1, thresholds and perceived intensity of Aδ- and C-fiber heat pain elicited by laser stimulation, non-painful cool sensations elicited by contact cold stimulation and mechanical vibrotactile sensations were assessed at the left hand before, immediately after and 20 min after deep cTBS delivered over the right operculo-insular cortex. In Experiment 2, Aδ-fiber heat pain and vibrotactile sensations elicited by stimulating the contra-lateral and ipsilateral hands were evaluated before and after deep cTBS or superficial cTBS delivered using a flat figure-of-eight coil. Only the

threshold to detect Aδ-fiber heat pain was significantly increased 20 min after deep cTBS. This effect was present at both hands. No effect was observed after superficial cTBS. Neuromodulation of the operculo-insular cortex using deep cTBS induces a bilateral reduction of the ability to perceive Aδ-fiber heat pain, without concomitantly affecting the ability to perceive innocuous warm, cold or vibrotactile sensations.

1. Introduction

There is increasing – but somewhat conflicting – evidence that the operculo-insular cortex plays an important role in pain perception (Starr et al., 2009; Davis et al., 2015; Segerdahl et al., 2015; Feinstein et al., 2016; Liberati et al., 2016). This has led some authors to propose that neuromodulation of the operculo-insular cortex could constitute a means to alleviate chronic pain (Ciampi de Andrade et al., 2012; Galhardoni et al., 2015; Segerdahl et al., 2015; Moisset et al., 2016). Supporting a central role of the operculo-insular cortex in nociception and pain is the observation that more than 40% of the spino-thalamic tract is relayed by thalamic neurons projecting to the insular cortex in primates (Dum et al., 2009). Second, brain responses elicited by painful stimuli have been consistently observed in the human operculo-insular cortex using functional magnetic resonance imaging, positron emission tomography, and intracerebral electro-encephalography (Peyron et al., 2002; Mazzola et al., 2012). Interestingly, intracerebral recordings performed in patients have shown that nociceptive stimuli elicit early-latency responses in both the contralateral and ipsilateral operculo-insular cortex (Frot et al., 1999; Peyron et al., 2002). Several authors have proposed

that the posterior part of the operculo-insular cortex could be more specifically involved in the processing of nociceptive inputs and in pain perception (Segerdahl et al., 2015). Indeed, direct intracerebral electrical stimulation of the dorsal-posterior insular cortex can elicit painful sensations, especially when the posterior part of the insular cortex is stimulated (Ostrowsky et al., 2002; Afif et al., 2008; Mazzola et al., 2009; Mazzola et al., 2012), but not when other brain areas activated by nociceptive stimuli were stimulated such as the primary somatosensory cortex (S1) or the anterior cingulate cortex (ACC) (Hutchison et al., 1999; Mazzola et al., 2006; Mazzola et al., 2012). However, it is important to note that painful sensations were reported in only 26 out of 101 patients (Ostrowsky et al., 2002; Mazzola et al., 2006; Afif et al., 2008; Mazzola et al., 2009; Stephani et al., 2011) and for only 10% of the stimuli delivered to this region (Ostrowsky et al., 2002; Mazzola et al., 2006; Afif et al., 2008; Mazzola et al., 2009). Finally, whether lesions of the posterior insula and adjacent parietal operculum impair the ability to perceive thermal sensations and/or pain remains debated. Garcia-Larrea et al. (2010) retrospectively studied 270 patients suffering from somatosensory abnormalities after stroke. Five of these patients had a selective impairment of thermonociception. All of these patients had lesions involving the posterior operculo-insular cortex. However, a later review of 24 patients with unilateral stroke lesions primarily affecting the insular cortex reported no changes in cold, heat or mechanical pain thresholds (Baier et al., 2014). Furthermore, Starr et al. (2009) reported two patients with extensive lesions of the insular cortex, and unscathed abilities to perceive and evaluate pain (see also Feinstein et

al. (2016)). In fact, these patients even exhibited increased pain ratings to noxious heat stimuli as compared to age-matched controls. The noxious stimuli also elicited stronger activity in primary and secondary somatosensory cortices (S1 and S2), suggesting a functional reorganization of nociceptive processing. Whether the perception of thermal and/or nociceptive stimuli depends on the function of the operculo-insular cortex in healthy individuals thus remains a very open question. In the present study, we attempted to address this question by characterizing the after-effects of repetitive transcranial magnetic stimulation (rTMS) delivered over the posterior operculo-insular cortex on the perception elicited by a set of somatosensory stimuli selectively activating heat- or cold-sensitive afferents of the spino-thalamic system, and mechano-sensitive afferents of the lemniscal system. Because of the deep location of the insula, the TMS pulses were delivered using a double-cone coil specifically designed to reach deep cortical targets such as the representation of the lower limb in the primary motor cortex (M1) (Stokic et al., 1997; Terao et al., 2000; Groppa et al., 2012; Deng et al., 2014). This procedure was recently proposed by Ciampi de Andrade et al. (2012), who also showed that repetitive TMS delivered at 10 Hz over the operculo-insular cortex using a double cone coil is safe and well tolerated. We chose to deliver repetitive TMS using a protocol referred to as continuous theta-burst stimulation (cTBS; Huang and Rothwell (2004)). Applied to the hand representation of the motor cortex, this protocol has been shown to have an inhibitory effect on motor-evoked potentials (MEPs) lasting at least 20 min after the stimulation (Huang et al., 2005). In addition to testing whether cTBS delivered over the operculo-insular cortex

differentially affects the ability to perceive thermal and/or nociceptive inputs conveyed by the spinothalamic system, we also examined whether the after-effects are restricted to the perception of sensory inputs originating from the hemibody contralateral to the operculo-insular cortex targeted by cTBS, or whether they affect similarly the perception of inputs originating from both hemibodies. As mentioned above, numerous studies reported bilateral operculo-insular activation by nociceptive stimuli (Coghill et al., 1999; Maihofner et al., 2002; Peyron et al., 2002; Garcia-Larrea et al., 2003; Iannetti et al., 2005; Mazzola et al., 2009; Mazzola et al., 2012). Therefore, modulating the excitability of one insula might affect not only the processing of inputs originating from the contralateral hemibody but also from the ipsilateral hemibody. Finally, deep cTBS delivered using a double-cone coil can be expected to affect not only the targeted structure but also more superficial structures such as S2 (Valmunen et al., 2009; Lockwood et al., 2013). For this reason, we also compared the after-effects of deep cTBS delivered using a double-cone coil to the after-effects of superficial cTBS delivered using a conventional flat figure-of-eight coil.

2. Methods

Ethical approval. The experiments were conducted according to the latest revision of the Declaration of Helsinki, except for registration in a database. Approval for the experimental procedures was obtained from the local ethics committee (Commission d'Ethique Biomedicale Hospitalo-Facultaire) of the Université catholique de Louvain (B403201316436). All participants

were informed of the experimental procedures, provided written informed consent and were financially compensated for their participation.

Subjects. A sample size of 10 participants was planned in both experiments. A neurologist screened all participants for contra-indications to TMS (Rossi et al., 2009). None of them had any history of psychiatric or neurological disorders including migraine and epilepsy or family history of seizure. None of the participants was allergic to lidocaine. All participants were right handed (Flinders Handedness Survey; Nicholls et al. (2013)). Eleven healthy volunteers (3 women/8 men; 29.2 ± 5.3 years; range 23–41 years) took part in Experiment 1. Eight healthy volunteers (3 women/5 men; 23.3 ± 1.7 years; range 20–26 years) took part in Experiment 2. In both experiments, cTBS was delivered over the right operculo-insular cortex. In one participant of Experiment 1, cTBS triggered a partial seizure starting with a very transient euphoria followed by a dystonic attitude of the left hemibody and hemiface, anxiety, a feeling of thoracic oppression and dysarthria lasting less than 1 min. Lateralization of the symptoms was difficult to confirm because the participant was positioned in left lateral decubitus when receiving cTBS. Subsequently, in one participant of Experiment 2, cTBS triggered similar symptoms with a dystonic attitude of the right hemibody and hemiface followed by a generalized tonicoclonic seizure lasting approximately 3 min, and acute post-ictal confusion. The two subjects fully recovered after the incident. The data of these two participants was excluded from the analyses, and the decision was taken to end the study. These two seizures induced by

deep cTBS of the operculo-insular cortex have been fully described elsewhere (Lenoir et al., 2018b).

Experimental design. In Experiment 1, we examined whether deep cTBS delivered using a double-cone coil over the right operculo-insular cortex differentially affects the perception of transient heat, cool and vibrotactile stimuli delivered to the contralateral hand by comparing detection thresholds and intensity of perception before cTBS (T0), immediately after cTBS (T1), 10 min after cTBS (T2) and 20 min after cTBS (T3) (Figure 1). In Experiment 2, we examined – in two separate sessions whose order was counterbalanced across participants – whether deep cTBS delivered using a double-cone coil and superficial cTBS delivered using a flat figure-of-eight coil over the right operculo-insular cortex differentially affects the perception of transient heat and vibrotactile stimuli delivered to the contralateral and ipsilateral hands. Detection thresholds were determined before (T0), immediately after (T1) and 20 min after (T3) cTBS. Reaction times, intensity and quality of perception elicited by suprathreshold stimuli were assessed before (T0) and 10 min after cTBS (T2). In both experiments, all assessments were completed within 30 min after ending cTBS. Our experimental design did not include a sham condition, because our aim was to assess the differential effect of deep vs. superficial cTBS delivered over the operculo-insular cortex. Furthermore, a control condition with sham cTBS would not have matched the strong sensations associated with the delivery of cTBS over the lateral aspect of the skull resulting in part from the peripheral activation of the temporalis muscle.

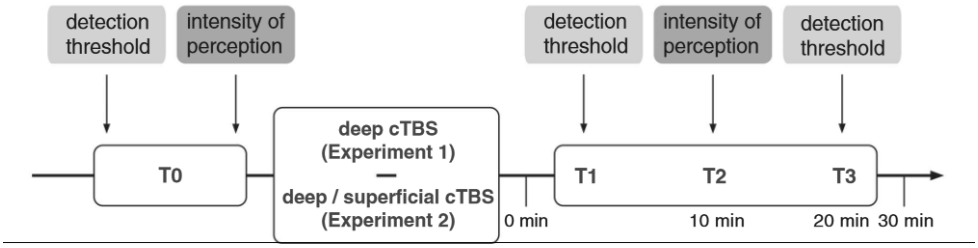

Figure 1. Experimental design. Both experiments followed the same procedure. Detection thresholds were monitored before (T0), immediately after (T1) and 20 min after cTBS (T3). The perceived intensity elicited by suprathreshold stimuli was monitored before (T0) and 10 min after cTBS (T2). Note that the threshold measurements at T0 and T1 and the perception evaluation at T0 and T2 were separated by approximately the same amount of time. In Experiment 1, thresholds and perception were assessed for four modalities: Aδ-heat, C-heat, Aδ-cool and Aβ-vibrotactile stimuli delivered on the contralateral hand (left) relative to the right insular cortex onto which deep cTBS was applied. In Experiment 2, sensory changes were assessed for two modalities: Aδ-heat and Aβ-vibrotactile stimuli delivered on the contralateral and ipsilateral hand at the same time points before and after deep cTBS of the operculo-insular cortex or superficial cTBS of the operculum. The experimental procedures were completed within 30 min following cTBS.

Determination of the dorsal posterior operculo-insular target. The target of cTBS was determined using individual 3D T1-weighted structural magnetic resonance imaging (MRI) data of the whole head (1 mm × 1mm × 1 mm; 3T Achieva; Philips Healthcare, Amsterdam, The Netherlands), acquired before the experiment. The right insular cortex was identified on the 3D MRI image of each participant (Ciampi de Andrade et al., 2012). A landmark was positioned over the dorsal-posterior region of the insular cortex,

corresponding to the dorsal portions of the anterior and posterior long gyrus (Figure 2; Nieuwenhuys (2012)).

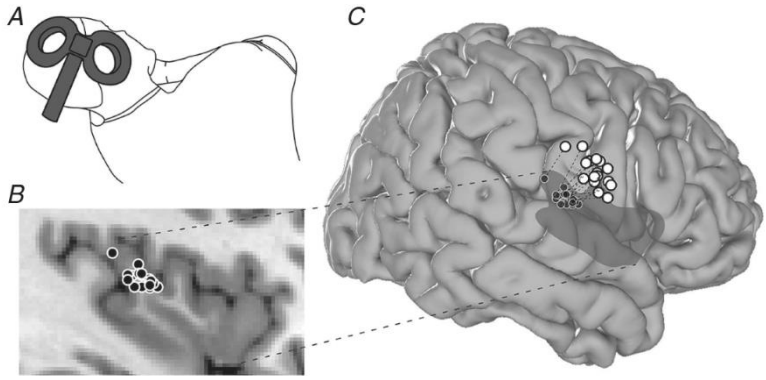

Figure 2. Localization of the target sites in the dorso-posterior insular cortex and the localization of the positions of the TMS coil. A, position of the TMS double cone coil with the handle pointing backwards during the cTBS protocol; the participants were lying in left lateral decubitus position. B, localization of the target sites in the dorso-posterior insular cortex (black circles; MNI coordinates x: [34 to 42], y: [−17 to−5], z: [4 to 14]) defined on individual 3D structural MRI image for the MRI-guided neuronavigation system. C, projections on the cortical surface of the position of the center of the TMS coil (white circles) at which cTBS was applied for all participants; the corresponding target markers in the dorsal posterior insula are indicated by the black circles; the location of the insula is indicated in dark grey. The apparent discrepancy between the target markers and the position of the coil is due to the 2D visualization of the different orientations of the TMS coil according to the individual curvature of the head (MNI Colin 27 brain reconstruction adapted from JuBrain; Mohlberg et al. (2012)).

The Visor2 neuronavigation system (Visor 2.1 and Visor 2.3.3, Advanced Neuro Technologies, Enschede, The Netherlands) was used to generate a 3D reconstruction of scalp and cortical volumes using the individual MRI data,

to coregister 3D space with the reconstructed MRI space using landmark-based markers (nasion and tragi) followed by head-shape matching (Wang et al., 1994; Gugino et al., 2001), and to accurately position and monitor the target of the TMS coil relative to the defined MRI target.

Continuous theta-burst stimulation. To reduce the scalp discomfort associated with the delivery of cTBS, 45 min prior to the experiment, 2.5 g of lidocaine cream (EMLA cream; AstraZeneca, Brussels, Belgium) was applied on the scalp of the participants where the coil would be positioned (Borckardt et al., 2006). Furthermore, during cTBS, participants were provided with ear plugs and a mouth guard to reduce discomfort due to the sound generated by the TMS pulses and teeth contact resulting from the peripheral activation of the temporalis muscle, respectively. During stimulation, the participants were comfortably positioned in left lateral decubitus. The stimulation consisted of trains of three biphasic pulses (280μs) delivered at 50 Hz, repeated every 200 ms (i.e. 5Hz; Huang and Rothwell (2004); Huang et al. (2009)) during 20 s (total number of pulses: 300; Di Lazzaro et al. (2005); Huang et al. (2005)). The TMS pulses were generated using a MagPro X100 magnetic stimulator (Magventure, Farum, Denmark). The direction of the current induced in the brain was set to the anterior–posterior posterior–anterior (AP-PA) direction. In both experiments, the TMS coil (double cone coil or figure-of-eight coil) was positioned tangentially to the scalp on the right temporoparietal region with the handle pointing towards the back of the head, approximately parallel to the midline (Fig. 2A). In Experiments 1 and 2, deep cTBS of the operculo-

insular cortex was delivered using an angled double-cone coil designed for deep stimulation (70 mm; D-B80 Butterfly Coil; MagVenture). The intensity of the TMS pulses was set individually to 80% of the average of the resting motor thresholds (rMT) obtained for the left and right tibialis anterior (TA). The TA-rMT was determined as the minimum intensity required to elicit MEPs 50µV (peak-to-peak amplitude between 20 and 50 ms after stimulus onset; Rossini et al. (2015)) in the contralateral TA in at least 5 out of 10 consecutive trials. This approach to determine stimulation intensity was used previously by Ciampi de Andrade et al. (2012), in a study aiming to modulate the insular cortex using a double-cone TMS coil, and is justified by the fact that the distance from the skull to the motor representation of the lower limbs in M1 is similar to the distance from the scalp to the insular cortex (respectively 47.1 ± 4.8 and 48.8 ± 4.2 mm; Ciampi de Andrade et al. (2012)). In Experiment 2, superficial cTBS over the operculo-insular cortex was delivered using a flat figure-of-eight coil (75 mm; C-B60 Butterfly Coil; MagVenture). The intensity of the TMS pulses was set individually to 80% of the average of the rMTs of the right and left first dorsal interosseous (FDI). Deep cTBS was delivered such as in Experiment 1.

Skin temperature. Skin temperature of the contralateral hand dorsum in Experiment 1 and of both hand dorsums in Experiment 2 was measured before and after each time point measurement, using an infrared thermometer (Raytek MI3, Raytek Corp., Santa Cruz, CA, USA).

Sensory stimulation. Transient heat stimuli consisted of radiant heat pulses (CO_2 laser; 100 ms duration; 6 mm diameter flat-top beam) delivered to the

hand dorsum and generated by a temperature-controlled CO_2 laser (Laser Stimulation Device; SIFEC, Ferrières, Belgium). These stimuli could be expected to generate responses related to the selective activation of heat-sensitive Aδ- and/or C-fibres (Towell et al., 1996; Mouraux et al., 2003; Plaghki and Mouraux, 2003). To avoid habituation and/or sensitization effects, the target of the laser was slightly displaced after each stimulus by approximately 2 cm. Transient cool stimuli consisted of fast cooling of the hand dorsum skin (200°C s^{-1}; 200 ms duration; 125 mm^2 probe surface) using a novel contact cold stimulator based on micro-Peltier elements (TCS; QST.Lab, Strasbourg, France). These stimuli would be expected to generate responses related to the selective activation of cool-sensitive Aδ-fibers (Simone and Kajander, 1997). Such as for laser stimuli, the location of the probe on the skin was slightly displaced after each stimulus by approximately 2 cm. Transient vibrotactile stimuli consisted of short lasting mechanical vibrations (300 Hz frequency; 100 ms duration; 20 mm diameter round-tipped probe) delivered to the index finger tip and generated by a piezo-electric actuator (VTS, Arsalis, UCL, Louvain-la-Neuve, Belgium). These stimuli could be expected to generate responses related to the selective activation of low-threshold Aβ-fibre mechanoreceptors.

Detection thresholds. Detection thresholds were determined using an adaptive staircase procedure based on the detection of the stimulus (Churyukanov et al., 2012). Participants were requested to press a button held in the contralateral hand as soon as they detected the stimulus delivered on the other hand dorsum. The intensity of the next stimulus was

decreased or increased by a fixed amount, depending on whether the previous stimulus was detected or undetected, respectively. The threshold was computed by averaging the intensities of the four stimuli at which a staircase reversal occurred (detected stimulus followed by undetected stimulus or the reverse). In Experiment 1, four different detection thresholds were assessed at the left hand dorsum using four randomly intermingled staircases: C-fiber heat detection threshold, Aδ-fiber heat detection threshold, cool detection threshold and vibrotactile detection threshold (Fig. 3).

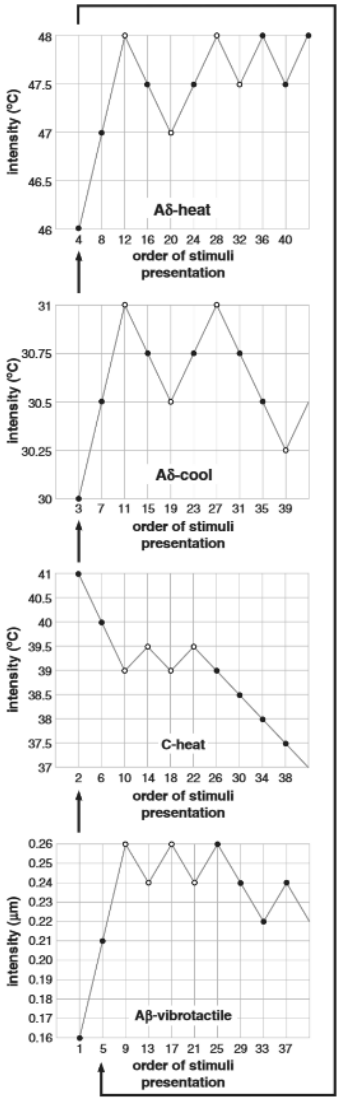

Figure 3. Example of the threshold intermingled staircase procedure for Experiment 1. In this representative participant, the first stimulus delivered was Aβ-vibrotactile (1; lower panel) followed by a C-heat stimulus (2) followed by a Aδ-cool stimulus (3) followed by an Aδ-heat stimulus (4; upper panel). The order is indicated by the arrows. This sequence was repeated until four reversals (open circles) were obtained for each modality. The order of the modalities was counterbalanced across participants. The different thresholds were computed within each modality by averaging stimulation intensities of the first four staircase reversals. In Experiment 2, the procedure was the same with alternative delivery of Aδ-heat and Aβ-vibrotactile stimuli. This procedure was conducted on one hand at a time. The order of the first tested hand was counterbalanced across participants.

In Experiment 2, two different detection thresholds were assessed at both the left hand dorsum and the right hand dorsum: Aδ-fiber heat detection threshold and vibrotactile detection threshold. The stimuli of these two modalities were alternatively delivered to one of the two hands, followed by the same procedure on the other hand. In both experiments, the time

interval between two successive stimuli varied between 10 and 20 s. For each type of stimulus, the staircase was ended as soon as four reversals had occurred. Several previous studies have shown that, for transient heat stimuli applied onto the skin, the detection threshold to C-fiber input is markedly lower than the detection threshold to Aδ-fiber input. Therefore, if detection of the stimulus is used as sole criterion, the estimated threshold will be related to the ability to detect input conveyed by heat-sensitive C-fibers. Conversely, if detection of the stimulus with a reaction time (RT) compatible with the conduction velocity of myelinated Aδ-fibers is used as criterion, the estimated threshold will be related to the ability to detect input conveyed by heat-sensitive Aδ-fibers (Towell et al., 1996; Mouraux et al., 2003; Plaghki and Mouraux, 2003). C-fiber heat detection thresholds were thus estimated with a staircase procedure using detection of the CO_2 laser stimulus as sole criterion. To reduce the number of steps required to estimate the threshold, the temperature of the first stimulus of the staircase was set close to the expected threshold (41°C; Meyer and Campbell (1981); Treede et al. (1995); Namer et al. (2009); Wooten et al. (2014)). Aδ-fiber heat detection thresholds were estimated with a staircase procedure using detection of the CO_2 laser stimulus with a RT<650 ms as criterion. The temperature of the first stimulus of the staircase was set to 46°C. For both staircases, step size was 1°C until the first reversal was obtained and then set to 0.5°C. Because transient innocuous cooling of the skin produces sensations strictly related to the activation of cool-sensitive Aδ-fibers (Mackenzie et al., 1975; Campero and Bostock, 2010), Aδ-fiber cool detection thresholds were estimated with a staircase procedure using

detection of the cool stimulus as sole criterion. The intensity of the first stimulus of the staircase was set to a temperature decrease of −1°C relative to baseline skin temperature. Step size was 0.5°C until the first reversal was obtained and then set to 0.25°C. Aβ-fiber vibrotactile detection thresholds were also estimated using detection as sole criterion. The intensity of the first stimulus of the staircase was set to 0.16 µm (detection threshold of 300 Hz vibration; Freeman and Johnson (1982); Bensmaia (2008)). Step size was 0.05 µm until the first reversal was obtained and then set to 0.02 µm. In both experiments, the modality of the first stimulus of the intermingled staircases was counterbalanced across participants. In Experiment 2, the hand which was tested first was also counterbalanced across participants. In both experiments, to reduce the number of steps required to estimate the threshold at T1 and T3, the intensity of the first stimulus of the staircase was set to the threshold obtained at the preceding time point.

Intensity of perception to suprathreshold stimuli. In Experiment 1, participants were asked to report verbally the intensity of perception elicited by supra-threshold high-intensity heat stimuli co-activating Aδ-and C-fiber heat-sensitive afferents, low-intensity heat stimuli preferentially activating low-threshold heat-sensitive C-fiber afferents, cool stimuli and vibrotactile stimuli. Ratings were provided using a numerical rating scale (NRS) ranging from 0 (no perception) to 100 (maximal conceivable intensity). For each of the four modalities, a block of 10 stimuli was delivered on the left hand dorsum of all participants. In Experiment 2, the same procedure was used to assess the intensity of the percept elicited by suprathreshold Aδ-heat and

Aβ-vibrotactile stimuli delivered to the left and right hands. In both experiments, the order of the blocks was counterbalanced across participants. Furthermore, in Experiment 2, reaction times to the suprathreshold stimuli were recorded, and participants were asked to describe the quality of the percept elicited by suprathreshold stimuli by selecting one item from a list of seven descriptors for Aδ-heat stimuli ('not perceived', 'light touch', 'touch', 'tingling', 'warm', 'pricking' and 'burning') and a list of five descriptors for Aβ-vibrotactile ('not perceived', 'light touch', 'touch', 'flutter' and 'vibration') (Ochoa and Torebjork, 1983; Nahra and Plaghki, 2003; Mouraux et al., 2010). Suprathreshold Aδ-heat stimuli consisted of 60°C CO_2 laser pulses. Suprathreshold C-heat stimuli consisted of CO_2 laser pulses delivered at a target temperature corresponding, for each participant, to the mean of Aδ- and C-fiber heat detection thresholds estimated before cTBS (44 ± 1.8°C), i.e. a temperature expected to be above the threshold of C-fibers, but below the threshold of Aδ-fibers. Suprathreshold Aδ-cool stimuli consisted of cooling of the skin down to 10°C. Supra-threshold Aβ-vibrotactile stimuli consisted of mechanical vibrations of 95 µm amplitude.

Statistics. Statistical analyses were conducted using SPSS Statistics version 25 (IBM Corp., Armonk, NY, USA). Significance threshold was set at $p<0.05$. In Experiment 1, to assess the differential effects of cTBS on the detection thresholds to heat, cool and vibrotactile stimuli, a two-way repeated-measures ANOVA (RM-ANOVA) was conducted with the factor 'time' (T0: before cTBS, T1: immediately after cTBS, T3: 20 min after cTBS) and

‘modality’ (Aδ-heat, C-heat, Aδ-cool, Aβ-vibrotactile). The same design was used to assess changes in perceived intensity to suprathreshold stimuli, except for the fact that the factor ‘time’ had only two levels (T0: before cTBS, T2: 10 min after cTBS). With this model, an interaction between the factors ‘time’ and ‘modality’ would indicate a differential effect of cTBS on the responses to the different types of stimuli. In Experiment 2, separate four-way RM-ANOVAs with the factors ‘time’, ‘treatment’ (deep vs. superficial cTBS), ‘modality’ (Aδ-heat vs. Aβ-vibrotactile) and ‘side’ (stimuli delivered to the contralateral vs. ipsilateral hand) were used to assess changes in detection thresholds, RTs and intensity of the perception elicited by suprathreshold stimuli. Because of the absence of any significant effect of ‘side’ (all $p>0.114$), measures from both sides were merged and further analyzed using three-way RM-ANOVAs with the factors ‘time’, ‘treatment’ and ‘modality’. With this model, a two-way interaction between the factors ‘time’ and ‘modality’ would indicate that both deep and superficial cTBS exert, at both hands, a differential effect on the responses to the two types of stimuli, but that the effects of deep and superficial cTBS are similar. A three-way interaction between the factors ‘time’ × ‘treatment’ × ‘modality’ would indicate that deep and superficial cTBS differentially modulate the responses to the two types of stimuli. When necessary a Greenhouse–Geisser correction was performed (denoted $F_{G\text{-}G}$). When justified, the effects were further assessed using univariate within-subjects contrasts and/or pairwise comparisons using a paired-sample Student’s *t* test, Bonferroni-corrected for multiple comparisons.

To test if cTBS affected the quality of perception in Experiment 2, a chi-square or Fisher's test was performed on the number of times each descriptor was used to qualify the sensation elicited by each stimulus. In addition, to examine whether the effects of cTBS on detection or perception of somatosensory stimuli was dependent on the intensity of the cTBS pulses, a linear Pearson's correlation was performed.

3. Results

M1 lower limb and insula distances from the scalp. The distance from the dorsal posterior insular cortex to the scalp, and from the lower limb representation in M1 to the scalp were measured in each individual MRI (n=16; scalp–insular cortex: 46 ± 4 mm; scalp–M1 lower limb: 45 ± 3 mm; Table 1). The mean difference between scalp–M1 lower limb and scalp–insula distances was −0.5 ± 3.9 mm. No significant difference between the two measures ($t_{(15)}$= 0.519; p= 0.612) was observed.

Table 1.	distance (mm)		cTBS intensity (% MSO)	
Experiment 1	**scalp - M1**	**scalp – insula**	**uncorrected**	**corrected**
Subject 1	47.5	46.1	39	41
Subject 2	45.9	48.3	46	44
Subject 3	42.6	44.8	50	48
Subject 4	42.1	39.8	32	35
Subject 5	41.1	44.1	50	47
Subject 6	49.7	48.1	37	39
Subject 7	48.2	44.9	60	64
Subject 8	48.0	47.5	36	37
Subject 9	42.7	48.3	47	41
Experiment 2				
Subject 1	49.2	50.6	39	31
Subject 2	43.7	46.6	34	27
Subject 3	44.7	41.3	37	30
Subject 4	47.0	41.3	38	30
Subject 5	43.2	41.2	27	22
Subject 6	43.3	53.2	33	26
Subject 7	43.7	44.4	33	26

Table 1. Distances and cTBS intensities relative to brain targets sites for both experiments. The distance from the scalp to the lower limb representation in M1 and from the scalp to the insular cortex were measured on the 3D MRI scans of each participants. The uncorrected cTBS intensities correspond to 80% of the average of the resting motor thresholds obtained for the right and left tibialis anterior, corrected cTBS intensities correspond to the distance-corrected intensities based on the intra-individual differences in distance between M1 and the insula.

Skin temperature. The skin temperature of the tested hand dorsum did not vary significantly over time, either in Experiment 1 (at T0: 30.9 ± 2.4°C; T1: 30.4 ± 1.7°C; T2: 30.5 ± 2°C) or in Experiment 2 (deep cTBS condition at T0: 32.6 ± 1.9°C; T1: 31.9 ± 1.9°C; T2: 32.3 ± 2.3°C; superficial cTBS condition at T0: 32.7 ± 1.5°C; T1: 31.9 ± 1.7°C; T2: 31.8 ± 2.4°C). Indeed, the one-way RM-

ANOVA did not reveal any significant difference in Experiment 1 (main effect of 'time'; $F_{(2,18)}$= 1.95; p= 0.171; η^2= 0.178) and neither the two-way RM-ANOVA in Experiment 2 when considering the temperatures of the contralateral and ipsilateral hands (main effect of 'time': $F_{(2,12)}$= 1.878; p= 0.195; η^2= 0.238; 'time' × 'treatment' interaction: $F_{(2,12)}$= 1.247; p= 0.322; η^2= 0.172; 'time' × 'treatment' × 'side' interaction: $F_{(1.137,6.821)}$= 0.911; p= 0.387; η^2= 0.132).

Experiment 1.

Detection thresholds. Figure 4 shows the individual changes in detection threshold for the different types of stimuli, immediately after cTBS (T1 vs.T0) and 20 min after cTBS (T3 vs. T0). In almost all participants, the detection threshold to Aδ-heat stimuli delivered to the contralateral hand was increased both at T1 and at T3. In contrast, cTBS did not appear to induce any reproducible change in the detection threshold to C-heat stimuli, Aδ-cool stimuli and Aβ-vibrotactile stimuli.

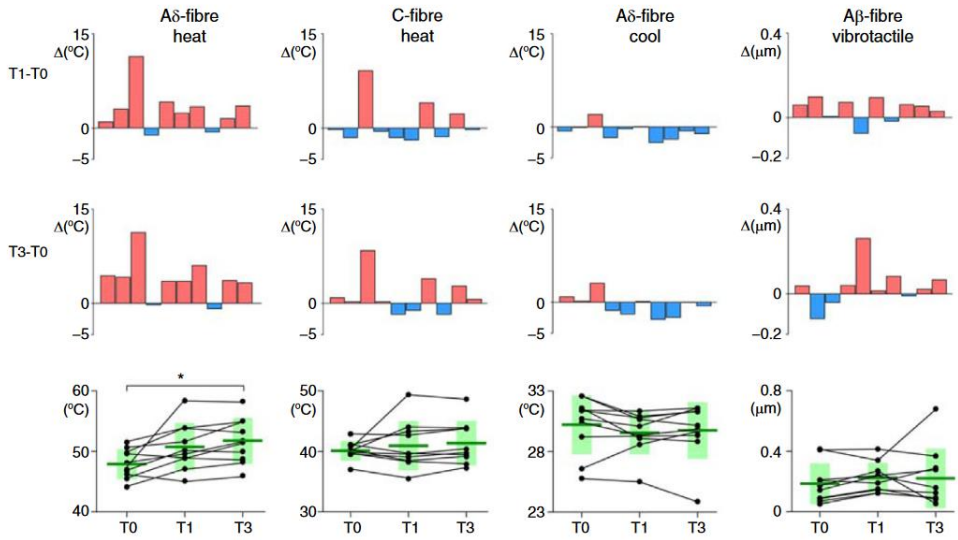

Figure 4. The effect of deep cTBS over the right operculo-insular cortex on detection thresholds in Experiment 1. Bar graphs represent the individual changes (increase in red, decrease in blue) in detection thresholds (n=10) immediately after cTBS (T1–T0) and 20 min after cTBS (T3–T0) for the four somatosensory modalities: Aδ-heat, C-heat, Aδ-cool and Aβ-vibrotactile delivered on the left contralateral hand. The lower graphs show the individual absolute thresholds at T0, T1 and T3; group-level average is displayed in green (mean ±SD).

This was confirmed by the RM-ANOVA, which revealed a significant a two-way 'time' × 'modality' interaction ($F_{(2.04,18.37)}$= 7.947; p= 0.003; η^2= 0.469) (Table 2). The univariate within-subjects contrasts showed a significant interaction for Aδ-heat vs. C-heat, Aδ-cool and Aβ-vibrotactile stimuli at T1 vs.T0 (Aδ-heat vs. C-heat: $F_{(1,9)}$= 7.321; p= 0.024; η^2= 0.449; Aδ-heat vs. Aδ-cool: $F_{(1,9)}$= 17.806; p= 0.002; η^2= 0.664; Aδ-heat vs. Aβ-vibrotactile: $F_{(1,9)}$= 7.742; p= 0.029; η^2= 0.428) and at T3 vs. T0 (Aδ-heat vs. C-heat: $F_{(1,9)}$= 20.879; p= 0.001; η^2= 0.699; Aδ-heat vs. Aδ-cool: $F_{(1,9)}$= 29.871; p= 0.0004;

η^2= 0.768; Aδ-heat vs. Aβ-vibrotactile: $F_{(1,9)}$= 13.399; p= 0.005; η^2= 0.598). Post hoc paired *t* tests showed that the increase in detection threshold for Aδ-heat stimuli was significant 20 min after cTBS (T3 vs.T0: $t_{(9)}$= −3.661; p= 0.009), but not immediately after cTBS (T1 vs.T0: $t_{(9)}$= −2.597; p= 0.057).

Table 2. **Experiment 1**

	main effect of 'time'			**main effect of 'modality'**			**interaction 'time' × 'modality'**		
	F value	p	η^2	F value	p	η^2	F value	p	η^2
threshold	$_{(G-G)}$2.85	.084	.241	$_{(G-G)}$943.4	**<.001***	.991	$_{(G-G)}$7.95	**.003***	.469
perception	22.22	**.001***	.702	22.28	**<.001***	.712	1.13	.354	.112

Table 2. Two-way RM-ANOVAs in Experiment 1. Repeated-measures ANOVAs for thresholds and intensity of perception with the factors 'time' (T0: before cTBS, T1: immediately after cTBS, T3: 20 minutes after cTBS; for thresholds) and (T0: before cTBS, T2: 10 minutes after cTBS; for perception) and 'modality' (Aδ-heat, C-heat, Aδ-cool, Aβ-vibrotactile).* p<.050. (G-G) indicates Greenhouse-Geisser correction.

Intensity of perception. As shown in Fig. 5, the intensity of the percept elicited by suprathreshold Aδ-heat stimuli was decreased 10 min after cTBS (T2) as compared to before cTBS (T0), in all but one participant. In contrast, cTBS did not appear to induce consistent changes in the intensity of the percept elicited by C-heat stimuli, Aδ-cool stimuli and Aβ-vibrotactile stimuli.

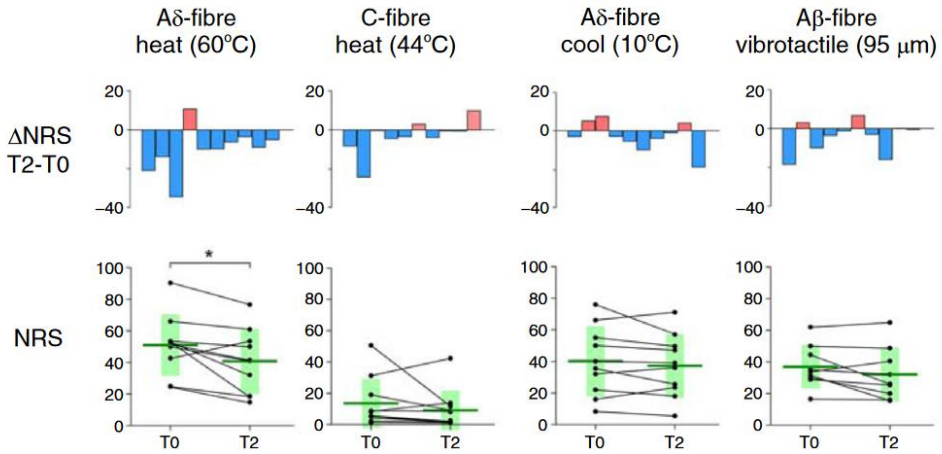

Figure 5. Effects of deep cTBS over the right operculo-insular cortex on perceived intensity in Experiment 1. Bar graphs represent the individual changes in perception (numerical rating scale, NRS; increase in red, decrease in blue; n=10 except for Aβ-vibrotactile where n=9 because of missing data) elicited by the four different suprathreshold stimuli delivered on the contralateral hand: Aδ-heat (60°C), C-heat (44°C), Aδ-cool (10°C) and Aβ-vibrotactile (95 µm) 10 min after cTBS (T2–T0). The lower graphs show the individual intensity of perception at T0 and T2; group-level average is displayed in green (mean ±SD).

The RM-ANOVA showed a significant main effect of 'time' ($F_{(3,27)}$= 21.222; p= 0.001; η^2= 0.702), a significant main effect of 'modality' ($F_{(3,27)}$= 22.284; p<0.0001; η^2= 0.712), but no 'time' × 'modality' interaction ($F_{(3,27)}$= 1.133; p= 0.354; η^2= 0.112) (Table 2). Paired sample *t* tests comparing, for each modality, the ratings obtained at T2 vs.T0 showed a significant decrease of the perception elicited by Aδ-heat stimuli ($t_{(9)}$= 2.74; p= 0.045), but not for C-heat stimuli ($t_{(9)}$= 1.166; p= 0.274), Aδ-cool stimuli ($t_{(9)}$= 2.138; p= 0.061) and Aβ-vibrotactile stimuli ($t_{(9)}$= 1,699; p= 0.128).

Experiment 2.

Detection thresholds. The three-way RM-ANOVA showed a significant three-way 'time' × 'treatment' × 'modality' interaction ($F_{(2,12)}$= 10.662; p= 0.002; η^2= 0.640), indicating that deep and superficial cTBS did not induce the same after-effects and, such as in Experiment 1, that cTBS did not exert the same effect on Aδ-heat and Aβ-vibrotactile detection thresholds. The univariate within-subjects contrasts showed a significant interaction 'time' × 'treatment' × 'modality' immediately after cTBS (T1 vs.T0: $F_{(1,6)}$= 8.890; p= 0.025; η^2= 0.597) and 20 min after cTBS (T3 vs.T0: $F_{(1,6)}$= 14.919; p= 0.008; η^2= 0.713). Post hoc pairwise comparisons showed that, such as in Experiment 1, the detection threshold for Aδ-heat stimuli was significantly increased 20 min after deep cTBS (T3 vs.T0: p= 0.022). In contrast, the detection threshold for Aδ-heat stimuli was not significantly changed immediately after deep cTBS (T1 vs.T0: p= 0.144). No significant changes in Aδ-heat detection thresholds were observed after superficial cTBS (T3 vs.T0: p= 0.969; T1 vs.T0: p= 0.320). Finally, there was no significant change in Aβ-vibrotactile detection thresholds, both after deep cTBS (T3 vs.T0: p= 1.0; T1 vs.T0: p= 0.685) and after superficial cTBS (T3 vs.T0: p= 1.0; T1 vs.T0: p=1.0) (Fig. 6).

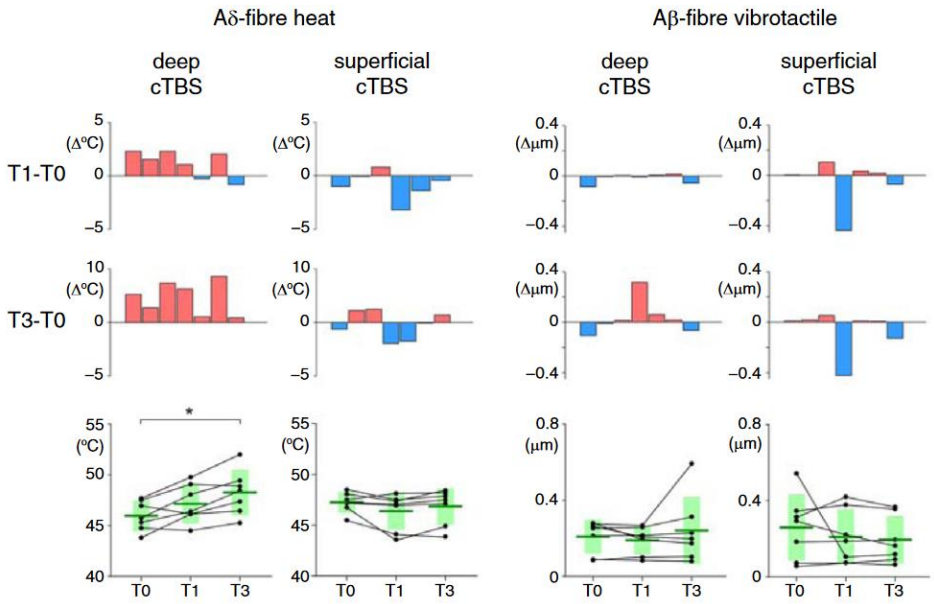

Figure 6. The effect of cTBS on detection thresholds in Experiment 2. Effects of deep and superficial cTBS of the operculo-insular cortex on Aδ-heat and Aβ-vibrotactile thresholds. Bar graphs represent the individual changes (increase in red, decrease in blue) in threshold (n=7) immediately after cTBS (T1–T0) and 20 min after cTBS (T3–T0). The lower graphs show the individual thresholds; group-level average is displayed in green (mean ±SD).

Intensity of perception. The intensity of perception elicited by suprathreshold Aδ-heat and Aβ-vibrotactile stimuli was not significantly affected after either deep cTBS or superficial cTBS (Table 3 and Fig. 7).

Table 3.

	Experiment2								
	main effect of 'time'			**interaction 'time' × 'modality'**			**interaction 'time' × 'modality' × 'treatment'**		
	F value	p	η^2	F value	p	η^2	F value	p	η^2
threshold	6.05	**.015***	.502	6.06	**.015***	.503	10.66	**.002***	.640
perception	.798	.406	.117	.078	.789	.013	2.303	.180	.277
RTs	.566	.480	.086	.053	.826	.009	.670	.444	.100

Table 3. Three-way RM-ANOVAs in Experiment 2. Repeated-measures ANOVAs with the factors 'time' (T0: before cTBS, T1: immediately after cTBS, T3: 20 minutes after cTBS; for thresholds) and (T0: before cTBS, T2: 10 minutes after cTBS; for perception and reaction time), 'modality' (Aδ-heat vs. Aβ-vibrotactile) and 'treatment' (deep vs. superficial cTBS).* p <.050.

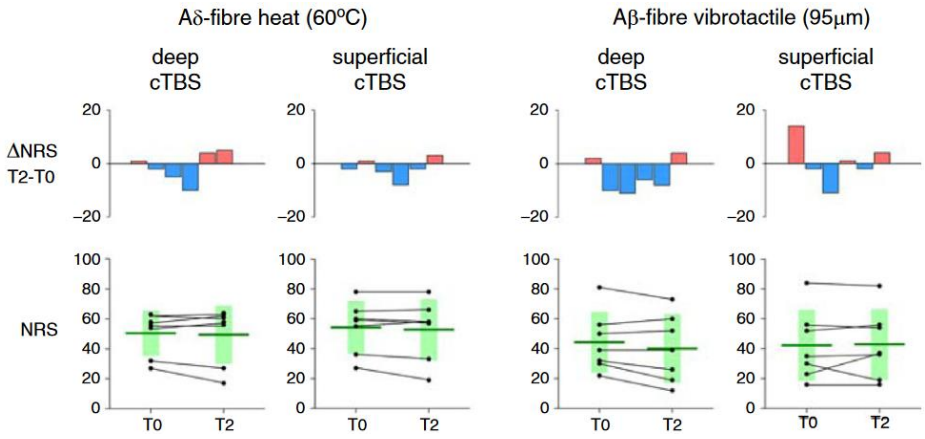

Figure 7. Effect of deep and superficial cTBS on intensity of perception in Experiment 2. Bar graphs indicate individual changes in perception (numerical rating scale, NRS; increase in red, decrease in blue; n=7) elicited by Aδ-heat (60°C) and Aβ-vibrotactile (95 μm) stimuli. The lower graphs show the individual perception; group-level average is displayed in green (mean ±SD).

Reaction time. The RTs elicited by suprathreshold Aδ-heat and Aβ-vibrotactile stimuli were not significantly affected after either deep or superficial cTBS (Table 3 and Fig. 8). The group-level average RT across conditions was 330 ± 50 ms for Aδ-heat stimuli and 227 ± 42 ms for Aβ-vibrotactile stimuli. During the threshold procedure, the RTs related to Aδ-heat stimuli detected within the time window criterion were similar before (at T0: 399 ± 75 ms) and after (at T3: 401 ± 35 ms) deep cTBS, and before (at T0: 452 ± 61 ms) and after (at T3: 435 ± 46 ms) superficial cTBS. This was also the case for the RTs related to Aβ-vibrotactile stimuli detected during the threshold procedure, before (at T0: 386 ± 71 ms) and after (at T3: 375 ± 125 ms) deep cTBS, and before (at T0: 369 ± 67 ms) and after (at T3: 361 ± 65 ms) superficial cTBS.

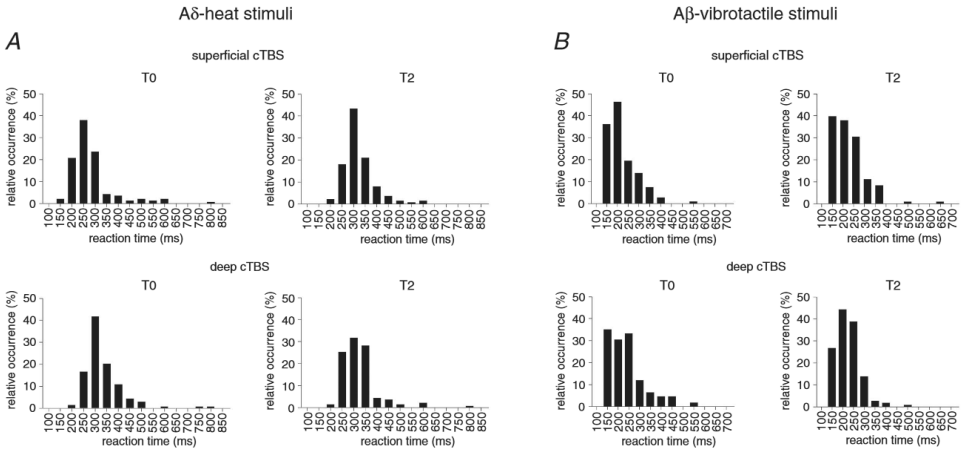

Figure 8. Relative frequency distribution of reaction times to suprathreshold Aδ-heat and Aβ-vibrotactile stimuli in Experiment 2. A, effect of deep and superficial cTBS on reaction times to suprathreshold Aδ-heat stimuli (60°C). The relative frequency distribution of RTs are displayed before (T0) and 10

min after (T2) cTBS. B, effect of deep and superficial cTBS on RTs to suprathreshold Aβ-vibrotactile stimuli (95 µm) at T0 and T2.

Quality of perception. The descriptors most often chosen to qualify the percept elicited by suprathreshold Aδ-heat stimuli and Aβ-vibrotactile stimuli before and after deep and superficial cTBS are shown in Fig. 9. Aδ-heat stimuli were most often considered as painful and described as burning or pricking (75–88%). The relative proportion of the different descriptors remained similar both after deep cTBS (Aδ-heat: p= 0.445; Aβ-vibrotactile: p= 0.071) and after superficial cTBS (Aδ-heat: p= 0.090; Aβ-vibrotactile: p= 0.321).

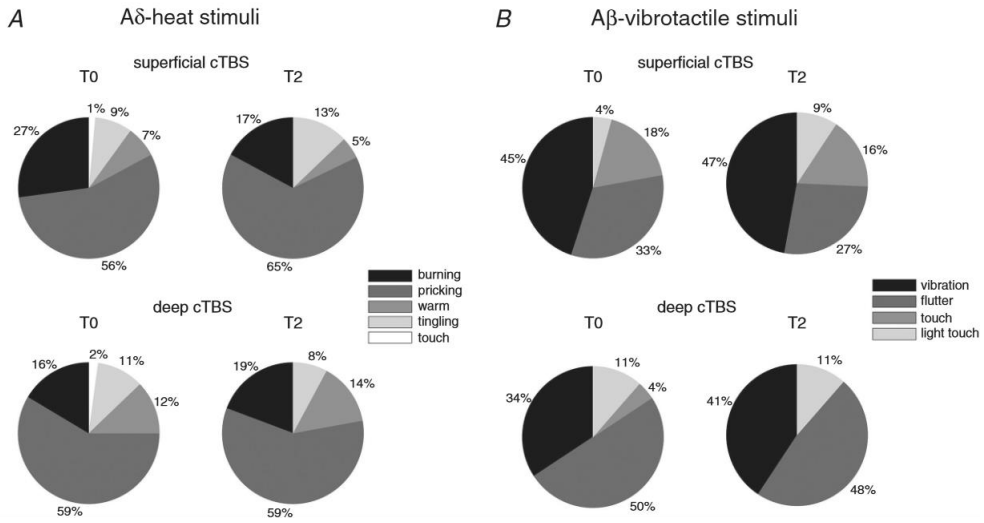

Figure 9. Quality of perception of suprathreshold stimuli in Experiment 2. A, quality of perception of suprathreshold Aδ-heat stimuli. B, quality of perception of suprathreshold Aβ-vibrotactile stimuli (95 µm). Pie charts represent the proportion of the use of each descriptor before (T0) and 10 min after (T2) cTBS. In both cases, all stimuli were perceived; in all conditions

Aδ-heat stimuli were mainly perceived as painful (burning or pricking) before and after deep or superficial cTBS.

Influence of cTBS intensity. The average intensity of TMS to deliver deep cTBS was 44 ± 8% of maximum stimulator output in Experiment 1 and 34 ± 9% in Experiment 2. There was a significant correlation between the magnitude of the increase in detection threshold of Aδ-heat stimuli 20 min after deep cTBS and the intensity of TMS (Fig. 10A). Specifically, taking the 16 participants of Experiments 1 and 2, there was a strong positive correlation between the increase in Aδ-heat thresholds at T3 vs. T0 and the intensity of cTBS pulses (r= 0.733; n= 16; p= 0.001; Pearson correlation; one observation has a standardized residual greater than the cut-off of three standard deviations, this participant was excluded for linear regression). When all the 17 participants of Experiments 1 and 2 were considered, there was still a significant positive correlation (r= 0.613; n= 17; p= 0.009; Pearson correlation). This indicates that increasing cTBS intensity led to a larger increase in Aδ-heat detection thresholds. On the contrary, there was no significant correlation between the change in Aβ-vibrotactile detection threshold 20 min after deep cTBS and the intensity of TMS (r= 0.110; n= 17; p= 0.676; Pearson correlation; Fig. 10B). Additionally, we estimated, for each participant, the intensity of cTBS pulses at the depth of the insular cortex using the attenuation coefficient for a batwing coil proposed by Cai et al. (2012) (Table 1). Taking into account coil–cortex distance did not improve the correlation between intensity of cTBS and the changes in Aδ-heat detection (r= 0.592; n= 16; p= 0.016 vs. r= 0.733; n= 16; p= 0.001; Pearson correlation; Fig. 10C).

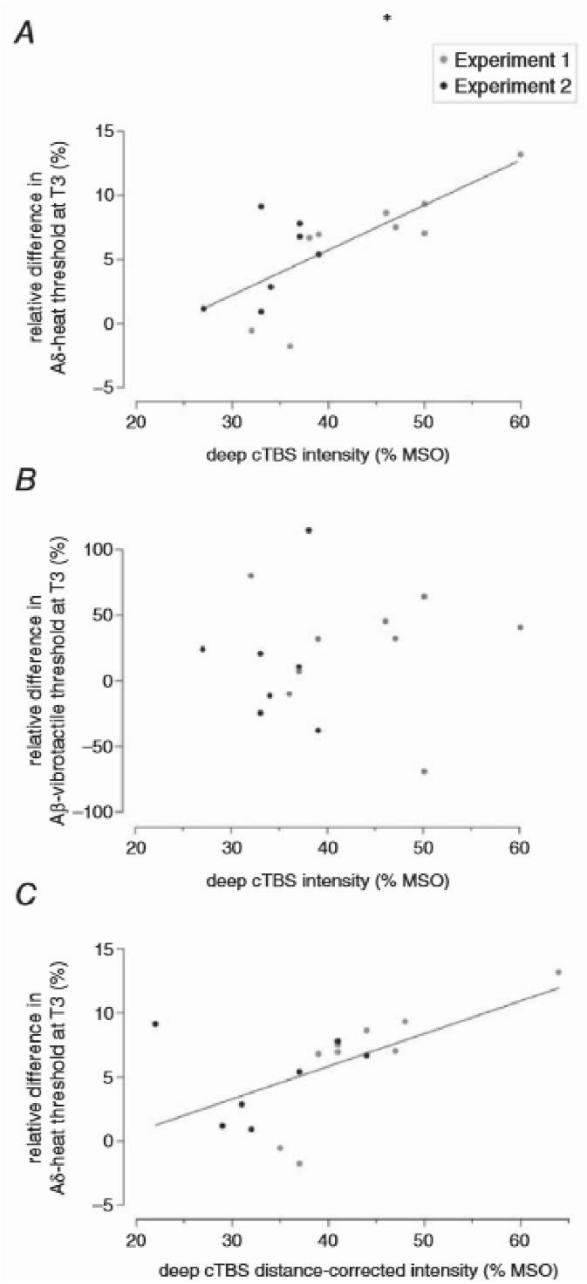

Figure 10. Relationship between the effect of deep cTBS on thresholds and intensity of cTBS pulses. A, linear regression for all the participants (Experiment 1 and 2) between the intensity of cTBS pulses used during deep

cTBS of the operculo-insular cortex and the relative difference in Aδ-heat threshold 20 min after cTBS (T3–T0). The increase of Aδ-heat threshold was significantly positively correlated with the intensity of cTBS pulses (r= 0.733; n= 16; p= 0.001; one observation, indicated by ∗, was excluded due to a standardized residual greater than 3 standard deviations; when all participants were included: r= 0.613; n= 17; p= 0.009). B, linear regression for all the participants (Experiment 1 and 2) between the intensity of cTBS pulses used during deep cTBS of the operculo-insular cortex and the relative difference in Aβ-vibrotactile threshold 20 min after cTBS (T3–T0). There was no significant correlation (r= 0.110; n= 17; p= 0.676). C, linear regression for all the participants (Experiment 1and 2) between the intensity of deep cTBS pulses, corrected for the coil–cortical target distance, used during deep cTBS of the operculo-insular cortex and the relative difference in Aδ-heat threshold 20 min after cTBS (T3–T0). The increase of Aδ-heat threshold was significantly positively correlated with the intensity of cTBS pulses (r= 0.592; n= 16; p= 0.016).

4. Discussion

Our results show that deep cTBS of the operculo-insular cortex selectively impairs the ability to perceive thermonociceptive input conveyed by Aδ-fiber thermo-nociceptors. Indeed, deep cTBS but not superficial cTBS of the right operculo-insular cortex induced a significant increase of Aδ-fiber heat detection thresholds, without concomitantly affecting the perception of thermal sensations conveyed by C-fibers, the perception of cold sensations conveyed by cool-sensitive Aδ-fibers, and the perception of vibrotactile input conveyed by low-threshold Aβ-fiber mechanoreceptors. The effect of operculo-insular cTBS on the perception of Aδ-fiber input was present at both the contralateral and the ipsilateral hand. Importantly, the magnitude of the increase in detection threshold was correlated with the intensity of

the cTBS pulses, indicating that the change was truly due to a neuro-modulatory effect of cTBS.

Deep operculo-insular cTBS selectively affects the perception of Aδ-fiber heat. Deep cTBS over the operculo-insular cortex induced a significant change in the ability to detect heat sensations related to the transient activation of Aδ-fiber thermonociceptors, without concomitantly affecting the detection of heat sensations conveyed by unmyelinated C-fibers, the detection of cold sensations conveyed by cool-sensitive Aδ-fibers, and the detection of vibrotactile sensations conveyed by large-diameter Aβ-fibers. The significant increase of Aδ-heat detection thresholds was present in both experiments after deep cTBS. Importantly, it was not observed in Experiment 2 after superficial cTBS, indicating that the increase in detection threshold after deep cTBS was not a consequence of response habituation (Greffrath et al., 2007; May et al., 2012) or decreased vigilance (Legrain et al., 2002; Legrain et al., 2012). Given that the criterion to determine Aδ-heat detection thresholds depended on whether participants detected the stimuli with a reaction time compatible with the conduction velocity of myelinated Aδ-fibers, whether the change in Aδ-heat detection thresholds could have been driven by an effect of cTBS on motor/sensorimotor processes should also be considered. This seems very unlikely as there was no significant difference in the average detection latency for Aδ-heat stimuli detected within the time window criterion during the threshold procedure, as well as in the detection latency for suprathreshold Aδ-heat stimuli. There was also no change in the detection latency of Aβ-vibrotactile stimuli. Finally,

there was a clear relationship between the intensity of the TMS pulses used to deliver cTBS and its after-effect on Aδ-heat detection threshold. Although our results allow us to conclude a differential effect of deep cTBS on the different modalities (with a significant effect on Aδ-heat perception), they do not allow us to conclude an absence of effect on the other modalities. Unfortunately, to answer this question, increasing the sample size is not possible for safety and ethical reasons given the induction of one suspected and one confirmed epileptic seizure in two participants after the deep cTBS protocol. It has been proposed that cTBS induces cortical inhibition through a local increase of γ-aminobutyric acid (GABA) (Stagg et al., 2009; Trippe et al., 2009). Supporting this interpretation, Jasmin et al. (2003) demonstrated in rodents that increasing GABA concentration in the insular cortex reduces pain behavior to noxious heat. Therefore, the modulation of thermonociception by cTBS observed in the present study could be explained, at least in part, by a GABAergic modulation of the operculo-insular cortex, as suggested by several authors (Enna and McCarson, 2006; Lefaucheur, 2006; Mylius et al., 2012; Denis et al., 2016; Moisset et al., 2016). Previous evidence suggesting a specific role of the operculo-insular cortex in thermonociception would predict that deep operculo-insular cTBS preferentially affects the perception of all inputs conveyed by the spinothalamic system; i.e. that deep operculo-insular cTBS would similarly affect the perception of heat and cold stimuli, as compared to vibrotactile stimuli. Other studies, suggesting that the processing of cold and heat may involve distinct operculo-insular subregions (Casey et al., 1996; Davis et al., 1998; Davis et al., 1999; Craig et al., 2000; Mano et al., 2017), would predict

that cTBS can differentially affect the detection of heat and cold stimuli, but would not predict a differential effect of cTBS on the detection of heat sensations conveyed by Aδ- and C-fibers. Studies investigating the relationship between the activity of the operculo-insular cortex and heat perception have revealed different patterns of activation depending on whether the stimulus is perceived as painful. Bornhovd et al. (2002) reported that heat-evoked BOLD responses in the operculo-insular cortex show a linear relationship with pain ratings but not for stimulus intensities below pain threshold. Frot et al. (2007) showed using intracerebral EEG recordings that the responses in the secondary somatosensory cortex correlate with the intensity of stimulation below pain threshold and exhibit a ceiling effect for stimulation intensities above pain threshold. Conversely, responses recorded in the posterior insula were of similar magnitude for intensities below pain threshold, but increased when the intensity of stimulation entered the painful range. Such observations could be related to our observation of a differential effect of cTBS on the ability to perceive sensations conveyed by heat-sensitive Aδ-fiber nociceptors having a high activation threshold vs. heat-sensitive C-fiber afferents and cool-sensitive Aδ-fiber afferents having low activation thresholds.

Deep cTBS over the right operculo-insular cortex similarly affects the perception of Aδ-fiber heat stimuli delivered to the left and right hands. In Experiment 2, we found that 20 min after deep cTBS, Aδ-heat detection thresholds were increased similarly at the contralateral hand and at the ipsilateral hand. This bilateral effect of cTBS is in line with the work of Denis

et al. (2016) who reported that high-frequency (150 Hz) intracerebral electrical stimulation of the insular cortex in epileptic patients increases heat pain thresholds bilaterally, without affecting cold and pressure pain thresholds. Currently, one can only speculate on the mechanism responsible for this bilateral effect. A first explanation could be that the operculo-insular cortex is involved in the processing of thermonociceptive inputs originating from both hemibodies. Supporting this view, it is well known that nociceptive stimuli elicit strong responses in both the contralateral and the ipsilateral operculo-insular cortex. For example, using intracerebral EEG, Frot et al. (1999) showed that nociceptive laser stimuli delivered to the hand dorsum elicit early-latency local field potentials in the left and right operculo-insular cortex. The latency of the response elicited in the ipsilateral operculo-insular cortex was, on average, delayed by 15 ms relative to the response elicited in the contralateral operculo-insular cortex, compatible with transcallosal interhemispheric conduction times. A second explanation could be that cTBS delivered over the operculo-insular cortex induces remote effects leading to a generalized modulation of thermonociception. For example, operculo-insular cTBS could activate descending projections involved in the modulation of nociceptive transmission at spinal level (Garcia-Larrea et al., 1999; Garcia-Larrea and Peyron, 2007; Onesti et al., 2013).

Deep vs. superficial operculo-insular cTBS and intensity of stimulation. In Experiment 2, we observed that, unlike deep operculo-insular cTBS delivered using a double-cone coil at 80% of the lower-limb resting motor

threshold, superficial operculo-insular cTBS delivered using a flat figure-of-eight coil at 80% of the upper-limb resting motor threshold had no effect on the ability to perceive Aδ-heat stimuli. This is an indication that the effects of deep operculo-insular cTBS could be due to neuromodulation of the deeply located insular cortex rather than neuromodulation of more superficial opercular areas such as S2. The recent work of Koyama et al. (2017), who showed that applying bilaterally transcranial direct current stimulation over the opercular cortex did not affect pain perception, is in line with our results. However, the differential effect of deep and superficial cTBS could also be due to the fact that the double-cone coil used to deliver deep cTBS generates a less focal magnetic field than the flat figure-of-eight coil used to deliver superficial cTBS. Hence, deep cTBS is likely to activate a larger area of both superficial and deep cortex (Deng et al., 2014). The differential effect of deep and superficial cTBS could also be due to the fact that during deep cTBS, intervening superficial structures are probably exposed to higher magnetic fields than during superficial cTBS (Deng et al., 2014; Lu and Ueno, 2017), which could lead to a differential modulatory effect on intracortical excitability (McAllister et al., 2009). Several other studies have reported that superficial TMS over the operculo-insular cortex can modulate thermonociception. Valmunen et al. (2009) found that, as compared to other targets (M1, S1, the occipital lobe), superficial 10 Hz repetitive TMS over the right S2 induces a long-lasting elevation of heat pain thresholds and a short-lasting impairment of the ability to discriminate different temperatures. Conversely, Ciampi de Andrade et al. (2012) did not observe any significant change in heat or pain detection thresholds after deep 10 Hz

repetitive TMS of the operculo-insular cortex delivered using the same double-cone coil that was used in the present study. However, their feasibility study included a limited number of participants, and the after-effects of repetitive TMS were assessed at a relatively late time point, 1 h after stimulation.

Deep operculo-insular cTBS could be associated with a higher risk of TMS-evoked seizures. Experiment 2 was stopped after the occurrence of a generalized TMS-induced seizure in one participant. Furthermore, in Experiment 1, deep cTBS triggered a short-lasting manifestation compatible with a partial TMS-induced seizure. Both TMS-induced adverse events were preceded by a sensation of mirth followed by a dystonic posture of the left or right hemibody, which tented to become diffuse. Both participants presented a dysarthric speech and had breathing difficulties associated to laryngeal sensation and thoraco-abominal heaviness. These clinical manifestations were very similar to the clinical manifestations of insular lobe seizures (Isnard et al., 2004; Wynford-Thomas and Powell, 2017). Therefore, in the present study, deep cTBS over the operculo-insular cortex may have triggered two epileptic seizures involving the insula. This was highly unexpected. To our knowledge, there is only one case of TMS-induced seizures reported during cTBS. This case occurred while stimulating the hand representation of M1 using a flat figure-of eight coil (Oberman and Pascual-Leone, 2009). Furthermore, our study is not the first study attempting to modulate relatively deep brain structures using various repetitive TMS protocols delivered with a double-cone coil, including TBS (Bakker et al.

(2015); for review Dunlop et al. (2015)), rTMS delivered at 1 Hz (Gerschlager et al., 2002; Vanneste et al., 2012; Vanneste and De Ridder, 2013; Nauczyciel et al., 2014; Schuwerk et al., 2014; Bradley, 2015; Modirrousta et al., 2015), at 5 Hz (Vanneste et al., 2011; Vanneste et al., 2012; Garg et al., 2016), at 10 Hz (Hayward et al., 2007; Vanneste et al., 2011; Ciampi de Andrade et al., 2012; Vanneste et al., 2012; Vanneste et al., 2014; Bakker et al., 2015; Dunlop et al., 2015; Kreuzer et al., 2015) and at 20 Hz (Rollnik et al., 2002; Vanneste et al., 2011; Benito et al., 2012) with comparable or even higher intensities of TMS. None of these studies, totalling 615 participants, reported any TMS-induced seizures. The main distinction between these studies and the present study appears to be the fact that we targeted the operculo-insular cortex, whereas the other studies targeted the dorsomedial prefrontal cortex, the cingulate cortex, the cerebellum or the lower limb motor representation in M1. Only two studies, including respectively five and seven participants, also targeted the operculo-insular cortex (Ciampi de Andrade et al., 2012; Bradley, 2015), using respectively 10 Hz and1 Hz repetitive TMS. Repetitive TMS delivered using a double-cone coil to target deep brain structures could be associated with a higher risk of TMS-induced seizures because the double-cone coil induces a less focal magnetic field than conventional flat-surface figure-of-eight coils and, therefore, synchronously activates a larger brain volume. The intensity at which the brain structures located between the coil and the target site are stimulated could also play a role (Rossi et al., 1999; Oberman et al., 2011; Deng et al., 2013; 2014). Finally, as our study is the first to apply deep cTBS over the operculo-insular cortex, the possibility that stimulation of this specific brain

structure could be associated with a higher risk of seizure should be considered. One possible reason could be that the insular cortex is highly connected with the operculum (Peyron et al., 2002) and numerous other brain structures (Augustine, 1996; Moayedi, 2014).

Operculo-insular cortex as an alternative rTMS target for pain relief? Most studies aiming at reducing pain with rTMS have targeted M1 (Poreisz et al., 2008; O'Connell et al., 2011; Onesti et al., 2013; Torta et al., 2013; Lefaucheur et al., 2014; O'Connell et al., 2014; Rossini et al., 2015). A few studies have examined the effects of applying rTMS to other targets, such as S1 (Poreisz et al., 2008; Antal and Paulus, 2010; Torta et al., 2013), the dorsolateral pre-frontal cortex (Nahmias et al., 2009; Fierro et al., 2010; Borckardt et al., 2011; Brighina et al., 2011; de Andrade et al., 2011; Taylor et al., 2012; Taylor et al., 2013; Ciampi de Andrade et al., 2014), ACC (Fan et al., 2012; Tzabazis et al., 2013), S2 (Valmunen et al., 2009; Fregni et al., 2011) and the insular cortex (Ciampi de Andrade et al., 2012). The mechanism underlying the analgesic effect of rTMS over M1 remains largely unknown. Garcia-Larrea and Peyron (2007) suggested that it could be due to the activation of cortico-thalamic projections which, in turn, would activate the lateral thalamus leading to a cascade of modulations of remote areas such as the ACC, the insular cortex and the orbitofrontal cortex, finally leading to the activation of descending inhibitory pain mechanisms (Garcia-Larrea et al., 1999). Because rTMS of M1 leads to changes in the activity of remote brain areas and because these same brain regions are implicated in the processing of nociceptive inputs and/or in pain perception (Treede et al.,

2000; Peyron et al., 2002; Apkarian et al., 2005), there is a growing interest in considering these non-motor areas as more direct targets for rTMS when it is applied to reduce pain. Future studies aiming to assess whether deep rTMS over the operculo-insular cortex may alleviate pain in chronic pain patients should consider the fact that deep cTBS delivered over that structure is associated with a higher risk of triggering a TMS-induced seizure.

5. Conclusion

Our study shows that neuromodulation of the operculo-insular cortex using deep cTBS induces a bilateral reduction of the ability to perceive transient Aδ-fiber heat pain, without concomitantly affecting the ability to perceive innocuous warm sensations conveyed by low-threshold heat-sensitive C-fibers, cold sensations conveyed by cool-sensitive Aδ-fibers and vibrotactile sensations conveyed by low-threshold Aβ-fiber mechano-receptors.

C. Publications related to this thesis

1. Temporal profile and limb-specificity of phasic pain-evoked changes in motor excitability. *Algoet M., Duqué J., Iannetti GD., Mouraux A. Neuroscience. 2018; 386: 240-255*
2. RIII reflex elicited by the preferential activation of nociceptors using concentric electrical stimulation of the skin. *Algoet M., van den Broeke E., Arguissain F. G., Jure F. A., Andersen O. K., Mouraux A. (in preparation)*
3. Lack of changes in motor outputs evaluated by TMS motor mapping following HFS of the human skin. *Algoet M., Huang G., Lambert J., Mouraux A. (in preparation)*
4. Feasibility of delivering transcranial magnetic stimulation inside flexible surface MRI coils during fMRI acquisition: a concurrent TMS-fMRI study. *Algoet M., Lenoir C., Dricot L., Mouraux A. (in preparation)*
5. Report of one confirmed generalized seizure and one suspected partial seizure induced by deep continuous theta burst stimulation of the right operculo-insular cortex. *Lenoir C.[#], Algoet M.[#], Vanderclausen C., Peeters A., Ferrao Santos S. and Mouraux A. Brain stimul. 2018; 11(5):1187-1188*

   # Both authors participated equally

6. Deep continuous theta burst stimulation of the operculo-insular cortex selectively affects Aδ-fiber heat pain. *Lenoir C.#, Algoet M.# and Mouraux A. J Physiol 2018; 596, 4767-4787*

Both authors participated equally

References

Abanoz Y, Abanoz Y, Gunduz A, Uludag M, Ornek NI, Uzun N, Unalan H, Kiziltan M (2018), Pattern of startle reflex to somatosensory stimuli changes after spinal cord injury. J Spinal Cord Med 41:36-41.

Abbruzzese G, Marchese R, Buccolieri A, Gasparetto B, Trompetto C (2001), Abnormalities of sensorimotor integration in focal dystonia: a transcranial magnetic stimulation study. Brain 124:537-545.

Abbruzzese G, Trompetto C (2002), Clinical and research methods for evaluating cortical excitability. J Clin Neurophysiol 19:307-321.

Adachi K, Murray GM, Lee JC, Sessle BJ (2008), Noxious lingual stimulation influences the excitability of the face primary motor cerebral cortex (face MI) in the rat. J Neurophysiol 100:1234-1244.

Adriaensen H, Gybels J, Handwerker HO, Van Hees J (1983), Response properties of thin myelinated (A-delta) fibers in human skin nerves. J Neurophysiol 49:111-122.

Afif A, Hoffmann D, Minotti L, Benabid AL, Kahane P (2008), Middle short gyrus of the insula implicated in pain processing. Pain 138:546-555.

Algoet M, Duque J, Iannetti GD, Mouraux A (2018), Temporal Profile and Limb-specificity of Phasic Pain-Evoked Changes in Motor Excitability. Neuroscience 386:240-255.

Ali Z, Meyer RA, Campbell JN (1996), Secondary hyperalgesia to mechanical but not heat stimuli following a capsaicin injection in hairy skin. Pain 68:401-411.

Allison K, Vicenzino B, Bennell KL, Wrigley TV, Grimaldi A, Hodges PW (2016), Kinematics and kinetics during stair ascent in individuals with Gluteal Tendinopathy. Clin Biomech (Bristol, Avon) 40:37-44.

Alvarez-Blanco S, Leon L, Valls-Sole J (2009), The startle reaction to somatosensory inputs: different response pattern to stimuli of upper and lower limbs. Exp Brain Res 195:285-292.

Amassian VE, Eberle L, Maccabee PJ, Cracco RQ (1992), Modelling magnetic coil excitation of human cerebral cortex with a peripheral nerve immersed in a brain-

shaped volume conductor: the significance of fiber bending in excitation. Electroencephalogr Clin Neurophysiol 85:291-301.

Amiez C, Kostopoulos P, Champod AS, Petrides M (2006), Local morphology predicts functional organization of the dorsal premotor region in the human brain. J Neurosci 26:2724-2731.

Andersen OK (2007), Studies of the organization of the human nociceptive withdrawal reflex. Focus on sensory convergence and stimulation site dependency. Acta Physiol (Oxf) 189 Suppl 654:1-35.

Andersen OK, Morch CD, Arendt-Nielsen L (2006), Modulation of heat evoked nociceptive withdrawal reflexes by painful intramuscular conditioning stimulation. Exp Brain Res 174:775-780.

Andersen OK, Sonnenborg F, Matjacic Z, Arendt-Nielsen L (2003), Foot-sole reflex receptive fields for human withdrawal reflexes in symmetrical standing position. Exp Brain Res 152:434-443.

Andersen OK, Sonnenborg FA, Arendt-Nielsen L (1999), Modular organization of human leg withdrawal reflexes elicited by electrical stimulation of the foot sole. Muscle Nerve 22:1520-1530.

Andersen OK, Sonnenborg FA, Arendt-Nielsen L (2001), Reflex receptive fields for human withdrawal reflexes elicited by non-painful and painful electrical stimulation of the foot sole. Clin Neurophysiol 112:641-649.

Andersson GB (1999), Epidemiological features of chronic low-back pain. Lancet 354:581-585.

Antal A, Paulus W (2010), Effects of transcranial theta-burst stimulation on acute pain perception. Restor Neurol Neurosci 28:477-484.

Apkarian AV, Baliki MN, Geha PY (2009), Towards a theory of chronic pain. Prog Neurobiol 87:81-97.

Apkarian AV, Bushnell MC, Treede RD, Zubieta JK (2005), Human brain mechanisms of pain perception and regulation in health and disease. Eur J Pain 9:463-484.

Apkarian AV, Gelnar PA, Krauss BR, Szeverenyi NM (2000), Cortical responses to thermal pain depend on stimulus size: a functional MRI study. J Neurophysiol 83:3113-3122.

Apkarian AV, Hashmi JA, Baliki MN (2011), Pain and the brain: specificity and plasticity of the brain in clinical chronic pain. Pain 152:S49-64.

Apkarian AV, Sosa Y, Sonty S, Levy RM, Harden RN, Parrish TB, Gitelman DR (2004), Chronic back pain is associated with decreased prefrontal and thalamic gray matter density. J Neurosci 24:10410-10415.

Arendt-Nielsen L, Graven-Nielsen T, Svarrer H, Svensson P (1996), The influence of low back pain on muscle activity and coordination during gait: a clinical and experimental study. Pain 64:231-240.

Arendt-Nielsen L, Mills KR (1985), The relationship between mean power frequency of the EMG spectrum and muscle fibre conduction velocity. Electroencephalogr Clin Neurophysiol 60:130-134.

Arendt-Nielsen L, Svensson P (2001), Referred muscle pain: basic and clinical findings. Clin J Pain 17:11-19.

Atkinson JH (2004), Chronic back pain: searching for causes and cures. J Rheumatol 31:2323-2325.

Attwell D, Laughlin SB (2001), An energy budget for signaling in the grey matter of the brain. J Cereb Blood Flow Metab 21:1133-1145.

Augustine JR (1996), Circuitry and functional aspects of the insular lobe in primates including humans. Brain Res Brain Res Rev 22:229-244.

Babiloni C, Brancucci A, Babiloni F, Capotosto P, Carducci F, Cincotti F, Arendt-Nielsen L, Chen AC, et al. (2003), Anticipatory cortical responses during the expectancy of a predictable painful stimulation. A high-resolution electroencephalography study. Eur J Neurosci 18:1692-1700.

Baier B, zu Eulenburg P, Geber C, Rohde F, Rolke R, Maihofner C, Birklein F, Dieterich M (2014), Insula and sensory insular cortex and somatosensory control in patients with insular stroke. Eur J Pain 18:1385-1393.

Bailey AZ, Asmussen MJ, Nelson AJ (2016), Short-latency afferent inhibition determined by the sensory afferent volley. J Neurophysiol 116:637-644.

Bakker N, Shahab S, Giacobbe P, Blumberger DM, Daskalakis ZJ, Kennedy SH, Downar J (2015), rTMS of the dorsomedial prefrontal cortex for major depression: safety, tolerability, effectiveness, and outcome predictors for 10 Hz versus intermittent theta-burst stimulation. Brain stimulation 8:208-215.

Baliki MN, Baria AT, Apkarian AV (2011), The cortical rhythms of chronic back pain. J Neurosci 31:13981-13990.

Baliki MN, Chialvo DR, Geha PY, Levy RM, Harden RN, Parrish TB, Apkarian AV (2006), Chronic pain and the emotional brain: specific brain activity associated with spontaneous fluctuations of intensity of chronic back pain. J Neurosci 26:12165-12173.

Baliki MN, Geha PY, Apkarian AV, Chialvo DR (2008), Beyond feeling: chronic pain hurts the brain, disrupting the default-mode network dynamics. J Neurosci 28:1398-1403.

Baliki MN, Mansour AR, Baria AT, Apkarian AV (2014), Functional reorganization of the default mode network across chronic pain conditions. PLoS One 9:e106133.

Bank PJ, Peper CE, Marinus J, Beek PJ, van Hilten JJ (2013), Motor consequences of experimentally induced limb pain: a systematic review. Eur J Pain 17:145-157.

Barker AT, Jalinous R, Freeston IL (1985), Non-invasive magnetic stimulation of human motor cortex. Lancet 1:1106-1107.

Bashir S, Perez JM, Horvath JC, Pascual-Leone A (2013), Differentiation of motor cortical representation of hand muscles by navigated mapping of optimal TMS current directions in healthy subjects. J Clin Neurophysiol 30:390-395.

Baudewig J, Paulus W, Frahm J (2000), Artifacts caused by transcranial magnetic stimulation coils and EEG electrodes in T(2)*-weighted echo-planar imaging. Magn Reson Imaging 18:479-484.

Baudewig J, Siebner HR, Bestmann S, Tergau F, Tings T, Paulus W, Frahm J (2001), Functional MRI of cortical activations induced by transcranial magnetic stimulation (TMS). Neuroreport 12:3543-3548.

Baumann TK, Simone DA, Shain CN, LaMotte RH (1991), Neurogenic hyperalgesia: the search for the primary cutaneous afferent fibers that contribute to capsaicin-induced pain and hyperalgesia. J Neurophysiol 66:212-227.

Baumer T, Bock F, Koch G, Lange R, Rothwell JC, Siebner HR, Munchau A (2006), Magnetic stimulation of human premotor or motor cortex produces interhemispheric facilitation through distinct pathways. J Physiol 572:857-868.

Benito J, Kumru H, Murillo N, Costa U, Medina J, Tormos JM, Pascual-Leone A, Vidal J (2012), Motor and gait improvement in patients with incomplete spinal cord injury induced by high-frequency repetitive transcranial magnetic stimulation. Topics in spinal cord injury rehabilitation 18:106-112.

Bensmaia SJ (2008), Tactile intensity and population codes. Behav Brain Res 190:165-173.

Bergmann TO, Karabanov A, Hartwigsen G, Thielscher A, Siebner HR (2016), Combining non-invasive transcranial brain stimulation with neuroimaging and electrophysiology: Current approaches and future perspectives. NeuroImage 140:4-19.

Berth A, Pap G, Neuman W, Awiszus F (2009), Central neuromuscular dysfunction of the deltoid muscle in patients with chronic rotator cuff tears. J Orthop Traumatol 10:135-141.

Bertolasi L, Priori A, Tinazzi M, Bertasi V, Rothwell JC (1998), Inhibitory action of forearm flexor muscle afferents on corticospinal outputs to antagonist muscles in humans. J Physiol 511 (Pt 3):947-956.

Bestmann S, Baudewig J, Frahm J (2003a), On the synchronization of transcranial magnetic stimulation and functional echo-planar imaging. J Magn Reson Imaging 17:309-316.

Bestmann S, Baudewig J, Siebner HR, Rothwell JC, Frahm J (2003b), Subthreshold high-frequency TMS of human primary motor cortex modulates interconnected frontal motor areas as detected by interleaved fMRI-TMS. NeuroImage 20:1685-1696.

Bestmann S, Baudewig J, Siebner HR, Rothwell JC, Frahm J (2004), Functional MRI of the immediate impact of transcranial magnetic stimulation on cortical and subcortical motor circuits. Eur J Neurosci 19:1950-1962.

Bestmann S, Baudewig J, Siebner HR, Rothwell JC, Frahm J (2005), BOLD MRI responses to repetitive TMS over human dorsal premotor cortex. NeuroImage 28:22-29.

Bestmann S, Duque J (2015), Transcranial Magnetic Stimulation: Decomposing the Processes Underlying Action Preparation. Neuroscientist.

Bestmann S, Duque J (2016), Transcranial Magnetic Stimulation: Decomposing the Processes Underlying Action Preparation. Neuroscientist 22:392-405.

Bestmann S, Feredoes E (2013), Combined neurostimulation and neuroimaging in cognitive neuroscience: past, present, and future. Ann N Y Acad Sci 1296:11-30.

Bestmann S, Oliviero A, Voss M, Dechent P, Lopez-Dolado E, Driver J, Baudewig J (2006), Cortical correlates of TMS-induced phantom hand movements revealed with concurrent TMS-fMRI. Neuropsychologia 44:2959-2971.

Bestmann S, Ruff CC, Blankenburg F, Weiskopf N, Driver J, Rothwell JC (2008c), Mapping causal interregional influences with concurrent TMS-fMRI. Exp Brain Res 191:383-402.

Bestmann S, Ruff CC, Driver J, Blankenburg F (2008a), Concurrent TMS and functional magnetic resonance imaging: methods and current advances. The Oxford Handbook of Transcranial Stimulation:569-592.

Bestmann S, Swayne O, Blankenburg F, Ruff CC, Haggard P, Weiskopf N, Josephs O, Driver J, et al. (2008b), Dorsal premotor cortex exerts state-dependent causal influences on activity in contralateral primary motor and dorsal premotor cortex. Cereb Cortex 18:1281-1291.

Bestmann S, Swayne O, Blankenburg F, Ruff CC, Teo J, Weiskopf N, Driver J, Rothwell JC, et al. (2010), The role of contralesional dorsal premotor cortex after stroke as studied with concurrent TMS-fMRI. J Neurosci 30:11926-11937.

Bhandari RN, Ogilvie J, Clarke RW (1999), Differences in opioidergic inhibition of spinal reflexes and Fos expression evoked by mechanical and chemical noxious stimuli in the decerebrated rabbit. Neuroscience 90:177-189.

Bikmullina R, Baumer T, Zittel S, Munchau A (2009), Sensory afferent inhibition within and between limbs in humans. Clin Neurophysiol 120:610-618.

Bikmullina R, Kicic D, Carlson S, Nikulin VV (2009), Electrophysiological correlates of short-latency afferent inhibition: a combined EEG and TMS study. Exp Brain Res 194:517-526.

Billot M, Neige C, Gagne M, Mercier C, Bouyer LJ (2018), Effect of Cutaneous Heat Pain on Corticospinal Excitability of the Tibialis Anterior at Rest and during Submaximal Contraction. Neural Plast 2018:8713218.

Biswal B, Yetkin FZ, Haughton VM, Hyde JS (1995), Functional connectivity in the motor cortex of resting human brain using echo-planar MRI. Magn Reson Med 34:537-541.

Blankenburg F, Ruff CC, Bestmann S, Bjoertomt O, Eshel N, Josephs O, Weiskopf N, Driver J (2008), Interhemispheric effect of parietal TMS on somatosensory response confirmed directly with concurrent TMS-fMRI. J Neurosci 28:13202-13208.

Blankenburg F, Ruff CC, Bestmann S, Bjoertomt O, Josephs O, Deichmann R, Driver J (2010), Studying the role of human parietal cortex in visuospatial attention with concurrent TMS-fMRI. Cereb Cortex 20:2702-2711.

Bliss TV, Collingridge GL (1993), A synaptic model of memory: long-term potentiation in the hippocampus. Nature 361:31-39.

Bohning DE, Denslow S, Bohning PA, Walker JA, George MS (2003a), A TMS coil positioning/holding system for MR image-guided TMS interleaved with fMRI. Clin Neurophysiol 114:2210-2219.

Bohning DE, Pecheny AP, Epstein CM, Speer AM, Vincent DJ, Dannels W, George MS (1997), Mapping transcranial magnetic stimulation (TMS) fields in vivo with MRI. Neuroreport 8:2535-2538.

Bohning DE, Shastri A, Lomarev MP, Lorberbaum JP, Nahas Z, George MS (2003b), BOLD-fMRI response vs. transcranial magnetic stimulation (TMS) pulse-train length: testing for linearity. J Magn Reson Imaging 17:279-290.

Bohning DE, Shastri A, McConnell KA, Nahas Z, Lorberbaum JP, Roberts DR, Teneback C, Vincent DJ, et al. (1999), A combined TMS/fMRI study of intensity-dependent TMS over motor cortex. Biol Psychiatry 45:385-394.

Bohning DE, Shastri A, McGavin L, McConnell KA, Nahas Z, Lorberbaum JP, Roberts DR, George MS (2000), Motor cortex brain activity induced by 1-Hz transcranial magnetic stimulation is similar in location and level to that for volitional movement. Invest Radiol 35:676-683.

Bohning DE, Shastri A, Nahas Z, Lorberbaum JP, Andersen SW, Dannels WR, Haxthausen EU, Vincent DJ, et al. (1998), Echoplanar BOLD fMRI of brain activation induced by concurrent transcranial magnetic stimulation. Invest Radiol 33:336-340.

Bonato C, Miniussi C, Rossini PM (2006), Transcranial magnetic stimulation and cortical evoked potentials: a TMS/EEG co-registration study. Clin Neurophysiol 117:1699-1707.

Borckardt JJ, Reeves ST, Beam W, Jensen MP, Gracely RH, Katz S, Smith AR, Madan A, et al. (2011), A randomized, controlled investigation of motor cortex transcranial magnetic stimulation (TMS) effects on quantitative sensory measures in healthy adults: evaluation of TMS device parameters. Clin J Pain 27:486-494.

Borckardt JJ, Smith AR, Hutcheson K, Johnson K, Nahas Z, Anderson B, Schneider MB, Reeves ST, et al. (2006), Reducing pain and unpleasantness during repetitive transcranial magnetic stimulation. J ECT 22:259-264.

Borghetti D, Sartucci F, Petacchi E, Guzzetta A, Piras MF, Murri L, Cioni G (2008), Transcranial magnetic stimulation mapping: a model based on spline interpolation. Brain Res Bull 77:143-148.

Bornhovd K, Quante M, Glauche V, Bromm B, Weiller C, Buchel C (2002), Painful stimuli evoke different stimulus-response functions in the amygdala, prefrontal, insula and somatosensory cortex: a single-trial fMRI study. Brain 125:1326-1336.

Boroojerdi B, Diefenbach K, Ferbert A (1996), Transcallosal inhibition in cortical and subcortical cerebral vascular lesions. J Neurol Sci 144:160-170.

Boroojerdi B, Foltys H, Krings T, Spetzger U, Thron A, Topper R (1999), Localization of the motor hand area using transcranial magnetic stimulation and functional magnetic resonance imaging. Clin Neurophysiol 110:699-704.

Bouhassira D, Danziger N, Attal N, Guirimand F (2003), Comparison of the pain suppressive effects of clinical and experimental painful conditioning stimuli. Brain 126:1068-1078.

Bouhassira D, Le Bars D, Bolgert F, Laplane D, Willer JC (1993), Diffuse noxious inhibitory controls in humans: a neurophysiological investigation of a patient with a form of Brown-Sequard syndrome. Ann Neurol 34:536-543.

Bradley (2015), The first steps of cortical somatosensory and nociceptive processing in humans, pp. 147. Université Claude Bernard Lyon 1.

Bradley, Cuthbert BN, Lang PJ (1990), Startle reflex modification: emotion or attention? Psychophysiology 27:513-522.

Bradnam L, Shanahan EM, Hendy K, Reed A, Skipworth T, Visser A, Lennon S (2016), Afferent inhibition and cortical silent periods in shoulder primary motor cortex and effect of a suprascapular nerve block in people experiencing chronic shoulder pain. Clin Neurophysiol 127:769-778.

Bragard D, Chen AC, Plaghki L (1996), Direct isolation of ultra-late (C-fibre) evoked brain potentials by CO2 laser stimulation of tiny cutaneous surface areas in man. Neurosci Lett 209:81-84.

Brascher AK, Becker S, Hoeppli ME, Schweinhardt P (2016), Different Brain Circuitries Mediating Controllable and Uncontrollable Pain. J Neurosci 36:5013-5025.

Brasil-Neto JP, Cohen LG, Panizza M, Nilsson J, Roth BJ, Hallett M (1992), Optimal focal transcranial magnetic activation of the human motor cortex: effects of coil orientation, shape of the induced current pulse, and stimulus intensity. J Clin Neurophysiol 9:132-136.

Brasil-Neto JP, McShane LM, Fuhr P, Hallett M, Cohen LG (1992), Topographic mapping of the human motor cortex with magnetic stimulation: factors affecting accuracy and reproducibility. Electroencephalogr Clin Neurophysiol 85:9-16.

Brasil-Neto JP, Valls-Sole J, Pascual-Leone A, Cammarota A, Amassian VE, Cracco R, Maccabee P, Cracco J, et al. (1993), Rapid modulation of human cortical motor outputs following ischaemic nerve block. Brain 116 (Pt 3):511-525.

Breivik H, Collett B, Ventafridda V, Cohen R, Gallacher D (2006), Survey of chronic pain in Europe: prevalence, impact on daily life, and treatment. Eur J Pain 10:287-333.

Breivik H, Eisenberg E, O'Brien T, Openminds (2013), The individual and societal burden of chronic pain in Europe: the case for strategic prioritisation and action to improve knowledge and availability of appropriate care. BMC Public Health 13:1229.

Brighina F, De Tommaso M, Giglia F, Scalia S, Cosentino G, Puma A, Panetta M, Giglia G, et al. (2011), Modulation of pain perception by transcranial magnetic stimulation of left prefrontal cortex. J Headache Pain 12:185-191.

Bromm B, Treede RD (1980), Withdrawal reflex, skin resistance reaction and pain ratings due to electrical stimuli in man. Pain 9:339-354.

Bromm B, Treede RD (1984), Nerve fibre discharges, cerebral potentials and sensations induced by CO2 laser stimulation. Hum Neurobiol 3:33-40.

Bromm B, Treede RD (1987), Human cerebral potentials evoked by CO2 laser stimuli causing pain. Exp Brain Res 67:153-162.

Bromm B, Treede RD (1987), Pain related cerebral potentials: late and ultralate components. Int J Neurosci 33:15-23.

Brown P, Rothwell JC, Thompson PD, Britton TC, Day BL, Marsden CD (1991), New observations on the normal auditory startle reflex in man. Brain 114 (Pt 4):1891-1902.

Brushart TM, Mesulam MM (1980), Transganglionic demonstration of central sensory projections from skin and muscle with HRP-lectin conjugates. Neurosci Lett 17:1-6.

Buckalew N, Haut MW, Morrow L, Weiner D (2008), Chronic pain is associated with brain volume loss in older adults: preliminary evidence. Pain Med 9:240-248.

Buhle JT, Silvers JA, Wager TD, Lopez R, Onyemekwu C, Kober H, Weber J, Ochsner KN (2014), Cognitive reappraisal of emotion: a meta-analysis of human neuroimaging studies. Cereb Cortex 24:2981-2990.

Bungert A, Chambers CD, Long E, Evans CJ (2012a), On the importance of specialized radiofrequency filtering for concurrent TMS/MRI. J Neurosci Methods 210:202-205.

Bungert A, Chambers CD, Phillips M, Evans CJ (2012b), Reducing image artefacts in concurrent TMS/fMRI by passive shimming. NeuroImage 59:2167-2174.

Burke D, Dickson HG, Skuse NF (1991), Task-dependent changes in the responses to low-threshold cutaneous afferent volleys in the human lower limb. J Physiol 432:445-458.

Burns E, Chipchase LS, Schabrun SM (2016a), Primary sensory and motor cortex function in response to acute muscle pain: A systematic review and meta-analysis. Eur J Pain 20:1203-1213.

Burns E, Chipchase LS, Schabrun SM (2016b), Reduced Short- and Long-Latency Afferent Inhibition Following Acute Muscle Pain: A Potential Role in the Recovery of Motor Output. Pain Med.

Butler JE, Taylor JL, Gandevia SC (2003), Responses of human motoneurons to corticospinal stimulation during maximal voluntary contractions and ischemia. J Neurosci 23:10224-10230.

Caccia MR, McComas AJ, Upton AR, Blogg T (1973), Cutaneous reflexes in small muscles of the hand. J Neurol Neurosurg Psychiatry 36:960-977.

Cai W, George JS, Chambers CD, Stokes MG, Verbruggen F, Aron AR (2012), Stimulating deep cortical structures with the batwing coil: how to determine the intensity for transcranial magnetic stimulation using coil-cortex distance. J Neurosci Methods 204:238-241.

Cairo TA, Liddle PF, Woodward TS, Ngan ET (2004), The influence of working memory load on phase specific patterns of cortical activity. Brain Res Cogn Brain Res 21:377-387.

Cambier J, Dehen H, Bathien N (1974), Upper limb cutaneous polysynaptic reflexes. J Neurol Sci 22:39-49.

Campbell, Carstens E, Watkins LR (1991), Comparison of human pain sensation and flexion withdrawal evoked by noxious radiant heat. Pain 45:259-268.

Campbell, Khan AA, Meyer RA, Raja SN (1988), Responses to heat of C-fiber nociceptors in monkey are altered by injury in the receptive field but not by adjacent injury. Pain 32:327-332.

Campbell, Meyer (1983), Sensitization of unmyelinated nociceptive afferents in monkey varies with skin type. J Neurophysiol 49:98-110.

Campbell, Meyer RA, LaMotte RH (1979), Sensitization of myelinated nociceptive afferents that innervate monkey hand. J Neurophysiol 42:1669-1679.

Campero M, Bostock H (2010), Unmyelinated afferents in human skin and their responsiveness to low temperature. Neurosci Lett 470:188-192.

Carstens E, Campell IG (1992), Responses of motor units during the hind limb flexion withdrawal reflex evoked by noxious skin heating: phasic and prolonged suppression by midbrain stimulation and comparison with simultaneously recorded dorsal horn units. Pain 48:215-226.

Casey KL, Minoshima S, Morrow TJ, Koeppe RA (1996), Comparison of human cerebral activation pattern during cutaneous warmth, heat pain, and deep cold pain. J Neurophysiol 76:571-581.

Caterina MJ, Schumacher MA, Tominaga M, Rosen TA, Levine JD, Julius D (1997), The capsaicin receptor: a heat-activated ion channel in the pain pathway. Nature 389:816-824.

Cattaneo L, Barchiesi G (2011), Transcranial Magnetic Mapping of the Short-Latency Modulations of Corticospinal Activity from the Ipsilateral Hemisphere during Rest. Frontiers in neural circuits 5:14.

Caumo W, Deitos A, Carvalho S, Leite J, Carvalho F, Dussan-Sarria JA, Lopes Tarrago Mda G, Souza A, et al. (2016), Motor Cortex Excitability and BDNF Levels in Chronic Musculoskeletal Pain According to Structural Pathology. Front Hum Neurosci 10:357.

Cavaleri R, Schabrun SM, Chipchase LS (2018), The reliability and validity of rapid transcranial magnetic stimulation mapping. Brain stimulation 11:1291-1295.

Ceko M, Shir Y, Ouellet JA, Ware MA, Stone LS, Seminowicz DA (2015), Partial recovery of abnormal insula and dorsolateral prefrontal connectivity to cognitive networks in chronic low back pain after treatment. Hum Brain Mapp 36:2075-2092.

Chan CW, Dallaire M (1989), Subjective pain sensation is linearly correlated with the flexion reflex in man. Brain Res 479:145-150.

Chang WJ, O'Connell NE, Beckenkamp PR, Alhassani G, Liston MB, Schabrun SM (2018), Altered Primary Motor Cortex Structure, Organization, and Function in Chronic Pain: A Systematic Review and Meta-Analysis. J Pain 19:341-359.

Chen R, Corwell B, Hallett M (1999), Modulation of motor cortex excitability by median nerve and digit stimulation. Exp Brain Res 129:77-86.

Cheng G, Randic M (2003), Involvement of intracellular calcium and protein phosphatases in long-term depression of A-fiber-mediated primary afferent neurotransmission. Brain Res Dev Brain Res 144:73-82.

Choi EY, Yeo BT, Buckner RL (2012), The organization of the human striatum estimated by intrinsic functional connectivity. J Neurophysiol 108:2242-2263.

Christensen LO, Petersen N, Andersen JB, Sinkjaer T, Nielsen JB (2000), Evidence for transcortical reflex pathways in the lower limb of man. Prog Neurobiol 62:251-272.

Churyukanov M, Plaghki L, Legrain V, Mouraux A (2012), Thermal detection thresholds of Adelta- and C-fibre afferents activated by brief CO2 laser pulses applied onto the human hairy skin. PLoS One 7:e35817.

Ciampi de Andrade D, Galhardoni R, Pinto LF, Lancelotti R, Rosi J, Jr., Marcolin MA, Teixeira MJ (2012), Into the island: a new technique of non-invasive cortical stimulation of the insula. Neurophysiol Clin 42:363-368.

Ciampi de Andrade D, Mhalla A, Adam F, Texeira MJ, Bouhassira D (2014), Repetitive transcranial magnetic stimulation induced analgesia depends on N-methyl-D-aspartate glutamate receptors. Pain 155:598-605.

Cincotta M, Borgheresi A, Jung P, Balestrieri F, Giovannelli F, Zaccara G, Ziemann U (2005), Physical interactions between induced electrical fields can have substantial effects on neuronal excitation during simultaneous TMS of two brain areas. Clin Neurophysiol 116:1733-1742.

Civardi C, Cantello R, Asselman P, Rothwell JC (2001), Transcranial magnetic stimulation can be used to test connections to primary motor areas from frontal and medial cortex in humans. NeuroImage 14:1444-1453.

Clark BD, Dacko SM, Cope TC (1993), Cutaneous stimulation fails to alter motor unit recruitment in the decerebrate cat. J Neurophysiol 70:1433-1439.

Clarke RW, Harris J (2001), The spatial organization of central sensitization of hind limb flexor reflexes in the decerebrated, spinalized rabbit. Eur J Pain 5:175-185.

Clarke RW, Harris J (2004), The organization of motor responses to noxious stimuli. Brain Res Brain Res Rev 46:163-172.

Clarke RW, Harris J, Ford TW, Taylor JS (1992), Prolonged potentiation of transmission through a withdrawal reflex pathway after noxious stimulation of the heel in the rabbit. Pain 49:65-70.

Classen J, Knorr U, Werhahn KJ, Schlaug G, Kunesch E, Cohen LG, Seitz RJ, Benecke R (1998), Multimodal output mapping of human central motor representation on different spatial scales. J Physiol 512 (Pt 1):163-179.

Classen J, Steinfelder B, Liepert J, Stefan K, Celnik P, Cohen LG, Hess A, Kunesch E, et al. (2000), Cutaneomotor integration in humans is somatotopically organized at various levels of the nervous system and is task dependent. Exp Brain Res 130:48-59.

Claus D, Harding AE, Hess CW, Mills KR, Murray NM, Thomas PK (1988), Central motor conduction in degenerative ataxic disorders: a magnetic stimulation study. J Neurol Neurosurg Psychiatry 51:790-795.

Clouston PD, Kiers L, Menkes D, Sander H, Chiappa K, Cros D (1995), Modulation of motor activity by cutaneous input: inhibition of the magnetic motor evoked potential by digital electrical stimulation. Electroencephalogr Clin Neurophysiol 97:114-125.

Coderre TJ, Melzack R (1985), Increased pain sensitivity following heat injury involves a central mechanism. Behav Brain Res 15:259-262.

Coghill RC, Sang CN, Maisog JM, Iadarola MJ (1999), Pain intensity processing within the human brain: a bilateral, distributed mechanism. J Neurophysiol 82:1934-1943.

Collins WR, Jr., Nulsen FE, Randt CT (1960), Relation of peripheral nerve fiber size and sensation in man. Arch Neurol 3:381-385.

Colon E, Liberati G, Mouraux A (2017), EEG frequency tagging using ultra-slow periodic heat stimulation of the skin reveals cortical activity specifically related to C fiber thermonociceptors. NeuroImage 146:266-274.

Cook AJ, Woolf CJ, Wall PD (1986), Prolonged C-fibre mediated facilitation of the flexion reflex in the rat is not due to changes in afferent terminal or motoneurone excitability. Neurosci Lett 70:91-96.

Cooke, Bliss TV (2006), Plasticity in the human central nervous system. Brain 129:1659-1673.

Cooke, Graziano MS (2003), Defensive movements evoked by air puff in monkeys. J Neurophysiol 90:3317-3329.

Cooke, Graziano MS (2004), Sensorimotor integration in the precentral gyrus: polysensory neurons and defensive movements. J Neurophysiol 91:1648-1660.

Cordes D, Haughton VM, Arfanakis K, Wendt GJ, Turski PA, Moritz CH, Quigley MA, Meyerand ME (2000), Mapping functionally related regions of brain with functional connectivity MR imaging. AJNR Am J Neuroradiol 21:1636-1644.

Corthout E, Barker AT, Cowey A (2001), Transcranial magnetic stimulation. Which part of the current waveform causes the stimulation? Exp Brain Res 141:128-132.

Craig AD, Chen K, Bandy D, Reiman EM (2000), Thermosensory activation of insular cortex. Nat Neurosci 3:184-190.

Crone C, Hultborn H, Mazieres L, Morin C, Nielsen J, Pierrot-Deseilligny E (1990), Sensitivity of monosynaptic test reflexes to facilitation and inhibition as a function of the test reflex size: a study in man and the cat. Exp Brain Res 81:35-45.

Curtis DR, Eccles JC (1959), The time courses of excitatory and inhibitory synaptic actions. J Physiol 145:529-546.

Dahl JB, Brennum J, Arendt-Nielsen L, Jensen TS, Kehlet H (1993), The effect of pre- versus postinjury infiltration with lidocaine on thermal and mechanical hyperalgesia after heat injury to the skin. Pain 53:43-51.

Danziger N, Fournier E, Bouhassira D, Michaud D, De Broucker T, Santarcangelo E, Carli G, Chertock L, et al. (1998), Different strategies of modulation can be operative during hypnotic analgesia: a neurophysiological study. Pain 75:85-92.

Davare M, Lemon R, Olivier E (2008), Selective modulation of interactions between ventral premotor cortex and primary motor cortex during precision grasping in humans. J Physiol 586:2735-2742.

Davare M, Montague K, Olivier E, Rothwell JC, Lemon RN (2009), Ventral premotor to primary motor cortical interactions during object-driven grasp in humans. Cortex 45:1050-1057.

Davare M, Rothwell JC, Lemon RN (2010), Causal connectivity between the human anterior intraparietal area and premotor cortex during grasp. Curr Biol 20:176-181.

Davis, Bushnell MC, Iannetti GD, St Lawrence K, Coghill R (2015), Evidence against pain specificity in the dorsal posterior insula. F1000Research 4:362.

Davis, Gendelman DS, Tischler MD, Gendelman PM (1982), A primary acoustic startle circuit: lesion and stimulation studies. J Neurosci 2:791-805.

Davis, Kwan CL, Crawley AP, Mikulis DJ (1998), Functional MRI study of thalamic and cortical activations evoked by cutaneous heat, cold, and tactile stimuli. J Neurophysiol 80:1533-1546.

Davis, Lozano RM, Manduch M, Tasker RR, Kiss ZH, Dostrovsky JO (1999), Thalamic relay site for cold perception in humans. J Neurophysiol 81:1970-1973.

Day SJ, Hulliger M (2001), Experimental simulation of cat electromyogram: evidence for algebraic summation of motor-unit action-potential trains. J Neurophysiol 86:2144-2158.

de Andrade DC, Mhalla A, Adam F, Texeira MJ, Bouhassira D (2011), Neuropharmacological basis of rTMS-induced analgesia: the role of endogenous opioids. Pain 152:320-326.

De Martino E, Seminowicz DA, Schabrun SM, Petrini L, Graven-Nielsen T (2019), High frequency repetitive transcranial magnetic stimulation to the left dorsolateral prefrontal cortex modulates sensorimotor cortex function in the transition to sustained muscle pain. NeuroImage 186:93-102.

De Martino E, Zandalasini M, Schabrun S, Petrini L, Graven-Nielsen T (2018), Experimental muscle hyperalgesia modulates sensorimotor cortical excitability, which is partially altered by unaccustomed exercise. Pain 159:2493-2502.

de Noordhout AM, Rapisarda G, Bogacz D, Gerard P, De Pasqua V, Pennisi G, Delwaide PJ (1999), Corticomotoneuronal synaptic connections in normal man: an electrophysiological study. Brain 122 (Pt 7):1327-1340.

de Tommaso M, Santostasi R, Devitofrancesco V, Franco G, Vecchio E, Delussi M, Livrea P, Katzarava Z (2011), A comparative study of cortical responses evoked by transcutaneous electrical vs CO(2) laser stimulation. Clin Neurophysiol 122:2482-2487.

de Weijer AD, Sommer IE, Bakker EJ, Bloemendaal M, Bakker CJ, Klomp DW, Bestmann S, Neggers SF (2014), A setup for administering TMS to medial and

lateral cortical areas during whole-brain FMRI recording. J Clin Neurophysiol 31:474-487.

Del Santo F, Gelli F, Spidalieri R, Rossi A (2007), Corticospinal drive during painful voluntary contractions at constant force output. Brain Res 1128:91-98.

Delvendahl I, Gattinger N, Berger T, Gleich B, Siebner HR, Mall V (2014), The role of pulse shape in motor cortex transcranial magnetic stimulation using full-sine stimuli. PLoS One 9:e115247.

Deng ZD, Lisanby SH, Peterchev AV (2013), Electric field depth-focality tradeoff in transcranial magnetic stimulation: simulation comparison of 50 coil designs. Brain stimulation 6:1-13.

Deng ZD, Lisanby SH, Peterchev AV (2014), Coil design considerations for deep transcranial magnetic stimulation. Clin Neurophysiol 125:1202-1212.

Denis DJ, Marouf R, Rainville P, Bouthillier A, Nguyen DK (2016), Effects of insular stimulation on thermal nociception. Eur J Pain 20:800-810.

Denslow S, Bohning DE, Bohning PA, Lomarev MP, George MS (2005), An increased precision comparison of TMS-induced motor cortex BOLD fMRI response for image-guided versus function-guided coil placement. Cogn Behav Neurol 18:119-126.

Denslow S, Lomarev M, Bohning DE, Mu Q, George MS (2004), A high resolution assessment of the repeatability of relative location and intensity of transcranial magnetic stimulation-induced and volitionally induced blood oxygen level-dependent response in the motor cortex. Cogn Behav Neurol 17:163-173.

Derosiere G, Billot M, Ward ET, Perrey S (2015), Adaptations of motor neural structures' activity to lapses in attention. Cereb Cortex 25:66-74.

Desmedt JE, Godaux E (1977), Ballistic contractions in man: characteristic recruitment pattern of single motor units of the tibialis anterior muscle. J Physiol 264:673-693.

Desmedt JE, Godaux E (1977), Fast motor units are not preferentially activated in rapid voluntary contractions in man. Nature 267:717-719.

Deuschl G, Michels R, Berardelli A, Schenck E, Inghilleri M, Lucking CH (1991), Effects of electric and magnetic transcranial stimulation on long latency reflexes. Exp Brain Res 83:403-410.

Devanne H, Lavoie BA, Capaday C (1997), Input-output properties and gain changes in the human corticospinal pathway. Exp Brain Res 114:329-338.

Devor M, Janig W, Michaelis M (1994), Modulation of activity in dorsal root ganglion neurons by sympathetic activation in nerve-injured rats. J Neurophysiol 71:38-47.

Deyo RA, Weinstein JN (2001), Low back pain. N Engl J Med 344:363-370.

Di Lazzaro V, Molinari M, Restuccia D, Leggio MG, Nardone R, Fogli D, Tonali P (1994), Cerebro-cerebellar interactions in man: neurophysiological studies in patients with focal cerebellar lesions. Electroencephalogr Clin Neurophysiol 93:27-34.

Di Lazzaro V, Oliviero A, Pilato F, Saturno E, Dileone M, Mazzone P, Insola A, Tonali PA, et al. (2004), The physiological basis of transcranial motor cortex stimulation in conscious humans. Clin Neurophysiol 115:255-266.

Di Lazzaro V, Oliviero A, Profice P, Insola A, Mazzone P, Tonali P, Rothwell JC (1999), Direct demonstration of interhemispheric inhibition of the human motor cortex produced by transcranial magnetic stimulation. Exp Brain Res 124:520-524.

Di Lazzaro V, Oliviero A, Profice P, Insola A, Mazzone P, Tonali P, Rothwell JC (1999), Effects of voluntary contraction on descending volleys evoked by transcranial electrical stimulation over the motor cortex hand area in conscious humans. Exp Brain Res 124:525-528.

Di Lazzaro V, Oliviero A, Profice P, Pennisi MA, Di Giovanni S, Zito G, Tonali P, Rothwell JC (2000), Muscarinic receptor blockade has differential effects on the excitability of intracortical circuits in the human motor cortex. Exp Brain Res 135:455-461.

Di Lazzaro V, Oliviero A, Profice P, Saturno E, Pilato F, Insola A, Mazzone P, Tonali P, et al. (1998), Comparison of descending volleys evoked by transcranial magnetic and electric stimulation in conscious humans. Electroencephalogr Clin Neurophysiol 109:397-401.

Di Lazzaro V, Oliviero A, Saturno E, Dileone M, Pilato F, Nardone R, Ranieri F, Musumeci G, et al. (2005), Effects of lorazepam on short latency afferent inhibition and short latency intracortical inhibition in humans. J Physiol 564:661-668.

Di Lazzaro V, Oliviero A, Saturno E, Pilato F, Insola A, Mazzone P, Profice P, Tonali P, et al. (2001), The effect on corticospinal volleys of reversing the direction of current induced in the motor cortex by transcranial magnetic stimulation. Exp Brain Res 138:268-273.

Di Lazzaro V, Oliviero A, Tonali PA, Marra C, Daniele A, Profice P, Saturno E, Pilato F, et al. (2002), Noninvasive in vivo assessment of cholinergic cortical circuits in AD using transcranial magnetic stimulation. Neurology 59:392-397.

Di Lazzaro V, Pilato F, Dileone M, Profice P, Ranieri F, Ricci V, Bria P, Tonali PA, et al. (2007), Segregating two inhibitory circuits in human motor cortex at the level of GABAA receptor subtypes: a TMS study. Clin Neurophysiol 118:2207-2214.

Di Lazzaro V, Pilato F, Saturno E, Oliviero A, Dileone M, Mazzone P, Insola A, Tonali PA, et al. (2005), Theta-burst repetitive transcranial magnetic stimulation suppresses specific excitatory circuits in the human motor cortex. J Physiol 565:945-950.

Di Lazzaro V, Rothwell JC (2014), Corticospinal activity evoked and modulated by non-invasive stimulation of the intact human motor cortex. J Physiol 592:4115-4128.

Di Lazzaro V, Ziemann U (2013), The contribution of transcranial magnetic stimulation in the functional evaluation of microcircuits in human motor cortex. Frontiers in neural circuits 7:18.

Dill T (2008), Contraindications to magnetic resonance imaging: non-invasive imaging. Heart 94:943-948.

Dolman AJ, Loggia ML, Edwards RR, Gollub RL, Kong J, Napadow V, Wasan AD (2014), Phenotype matters: the absence of a positive association between cortical thinning and chronic low back pain when controlling for salient clinical variables. Clin J Pain 30:839-845.

Donaldson TS (1968), Robustness of the *F*-test to errors of both kinds and the correlation between the numerator and denominator of the *F*-ratio. J Am Stat Assoc 63:660-676.

Donoghue JP, Leibovic S, Sanes JN (1992), Organization of the forelimb area in squirrel monkey motor cortex: representation of digit, wrist, and elbow muscles. Exp Brain Res 89:1-19.

Dowdle LT, Brown TR, George MS, Hanlon CA (2018), Single pulse TMS to the DLPFC, compared to a matched sham control, induces a direct, causal increase in caudate, cingulate, and thalamic BOLD signal. Brain stimulation 11:789-796.

Dowman R (1991), Spinal and supraspinal correlates of nociception in man. Pain 45:269-281.

Dowman R (1992), Possible startle response contamination of the spinal nociceptive withdrawal reflex. Pain 49:187-197.

Downar J, Crawley AP, Mikulis DJ, Davis KD (2002), A cortical network sensitive to stimulus salience in a neutral behavioral context across multiple sensory modalities. J Neurophysiol 87:615-620.

Dube JA, Mercier C (2011), Effect of pain and pain expectation on primary motor cortex excitability. Clin Neurophysiol 122:2318-2323.

Dum RP, Levinthal DJ, Strick PL (2009), The spinothalamic system targets motor and sensory areas in the cerebral cortex of monkeys. J Neurosci 29:14223-14235.

Dum RP, Strick PL (2005), Frontal lobe inputs to the digit representations of the motor areas on the lateral surface of the hemisphere. J Neurosci 25:1375-1386.

Dunlop K, Gaprielian P, Blumberger D, Daskalakis ZJ, Kennedy SH, Giacobbe P, Downar J (2015), MRI-guided dmPFC-rTMS as a Treatment for Treatment-resistant Major Depressive Disorder. Journal of visualized experiments : JoVE:e53129.

Duque J, Greenhouse I, Labruna L, Ivry RB (2017), Physiological Markers of Motor Inhibition during Human Behavior. Trends Neurosci 40:219-236.

Duque J, Hummel F, Celnik P, Murase N, Mazzocchio R, Cohen LG (2005), Transcallosal inhibition in chronic subcortical stroke. NeuroImage 28:940-946.

Eccles RM, Lundberg A (1959), Supraspinal control of interneurones mediating spinal reflexes. J Physiol 147:565-584.

Eckert N, Riley ZA (2013), The nociceptive withdrawal reflex does not adapt to joint position change and short-term motor practice. F1000Research 2:158.

Elgueta-Cancino E, Marinovic W, Jull G, Hodges PW (2019), Motor cortex representation of deep and superficial neck flexor muscles in individuals with and without neck pain. Hum Brain Mapp 40:2759-2770.

Ellaway PH, Davey NJ, Maskill DW, Rawlinson SR, Lewis HS, Anissimova NP (1998), Variability in the amplitude of skeletal muscle responses to magnetic stimulation of the motor cortex in man. Electroencephalogr Clin Neurophysiol 109:104-113.

Elliott AM, Smith BH, Penny KI, Smith WC, Chambers WA (1999), The epidemiology of chronic pain in the community. Lancet 354:1248-1252.

Ellrich J, Treede RD (1998), Convergence of nociceptive and non-nociceptive inputs onto spinal reflex pathways to the tibialis anterior muscle in humans. Acta Physiol Scand 163:391-401.

Elster A, *Frequency Encoding: How does frequency-encoding work?*, Questions and Answers in MRI, retrieved March 28, 2021 from http://mriquestionscom/frequency-encodinghtml, 2021a.

Elster A, *Phase-encoding Gradients: Why do some gradients change frequency and others change phase? It seems like they should do all work the same way.*, Questions and Answers in MRI, retrieved March 28, 2021 from http://mriquestionscom/phase-encoding-gradienthtml, 2021b.

Elster A, *Phase Encoding Steps: If each pixel is assigned a unique phase and frequency, why can't you use just a single phase-encoding step to decode spatial information?*, Questions and Answers in MRI, retrieved March 28, 2021 from http://mriquestionscom/single-pe-stephtml, 2021c.

Elster A, *Intro to Phase-encoding - I: I understand frequency-encoding, but I just don't get phase-encoding. Can you explain?*, Questions and Answers in MRI, retrieved March 28, 2021 from http://mriquestionscom/what-is-phase-encodinghtml, 2021d.

Elster A, *Phase Encoding Intro II: I understand the 2-pixel example, but I still can't put it all together with the whole image and frequency encoding. Can you help?*,

Questions and Answers in MRI, retrieved March 28, 2021 from http://mriquestionscom/pe-and-fe-togetherhtml, 2021e.

Elster A, *2D Fourier Transform: I think I see how to calculate pixel values in your simple examples, but how do you do this in a real image with thousands of pixels?*, Questions and Answers in MRI, retrieved March 28, 2021 from http://mriquestionscom/2dft-reconstructionhtml, 2021f.

Elster A, *k-space: What is k-space?*, Questions and Answers in MRI, retrieved March 28, 2021 from http://mriquestionscom/what-is-k-spacehtml, 2021g.

Elster A, *"Geography" of k-space: If the points in k-space don't correspond to points in the image, what do they mean?*, Questions and Answers in MRI, retrieved March 28, 2021 from http://mriquestionscom/parts-of-k-spacehtml, 2021h.

Elster A, *Location of Spatial Frequencies: Exactly where are the spatial frequencies are located in k-space?*, Questions and Answers in MRI, retrieved March 28, 2021 from http://mriquestionscom/locations-in-k-spacehtml, 2021i.

Emborg J, Spaich EG, Andersen OK (2009), Withdrawal reflexes examined during human gait by ground reaction forces: site and gait phase dependency. Med Biol Eng Comput 47:29-39.

Engberg I, Lundberg A, Ryall RW (1968), Is the tonic decerebrate inhibition of reflex paths mediated by monoaminergic pathways? Acta Physiol Scand 72:123-133.

Engberg I, Lundberg A, Ryall RW (1968), Reticulospinal inhibition of transmission in reflex pathways. J Physiol 194:201-223.

Enna SJ, McCarson KE (2006), The role of GABA in the mediation and perception of pain. Adv Pharmacol 54:1-27.

Epstein CM (2008), TMS stimulation coils. In: Wassermann, EM, Epstein CM, Ziemann, U, Walsh, V, Paus, T, Lisanby, SH; The Oxford Handbook of Transcranial stimulation Oxford: Oxford University Press:25-32.

Ertekin C, Ertekin N, Karcioglu M (1975), Conduction velocity along human nociceptive reflex afferent nerve fibres. J Neurol Neurosurg Psychiatry 38:959-965.

Espiritu MG, Lin CS, Burke D (2003), Motoneuron excitability and the F wave. Muscle Nerve 27:720-727.

Fan J, Wu T, Lee KS, Li X (2012), Magnetically induced deep brain stimulation of neuronal firing for pain relief. Annual International Conference of the IEEE Engineering in Medicine and Biology Society IEEE Engineering in Medicine and Biology Society Annual International Conference 2012:731-734.

Farina D, Arendt-Nielsen L, Graven-Nielsen T (2005a), Experimental muscle pain decreases voluntary EMG activity but does not affect the muscle potential evoked by transcutaneous electrical stimulation. Clin Neurophysiol 116:1558-1565.

Farina D, Arendt-Nielsen L, Merletti R, Graven-Nielsen T (2004a), Effect of experimental muscle pain on motor unit firing rate and conduction velocity. J Neurophysiol 91:1250-1259.

Farina D, Merletti R, Enoka RM (2004b), The extraction of neural strategies from the surface EMG. J Appl Physiol (1985) 96:1486-1495.

Farina S, Tinazzi M, Le Pera D, Valeriani M (2003), Pain-related modulation of the human motor cortex. Neurol Res 25:130-142.

Farina S, Valeriani M, Rosso T, Aglioti S, Tamburin S, Fiaschi A, Tinazzi M (2001), Transient inhibition of the human motor cortex by capsaicin-induced pain. A study with transcranial magnetic stimulation. Neurosci Lett 314:97-101.

Feinstein JS, Khalsa SS, Salomons TV, Prkachin KM, Frey-Law LA, Lee JE, Tranel D, Rudrauf D (2016), Preserved emotional awareness of pain in a patient with extensive bilateral damage to the insula, anterior cingulate, and amygdala. Brain structure & function 221:1499-1511.

Feise RJ (2002), Do multiple outcome measures require p-value adjustment? BMC Med Res Methodol 2:8.

Ferbert A, Priori A, Rothwell JC, Day BL, Colebatch JG, Marsden CD (1992), Interhemispheric inhibition of the human motor cortex. J Physiol 453:525-546.

Feredoes E, Heinen K, Weiskopf N, Ruff C, Driver J (2011), Causal evidence for frontal involvement in memory target maintenance by posterior brain areas during distracter interference of visual working memory. Proc Natl Acad Sci U S A 108:17510-17515.

Ferreri F, Ponzo D, Hukkanen T, Mervaala E, Kononen M, Pasqualetti P, Vecchio F, Rossini PM, et al. (2012), Human brain cortical correlates of short-latency afferent inhibition: a combined EEG-TMS study. J Neurophysiol 108:314-323.

Fierro B, De Tommaso M, Giglia F, Giglia G, Palermo A, Brighina F (2010), Repetitive transcranial magnetic stimulation (rTMS) of the dorsolateral prefrontal cortex (DLPFC) during capsaicin-induced pain: modulatory effects on motor cortex excitability. Exp Brain Res 203:31-38.

Filbrich L, Alamia A, Blandiaux S, Burns S, Legrain V (2017b), Shaping visual space perception through bodily sensations: Testing the impact of nociceptive stimuli on visual perception in peripersonal space with temporal order judgments. PLoS One 12:e0182634.

Filbrich L, Alamia A, Burns S, Legrain V (2017a), Orienting attention in visual space by nociceptive stimuli: investigation with a temporal order judgment task based on the adaptive PSI method. Exp Brain Res 235:2069-2079.

Filbrich L, Halicka M, Alamia A, Legrain V (2018), Investigating the spatial characteristics of the crossmodal interaction between nociception and vision using gaze direction. Conscious Cogn 57:106-115.

Fiori F, Chiappini E, Candidi M, Romei V, Borgomaneri S, Avenanti A (2017), Long-latency interhemispheric interactions between motor-related areas and the primary motor cortex: a dual site TMS study. Sci Rep 7:14936.

Fiori F, Chiappini E, Soriano M, Paracampo R, Romei V, Borgomaneri S, Avenanti A (2016), Long-latency modulation of motor cortex excitability by ipsilateral posterior inferior frontal gyrus and pre-supplementary motor area. Sci Rep 6:38396.

Fischer M, Orth M (2011), Short-latency sensory afferent inhibition: conditioning stimulus intensity, recording site, and effects of 1 Hz repetitive TMS. Brain stimulation 4:202-209.

Floeter MK (2003), Cutaneous silent periods. Muscle Nerve 28:391-401.

Floeter MK, Gerloff C, Kouri J, Hallett M (1998), Cutaneous withdrawal reflexes of the upper extremity. Muscle Nerve 21:591-598.

Fossataro C, Burin D, Ronga I, Galigani M, Rossi Sebastiano A, Pia L, Garbarini F (2020), Agent-dependent modulation of corticospinal excitability during painful transcutaneous electrical stimulation. NeuroImage 217:116897.

Fox, Corbetta M, Snyder AZ, Vincent JL, Raichle ME (2006), Spontaneous neuronal activity distinguishes human dorsal and ventral attention systems. Proc Natl Acad Sci U S A 103:10046-10051.

Fox, Halko MA, Eldaief MC, Pascual-Leone A (2012), Measuring and manipulating brain connectivity with resting state functional connectivity magnetic resonance imaging (fcMRI) and transcranial magnetic stimulation (TMS). NeuroImage 62:2232-2243.

Fox, Narayana S, Tandon N, Sandoval H, Fox SP, Kochunov P, Lancaster JL (2004), Column-based model of electric field excitation of cerebral cortex. Hum Brain Mapp 22:1-14.

Fox, Raichle ME (2007), Spontaneous fluctuations in brain activity observed with functional magnetic resonance imaging. Nat Rev Neurosci 8:700-711.

Fox P, Ingham R, George MS, Mayberg H, Ingham J, Roby J, Martin C, Jerabek P (1997), Imaging human intra-cerebral connectivity by PET during TMS. Neuroreport 8:2787-2791.

Freeman AW, Johnson KO (1982), A model accounting for effects of vibratory amplitude on responses of cutaneous mechanoreceptors in macaque monkey. J Physiol 323:43-64.

Fregni F, Potvin K, Dasilva D, Wang X, Lenkinski RE, Freedman SD, Pascual-Leone A (2011), Clinical effects and brain metabolic correlates in non-invasive cortical neuromodulation for visceral pain. Eur J Pain 15:53-60.

Friston KJ, Frith CD, Liddle PF, Frackowiak RS (1993), Functional connectivity: the principal-component analysis of large (PET) data sets. J Cereb Blood Flow Metab 13:5-14.

Fritz HC, McAuley JH, Wittfeld K, Hegenscheid K, Schmidt CO, Langner S, Lotze M (2016), Chronic Back Pain Is Associated With Decreased Prefrontal and Anterior Insular Gray Matter: Results From a Population-Based Cohort Study. J Pain 17:111-118.

Frot M, Magnin M, Mauguiere F, Garcia-Larrea L (2007), Human SII and posterior insula differently encode thermal laser stimuli. Cereb Cortex 17:610-620.

Frot M, Magnin M, Mauguiere F, Garcia-Larrea L (2013), Cortical representation of pain in primary sensory-motor areas (S1/M1)--a study using intracortical recordings in humans. Hum Brain Mapp 34:2655-2668.

Frot M, Rambaud L, Guenot M, Mauguiere F (1999), Intracortical recordings of early pain-related CO2-laser evoked potentials in the human second somatosensory (SII) area. Clin Neurophysiol 110:133-145.

Fuglsang-Frederiksen A, Ronager J (1988), The motor unit firing rate and the power spectrum of EMG in humans. Electroencephalogr Clin Neurophysiol 70:68-72.

Fujiwara T, Rothwell JC (2004), The after effects of motor cortex rTMS depend on the state of contraction when rTMS is applied. Clin Neurophysiol 115:1514-1518.

Galhardoni R, Correia GS, Araujo H, Yeng LT, Fernandes DT, Kaziyama HH, Marcolin MA, Bouhassira D, et al. (2015), Repetitive transcranial magnetic stimulation in chronic pain: a review of the literature. Arch Phys Med Rehabil 96:S156-172.

Garcia-Larrea L, Frot M, Valeriani M (2003), Brain generators of laser-evoked potentials: from dipoles to functional significance. Neurophysiol Clin 33:279-292.

Garcia-Larrea L, Perchet C, Creac'h C, Convers P, Peyron R, Laurent B, Mauguiere F, Magnin M (2010), Operculo-insular pain (parasylvian pain): a distinct central pain syndrome. Brain 133:2528-2539.

Garcia-Larrea L, Peyron R (2007), Motor cortex stimulation for neuropathic pain: From phenomenology to mechanisms. NeuroImage 37 Suppl 1:S71-79.

Garcia-Larrea L, Peyron R, Mertens P, Gregoire MC, Lavenne F, Le Bars D, Convers P, Mauguiere F, et al. (1999), Electrical stimulation of motor cortex for pain control: a combined PET-scan and electrophysiological study. Pain 83:259-273.

Garg S, Sinha VK, Tikka SK, Mishra P, Goyal N (2016), The efficacy of cerebellar vermal deep high frequency (theta range) repetitive transcranial magnetic stimulation (rTMS) in schizophrenia: A randomized rater blind-sham controlled study. Psychiatry Res 243:413-420.

George MS, Lisanby SH, Sackeim HA (1999), Transcranial magnetic stimulation: applications in neuropsychiatry. Arch Gen Psychiatry 56:300-311.

Gerschlager W, Christensen LO, Bestmann S, Rothwell JC (2002), rTMS over the cerebellum can increase corticospinal excitability through a spinal mechanism involving activation of peripheral nerve fibres. Clin Neurophysiol 113:1435-1440.

Gibbs J, Harrison LM, Stephens JA (1995), Cutaneomuscular reflexes recorded from the lower limb in man during different tasks. J Physiol 487:237-242.

Giehl J, Meyer-Brandis G, Kunz M, Lautenbacher S (2014), Responses to tonic heat pain in the ongoing EEG under conditions of controlled attention. Somatosens Mot Res 31:40-48.

Gilio F, Bettolo CM, Conte A, Iacovelli E, Frasca V, Serrao M, Giacomelli E, Gabriele M, et al. (2008), Influence of the corticospinal tract on the cutaneous silent period: a study in patients with pyramidal syndrome. Neurosci Lett 433:109-113.

Glass GV, Peckham PD, Sanders JR (1972), Consequences of failure to meet assumptions underlying the fixed effects analysis of variance and covariance. Rev Educ Res 42:237-288.

Gogan P (1970), The startle and orienting reactions in man. A study of their characteristics and habituation. Brain Res 18:117-135.

Grachev ID, Fredrickson BE, Apkarian AV (2000), Abnormal brain chemistry in chronic back pain: an in vivo proton magnetic resonance spectroscopy study. Pain 89:7-18.

Grachev ID, Thomas PS, Ramachandran TS (2002), Decreased levels of N-acetylaspartate in dorsolateral prefrontal cortex in a case of intractable severe sympathetically mediated chronic pain (complex regional pain syndrome, type I). Brain Cogn 49:102-113.

Grandjean J, Derosiere G, Vassiliadis P, Quemener L, Wilde Y, Duque J (2018), Towards assessing corticospinal excitability bilaterally: Validation of a double-coil TMS method. J Neurosci Methods 293:162-168.

Grant G, Arvidsson J, Robertson B, Ygge J (1979), Transganglionic transport of horseradish peroxidase in primary sensory neurons. Neurosci Lett 12:23-28.

Graven-Nielsen T (2006), Fundamentals of muscle pain, referred pain, and deep tissue hyperalgesia. Scand J Rheumatol Suppl 122:1-43.

Graven-Nielsen T, Arendt-Nielsen L, Mense S (2002), Thermosensitivity of muscle: high-intensity thermal stimulation of muscle tissue induces muscle pain in humans. J Physiol 540:647-656.

Graven-Nielsen T, Lund H, Arendt-Nielsen L, Danneskiold-Samsoe B, Bliddal H (2002), Inhibition of maximal voluntary contraction force by experimental muscle pain: a centrally mediated mechanism. Muscle Nerve 26:708-712.

Graven-Nielsen T, McArdle A, Phoenix J, Arendt-Nielsen L, Jensen TS, Jackson MJ, Edwards RH (1997), In vivo model of muscle pain: quantification of intramuscular chemical, electrical, and pressure changes associated with saline-induced muscle pain in humans. Pain 69:137-143.

Graven-Nielsen T, Svensson P, Arendt-Nielsen L (1997), Effects of experimental muscle pain on muscle activity and co-ordination during static and dynamic motor function. Electroencephalogr Clin Neurophysiol 105:156-164.

Greffrath W, Baumgartner U, Treede RD (2007), Peripheral and central components of habituation of heat pain perception and evoked potentials in humans. Pain 132:301-311.

Grimby L (1963), Normal plantar response: integration of flexor and extensor reflex components. J Neurol Neurosurg Psychiatry 26:39-50.

Groetzner P, Weidner C (2010), The human vasodilator axon reflex - an exclusively peripheral phenomenon? Pain 149:71-75.

Gronroos M, Pertovaara A (1993), Capsaicin-induced central facilitation of a nociceptive flexion reflex in humans. Neurosci Lett 159:215-218.

Groppa S, Oliviero A, Eisen A, Quartarone A, Cohen LG, Mall V, Kaelin-Lang A, Mima T, et al. (2012), A practical guide to diagnostic transcranial magnetic stimulation: report of an IFCN committee. Clin Neurophysiol 123:858-882.

Groppe DM, Urbach TP, Kutas M (2011), Mass univariate analysis of event-related brain potentials/fields I: a critical tutorial review. Psychophysiology 48:1711-1725.

Gugino LD, Romero JR, Aglio L, Titone D, Ramirez M, Pascual-Leone A, Grimson E, Weisenfeld N, et al. (2001), Transcranial magnetic stimulation coregistered with

MRI: a comparison of a guided versus blind stimulation technique and its effect on evoked compound muscle action potentials. Clin Neurophysiol 112:1781-1792.

Hagbarth KE (1960), Spinal withdrawal reflexes in the human lower limbs. J Neurol Neurosurg Psychiatry 23:222-227.

Hallett M (2000), Transcranial magnetic stimulation and the human brain. Nature 406:147-150.

Hallett M (2007), Transcranial magnetic stimulation: a primer. Neuron 55:187-199.

Hallett M, Di Iorio R, Rossini PM, Park JE, Chen R, Celnik P, Strafella AP, Matsumoto H, et al. (2017), Contribution of transcranial magnetic stimulation to assessment of brain connectivity and networks. Clin Neurophysiol 128:2125-2139.

Hampson M, Hoffman RE (2010), Transcranial magnetic stimulation and connectivity mapping: tools for studying the neural bases of brain disorders. Front Syst Neurosci 4.

Hanajima R, Ugawa Y, Machii K, Mochizuki H, Terao Y, Enomoto H, Furubayashi T, Shiio Y, et al. (2001), Interhemispheric facilitation of the hand motor area in humans. J Physiol 531:849-859.

Hanakawa T, Mima T, Matsumoto R, Abe M, Inouchi M, Urayama S, Anami K, Honda M, et al. (2009), Stimulus-response profile during single-pulse transcranial magnetic stimulation to the primary motor cortex. Cereb Cortex 19:2605-2615.

Hanlon CA, Canterberry M, Taylor JJ, DeVries W, Li X, Brown TR, George MS (2013), Probing the frontostriatal loops involved in executive and limbic processing via interleaved TMS and functional MRI at two prefrontal locations: a pilot study. PLoS One 8:e67917.

Hanlon CA, Dowdle LT, Moss H, Canterberry M, George MS (2016), Mobilization of Medial and Lateral Frontal-Striatal Circuits in Cocaine Users and Controls: An Interleaved TMS/BOLD Functional Connectivity Study. Neuropsychopharmacology 41:3032-3041.

Hansen N, Klein T, Magerl W, Treede RD (2007), Psychophysical evidence for long-term potentiation of C-fiber and Adelta-fiber pathways in humans by analysis of pain descriptors. J Neurophysiol 97:2559-2563.

Hardy JD (1953), Thresholds of pain and reflex contraction as related to noxious stimulation. J Appl Physiol 5:725-739.

Hardy JD, Wolff HG, Goodell H (1950), Experimental evidence on the nature of cutaneous hyperalgesia. J Clin Invest 29:115-140.

Harrison PJ, Jankowska E (1985), Sources of input to interneurones mediating group I non-reciprocal inhibition of motoneurones in the cat. J Physiol 361:379-401.

Harwell MR, Rubinstein EN, Hayes WS, Olds CC (1992), Summarizing Monte Carlo results in methodological research: the one- and two-factor fixed effects ANOVA cases. J Educ Stat 17:315-339.

Hasan A, Galea JM, Casula EP, Falkai P, Bestmann S, Rothwell JC (2013), Muscle and timing-specific functional connectivity between the dorsolateral prefrontal cortex and the primary motor cortex. J Cogn Neurosci 25:558-570.

Hashmi JA, Baria AT, Baliki MN, Huang L, Schnitzer TJ, Apkarian AV (2012), Brain networks predicting placebo analgesia in a clinical trial for chronic back pain. Pain 153:2393-2402.

Hawco C, Armony JL, Daskalakis ZJ, Berlim MT, Chakravarty MM, Pike GB, Lepage M (2017), Differing Time of Onset of Concurrent TMS-fMRI during Associative Memory Encoding: A Measure of Dynamic Connectivity. Front Hum Neurosci 11:404.

Hayashi K, Shiozawa S, Ozaki N, Mizumura K, Graven-Nielsen T (2013), Repeated intramuscular injections of nerve growth factor induced progressive muscle hyperalgesia, facilitated temporal summation, and expanded pain areas. Pain 154:2344-2352.

Hayward G, Mehta MA, Harmer C, Spinks TJ, Grasby PM, Goodwin GM (2007), Exploring the physiological effects of double-cone coil TMS over the medial frontal cortex on the anterior cingulate cortex: an H2(15)O PET study. Eur J Neurosci 25:2224-2233.

Heales LJ, Hug F, MacDonald DA, Vicenzino B, Hodges PW (2016), Is synergistic organisation of muscle coordination altered in people with lateral epicondylalgia? A case-control study. Clin Biomech (Bristol, Avon) 35:124-131.

Heinen, Glocker FX, Fietzek U, Meyer BU, Lucking CH, Korinthenberg R (1998), Absence of transcallosal inhibition following focal magnetic stimulation in preschool children. Ann Neurol 43:608-612.

Heinen, Ruff CC, Bjoertomt O, Schenkluhn B, Bestmann S, Blankenburg F, Driver J, Chambers CD (2011), Concurrent TMS-fMRI reveals dynamic interhemispheric influences of the right parietal cortex during exogenously cued visuospatial attention. Eur J Neurosci 33:991-1000.

Heinricher MM, Tavares I, Leith JL, Lumb BM (2009), Descending control of nociception: Specificity, recruitment and plasticity. Brain Res Rev 60:214-225.

Helmich RC, Baumer T, Siebner HR, Bloem BR, Munchau A (2005), Hemispheric asymmetry and somatotopy of afferent inhibition in healthy humans. Exp Brain Res 167:211-219.

Henderson LA, Gandevia SC, Macefield VG (2007), Somatotopic organization of the processing of muscle and cutaneous pain in the left and right insula cortex: a single-trial fMRI study. Pain 128:20-30.

Henriksen M, Rosager S, Aaboe J, Bliddal H (2011), Adaptations in the gait pattern with experimental hamstring pain. J Electromyogr Kinesiol 21:746-753.

Herwig U, Kolbel K, Wunderlich AP, Thielscher A, von Tiesenhausen C, Spitzer M, Schonfeldt-Lecuona C (2002), Spatial congruence of neuronavigated transcranial magnetic stimulation and functional neuroimaging. Clin Neurophysiol 113:462-468.

Herwig U, Padberg F, Unger J, Spitzer M, Schonfeldt-Lecuona C (2001), Transcranial magnetic stimulation in therapy studies: examination of the reliability of "standard" coil positioning by neuronavigation. Biol Psychiatry 50:58-61.

Herwig U, Satrapi P, Schonfeldt-Lecuona C (2003), Using the international 10-20 EEG system for positioning of transcranial magnetic stimulation. Brain Topogr 16:95-99.

Hjornevik T, Jacobsen LM, Qu H, Bjaalie JG, Gjerstad J, Willoch F (2008), Metabolic plasticity in the supraspinal pain modulating circuitry after noxious stimulus-induced spinal cord LTP. Pain 140:456-464.

Hodges PW, Moseley GL, Gabrielsson A, Gandevia SC (2003), Experimental muscle pain changes feedforward postural responses of the trunk muscles. Exp Brain Res 151:262-271.

Hodges PW, Tucker K (2011), Moving differently in pain: a new theory to explain the adaptation to pain. Pain 152:S90-98.

Holmberg H, Schouenborg J (1996), Postnatal development of the nociceptive withdrawal reflexes in the rat: a behavioural and electromyographic study. J Physiol 493 (Pt 1):239-252.

Homberg V, Stephan KM, Netz J (1991), Transcranial stimulation of motor cortex in upper motor neurone syndrome: its relation to the motor deficit. Electroencephalogr Clin Neurophysiol 81:377-388.

Honey GD, Bullmore ET, Sharma T (2000), Prolonged reaction time to a verbal working memory task predicts increased power of posterior parietal cortical activation. NeuroImage 12:495-503.

Huang YZ, Edwards MJ, Rounis E, Bhatia KP, Rothwell JC (2005), Theta burst stimulation of the human motor cortex. Neuron 45:201-206.

Huang YZ, Rothwell JC (2004), The effect of short-duration bursts of high-frequency, low-intensity transcranial magnetic stimulation on the human motor cortex. Clin Neurophysiol 115:1069-1075.

Huang YZ, Rothwell JC, Lu CS, Wang J, Weng YH, Lai SC, Chuang WL, Hung J, et al. (2009), The effect of continuous theta burst stimulation over premotor cortex on circuits in primary motor cortex and spinal cord. Clin Neurophysiol 120:796-801.

Hubbard CS, Khan SA, Keaser ML, Mathur VA, Goyal M, Seminowicz DA (2014), Altered Brain Structure and Function Correlate with Disease Severity and Pain Catastrophizing in Migraine Patients. eNeuro 1:e20 14.

Huettel SA, Song AW, McCarthy G (2014), Functional Magnetic Resonance Imaging, third edition. Sinauer Associates, Sunderlalnd, MA.

Hugon M (1973), Exteroceptive Reflexes to Stimulation of the Sural Nerve in Normal Man. New Developments in Electromyography and Clinical Neurophysiology 3:713-729.

Huishi Zhang C, Sohrabpour A, Lu Y, He B (2016), Spectral and spatial changes of brain rhythmic activity in response to the sustained thermal pain stimulation. Hum Brain Mapp 37:2976-2991.

Hutchison WD, Davis KD, Lozano AM, Tasker RR, Dostrovsky JO (1999), Pain-related neurons in the human cingulate cortex. Nat Neurosci 2:403-405.

Hutton C, Bork A, Josephs O, Deichmann R, Ashburner J, Turner R (2002), Image distortion correction in fMRI: A quantitative evaluation. NeuroImage 16:217-240.

Iannetti GD, Mouraux A (2010), From the neuromatrix to the pain matrix (and back). Exp Brain Res 205:1-12.

Iannetti GD, Zambreanu L, Cruccu G, Tracey I (2005), Operculoinsular cortex encodes pain intensity at the earliest stages of cortical processing as indicated by amplitude of laser-evoked potentials in humans. Neuroscience 131:199-208.

Ikeda H, Heinke B, Ruscheweyh R, Sandkuhler J (2003), Synaptic plasticity in spinal lamina I projection neurons that mediate hyperalgesia. Science 299:1237-1240.

Ikeda H, Stark J, Fischer H, Wagner M, Drdla R, Jager T, Sandkuhler J (2006), Synaptic amplifier of inflammatory pain in the spinal dorsal horn. Science 312:1659-1662.

Ilmoniemi RJ, Virtanen J, Ruohonen J, Karhu J, Aronen HJ, Naatanen R, Katila T (1997), Neuronal responses to magnetic stimulation reveal cortical reactivity and connectivity. Neuroreport 8:3537-3540.

Inghilleri M, Berardelli A, Cruccu G, Manfredi M, Priori A, Rothwell JC (1995), Inhibition of hand muscle motoneurones by peripheral nerve stimulation in the relaxed human subject. Antidromic versus orthodromic input. Electroencephalogr Clin Neurophysiol 97:63-68.

Inghilleri M, Cruccu G, Argenta M, Polidori L, Manfredi M (1997), Silent period in upper limb muscles after noxious cutaneous stimulation in man. Electroencephalogr Clin Neurophysiol 105:109-115.

Inui K, Kakigi R (2012), Pain perception in humans: use of intraepidermal electrical stimulation. J Neurol Neurosurg Psychiatry 83:551-556.

Inui K, Tran TD, Hoshiyama M, Kakigi R (2002), Preferential stimulation of Adelta fibers by intra-epidermal needle electrode in humans. Pain 96:247-252.

Inui K, Tran TD, Qiu Y, Wang X, Hoshiyama M, Kakigi R (2003), A comparative magnetoencephalographic study of cortical activations evoked by noxious and innocuous somatosensory stimulations. Neuroscience 120:235-248.

Inui K, Tsuji T, Kakigi R (2006), Temporal analysis of cortical mechanisms for pain relief by tactile stimuli in humans. Cereb Cortex 16:355-365.

Isnard J, Guenot M, Sindou M, Mauguiere F (2004), Clinical manifestations of insular lobe seizures: a stereo-electroencephalographic study. Epilepsia 45:1079-1090.

Ivo R, Nicklas A, Dargel J, Sobottke R, Delank KS, Eysel P, Weber B (2013), Brain structural and psychometric alterations in chronic low back pain. Eur Spine J 22:1958-1964.

Iwata, Hanajima R, Furubayashi T, Terao Y, Uesugi H, Shiio Y, Enomoto H, Mochizuki H, et al. (2004), Facilitatory effect on the motor cortex by electrical stimulation over the cerebellum in humans. Exp Brain Res 159:418-424.

Iwata, Ugawa Y (2005), The effects of cerebellar stimulation on the motor cortical excitability in neurological disorders: a review. Cerebellum 4:218-223.

Iwata Y, Jono Y, Mizusawa H, Kinoshita A, Hiraoka K (2016), Interhemispheric Inhibition Induced by Transcranial Magnetic Stimulation Over Primary Sensory Cortex. Front Hum Neurosci 10:438.

Jasmin L, Rabkin SD, Granato A, Boudah A, Ohara PT (2003), Analgesia and hyperalgesia from GABA-mediated modulation of the cerebral cortex. Nature 424:316-320.

Jenner JR, Stephens JA (1982), Cutaneous reflex responses and their central nervous pathways studied in man. J Physiol 333:405-419.

Jensen TS, Finnerup NB (2014), Allodynia and hyperalgesia in neuropathic pain: clinical manifestations and mechanisms. Lancet Neurol 13:924-935.

Jesunathadas M, Aidoor SS, Keenan KG, Farina D, Enoka RM (2012), Influence of amplitude cancellation on the accuracy of determining the onset of muscle activity from the surface electromyogram. J Electromyogr Kinesiol 22:494-500.

Jezzard P, Balaban RS (1995), Correction for geometric distortion in echo planar images from B0 field variations. Magn Reson Med 34:65-73.

Johansson H, Sojka P (1991), Pathophysiological mechanisms involved in genesis and spread of muscular tension in occupational muscle pain and in chronic musculoskeletal pain syndromes: a hypothesis. Med Hypotheses 35:196-203.

Jonker ZD, van der Vliet R, Hauwert CM, Gaiser C, Tulen JHM, van der Geest JN, Donchin O, Ribbers GM, et al. (2019), TMS motor mapping: Comparing the absolute reliability of digital reconstruction methods to the golden standard. Brain stimulation 12:309-313.

Jovanovic K, Anastasijevic R, Vuco J (1990), Reflex effects on gamma fusimotor neurones of chemically induced discharges in small-diameter muscle afferents in decerebrate cats. Brain Res 521:89-94.

Julkunen P (2014), Methods for estimating cortical motor representation size and location in navigated transcranial magnetic stimulation. J Neurosci Methods 232:125-133.

Jung J, Bungert A, Bowtell R, Jackson SR (2016), Vertex Stimulation as a Control Site for Transcranial Magnetic Stimulation: A Concurrent TMS/fMRI Study. Brain stimulation 9:58-64.

Kahya MC, Yavuz SU, Turker KS (2010), Cutaneous silent period in human FDI motor units. Exp Brain Res 205:455-463.

Kakigi R, Endo C, Neshige R, Kuroda Y, Shibasaki H (1991), Estimation of conduction velocity of A delta fibers in humans. Muscle Nerve 14:1193-1196.

Kalezic I, Bugaychenko LA, Kostyukov AI, Pilyavskii AI, Ljubisavljevic M, Windhorst U, Johansson H (2004), Fatigue-related depression of the feline monosynaptic gastrocnemius-soleus reflex. J Physiol 556:283-296.

Kammer T, Beck S, Thielscher A, Laubis-Herrmann U, Topka H (2001), Motor thresholds in humans: a transcranial magnetic stimulation study comparing different pulse waveforms, current directions and stimulator types. Clin Neurophysiol 112:250-258.

Kaneko K, Kawai S, Taguchi T, Fuchigami Y, Yonemura H, Fujimoto H (1998), Cortical motor neuron excitability during cutaneous silent period. Electroencephalogr Clin Neurophysiol 109:364-368.

Karabanov AN, Chao CC, Paine R, Hallett M (2013), Mapping different intra-hemispheric parietal-motor networks using twin Coil TMS. Brain stimulation 6:384-389.

Karlsson S, Yu J, Akay M (1999), Enhancement of spectral analysis of myoelectric signals during static contractions using wavelet methods. IEEE Trans Biomed Eng 46:670-684.

Karlsson S, Yu J, Akay M (2000), Time-frequency analysis of myoelectric signals during dynamic contractions: a comparative study. IEEE Trans Biomed Eng 47:228-238.

Kastrup O, Leonhardt G, Kurthen M, Hufnagel A (2000), Cortical motor reorganization following early brain damage and hemispherectomy demonstrated by transcranial magnetic stimulation. Clin Neurophysiol 111:1346-1352.

Kemna LJ, Gembris D (2003), Repetitive transcranial magnetic stimulation induces different responses in different cortical areas: a functional magnetic resonance study in humans. Neurosci Lett 336:85-88.

Khasabov SG, Rogers SD, Ghilardi JR, Peters CM, Mantyh PW, Simone DA (2002), Spinal neurons that possess the substance P receptor are required for the development of central sensitization. J Neurosci 22:9086-9098.

Kiers L, Cros D, Chiappa KH, Fang J (1993), Variability of motor potentials evoked by transcranial magnetic stimulation. Electroencephalogr Clin Neurophysiol 89:415-423.

Kiziltan ME, Gunduz A, Apaydin H, Ertan S, Kiziltan G (2015), Auditory startle reflex and startle reflex to somatosensory inputs in generalized dystonia. Clin Neurophysiol 126:1740-1745.

Klein T, Magerl W, Hopf HC, Sandkuhler J, Treede RD (2004), Perceptual correlates of nociceptive long-term potentiation and long-term depression in humans. J Neurosci 24:964-971.

Klein T, Magerl W, Nickel U, Hopf HC, Sandkuhler J, Treede RD (2007), Effects of the NMDA-receptor antagonist ketamine on perceptual correlates of long-term potentiation within the nociceptive system. Neuropharmacology 52:655-661.

Klein T, Magerl W, Treede RD (2006), Perceptual correlate of nociceptive long-term potentiation (LTP) in humans shares the time course of early-LTP. J Neurophysiol 96:3551-3555.

Klein T, Stahn S, Magerl W, Treede RD (2008), The role of heterosynaptic facilitation in long-term potentiation (LTP) of human pain sensation. Pain 139:507-519.

Kniffki KD, Schomburg ED, Steffens H (1981), Synaptic effects from chemically activated fine muscle afferents upon alpha-motoneurones in decerebrate and spinal cats. Brain Res 206:361-370.

Knikou M (2008), The H-reflex as a probe: pathways and pitfalls. J Neurosci Methods 171:1-12.

Koch G, Cercignani M, Pecchioli C, Versace V, Oliveri M, Caltagirone C, Rothwell J, Bozzali M (2010), In vivo definition of parieto-motor connections involved in planning of grasping movements. NeuroImage 51:300-312.

Koch G, Fernandez Del Olmo M, Cheeran B, Ruge D, Schippling S, Caltagirone C, Rothwell JC (2007), Focal stimulation of the posterior parietal cortex increases the excitability of the ipsilateral motor cortex. J Neurosci 27:6815-6822.

Koch G, Fernandez Del Olmo M, Cheeran B, Schippling S, Caltagirone C, Driver J, Rothwell JC (2008), Functional interplay between posterior parietal and ipsilateral motor cortex revealed by twin-coil transcranial magnetic stimulation during reach planning toward contralateral space. J Neurosci 28:5944-5953.

Koch G, Franca M, Del Olmo MF, Cheeran B, Milton R, Alvarez Sauco M, Rothwell JC (2006), Time course of functional connectivity between dorsal premotor and contralateral motor cortex during movement selection. J Neurosci 26:7452-7459.

Koch G, Ruge D, Cheeran B, Fernandez Del Olmo M, Pecchioli C, Marconi B, Versace V, Lo Gerfo E, et al. (2009), TMS activation of interhemispheric pathways between the posterior parietal cortex and the contralateral motor cortex. J Physiol 587:4281-4292.

Kodaira M, Inui K, Kakigi R (2014), Evaluation of nociceptive Adelta- and C-fiber dysfunction with lidocaine using intraepidermal electrical stimulation. Clin Neurophysiol 125:1870-1877.

Kofler M (2003), Functional organization of exteroceptive inhibition following nociceptive electrical fingertip stimulation in humans. Clin Neurophysiol 114:973-980.

Kofler M, Fuhr P, Leis AA, Glocker FX, Kronenberg MF, Wissel J, Stetkarova I (2001), Modulation of upper extremity motor evoked potentials by cutaneous afferents in humans. Clin Neurophysiol 112:1053-1063.

Kofler M, Glocker FX, Leis AA, Seifert C, Wissel J, Kronenberg MF, Fuhr P (1998), Modulation of upper extremity motoneurone excitability following noxious finger tip stimulation in man: a study with transcranial magnetic stimulation. Neurosci Lett 246:97-100.

Kofler M, Valls-Sole J, Fuhr P, Schindler C, Zaccaria BR, Saltuari L (2008), Sensory modulation of voluntary and TMS-induced activation in hand muscles. Exp Brain Res 188:399-409.

Kojima S, Onishi H, Miyaguchi S, Kotan S, Sugawara K, Kirimoto H, Tamaki H (2015), Effects of cathodal transcranial direct current stimulation to primary somatosensory cortex on short-latency afferent inhibition. Neuroreport 26:634-637.

Komssi S, Aronen HJ, Huttunen J, Kesaniemi M, Soinne L, Nikouline VV, Ollikainen M, Roine RO, et al. (2002), Ipsi- and contralateral EEG reactions to transcranial magnetic stimulation. Clin Neurophysiol 113:175-184.

Komssi S, Kahkonen S, Ilmoniemi RJ (2004), The effect of stimulus intensity on brain responses evoked by transcranial magnetic stimulation. Hum Brain Mapp 21:154-164.

Kornelsen J, Sboto-Frankenstein U, McIver T, Gervai P, Wacnik P, Berrington N, Tomanek B (2013), Default mode network functional connectivity altered in failed back surgery syndrome. J Pain 14:483-491.

Korotkov A, Ljubisavljevic M, Thunberg J, Kataeva G, Roudas M, Pakhomov S, Radovanovic S, Lyskov E, et al. (2002), Changes in human regional cerebral blood flow following hypertonic saline induced experimental muscle pain: a positron emission tomography study. Neurosci Lett 335:119-123.

Koyama S, Nakagawa K, Tanaka S (2017), Transcranial direct current stimulation over the opercular somatosensory region does not influence experimentally induced pain: a triple blind, sham-controlled study. Neuroreport 28:158-162.

Kranz H, Adorjani C, Baumgartner G (1973), The effect of nociceptive cutaneous stimuli on human motoneurons. Brain 96:571-590.

Kraus D, Gharabaghi A (2015), Projecting Navigated TMS Sites on the Gyral Anatomy Decreases Inter-subject Variability of Cortical Motor Maps. Brain stimulation 8:831-837.

Krause P, Forderreuther S, Straube A (2006), TMS motor cortical brain mapping in patients with complex regional pain syndrome type I. Clin Neurophysiol 117:169-176.

Kreuzer PM, Schecklmann M, Lehner A, Wetter TC, Poeppl TB, Rupprecht R, de Ridder D, Landgrebe M, et al. (2015), The ACDC pilot trial: targeting the anterior cingulate by double cone coil rTMS for the treatment of depression. Brain stimulation 8:240-246.

Kronschlager MT, Drdla-Schutting R, Gassner M, Honsek SD, Teuchmann HL, Sandkuhler J (2016), Gliogenic LTP spreads widely in nociceptive pathways. Science 354:1144-1148.

Kruger L, Sampogna SL, Rodin BE, Clague J, Brecha N, Yeh Y (1985), Thin-fiber cutaneous innervation and its intraepidermal contribution studied by labeling methods and neurotoxin treatment in rats. Somatosens Res 2:335-356.

Krummenacher P, Candia V, Folkers G, Schedlowski M, Schonbachler G (2010), Prefrontal cortex modulates placebo analgesia. Pain 148:368-374.

Kucyi A, Davis KD (2015), The dynamic pain connectome. Trends Neurosci 38:86-95.

Kucyi A, Hodaie M, Davis KD (2012), Lateralization in intrinsic functional connectivity of the temporoparietal junction with salience- and attention-related brain networks. J Neurophysiol 108:3382-3392.

Kucyi A, Moayedi M, Weissman-Fogel I, Goldberg MB, Freeman BV, Tenenbaum HC, Davis KD (2014), Enhanced medial prefrontal-default mode network functional connectivity in chronic pain and its association with pain rumination. J Neurosci 34:3969-3975.

Kugelberg E (1948), Demonstration of A and C fibre components in the Babinski plantar response and the pathological flexion reflex. Brain 71:304-319.

Kugelberg E, Eklund K, Grimby L (1960), An electromyographic study of the nociceptive reflexes of the lower limb. Mechanism of the plantar responses. Brain 83:394-410.

Kujirai T, Caramia MD, Rothwell JC, Day BL, Thompson PD, Ferbert A, Wroe S, Asselman P, et al. (1993), Corticocortical inhibition in human motor cortex. J Physiol 471:501-519.

Kumru H, Opisso E, Valls-Sole J, Kofler M (2009), The effect of a prepulse stimulus on the EMG rebound following the cutaneous silent period. J Physiol 587:587-595.

Kupers RC, Svensson P, Jensen TS (2004), Central representation of muscle pain and mechanical hyperesthesia in the orofacial region: a positron emission tomography study. Pain 108:284-293.

Laakso I, Hirata A, Ugawa Y (2014), Effects of coil orientation on the electric field induced by TMS over the hand motor area. Phys Med Biol 59:203-218.

LaMotte RH, Lundberg LE, Torebjork HE (1992), Pain, hyperalgesia and activity in nociceptive C units in humans after intradermal injection of capsaicin. J Physiol 448:749-764.

LaMotte RH, Shain CN, Simone DA, Tsai EF (1991), Neurogenic hyperalgesia: psychophysical studies of underlying mechanisms. J Neurophysiol 66:190-211.

LaMotte RH, Thalhammer JG, Robinson CJ (1983), Peripheral neural correlates of magnitude of cutaneous pain and hyperalgesia: a comparison of neural events in monkey with sensory judgments in human. J Neurophysiol 50:1-26.

Landgren S, Phillips CG, Porter R (1962), Minimal synaptic actions of pyramidal impulses on some alpha motoneurones of the baboon's hand and forearm. J Physiol 161:91-111.

Lang S, Klein T, Magerl W, Treede RD (2007), Modality-specific sensory changes in humans after the induction of long-term potentiation (LTP) in cutaneous nociceptive pathways. Pain 128:254-263.

Larsen DB, Graven-Nielsen T, Hirata RP, Boudreau SA (2018), Differential Corticomotor Excitability Responses to Hypertonic Saline-Induced Muscle Pain in Forearm and Hand Muscles. Neural Plast 2018:7589601.

Laursen RJ, Graven-Nielsen T, Jensen TS, Arendt-Nielsen L (1997), Quantification of local and referred pain in humans induced by intramuscular electrical stimulation. Eur J Pain 1:105-113.

Lavand'homme P, De Kock M, Waterloos H (2005), Intraoperative epidural analgesia combined with ketamine provides effective preventive analgesia in patients undergoing major digestive surgery. Anesthesiology 103:813-820.

Le Pera D, Graven-Nielsen T, Valeriani M, Oliviero A, Di Lazzaro V, Tonali PA, Arendt-Nielsen L (2001), Inhibition of motor system excitability at cortical and spinal level by tonic muscle pain. Clin Neurophysiol 112:1633-1641.

Lee, Mouraux A, Iannetti GD (2009), Characterizing the cortical activity through which pain emerges from nociception. J Neurosci 29:7909-7916.

Lee M, Silverman SM, Hansen H, Patel VB, Manchikanti L (2011), A comprehensive review of opioid-induced hyperalgesia. Pain physician 14:145-161.

Lefaucheur JP (2006), The use of repetitive transcranial magnetic stimulation (rTMS) in chronic neuropathic pain. Neurophysiol Clin 36:117-124.

Lefaucheur JP, Andre-Obadia N, Antal A, Ayache SS, Baeken C, Benninger DH, Cantello RM, Cincotta M, et al. (2014), Evidence-based guidelines on the therapeutic use of repetitive transcranial magnetic stimulation (rTMS). Clin Neurophysiol 125:2150-2206.

Legrain V, Guerit JM, Bruyer R, Plaghki L (2002), Attentional modulation of the nociceptive processing into the human brain: selective spatial attention, probability of stimulus occurrence, and target detection effects on laser evoked potentials. Pain 99:21-39.

Legrain V, Mancini F, Sambo CF, Torta DM, Ronga I, Valentini E (2012), Cognitive aspects of nociception and pain: bridging neurophysiology with cognitive psychology. Neurophysiol Clin 42:325-336.

Legrain V, Mouraux A (2013), Activating selectively and reliably nociceptive afferents with concentric electrode stimulation: yes we can! Provided that low stimulus intensities are used! Clin Neurophysiol 124:424.

Leis AA, Stokic DS, Fuhr P, Kofler M, Kronenberg MF, Wissel J, Glocker FX, Seifert C, et al. (2000), Nociceptive fingertip stimulation inhibits synergistic motoneuron pools in the human upper limb. Neurology 55:1305-1309.

Leitao J, Thielscher A, Tuennerhoff J, Noppeney U (2017), Comparing TMS perturbations to occipital and parietal cortices in concurrent TMS-fMRI studies-Methodological considerations. PLoS One 12:e0181438.

Leitao J, Thielscher A, Tunnerhoff J, Noppeney U (2015), Concurrent TMS-fMRI Reveals Interactions between Dorsal and Ventral Attentional Systems. J Neurosci 35:11445-11457.

Leitao J, Thielscher A, Werner S, Pohmann R, Noppeney U (2013), Effects of parietal TMS on visual and auditory processing at the primary cortical level -- a concurrent TMS-fMRI study. Cereb Cortex 23:873-884.

Lenoir C, Algoet M, Vanderclausen C, Peeters A, Santos SF, Mouraux A (2018b), Report of one confirmed generalized seizure and one suspected partial seizure induced by deep continuous theta burst stimulation of the right operculo-insular cortex. Brain stimulation.

Lenoir C, Huang G, Vandermeeren Y, Hatem SM, Mouraux A (2017), Human primary somatosensory cortex is differentially involved in vibrotaction and nociception. J Neurophysiol 118:317-330.

Lenoir C, Plaghki L, Mouraux A, van den Broeke EN (2018c), Quickly responding C-fibre nociceptors contribute to heat hypersensitivity in the area of secondary hyperalgesia. J Physiol.

Levinsson A, Luo XL, Holmberg H, Schouenborg J (1999), Developmental tuning in a spinal nociceptive system: effects of neonatal spinalization. J Neurosci 19:10397-10403.

Li X, Aruin A (2005), Muscle activity onset time detection using teager-kaiser energy operator. Conf Proc IEEE Eng Med Biol Soc 7:7549-7552.

Li X, Large CH, Ricci R, Taylor JJ, Nahas Z, Bohning DE, Morgan P, George MS (2011), Using interleaved transcranial magnetic stimulation/functional magnetic resonance imaging (fMRI) and dynamic causal modeling to understand the discrete circuit specific changes of medications: lamotrigine and valproic acid changes in motor or prefrontal effective connectivity. Psychiatry Res 194:141-148.

Li X, Nahas Z, Kozel FA, Anderson B, Bohning DE, George MS (2004), Acute left prefrontal transcranial magnetic stimulation in depressed patients is associated with immediately increased activity in prefrontal cortical as well as subcortical regions. Biol Psychiatry 55:882-890.

Li X, Ricci R, Large CH, Anderson B, Nahas Z, Bohning DE, George MS (2010), Interleaved transcranial magnetic stimulation and fMRI suggests that lamotrigine and valproic acid have different effects on corticolimbic activity. Psychopharmacology (Berl) 209:233-244.

Li X, Teneback CC, Nahas Z, Kozel FA, Large C, Cohn J, Bohning DE, George MS (2004), Interleaved transcranial magnetic stimulation/functional MRI confirms that lamotrigine inhibits cortical excitability in healthy young men. Neuropsychopharmacology 29:1395-1407.

Li X, Zhou P, Aruin AS (2007), Teager-Kaiser energy operation of surface EMG improves muscle activity onset detection. Ann Biomed Eng 35:1532-1538.

Liang M, Lee MC, O'Neill J, Dickenson AH, Iannetti GD (2016), Brain potentials evoked by intraepidermal electrical stimuli reflect the central sensitization of nociceptive pathways. J Neurophysiol 116:286-295.

Liberati G, Klocker A, Safronova MM, Ferrao Santos S, Ribeiro Vaz JG, Raftopoulos C, Mouraux A (2016), Nociceptive Local Field Potentials Recorded from the Human Insula Are Not Specific for Nociception. PLoS Biol 14:e1002345.

Liepert J, Bauder H, Wolfgang HR, Miltner WH, Taub E, Weiller C (2000), Treatment-induced cortical reorganization after stroke in humans. Stroke 31:1210-1216.

Liepert J, Miltner WH, Bauder H, Sommer M, Dettmers C, Taub E, Weiller C (1998), Motor cortex plasticity during constraint-induced movement therapy in stroke patients. Neurosci Lett 250:5-8.

Lin Q, Peng YB, Willis WD (1996), Inhibition of primate spinothalamic tract neurons by spinal glycine and GABA is reduced during central sensitization. J Neurophysiol 76:1005-1014.

Liu, Sandkuhler J (1995), Long-term potentiation of C-fiber-evoked potentials in the rat spinal dorsal horn is prevented by spinal N-methyl-D-aspartic acid receptor blockage. Neurosci Lett 191:43-46.

Liu, Sandkuhler J (1997), Characterization of long-term potentiation of C-fiber-evoked potentials in spinal dorsal horn of adult rat: essential role of NK1 and NK2 receptors. J Neurophysiol 78:1973-1982.

Lix LM, Keselman JC, Keselman HJ (1996), Consequences of assumption violations revisited: a quantitative review of alternatives to the one-way analysis of variance F test. Rev Educ Res 66:579-619.

Lockwood PL, Iannetti GD, Haggard P (2013), Transcranial magnetic stimulation over human secondary somatosensory cortex disrupts perception of pain intensity. Cortex 49:2201-2209.

Loggia ML, Edwards RR, Kim J, Vangel MG, Wasan AD, Gollub RL, Harris RE, Park K, et al. (2012), Disentangling linear and nonlinear brain responses to evoked deep tissue pain. Pain 153:2140-2151.

Loggia ML, Kim J, Gollub RL, Vangel MG, Kirsch I, Kong J, Wasan AD, Napadow V (2013), Default mode network connectivity encodes clinical pain: an arterial spin labeling study. Pain 154:24-33.

Lowe MJ, Mock BJ, Sorenson JA (1998), Functional connectivity in single and multislice echoplanar imaging using resting-state fluctuations. NeuroImage 7:119-132.

Lu M, Ueno S (2017), Comparison of the induced fields using different coil configurations during deep transcranial magnetic stimulation. PLoS One 12:e0178422.

Lund JP, Donga R, Widmer CG, Stohler CS (1991), The pain-adaptation model: a discussion of the relationship between chronic musculoskeletal pain and motor activity. Can J Physiol Pharmacol 69:683-694.

Lundberg A (1979), Multisensory control of spinal reflex pathways. Prog Brain Res 50:11-28.

Lundberg A, Voorhoeve P (1962), Effects from the pyramidal tract on spinal reflex arcs. Acta Physiol Scand 56:201-219.

Lynn B, Schutterle S, Pierau FK (1996), The vasodilator component of neurogenic inflammation is caused by a special subclass of heat-sensitive nociceptors in the skin of the pig. J Physiol 494 (Pt 2):587-593.

Macefield (2009), Long Loop Reflexes. Encyclopedia of Neuroscience Springer, Berlin, Heidelberg In: Binder M.D., Hirokawa N., Windhorst U. (eds).

Macefield, Gandevia SC, Henderson LA (2007), Discrete changes in cortical activation during experimentally induced referred muscle pain: a single-trial fMRI study. Cereb Cortex 17:2050-2059.

Mackenzie RA, Burke D, Skuse NF, Lethlean AK (1975), Fibre function and perception during cutaneous nerve block. J Neurol Neurosurg Psychiatry 38:865-873.

Madeleine P, Leclerc F, Arendt-Nielsen L, Ravier P, Farina D (2006), Experimental muscle pain changes the spatial distribution of upper trapezius muscle activity during sustained contraction. Clin Neurophysiol 117:2436-2445.

Maeda L, Ono M, Koyama T, Oshiro Y, Sumitani M, Mashimo T, Shibata M (2011), Human brain activity associated with painful mechanical stimulation to muscle and bone. J Anesth 25:523-530.

Magerl W, Fuchs PN, Meyer RA, Treede RD (2001), Roles of capsaicin-insensitive nociceptors in cutaneous pain and secondary hyperalgesia. Brain 124:1754-1764.

Maihofner C, Handwerker HO (2005), Differential coding of hyperalgesia in the human brain: a functional MRI study. NeuroImage 28:996-1006.

Maihofner C, Kaltenhauser M, Neundorfer B, Lang E (2002), Temporo-spatial analysis of cortical activation by phasic innocuous and noxious cold stimuli--a magnetoencephalographic study. Pain 100:281-290.

Mainero C, Boshyan J, Hadjikhani N (2011), Altered functional magnetic resonance imaging resting-state connectivity in periaqueductal gray networks in migraine. Ann Neurol 70:838-845.

Malcolm MP, Triggs WJ, Light KE, Shechtman O, Khandekar G, Gonzalez Rothi LJ (2006), Reliability of motor cortex transcranial magnetic stimulation in four muscle representations. Clin Neurophysiol 117:1037-1046.

Manganotti P, Zanette G, Bonato C, Tinazzi M, Polo A, Fiaschi A (1997), Crossed and direct effects of digital nerves stimulation on motor evoked potential: a study with magnetic brain stimulation. Electroencephalogr Clin Neurophysiol 105:280-289.

Mano H, Yoshida W, Shibata K, Zhang S, Koltzenburg M, Kawato M, Seymour B (2017), Thermosensory Perceptual Learning Is Associated with Structural Brain Changes in Parietal-Opercular (SII) Cortex. J Neurosci 37:9380-9388.

Mansour ZM, Lepping RJ, Honea RA, Brooks WM, Yeh HW, Burns JM, Sharma NK (2017), Structural Brain Imaging in People With Low Back Pain. Spine (Phila Pa 1976) 42:726-732.

Mantyh PW, Rogers SD, Honore P, Allen BJ, Ghilardi JR, Li J, Daughters RS, Lappi DA, et al. (1997), Inhibition of hyperalgesia by ablation of lamina I spinal neurons expressing the substance P receptor. Science 278:275-279.

Mao CP, Yang HJ (2015), Smaller Amygdala Volumes in Patients With Chronic Low Back Pain Compared With Healthy Control Individuals. J Pain 16:1366-1376.

Maris E, Oostenveld R (2007), Nonparametric statistical testing of EEG- and MEG-data. J Neurosci Methods 164:177-190.

Martel M, Harvey MP, Houde F, Balg F, Goffaux P, Leonard G (2017), Unravelling the effect of experimental pain on the corticomotor system using transcranial magnetic stimulation and electroencephalography. Exp Brain Res 235:1223-1231.

Martin PG, Smith JL, Butler JE, Gandevia SC, Taylor JL (2006), Fatigue-sensitive afferents inhibit extensor but not flexor motoneurons in humans. J Neurosci 26:4796-4802.

Martin PG, Weerakkody N, Gandevia SC, Taylor JL (2008), Group III and IV muscle afferents differentially affect the motor cortex and motoneurones in humans. J Physiol 586:1277-1289.

Masse-Alarie H, Beaulieu LD, Preuss R, Schneider C (2016), Corticomotor control of lumbar multifidus muscles is impaired in chronic low back pain: concurrent evidence from ultrasound imaging and double-pulse transcranial magnetic stimulation. Exp Brain Res 234:1033-1045.

Masse-Alarie H, Bergin MJG, Schneider C, Schabrun S, Hodges PW (2017), "Discrete peaks" of excitability and map overlap reveal task-specific organization of primary motor cortex for control of human forearm muscles. Hum Brain Mapp 38:6118-6132.

Massimini M, Ferrarelli F, Huber R, Esser SK, Singh H, Tononi G (2005), Breakdown of cortical effective connectivity during sleep. Science 309:2228-2232.

Matre DA, Sinkjaer T, Knardahl S, Andersen JB, Arendt-Nielsen L (1999), The influence of experimental muscle pain on the human soleus stretch reflex during sitting and walking. Clin Neurophysiol 110:2033-2043.

Matre DA, Sinkjaer T, Svensson P, Arendt-Nielsen L (1998), Experimental muscle pain increases the human stretch reflex. Pain 75:331-339.

Matsumoto H, Hanajima R, Hamada M, Terao Y, Yugeta A, Inomata-Terada S, Nakatani-Enomoto S, Tsuji S, et al. (2008), Double-pulse magnetic brain stem stimulation: mimicking successive descending volleys. J Neurophysiol 100:3437-3444.

Mavromatis N, Neige C, Gagne M, Reilly KT, Mercier C (2017), Effect of Experimental Hand Pain on Training-Induced Changes in Motor Performance and Corticospinal Excitability. Brain sciences 7.

May A (2008), Chronic pain may change the structure of the brain. Pain 137:7-15.

May A (2011), Structural brain imaging: a window into chronic pain. Neuroscientist 17:209-220.

May A, Rodriguez-Raecke R, Schulte A, Ihle K, Breimhorst M, Birklein F, Jurgens TP (2012), Within-session sensitization and between-session habituation: a robust physiological response to repetitive painful heat stimulation. Eur J Pain 16:401-409.

Mayberg HS, Liotti M, Brannan SK, McGinnis S, Mahurin RK, Jerabek PA, Silva JA, Tekell JL, et al. (1999), Reciprocal limbic-cortical function and negative mood: converging PET findings in depression and normal sadness. Am J Psychiatry 156:675-682.

Mazzocchio R, Rothwell JC, Day BL, Thompson PD (1994), Effect of tonic voluntary activity on the excitability of human motor cortex. J Physiol 474:261-267.

Mazzocchio R, Rothwell JC, Rossi A (1995), Distribution of Ia effects onto human hand muscle motoneurones as revealed using an H reflex technique. J Physiol 489 (Pt 1):263-273.

Mazzola L, Faillenot I, Barral FG, Mauguiere F, Peyron R (2012), Spatial segregation of somato-sensory and pain activations in the human operculo-insular cortex. NeuroImage 60:409-418.

Mazzola L, Isnard J, Mauguiere F (2006), Somatosensory and pain responses to stimulation of the second somatosensory area (SII) in humans. A comparison with SI and insular responses. Cereb Cortex 16:960-968.

Mazzola L, Isnard J, Peyron R, Guenot M, Mauguiere F (2009), Somatotopic organization of pain responses to direct electrical stimulation of the human insular cortex. Pain 146:99-104.

Mazzola L, Isnard J, Peyron R, Mauguiere F (2012), Stimulation of the human cortex and the experience of pain: Wilder Penfield's observations revisited. Brain 135:631-640.

McAllister SM, Rothwell JC, Ridding MC (2009), Selective modulation of intracortical inhibition by low-intensity Theta Burst Stimulation. Clin Neurophysiol 120:820-826.

McLellan DL (1973), The electromyographic silent period produced by supramaximal electrical stimulation in normal man. J Neurol Neurosurg Psychiatry 36:334-341.

Megirian D (1962), Bilateral facilitatory and inhibitory skin areas of spinal motoneurones of cat. J Neurophysiol 25:127-137.

Meinck HM, Kuster S, Benecke R, Conrad B (1985), The flexor reflex--influence of stimulus parameters on the reflex response. Electroencephalogr Clin Neurophysiol 61:287-298.

Meinck HM, Piesiur-Strehlow B, Koehler W (1981), Some principles of flexor reflex generation in human leg muscles. Electroencephalogr Clin Neurophysiol 52:140-150.

Meister IG, Boroojerdi B, Foltys H, Sparing R, Huber W, Topper R (2003), Motor cortex hand area and speech: implications for the development of language. Neuropsychologia 41:401-406.

Mercier C, Gagne M, Reilly KT, Bouyer LJ (2016), Effect of Experimental Cutaneous Hand Pain on Corticospinal Excitability and Short Afferent Inhibition. Brain sciences 6.

Merton PA (1951), The silent period in a muscle of the human hand. J Physiol 114:183-198.

Metman LV, Bellevich JS, Jones SM, Barber MD, Streletz LJ (1993), Topographic mapping of human motor cortex with transcranial magnetic stimulation: Homunculus revisited. Brain Topogr 6:13-19.

Meyer, Campbell JN (1981), Myelinated nociceptive afferents account for the hyperalgesia that follows a burn to the hand. Science 213:1527-1529.

Meyer, Roricht S, Grafin von Einsiedel H, Kruggel F, Weindl A (1995), Inhibitory and excitatory interhemispheric transfers between motor cortical areas in normal humans and patients with abnormalities of the corpus callosum. Brain 118 (Pt 2):429-440.

Meyer, Roricht S, Woiciechowsky C (1998), Topography of fibers in the human corpus callosum mediating interhemispheric inhibition between the motor cortices. Ann Neurol 43:360-369.

Mhalla A, de Andrade DC, Baudic S, Perrot S, Bouhassira D (2010), Alteration of cortical excitability in patients with fibromyalgia. Pain 149:495-500.

Mills KR, Boniface SJ, Schubert M (1992), Magnetic brain stimulation with a double coil: the importance of coil orientation. Electroencephalogr Clin Neurophysiol 85:17-21.

Miranda PC, de Carvalho M, Conceicao I, Luis ML, Ducla-Soares E (1997), A new method for reproducible coil positioning in transcranial magnetic stimulation mapping. Electroencephalogr Clin Neurophysiol 105:116-123.

Misra G, Ofori E, Chung JW, Coombes SA (2017), Pain-Related Suppression of Beta Oscillations Facilitates Voluntary Movement. Cereb Cortex 27:2592-2606.

Moayedi M (2014), All roads lead to the insula. Pain 155:1920-1921.

Moayedi M, Liang M, Sim AL, Hu L, Haggard P, Iannetti GD (2015), Laser-Evoked Vertex Potentials Predict Defensive Motor Actions. Cereb Cortex 25:4789-4798.

Mochizuki H, Huang YZ, Rothwell JC (2004), Interhemispheric interaction between human dorsal premotor and contralateral primary motor cortex. J Physiol 561:331-338.

Modirrousta M, Meek BP, Sareen J, Enns MW (2015), Impaired trial-by-trial adjustment of cognitive control in obsessive compulsive disorder improves after deep repetitive transcranial magnetic stimulation. BMC Neurosci 16:63.

Mohlberg H, Eickhoff S, Schleicher A, Zilles K, Amunts K (2012), A new processing pipeline and release of cytoarchitectonic probabilistic maps – JuBrain. 18th Annual Meeting of the Organization for Human Brain Mapping. OHBM 18, Beijing, China, 10 Jun 2012 https://wwwjubrainfz-juelichde.

Moiniche S, Dahl JB, Kehlet H (1993), Time course of primary and secondary hyperalgesia after heat injury to the skin. Br J Anaesth 71:201-205.

Moisa M, Pohmann R, Ewald L, Thielscher A (2009), New coil positioning method for interleaved transcranial magnetic stimulation (TMS)/functional MRI (fMRI) and its validation in a motor cortex study. J Magn Reson Imaging 29:189-197.

Moisa M, Siebner HR, Pohmann R, Thielscher A (2012), Uncovering a context-specific connectional fingerprint of human dorsal premotor cortex. J Neurosci 32:7244-7252.

Moisset X, de Andrade DC, Bouhassira D (2016), From pulses to pain relief: an update on the mechanisms of rTMS-induced analgesic effects. Eur J Pain 20:689-700.

Morch CD, Andersen OK, Graven-Nielsen T, Arendt-Nielsen L (2007), Nociceptive withdrawal reflexes evoked by uniform-temperature laser heat stimulation of large skin areas in humans. J Neurosci Methods 160:85-92.

Mortifee P, Stewart H, Schulzer M, Eisen A (1994), Reliability of transcranial magnetic stimulation for mapping the human motor cortex. Electroencephalogr Clin Neurophysiol 93:131-137.

Motogi J, Sugiyama Y, Laakso I, Hirata A, Inui K, Tamura M, Muragaki Y (2016), Why intra-epidermal electrical stimulation achieves stimulation of small fibres selectively: a simulation study. Phys Med Biol 61:4479-4490.

Mouraux A, De Paepe AL, Marot E, Plaghki L, Iannetti GD, Legrain V (2013), Unmasking the obligatory components of nociceptive event-related brain potentials. J Neurophysiol 110:2312-2324.

Mouraux A, Diukova A, Lee MC, Wise RG, Iannetti GD (2011), A multisensory investigation of the functional significance of the "pain matrix". NeuroImage 54:2237-2249.

Mouraux A, Guerit JM, Plaghki L (2003), Non-phase locked electroencephalogram (EEG) responses to CO2 laser skin stimulations may reflect central interactions

between A partial partial differential- and C-fibre afferent volleys. Clin Neurophysiol 114:710-722.

Mouraux A, Iannetti GD, Plaghki L (2010), Low intensity intra-epidermal electrical stimulation can activate Adelta-nociceptors selectively. Pain 150:199-207.

Mouraux A, Marot E, Legrain V (2014), Short trains of intra-epidermal electrical stimulation to elicit reliable behavioral and electrophysiological responses to the selective activation of nociceptors in humans. Neurosci Lett 561:69-73.

Munger BL, Halata Z (1983), The sensory innervation of primate facial skin. I. Hairy skin. Brain Res 286:45-80.

Murase N, Duque J, Mazzocchio R, Cohen LG (2004), Influence of interhemispheric interactions on motor function in chronic stroke. Ann Neurol 55:400-409.

Mylius V, Borckardt JJ, Lefaucheur JP (2012), Noninvasive cortical modulation of experimental pain. Pain 153:1350-1363.

Nagasako EM, Oaklander AL, Dworkin RH (2003), Congenital insensitivity to pain: an update. Pain 101:213-219.

Nahas Z, Lomarev M, Roberts DR, Shastri A, Lorberbaum JP, Teneback C, McConnell K, Vincent DJ, et al. (2001), Unilateral left prefrontal transcranial magnetic stimulation (TMS) produces intensity-dependent bilateral effects as measured by interleaved BOLD fMRI. Biol Psychiatry 50:712-720.

Nahmias F, Debes C, de Andrade DC, Mhalla A, Bouhassira D (2009), Diffuse analgesic effects of unilateral repetitive transcranial magnetic stimulation (rTMS) in healthy volunteers. Pain 147:224-232.

Nahra H, Plaghki L (2003), The effects of A-fiber pressure block on perception and neurophysiological correlates of brief non-painful and painful CO2 laser stimuli in humans. Eur J Pain 7:189-199.

Najib U, Bashir S, Edwards D, Rotenberg A, Pascual-Leone A (2011), Transcranial brain stimulation: clinical applications and future directions. Neurosurg Clin N Am 22:233-251, ix.

Nakamura Y, Paur R, Zimmermann R, Bromm B (2002), Attentional modulation of human pain processing in the secondary somatosensory cortex: a magnetoencephalographic study. Neurosci Lett 328:29-32.

Namer B, Barta B, Orstavik K, Schmidt R, Carr R, Schmelz M, Handwerker HO (2009), Microneurographic assessment of C-fibre function in aged healthy subjects. J Physiol 587:419-428.

Nash PG, Macefield VG, Klineberg IJ, Gustin SM, Murray GM, Henderson LA (2010), Changes in human primary motor cortex activity during acute cutaneous and muscle orofacial pain. J Orofac Pain 24:379-390.

Nathan PW, Smith MC, Cook AW (1986), Sensory effects in man of lesions of the posterior columns and of some other afferent pathways. Brain 109 (Pt 5):1003-1041.

Nauczyciel C, Le Jeune F, Naudet F, Douabin S, Esquevin A, Verin M, Dondaine T, Robert G, et al. (2014), Repetitive transcranial magnetic stimulation over the orbitofrontal cortex for obsessive-compulsive disorder: a double-blind, crossover study. Translational psychiatry 4:e436.

Navarro de Lara LI, Windischberger C, Kuehne A, Woletz M, Sieg J, Bestmann S, Weiskopf N, Strasser B, et al. (2015), A novel coil array for combined TMS/fMRI experiments at 3 T. Magn Reson Med 74:1492-1501.

Neef NE, Hoang TN, Neef A, Paulus W, Sommer M (2015), Speech dynamics are coded in the left motor cortex in fluent speakers but not in adults who stutter. Brain 138:712-725.

Neziri AY, Andersen OK, Petersen-Felix S, Radanov B, Dickenson AH, Scaramozzino P, Arendt-Nielsen L, Curatolo M (2010), The nociceptive withdrawal reflex: normative values of thresholds and reflex receptive fields. Eur J Pain 14:134-141.

Ni Z, Gunraj C, Nelson AJ, Yeh IJ, Castillo G, Hoque T, Chen R (2009), Two phases of interhemispheric inhibition between motor related cortical areas and the primary motor cortex in human. Cereb Cortex 19:1654-1665.

Nicholls ME, Thomas NA, Loetscher T, Grimshaw GM (2013), The Flinders Handedness survey (FLANDERS): a brief measure of skilled hand preference. Cortex 49:2914-2926.

Nichols ML, Allen BJ, Rogers SD, Ghilardi JR, Honore P, Luger NM, Finke MP, Li J, et al. (1999), Transmission of chronic nociception by spinal neurons expressing the substance P receptor. Science 286:1558-1561.

Nickel MM, Ta Dinh S, May ES, Tiemann L, Hohn VD, Gross J, Ploner M (2020), Neural oscillations and connectivity characterizing the state of tonic experimental pain in humans. Hum Brain Mapp 41:17-29.

Niddam DM, Yeh TC, Wu YT, Lee PL, Ho LT, Arendt-Nielsen L, Chen AC, Hsieh JC (2002), Event-related functional MRI study on central representation of acute muscle pain induced by electrical stimulation. NeuroImage 17:1437-1450.

Niehaus L, Meyer BU, Weyh T (2000), Influence of pulse configuration and direction of coil current on excitatory effects of magnetic motor cortex and nerve stimulation. Clin Neurophysiol 111:75-80.

Nielsen J, Petersen N (1994), Is presynaptic inhibition distributed to corticospinal fibres in man? J Physiol 477:47-58.

Nielsen J, Petersen N, Fedirchuk B (1997), Evidence suggesting a transcortical pathway from cutaneous foot afferents to tibialis anterior motoneurones in man. J Physiol 501 (Pt 2):473-484.

Nieuwenhuys R (2012), The insular cortex: a review. Prog Brain Res 195:123-163.

Noda Y, Cash RF, Zomorrodi R, Dominguez LG, Farzan F, Rajji TK, Barr MS, Chen R, et al. (2016), A combined TMS-EEG study of short-latency afferent inhibition in the motor and dorsolateral prefrontal cortex. J Neurophysiol 116:938-948.

Nolano M, Simone DA, Wendelschafer-Crabb G, Johnson T, Hazen E, Kennedy WR (1999), Topical capsaicin in humans: parallel loss of epidermal nerve fibers and pain sensation. Pain 81:135-145.

Northoff G, Richter A, Gessner M, Schlagenhauf F, Fell J, Baumgart F, Kaulisch T, Kotter R, et al. (2000), Functional dissociation between medial and lateral prefrontal cortical spatiotemporal activation in negative and positive emotions: a combined fMRI/MEG study. Cereb Cortex 10:93-107.

Novikov PA, Nazarova MA, Nikulin VV (2018), TMSmap - Software for Quantitative Analysis of TMS Mapping Results. Front Hum Neurosci 12:239.

Novotny GE, Gommert-Novotny E (1988), Intraepidermal nerves in human digital skin. Cell Tissue Res 254:111-117.

O'Connell NE, Wand BM, Marston L, Spencer S, Desouza LH (2011), Non-invasive brain stimulation techniques for chronic pain. A report of a Cochrane systematic review and meta-analysis. Eur J Phys Rehabil Med 47:309-326.

O'Connell NE, Wand BM, Marston L, Spencer S, Desouza LH (2014), Non-invasive brain stimulation techniques for chronic pain. The Cochrane database of systematic reviews:CD008208.

Oberman, Edwards D, Eldaief M, Pascual-Leone A (2011), Safety of theta burst transcranial magnetic stimulation: a systematic review of the literature. J Clin Neurophysiol 28:67-74.

Oberman, Pascual-Leone A (2009), Report of seizure induced by continuous theta burst stimulation. Brain stimulation 2:246-247.

Ochoa J, Torebjork E (1983), Sensations evoked by intraneural microstimulation of single mechanoreceptor units innervating the human hand. J Physiol 342:633-654.

Ohsawa I, Inui K (2009), Use of tripolar electrodes for minimization of current spread in uncut peripheral nerve stimulation. Neurosci Res 64:63-66.

On AY, Uludag B, Taskiran E, Ertekin C (2004), Differential corticomotor control of a muscle adjacent to a painful joint. Neurorehabil Neural Repair 18:127-133.

Onesti E, Gabriele M, Cambieri C, Ceccanti M, Raccah R, Di Stefano G, Biasiotta A, Truini A, et al. (2013), H-coil repetitive transcranial magnetic stimulation for pain relief in patients with diabetic neuropathy. Eur J Pain 17:1347-1356.

Opitz A, Legon W, Rowlands A, Bickel WK, Paulus W, Tyler WJ (2013), Physiological observations validate finite element models for estimating subject-specific electric field distributions induced by transcranial magnetic stimulation of the human motor cortex. NeuroImage 81:253-264.

Ortu E, Deriu F, Suppa A, Tolu E, Rothwell JC (2008), Effects of volitional contraction on intracortical inhibition and facilitation in the human motor cortex. J Physiol 586:5147-5159.

Ostrowsky K, Magnin M, Ryvlin P, Isnard J, Guenot M, Mauguiere F (2002), Representation of pain and somatic sensation in the human insula: a study of responses to direct electrical cortical stimulation. Cereb Cortex 12:376-385.

Owen DG, Clarke CF, Bureau Y, Ganapathy S, Prato FS, St Lawrence KS (2012), Measuring the neural response to continuous intramuscular infusion of hypertonic saline by perfusion MRI. J Magn Reson Imaging 35:669-677.

Owen DG, Clarke CF, Ganapathy S, Prato FS, St Lawrence KS (2010), Using perfusion MRI to measure the dynamic changes in neural activation associated with tonic muscular pain. Pain 148:375-386.

Padel Y, Relova JL (1991), Somatosensory responses in the cat motor cortex. I. Identification and course of an afferent pathway. J Neurophysiol 66:2041-2058.

Parker RS, Lewis GN, Rice DA, McNair PJ (2016), Is Motor Cortical Excitability Altered in People with Chronic Pain? A Systematic Review and Meta-Analysis. Brain stimulation 9:488-500.

Pascual-Leone A, Grafman J, Hallett M (1994), Modulation of cortical motor output maps during development of implicit and explicit knowledge. Science 263:1287-1289.

Pascual-Leone A, Nguyet D, Cohen LG, Brasil-Neto JP, Cammarota A, Hallett M (1995), Modulation of muscle responses evoked by transcranial magnetic stimulation during the acquisition of new fine motor skills. J Neurophysiol 74:1037-1045.

Pascual-Leone A, Rubio B, Pallardo F, Catala MD (1996), Rapid-rate transcranial magnetic stimulation of left dorsolateral prefrontal cortex in drug-resistant depression. Lancet 348:233-237.

Pascual-Leone A, Wassermann EM, Sadato N, Hallett M (1995), The role of reading activity on the modulation of motor cortical outputs to the reading hand in Braille readers. Ann Neurol 38:910-915.

Pattany PM, Yezierski RP, Widerstrom-Noga EG, Bowen BC, Martinez-Arizala A, Garcia BR, Quencer RM (2002), Proton magnetic resonance spectroscopy of the thalamus in patients with chronic neuropathic pain after spinal cord injury. AJNR Am J Neuroradiol 23:901-905.

Patton HD, Amassian VE (1954), Single and multiple-unit analysis of cortical stage of pyramidal tract activation. J Neurophysiol 17:345-363.

Pauli WM, O'Reilly RC, Yarkoni T, Wager TD (2016), Regional specialization within the human striatum for diverse psychological functions. Proc Natl Acad Sci U S A 113:1907-1912.

Paus T (2005), Inferring causality in brain images: a perturbation approach. Philos Trans R Soc Lond B Biol Sci 360:1109-1114.

Paus T (2008), Combining brain imaging with brain stimulation: causality and connectivity. The Oxford Handbook of Transcranial Stimulation:539-547.

Paus T, Jech R, Thompson CJ, Comeau R, Peters T, Evans AC (1997), Transcranial magnetic stimulation during positron emission tomography: a new method for studying connectivity of the human cerebral cortex. J Neurosci 17:3178-3184.

Pedersen JL, Kehlet H (1998), Secondary hyperalgesia to heat stimuli after burn injury in man. Pain 76:377-384.

Pellegrini M, Zoghi M, Jaberzadeh S (2018), The effect of transcranial magnetic stimulation test intensity on the amplitude, variability and reliability of motor evoked potentials. Brain Res 1700:190-198.

Pellicciari MC, Miniussi C, Ferrari C, Koch G, Bortoletto M (2016), Ongoing cumulative effects of single TMS pulses on corticospinal excitability: An intra- and inter-block investigation. Clin Neurophysiol 127:621-628.

Peng W, Hu L, Zhang Z, Hu Y (2014), Changes of spontaneous oscillatory activity to tonic heat pain. PLoS One 9:e91052.

Perchet C, Frot M, Charmarty A, Flores C, Mazza S, Magnin M, Garcia-Larrea L (2012), Do we activate specifically somatosensory thin fibres with the concentric planar electrode? A scalp and intracranial EEG study. Pain 153:1244-1252.

Pereon Y, Guiheneuc P (1995), Late facilitations of motor evoked potentials by contralateral mixed nerve stimulation. Electroencephalogr Clin Neurophysiol 97:126-130.

Peterchev AV (2014), Reduction of TMS strength near MRI scanner could be explained by electromagnetic coupling to MRI magnet. Brain stimulation 7:916-917.

Peters JC, Reithler J, Schuhmann T, de Graaf T, Uludag K, Goebel R, Sack AT (2013), On the feasibility of concurrent human TMS-EEG-fMRI measurements. J Neurophysiol 109:1214-1227.

Petersen NT, Taylor JL, Gandevia SC (2002), The effect of electrical stimulation of the corticospinal tract on motor units of the human biceps brachii. J Physiol 544:277-284.

Peterson CL, Riley ZA, Krepkovich ET, Murray WM, Perreault EJ (2014), Withdrawal reflexes in the upper limb adapt to arm posture and stimulus location. Muscle Nerve 49:716-723.

Petrides M (2005), Lateral prefrontal cortex: architectonic and functional organization. Philos Trans R Soc Lond B Biol Sci 360:781-795.

Pettorossi VE, Della Torre G, Bortolami R, Brunetti O (1999), The role of capsaicin-sensitive muscle afferents in fatigue-induced modulation of the monosynaptic reflex in the rat. J Physiol 515 (Pt 2):599-607.

Peyron R, Frot M, Schneider F, Garcia-Larrea L, Mertens P, Barral FG, Sindou M, Laurent B, et al. (2002), Role of operculoinsular cortices in human pain processing: converging evidence from PET, fMRI, dipole modeling, and intracerebral recordings of evoked potentials. NeuroImage 17:1336-1346.

Peyron R, Laurent B, Garcia-Larrea L (2000), Functional imaging of brain responses to pain. A review and meta-analysis (2000). Neurophysiol Clin 30:263-288.

Pfau DB, Klein T, Putzer D, Pogatzki-Zahn EM, Treede RD, Magerl W (2011), Analysis of hyperalgesia time courses in humans after painful electrical high-frequency stimulation identifies a possible transition from early to late LTP-like pain plasticity. Pain 152:1532-1539.

Philiastides MG, Auksztulewicz R, Heekeren HR, Blankenburg F (2011), Causal role of dorsolateral prefrontal cortex in human perceptual decision making. Curr Biol 21:980-983.

Pinto AD, Chen R (2001), Suppression of the motor cortex by magnetic stimulation of the cerebellum. Exp Brain Res 140:505-510.

Plaghki, Bragard D, Le Bars D, Willer JC, Godfraind JM (1998), Facilitation of a nociceptive flexion reflex in man by nonnoxious radiant heat produced by a laser. J Neurophysiol 79:2557-2567.

Plaghki, Mouraux A (2002), Brain responses to signals ascending through C-fibers. Int Congress Series 1232:181-192.

Plaghki, Mouraux A (2003), How do we selectively activate skin nociceptors with a high power infrared laser? Physiology and biophysics of laser stimulation. Neurophysiol Clin 33:269-277.

Plaghki L, Delisle D, Godfraind JM (1994), Heterotopic nociceptive conditioning stimuli and mental task modulate differently the perception and physiological correlates of short CO2 laser stimuli. Pain 57:181-192.

Ploner M, Gross J, Timmermann L, Pollok B, Schnitzler A (2006), Pain suppresses spontaneous brain rhythms. Cereb Cortex 16:537-540.

Poreisz C, Antal A, Boros K, Brepohl N, Csifcsak G, Paulus W (2008), Attenuation of N2 amplitude of laser-evoked potentials by theta burst stimulation of primary somatosensory cortex. Exp Brain Res 185:611-621.

Poreisz C, Csifcsak G, Antal A, Levold M, Hillers F, Paulus W (2008), Theta burst stimulation of the motor cortex reduces laser-evoked pain perception. Neuroreport 19:193-196.

Raffin E, Pellegrino G, Di Lazzaro V, Thielscher A, Siebner HR (2015), Bringing transcranial mapping into shape: Sulcus-aligned mapping captures motor somatotopy in human primary motor hand area. NeuroImage 120:164-175.

Raichle ME (2015), The brain's default mode network. Annu Rev Neurosci 38:433-447.

Raichle ME, MacLeod AM, Snyder AZ, Powers WJ, Gusnard DA, Shulman GL (2001), A default mode of brain function. Proc Natl Acad Sci U S A 98:676-682.

Raij TT, Forss N, Stancak A, Hari R (2004), Modulation of motor-cortex oscillatory activity by painful Adelta- and C-fiber stimuli. NeuroImage 23:569-573.

Raij TT, Vartiainen NV, Jousmaki V, Hari R (2003), Effects of interstimulus interval on cortical responses to painful laser stimulation. J Clin Neurophysiol 20:73-79.

Raja SN, Campbell JN, Meyer RA (1984), Evidence for different mechanisms of primary and secondary hyperalgesia following heat injury to the glabrous skin. Brain 107 (Pt 4):1179-1188.

Raja SN, Carr DB, Cohen M, Finnerup NB, Flor H, Gibson S, Keefe FJ, Mogil JS, et al. (2020), The revised International Association for the Study of Pain definition of pain: concepts, challenges, and compromises. Pain 161:1976-1982.

Rall W, Burke RE, Smith TG, Nelson PG, Frank K (1967), Dendritic location of synapses and possible mechanisms for the monosynaptic EPSP in motoneurons. J Neurophysiol 30:1169-1193.

Randic M, Jiang MC, Cerne R (1993), Long-term potentiation and long-term depression of primary afferent neurotransmission in the rat spinal cord. J Neurosci 13:5228-5241.

Reeh PW, Bayer J, Kocher L, Handwerker HO (1987), Sensitization of nociceptive cutaneous nerve fibers from the rat's tail by noxious mechanical stimulation. Exp Brain Res 65:505-512.

Reinert A, Kaske A, Mense S (1998), Inflammation-induced increase in the density of neuropeptide-immunoreactive nerve endings in rat skeletal muscle. Exp Brain Res 121:174-180.

Rhudy JL, France CR (2007), Defining the nociceptive flexion reflex (NFR) threshold in human participants: a comparison of different scoring criteria. Pain 128:244-253.

Ricci R, Salatino A, Li X, Funk AP, Logan SL, Mu Q, Johnson KA, Bohning DE, et al. (2012), Imaging the neural mechanisms of TMS neglect-like bias in healthy volunteers with the interleaved TMS/fMRI technique: preliminary evidence. Front Hum Neurosci 6:326.

Ridding MC, Rothwell JC (1997), Stimulus/response curves as a method of measuring motor cortical excitability in man. Electroencephalogr Clin Neurophysiol 105:340-344.

Ridding MC, Taylor JL, Rothwell JC (1995), The effect of voluntary contraction on cortico-cortical inhibition in human motor cortex. J Physiol 487 (Pt 2):541-548.

Ringkamp M, Peng YB, Wu G, Hartke TV, Campbell JN, Meyer RA (2001), Capsaicin responses in heat-sensitive and heat-insensitive A-fiber nociceptors. J Neurosci 21:4460-4468.

Rittig-Rasmussen B, Kasch H, Fuglsang-Frederiksen A, Svensson P, Jensen TS (2014), The role of neuroplasticity in experimental neck pain: a study of potential mechanisms impeding clinical outcomes of training. Man Ther 19:288-293.

Ro JY, Capra NF (2001), Modulation of jaw muscle spindle afferent activity following intramuscular injections with hypertonic saline. Pain 92:117-127.

Roby-Brami A, Bussel B (1987), Long-latency spinal reflex in man after flexor reflex afferent stimulation. Brain 110 (Pt 3):707-725.

Roland MO (1986), A critical review of the evidence for a pain-spasm-pain cycle in spinal disorders. Clin Biomech (Bristol, Avon) 1:102-109.

Rollnik JD, Wustefeld S, Dauper J, Karst M, Fink M, Kossev A, Dengler R (2002), Repetitive transcranial magnetic stimulation for the treatment of chronic pain - a pilot study. Eur Neurol 48:6-10.

Romaniello A, Cruccu G, McMillan AS, Arendt-Nielsen L, Svensson P (2000), Effect of experimental pain from trigeminal muscle and skin on motor cortex excitability in humans. Brain Res 882:120-127.

Romaniello A, Truini A, Galeotti F, De Lena C, Willer JC, Cruccu G (2004), Cutaneous silent period in hand muscle is evoked by laser stimulation of the palm, but not the hand dorsum. Muscle Nerve 29:870-872.

Rossi, Decchi B (1995), Cutaneous nociceptive facilitation of Ib heteronymous pathways to lower limb motoneurones in humans. Brain Res 700:164-172.

Rossi, Decchi B (1997), Changes in Ib heteronymous inhibition to soleus motoneurones during cutaneous and muscle nociceptive stimulation in humans. Brain Res 774:55-61.

Rossi, Decchi B, Ginanneschi F (1999), Presynaptic excitability changes of group Ia fibres to muscle nociceptive stimulation in humans. Brain Res 818:12-22.

Rossi, Hallett M, Rossini PM, Pascual-Leone A, Safety of TMSCG (2009), Safety, ethical considerations, and application guidelines for the use of transcranial magnetic stimulation in clinical practice and research. Clin Neurophysiol 120:2008-2039.

Rossi, Mazzocchio R, Decchi B (2003), Effect of chemically activated fine muscle afferents on spinal recurrent inhibition in humans. Clin Neurophysiol 114:279-287.

Rossini PM, Barker AT, Berardelli A, Caramia MD, Caruso G, Cracco RQ, Dimitrijevic MR, Hallett M, et al. (1994), Non-invasive electrical and magnetic stimulation of the brain, spinal cord and roots: basic principles and procedures for routine clinical application. Report of an IFCN committee. Electroencephalogr Clin Neurophysiol 91:79-92.

Rossini PM, Burke D, Chen R, Cohen LG, Daskalakis Z, Di Iorio R, Di Lazzaro V, Ferreri F, et al. (2015), Non-invasive electrical and magnetic stimulation of the brain, spinal cord, roots and peripheral nerves: Basic principles and procedures for routine clinical and research application. An updated report from an I.F.C.N. Committee. Clin Neurophysiol 126:1071-1107.

Rossini PM, Caramia MD, Zarola F (1987), Mechanisms of nervous propagation along central motor pathways: noninvasive evaluation in healthy subjects and in patients with neurological disease. Neurosurgery 20:183-191.

Rothman KJ (1990), No adjustments are needed for multiple comparisons. Epidemiology 1:43-46.

Ruff CC, Bestmann S, Blankenburg F, Bjoertomt O, Josephs O, Weiskopf N, Deichmann R, Driver J (2008), Distinct causal influences of parietal versus frontal areas on human visual cortex: evidence from concurrent TMS-fMRI. Cereb Cortex 18:817-827.

Ruff CC, Blankenburg F, Bjoertomt O, Bestmann S, Freeman E, Haynes JD, Rees G, Josephs O, et al. (2006), Concurrent TMS-fMRI and psychophysics reveal frontal influences on human retinotopic visual cortex. Curr Biol 16:1479-1488.

Ruff CC, Blankenburg F, Bjoertomt O, Bestmann S, Weiskopf N, Driver J (2009), Hemispheric differences in frontal and parietal influences on human occipital cortex: direct confirmation with concurrent TMS-fMRI. J Cogn Neurosci 21:1146-1161.

Ruff CC, Driver J, Bestmann S (2009), Combining TMS and fMRI: from 'virtual lesions' to functional-network accounts of cognition. Cortex 45:1043-1049.

Ruohonen, Ilmoniemi (2005), Basic Physics and Design of Transcranial Magnetic Stimulation Devices and Coils. In: Mark Hallett and Sudhansu Chokroverty, Magnetic stimulation in clinical neurophysiology, second edition Philadelphia, Pennsylvania: Butterworths:17-30.

Rusjan PM, Barr MS, Farzan F, Arenovich T, Maller JJ, Fitzgerald PB, Daskalakis ZJ (2010), Optimal transcranial magnetic stimulation coil placement for targeting the dorsolateral prefrontal cortex using novel magnetic resonance image-guided neuronavigation. Hum Brain Mapp 31:1643-1652.

Rygh LJ, Svendsen F, Fiska A, Haugan F, Hole K, Tjolsen A (2005), Long-term potentiation in spinal nociceptive systems--how acute pain may become chronic. Psychoneuroendocrinology 30:959-964.

Sack AT, Kohler A, Bestmann S, Linden DE, Dechent P, Goebel R, Baudewig J (2007), Imaging the brain activity changes underlying impaired visuospatial judgments: simultaneous FMRI, TMS, and behavioral studies. Cereb Cortex 17:2841-2852.

Sailer A, Molnar GF, Cunic DI, Chen R (2002), Effects of peripheral sensory input on cortical inhibition in humans. J Physiol 544:617-629.

Sailer A, Molnar GF, Paradiso G, Gunraj CA, Lang AE, Chen R (2003), Short and long latency afferent inhibition in Parkinson's disease. Brain 126:1883-1894.

Saito Y, Yokota T, Yuasa T (1995), Suppression of motor cortical excitability by magnetic stimulation of the cerebellum. Brain Res 694:200-206.

Salerno A, Thomas E, Olive P, Blotman F, Picot MC, Georgesco M (2000), Motor cortical dysfunction disclosed by single and double magnetic stimulation in patients with fibromyalgia. Clin Neurophysiol 111:994-1001.

Sallet J, Mars RB, Noonan MP, Neubert FX, Jbabdi S, O'Reilly JX, Filippini N, Thomas AG, et al. (2013), The organization of dorsal frontal cortex in humans and macaques. J Neurosci 33:12255-12274.

Salo KS, Vaalto SMI, Koponen LM, Nieminen JO, Ilmoniemi RJ (2019), The effect of experimental pain on short-interval intracortical inhibition with multi-locus transcranial magnetic stimulation. Exp Brain Res 237:1503-1510.

Salvador R, Silva S, Basser PJ, Miranda PC (2011), Determining which mechanisms lead to activation in the motor cortex: a modeling study of transcranial magnetic stimulation using realistic stimulus waveforms and sulcal geometry. Clin Neurophysiol 122:748-758.

Sandkuhler J (2009), Models and mechanisms of hyperalgesia and allodynia. Physiol Rev 89:707-758.

Sandkuhler J, Liu X (1998), Induction of long-term potentiation at spinal synapses by noxious stimulation or nerve injury. Eur J Neurosci 10:2476-2480.

Sandrini G, Alfonsi E, Bono G, Facchinetti F, Montalbetti L, Nappi G (1986), Circadian variations of human flexion reflex. Pain 25:403-410.

Sandrini G, Arrigo A, Bono G, Nappi G (1993), The nociceptive flexion reflex as a tool for exploring pain control systems in headache and other pain syndromes. Cephalalgia 13:21-27.

Sandrini G, Serrao M, Rossi P, Romaniello A, Cruccu G, Willer JC (2005), The lower limb flexion reflex in humans. Prog Neurobiol 77:353-395.

Schabrun SM, Christensen SW, Mrachacz-Kersting N, Graven-Nielsen T (2016), Motor Cortex Reorganization and Impaired Function in the Transition to Sustained Muscle Pain. Cereb Cortex 26:1878-1890.

Schabrun SM, Elgueta-Cancino EL, Hodges PW (2017), Smudging of the Motor Cortex Is Related to the Severity of Low Back Pain. Spine (Phila Pa 1976) 42:1172-1178.

Schabrun SM, Hodges PW (2012), Muscle pain differentially modulates short interval intracortical inhibition and intracortical facilitation in primary motor cortex. J Pain 13:187-194.

Schabrun SM, Hodges PW, Vicenzino B, Jones E, Chipchase LS (2015), Novel adaptations in motor cortical maps: the relation to persistent elbow pain. Med Sci Sports Exerc 47:681-690.

Schabrun SM, Jones E, Elgueta Cancino EL, Hodges PW (2014), Targeting chronic recurrent low back pain from the top-down and the bottom-up: a combined transcranial direct current stimulation and peripheral electrical stimulation intervention. Brain stimulation 7:451-459.

Schabrun SM, Jones E, Kloster J, Hodges PW (2013), Temporal association between changes in primary sensory cortex and corticomotor output during muscle pain. Neuroscience 235:159-164.

Schabrun SM, Ridding MC (2007), The influence of correlated afferent input on motor cortical representations in humans. Exp Brain Res 183:41-49.

Schieber MH (2001), Constraints on somatotopic organization in the primary motor cortex. J Neurophysiol 86:2125-2143.

Schmelz M, Michael K, Weidner C, Schmidt R, Torebjork HE, Handwerker HO (2000), Which nerve fibers mediate the axon reflex flare in human skin? Neuroreport 11:645-648.

Schmidt-Wilcke T, Ichesco E, Hampson JP, Kairys A, Peltier S, Harte S, Clauw DJ, Harris RE (2014), Resting state connectivity correlates with drug and placebo response in fibromyalgia patients. NeuroImage Clinical 6:252-261.

Schmidt-Wilcke T, Leinisch E, Ganssbauer S, Draganski B, Bogdahn U, Altmeppen J, May A (2006), Affective components and intensity of pain correlate with structural differences in gray matter in chronic back pain patients. Pain 125:89-97.

Schmierer K, Niehaus L, Roricht S, Meyer BU (2000), Conduction deficits of callosal fibres in early multiple sclerosis. J Neurol Neurosurg Psychiatry 68:633-638.

Schneider C, Zytnicki D, Capaday C (2001), Quantitative evidence for multiple widespread representations of individual muscles in the cat motor cortex. Neurosci Lett 310:183-187.

Schomburg ED (1990), Spinal sensorimotor systems and their supraspinal control. Neurosci Res 7:265-340.

Schomburg ED, Steffens H (2002), Only minor spinal motor reflex effects from feline group IV muscle nociceptors. Neurosci Res 44:213-223.

Schomburg ED, Steffens H, Kniffki KD (1999), Contribution of group III and IV muscle afferents to multisensorial spinal motor control in cats. Neurosci Res 33:195-206.

Schomburg ED, Steffens H, Mense S (2000), Contribution of TTX-resistant C-fibres and Adelta-fibres to nociceptive flexor-reflex and non-flexor-reflex pathways in cats. Neurosci Res 37:277-287.

Schouenborg J (2002), Modular organisation and spinal somatosensory imprinting. Brain Res Brain Res Rev 40:80-91.

Schouenborg J, Kalliomaki J (1990), Functional organization of the nociceptive withdrawal reflexes. I. Activation of hindlimb muscles in the rat. Exp Brain Res 83:67-78.

Schouenborg J, Weng HR (1994), Sensorimotor transformation in a spinal motor system. Exp Brain Res 100:170-174.

Schulz E, Tiemann L, Witkovsky V, Schmidt P, Ploner M (2012), gamma Oscillations are involved in the sensorimotor transformation of pain. J Neurophysiol 108:1025-1031.

Schuwerk T, Schecklmann M, Langguth B, Dohnel K, Sodian B, Sommer M (2014), Inhibiting the posterior medial prefrontal cortex by rTMS decreases the discrepancy between self and other in Theory of Mind reasoning. Behav Brain Res 274:312-318.

Schwenkreis P, Janssen F, Rommel O, Pleger B, Volker B, Hosbach I, Dertwinkel R, Maier C, et al. (2003), Bilateral motor cortex disinhibition in complex regional pain syndrome (CRPS) type I of the hand. Neurology 61:515-519.

Schwenkreis P, Scherens A, Ronnau AK, Hoffken O, Tegenthoff M, Maier C (2010), Cortical disinhibition occurs in chronic neuropathic, but not in chronic nociceptive pain. BMC Neurosci 11:73.

Schwenkreis P, Voigt M, Hasenbring M, Tegenthoff M, Vorgerd M, Kley RA (2011), Central mechanisms during fatiguing muscle exercise in muscular dystrophy and fibromyalgia syndrome: a study with transcranial magnetic stimulation. Muscle Nerve 43:479-484.

Seeley WW, Menon V, Schatzberg AF, Keller J, Glover GH, Kenna H, Reiss AL, Greicius MD (2007), Dissociable intrinsic connectivity networks for salience processing and executive control. J Neurosci 27:2349-2356.

Segerdahl AR, Mezue M, Okell TW, Farrar JT, Tracey I (2015), The dorsal posterior insula subserves a fundamental role in human pain. Nat Neurosci 18:499-500.

Seifert F, Maihofner C (2009), Central mechanisms of experimental and chronic neuropathic pain: findings from functional imaging studies. Cell Mol Life Sci 66:375-390.

Seifert F, Maihofner C (2011), Functional and structural imaging of pain-induced neuroplasticity. Current opinion in anaesthesiology 24:515-523.

Seminowicz DA, Moayedi M (2017), The Dorsolateral Prefrontal Cortex in Acute and Chronic Pain. J Pain 18:1027-1035.

Seminowicz DA, Wideman TH, Naso L, Hatami-Khoroushahi Z, Fallatah S, Ware MA, Jarzem P, Bushnell MC, et al. (2011), Effective treatment of chronic low back pain in humans reverses abnormal brain anatomy and function. J Neurosci 31:7540-7550.

Serra J, Campero M, Ochoa J (1998), Flare and hyperalgesia after intradermal capsaicin injection in human skin. J Neurophysiol 80:2801-2810.

Serrao M, Parisi L, Pierelli F, Rossi P (2001), Cutaneous afferents mediating the cutaneous silent period in the upper limbs: evidences for a role of low-threshold sensory fibres. Clin Neurophysiol 112:2007-2014.

Serrao M, Pierelli F, Don R, Ranavolo A, Cacchio A, Curra A, Sandrini G, Frascarelli M, et al. (2006), Kinematic and electromyographic study of the nociceptive withdrawal reflex in the upper limbs during rest and movement. J Neurosci 26:3505-3513.

Serrao M, Ranavolo A, Andersen OK, Don R, Draicchio F, Conte C, Di Fabio R, Perrotta A, et al. (2012), Reorganization of multi-muscle and joint withdrawal reflex during arm movements in post-stroke hemiparetic patients. Clin Neurophysiol 123:527-540.

Seyal M, Mull B, Bhullar N, Ahmad T, Gage B (1999), Anticipation and execution of a simple reading task enhance corticospinal excitability. Clin Neurophysiol 110:424-429.

Shahani (1968), Effects of sleep on human reflexes with a double component. J Neurol Neurosurg Psychiatry 31:574-579.

Shahani, Young RR (1971), Human flexor reflexes. J Neurol Neurosurg Psychiatry 34:616-627.

Shahani B (1970), Flexor reflex afferent nerve fibres in man. J Neurol Neurosurg Psychiatry 33:786-791.

Sherrington CS (1910), Flexion-reflex of the limb, crossed extension-reflex, and reflex stepping and standing. J Physiol 40:28-121.

Shields J, Park JE, Srivanitchapoom P, Paine R, Thirugnanasambandam N, Kukke SN, Hallett M (2016), Probing the interaction of the ipsilateral posterior parietal cortex with the premotor cortex using a novel transcranial magnetic stimulation technique. Clin Neurophysiol 127:1475-1480.

Shitara H, Shinozaki T, Takagishi K, Honda M, Hanakawa T (2011), Time course and spatial distribution of fMRI signal changes during single-pulse transcranial magnetic stimulation to the primary motor cortex. NeuroImage 56:1469-1479.

Shitara H, Shinozaki T, Takagishi K, Honda M, Hanakawa T (2013), Movement and afferent representations in human motor areas: a simultaneous neuroimaging and transcranial magnetic/peripheral nerve-stimulation study. Front Hum Neurosci 7:554.

Siebner HR, Bergmann TO, Bestmann S, Massimini M, Johansen-Berg H, Mochizuki H, Bohning DE, Boorman ED, et al. (2009a), Consensus paper: combining transcranial stimulation with neuroimaging. Brain stimulation 2:58-80.

Siebner HR, Hartwigsen G, Kassuba T, Rothwell JC (2009b), How does transcranial magnetic stimulation modify neuronal activity in the brain? Implications for studies of cognition. Cortex 45:1035-1042.

Siebner HR, Lee L, Bestmann S (2003), Interleaving TMS with functional MRI: now that it is technically feasible how should it be used? Clin Neurophysiol 114:1997-1999.

Silvanto J, Lavie N, Walsh V (2006), Stimulation of the human frontal eye fields modulates sensitivity of extrastriate visual cortex. J Neurophysiol 96:941-945.

Simone DA, Kajander KC (1997), Responses of cutaneous A-fiber nociceptors to noxious cold. J Neurophysiol 77:2049-2060.

Simone DA, Sorkin LS, Oh U, Chung JM, Owens C, LaMotte RH, Willis WD (1991), Neurogenic hyperalgesia: central neural correlates in responses of spinothalamic tract neurons. J Neurophysiol 66:228-246.

Sinitsyn DO, Chernyavskiy AY, Poydasheva AG, Bakulin IS, Suponeva NA, Piradov MA (2019), Optimization of the Navigated TMS Mapping Algorithm for Accurate Estimation of Cortical Muscle Representation Characteristics. Brain sciences 9.

Skljarevski V, Ramadan NM (2002), The nociceptive flexion reflex in humans -- review article. Pain 96:3-8.

Sohn MK, Graven-Nielsen T, Arendt-Nielsen L, Svensson P (2000), Inhibition of motor unit firing during experimental muscle pain in humans. Muscle Nerve 23:1219-1226.

Solnik S, DeVita P, Rider P, Long B, Hortobagyi T (2008), Teager-Kaiser Operator improves the accuracy of EMG onset detection independent of signal-to-noise ratio. Acta of bioengineering and biomechanics 10:65-68.

Solnik S, Rider P, Steinweg K, DeVita P, Hortobagyi T (2010), Teager-Kaiser energy operator signal conditioning improves EMG onset detection. Eur J Appl Physiol 110:489-498.

Solomonow M, Baten C, Smit J, Baratta R, Hermens H, D'Ambrosia R, Shoji H (1990), Electromyogram power spectra frequencies associated with motor unit recruitment strategies. J Appl Physiol (1985) 68:1177-1185.

Sommer M, Alfaro A, Rummel M, Speck S, Lang N, Tings T, Paulus W (2006), Half sine, monophasic and biphasic transcranial magnetic stimulation of the human motor cortex. Clin Neurophysiol 117:838-844.

Sommer M, Ciocca M, Chieffo R, Hammond P, Neef A, Paulus W, Rothwell JC, Hannah R (2018), TMS of primary motor cortex with a biphasic pulse activates two independent sets of excitable neurones. Brain stimulation 11:558-565.

Sommer M, Paulus W (2008), TMS waveform and current direction. In: Wassermann, EM, Epstein CM, Ziemann, U, Walsh, V, Paus, T, Lisanby, SH; The Oxford Handbook of Transcranial stimulation Oxford: Oxford University Press:7-12.

Sonnenborg FA, Andersen OK, Arendt-Nielsen L, Treede RD (2001), Withdrawal reflex organisation to electrical stimulation of the dorsal foot in humans. Exp Brain Res 136:303-312.

Spiegel J, Hansen C, Treede RD (1996), Laser-evoked potentials after painful hand and foot stimulation in humans: evidence for generation of the middle-latency component in the secondary somatosensory cortex. Neurosci Lett 216:179-182.

Stagg CJ, Wylezinska M, Matthews PM, Johansen-Berg H, Jezzard P, Rothwell JC, Bestmann S (2009), Neurochemical effects of theta burst stimulation as assessed by magnetic resonance spectroscopy. J Neurophysiol 101:2872-2877.

Stancak A, Polacek H, Vrana J, Mlynar J (2007), Cortical oscillatory changes during warming and heating in humans. Neuroscience 147:842-852.

Starr CJ, Sawaki L, Wittenberg GF, Burdette JH, Oshiro Y, Quevedo AS, Coghill RC (2009), Roles of the insular cortex in the modulation of pain: insights from brain lesions. J Neurosci 29:2684-2694.

Stephani C, Fernandez-Baca Vaca G, Maciunas R, Koubeissi M, Luders HO (2011), Functional neuroanatomy of the insular lobe. Brain structure & function 216:137-149.

Stokic DS, McKay WB, Scott L, Sherwood AM, Dimitrijevic MR (1997), Intracortical inhibition of lower limb motor-evoked potentials after paired transcranial magnetic stimulation. Exp Brain Res 117:437-443.

Strutton PH, Theodorou S, Catley M, McGregor AH, Davey NJ (2005), Corticospinal excitability in patients with chronic low back pain. Journal of spinal disorders & techniques 18:420-424.

Stubhaug A, Breivik H, Eide PK, Kreunen M, Foss A (1997), Mapping of punctuate hyperalgesia around a surgical incision demonstrates that ketamine is a powerful suppressor of central sensitization to pain following surgery. Acta Anaesthesiol Scand 41:1124-1132.

Suppa A, Biasiotta A, Belvisi D, Marsili L, La Cesa S, Truini A, Cruccu G, Berardelli A (2013), Heat-evoked experimental pain induces long-term potentiation-like plasticity in human primary motor cortex. Cereb Cortex 23:1942-1951.

Suzuki R, Morcuende S, Webber M, Hunt SP, Dickenson AH (2002), Superficial NK1-expressing neurons control spinal excitability through activation of descending pathways. Nat Neurosci 5:1319-1326.

Svensson P, Arendt-Nielsen L, Houe L (1996), Sensory-motor interactions of human experimental unilateral jaw muscle pain: a quantitative analysis. Pain 64:241-249.

Svensson P, De Laat A, Graven-Nielsen T, Arendt-Nielsen L (1998), Experimental jaw-muscle pain does not change heteronymous H-reflexes in the human temporalis muscle. Exp Brain Res 121:311-318.

Svensson P, Miles TS, McKay D, Ridding MC (2003), Suppression of motor evoked potentials in a hand muscle following prolonged painful stimulation. Eur J Pain 7:55-62.

Svensson P, Minoshima S, Beydoun A, Morrow TJ, Casey KL (1997), Cerebral processing of acute skin and muscle pain in humans. J Neurophysiol 78:450-460.

Szolcsanyi J, Anton F, Reeh PW, Handwerker HO (1988), Selective excitation by capsaicin of mechano-heat sensitive nociceptors in rat skin. Brain Res 446:262-268.

Tagliazucchi E, Balenzuela P, Fraiman D, Chialvo DR (2010), Brain resting state is disrupted in chronic back pain patients. Neurosci Lett 485:26-31.

Takahashi K, Taguchi T, Tanaka S, Sadato N, Qiu Y, Kakigi R, Mizumura K (2011), Painful muscle stimulation preferentially activates emotion-related brain regions compared to painful skin stimulation. Neurosci Res 70:285-293.

Tamburin S, Fiaschi A, Andreoli A, Marani S, Zanette G (2005), Sensorimotor integration to cutaneous afferents in humans: the effect of the size of the receptive field. Exp Brain Res 167:362-369.

Tamburin S, Manganotti P, Zanette G, Fiaschi A (2001), Cutaneomotor integration in human hand motor areas: somatotopic effect and interaction of afferents. Exp Brain Res 141:232-241.

Tarkka IM, Treede RD, Bromm B (1992), Sensory and movement-related cortical potentials in nociceptive and auditory reaction time tasks. Acta Neurol Scand 86:359-364.

Taylor (2006), Stimulation at the cervicomedullary junction in human subjects. J Electromyogr Kinesiol 16:215-223.

Taylor, Nobre AC, Rushworth MF (2007a), FEF TMS affects visual cortical activity. Cereb Cortex 17:391-399.

Taylor, Nobre AC, Rushworth MF (2007b), Subsecond changes in top down control exerted by human medial frontal cortex during conflict and action selection: a combined transcranial magnetic stimulation electroencephalography study. J Neurosci 27:11343-11353.

Taylor, Pettit JS, Harris PJ, Ford TW, Clarke RW (1990), Noxious stimulation of the toes evokes long-lasting, naloxone-reversible suppression of the sural-gastrocnemius reflex in the rabbit. Brain Res 531:263-268.

Taylor JJ, Borckardt JJ, Canterberry M, Li X, Hanlon CA, Brown TR, George MS (2013), Naloxone-reversible modulation of pain circuitry by left prefrontal rTMS. Neuropsychopharmacology 38:1189-1197.

Taylor JJ, Borckardt JJ, George MS (2012), Endogenous opioids mediate left dorsolateral prefrontal cortex rTMS-induced analgesia. Pain 153:1219-1225.

Te M, Baptista AF, Chipchase LS, Schabrun SM (2017), Primary Motor Cortex Organization Is Altered in Persistent Patellofemoral Pain. Pain Med 18:2224-2234.

Terada K, Umeoka S, Usui N, Baba K, Usui K, Fujitani S, Matsuda K, Tottori T, et al. (2012), Uneven interhemispheric connections between left and right primary sensori-motor areas. Hum Brain Mapp 33:14-26.

Terao Y, Ugawa Y, Hanajima R, Machii K, Furubayashi T, Mochizuki H, Enomoto H, Shiio Y, et al. (2000), Predominant activation of I1-waves from the leg motor area by transcranial magnetic stimulation. Brain Res 859:137-146.

Thalhammer JG, LaMotte RH (1982), Spatial properties of nociceptor sensitization following heat injury of the skin. Brain Res 231:257-265.

Thickbroom GW, Byrnes ML, Stell R, Mastaglia FL (2003), Reversible reorganisation of the motor cortical representation of the hand in cervical dystonia. Mov Disord 18:395-402.

Thickbroom GW, Sammut R, Mastaglia FL (1998), Magnetic stimulation mapping of motor cortex: factors contributing to map area. Electroencephalogr Clin Neurophysiol 109:79-84.

Thunberg J, Ljubisavljevic M, Djupsjobacka M, Johansson H (2002), Effects on the fusimotor-muscle spindle system induced by intramuscular injections of hypertonic saline. Exp Brain Res 142:319-326.

Thunberg J, Lyskov E, Korotkov A, Ljubisavljevic M, Pakhomov S, Katayeva G, Radovanovic S, Medvedev S, et al. (2005), Brain processing of tonic muscle pain induced by infusion of hypertonic saline. Eur J Pain 9:185-194.

Tokimura H, Di Lazzaro V, Tokimura Y, Oliviero A, Profice P, Insola A, Mazzone P, Tonali P, et al. (2000), Short latency inhibition of human hand motor cortex by somatosensory input from the hand. J Physiol 523 Pt 2:503-513.

Tokimura H, Tokimura Y, Oliviero A, Asakura T, Rothwell JC (1996), Speech-induced changes in corticospinal excitability. Ann Neurol 40:628-634.

Tomasino B, Gremese M (2016), The Cognitive Side of M1. Front Hum Neurosci 10:298.

Torebjork HE, Hallin RG (1973), Perceptual changes accompanying controlled preferential blocking of A and C fibre responses in intact human skin nerves. Exp Brain Res 16:321-332.

Torebjork HE, Lundberg LE, LaMotte RH (1992), Central changes in processing of mechanoreceptive input in capsaicin-induced secondary hyperalgesia in humans. J Physiol 448:765-780.

Torta DM, Filbrich L, Van Den Broeke EN, Legrain V (2018), No perceptual prioritization of non-nociceptive vibrotactile and visual stimuli presented on a sensitized body part. Sci Rep 8:5359.

Torta DM, Legrain V, Algoet M, Olivier E, Duque J, Mouraux A (2013), Theta burst stimulation applied over primary motor and somatosensory cortices produces analgesia unrelated to the changes in nociceptive event-related potentials. PLoS One 8:e73263.

Torta DM, Van Den Broeke EN, Filbrich L, Jacob B, Lambert J, Mouraux A (2017), Intense pain influences the cortical processing of visual stimuli projected onto the sensitized skin. Pain 158:691-697.

Towell AD, Purves AM, Boyd SG (1996), CO2 laser activation of nociceptive and non-nociceptive thermal afferents from hairy and glabrous skin. Pain 66:79-86.

Tran TD, Lam K, Hoshiyama M, Kakigi R (2001), A new method for measuring the conduction velocities of Abeta-, Adelta- and C-fibers following electric and CO(2) laser stimulation in humans. Neurosci Lett 301:187-190.

Traverse E, Brun C, Harnois E, Mercier C (2020), Impact of Experimental Tonic Pain on Corrective Motor Responses to Mechanical Perturbations. Neural Plast 2020:8864407.

Treede RD, Apkarian VA, Bromm B, Greenspan JD, Lenz FA (2000), Cortical representation of pain: functional characterization of nociceptive areas near the lateral sulcus. Pain 87:113-119.

Treede RD, Kenshalo DR, Gracely RH, Jones AK (1999), The cortical representation of pain. Pain 79:105-111.

Treede RD, Meyer RA, Campbell JN (1998), Myelinated mechanically insensitive afferents from monkey hairy skin: heat-response properties. J Neurophysiol 80:1082-1093.

Treede RD, Meyer RA, Raja SN, Campbell JN (1992), Peripheral and central mechanisms of cutaneous hyperalgesia. Prog Neurobiol 38:397-421.

Treede RD, Meyer RA, Raja SN, Campbell JN (1995), Evidence for two different heat transduction mechanisms in nociceptive primary afferents innervating monkey skin. J Physiol 483 (Pt 3):747-758.

Triggs WJ, Calvanio R, Macdonell RA, Cros D, Chiappa KH (1994), Physiological motor asymmetry in human handedness: evidence from transcranial magnetic stimulation. Brain Res 636:270-276.

Trippe J, Mix A, Aydin-Abidin S, Funke K, Benali A (2009), theta burst and conventional low-frequency rTMS differentially affect GABAergic neurotransmission in the rat cortex. Exp Brain Res 199:411-421.

Trompetto C, Buccolieri A, Marchese R, Marinelli L, Michelozzi G, Abbruzzese G (2003), Impairment of transcallosal inhibition in patients with corticobasal degeneration. Clin Neurophysiol 114:2181-2187.

Tsang P, Jacobs MF, Lee KG, Asmussen MJ, Zapallow CM, Nelson AJ (2014), Continuous theta-burst stimulation over primary somatosensory cortex modulates short-latency afferent inhibition. Clin Neurophysiol 125:2253-2259.

Tsao H, Danneels L, Hodges PW (2011), Individual fascicles of the paraspinal muscles are activated by discrete cortical networks in humans. Clin Neurophysiol 122:1580-1587.

Tsao H, Galea MP, Hodges PW (2008), Reorganization of the motor cortex is associated with postural control deficits in recurrent low back pain. Brain 131:2161-2171.

Tsao H, Tucker KJ, Hodges PW (2011), Changes in excitability of corticomotor inputs to the trunk muscles during experimentally-induced acute low back pain. Neuroscience 181:127-133.

Tucker KJ, Hodges PW (2009), Motoneurone recruitment is altered with pain induced in non-muscular tissue. Pain 141:151-155.

Tucker KJ, Hodges PW (2010), Changes in motor unit recruitment strategy during pain alters force direction. Eur J Pain 14:932-938.

Turken AU, Swick D (1999), Response selection in the human anterior cingulate cortex. Nat Neurosci 2:920-924.

Tzabazis A, Aparici CM, Rowbotham MC, Schneider MB, Etkin A, Yeomans DC (2013), Shaped magnetic field pulses by multi-coil repetitive transcranial magnetic stimulation (rTMS) differentially modulate anterior cingulate cortex responses and pain in volunteers and fibromyalgia patients. Molecular pain 9:33.

Uematsu H, Shibata M, Miyauchi S, Mashimo T (2011), Brain imaging of mechanically induced muscle versus cutaneous pain. Neurosci Res 70:78-84.

Ugawa Y, Day BL, Rothwell JC, Thompson PD, Merton PA, Marsden CD (1991), Modulation of motor cortical excitability by electrical stimulation over the cerebellum in man. J Physiol 441:57-72.

Ugawa Y, Hanajima R, Kanazawa I (1993), Interhemispheric facilitation of the hand area of the human motor cortex. Neurosci Lett 160:153-155.

Ugawa Y, Hanajima R, Kanazawa I (1994), Motor cortex inhibition in patients with ataxia. Electroencephalogr Clin Neurophysiol 93:225-229.

Ugawa Y, Terao Y, Hanajima R, Sakai K, Furubayashi T, Machii K, Kanazawa I (1997), Magnetic stimulation over the cerebellum in patients with ataxia. Electroencephalogr Clin Neurophysiol 104:453-458.

Ugawa Y, Uesaka Y, Terao Y, Hanajima R, Kanazawa I (1995), Magnetic stimulation over the cerebellum in humans. Ann Neurol 37:703-713.

Uncini A, Kujirai T, Gluck B, Pullman S (1991), Silent period induced by cutaneous stimulation. Electroencephalogr Clin Neurophysiol 81:344-352.

Ung H, Brown JE, Johnson KA, Younger J, Hush J, Mackey S (2014), Multivariate classification of structural MRI data detects chronic low back pain. Cereb Cortex 24:1037-1044.

Urban, Gebhart GF (1999), Supraspinal contributions to hyperalgesia. Proc Natl Acad Sci U S A 96:7687-7692.

Urban, Solinski M, Best C, Rolke R, Hopf HC, Dieterich M (2004), Different short-term modulation of cortical motor output to distal and proximal upper-limb muscles during painful sensory nerve stimulation. Muscle Nerve 29:663-669.

Uy J, Ridding MC, Miles TS (2002), Stability of maps of human motor cortex made with transcranial magnetic stimulation. Brain Topogr 14:293-297.

Valentin J (2002), Basic Anatomical and Physiological Data for Use in Radiological Protection: Reference Values. ICRP PUBLICATION 89.

Valentini E, Hu L, Chakrabarti B, Hu Y, Aglioti SM, Iannetti GD (2012a), The primary somatosensory cortex largely contributes to the early part of the cortical response elicited by nociceptive stimuli. NeuroImage 59:1571-1581.

Valentini E, Liang M, Aglioti SM, Iannetti GD (2012b), Seeing touch and pain in a stranger modulates the cortical responses elicited by somatosensory but not auditory stimulation. Hum Brain Mapp 33:2873-2884.

Valeriani M, Restuccia D, Di Lazzaro V, Oliviero A, Le Pera D, Profice P, Saturno E, Tonali P (2001), Inhibition of biceps brachii muscle motor area by painful heat stimulation of the skin. Exp Brain Res 139:168-172.

Valeriani M, Restuccia D, Di Lazzaro V, Oliviero A, Profice P, Le Pera D, Saturno E, Tonali P (1999), Inhibition of the human primary motor area by painful heat stimulation of the skin. Clin Neurophysiol 110:1475-1480.

Valls-Sole J, Kumru H, Kofler M (2008), Interaction between startle and voluntary reactions in humans. Exp Brain Res 187:497-507.

Valmunen T, Pertovaara A, Taiminen T, Virtanen A, Parkkola R, Jaaskelainen SK (2009), Modulation of facial sensitivity by navigated rTMS in healthy subjects. Pain 142:149-158.

van de Ruit M, Perenboom MJ, Grey MJ (2015), TMS brain mapping in less than two minutes. Brain stimulation 8:231-239.

van den Broeke EN, de Vries B, Lambert J, Torta DM, Mouraux A (2017), Phase-locked and non-phase-locked EEG responses to pinprick stimulation before and

after experimentally-induced secondary hyperalgesia. Clin Neurophysiol 128:1445-1456.

van den Broeke EN, Lambert J, Huang G, Mouraux A (2016a), Central Sensitization of Mechanical Nociceptive Pathways Is Associated with a Long-Lasting Increase of Pinprick-Evoked Brain Potentials. Front Hum Neurosci 10:531.

van den Broeke EN, Lenoir C, Mouraux A (2016b), Secondary hyperalgesia is mediated by heat-insensitive A-fibre nociceptors. J Physiol 594:6767-6776.

van den Broeke EN, Mouraux A (2014a), Enhanced brain responses to C-fiber input in the area of secondary hyperalgesia induced by high-frequency electrical stimulation of the skin. J Neurophysiol 112:2059-2066.

van den Broeke EN, Mouraux A (2014b), High-frequency electrical stimulation of the human skin induces heterotopical mechanical hyperalgesia, heat hyperalgesia, and enhanced responses to nonnociceptive vibrotactile input. J Neurophysiol 111:1564-1573.

van den Broeke EN, van Heck CH, Ceelen LA, van Rijn CM, van Goor H, Wilder-Smith OH (2012), The effect of high-frequency conditioning stimulation of human skin on reported pain intensity and event-related potentials. J Neurophysiol 108:2276-2281.

van den Broeke EN, van Rijn CM, Biurrun Manresa JA, Andersen OK, Arendt-Nielsen L, Wilder-Smith OH (2010), Neurophysiological correlates of nociceptive heterosynaptic long-term potentiation in humans. J Neurophysiol 103:2107-2113.

Vanderclausen C, Filbrich L, Alamia A, Legrain V (2017), Investigating peri-limb interaction between nociception and vision using spatial depth. Neurosci Lett 654:111-116.

Vanneste S, De Ridder D (2013), Differences between a single session and repeated sessions of 1 Hz TMS by double-cone coil prefrontal stimulation for the improvement of tinnitus. Brain stimulation 6:155-159.

Vanneste S, Ost J, Langguth B, De Ridder D (2014), TMS by double-cone coil prefrontal stimulation for medication resistant chronic depression: a case report. Neurocase 20:61-68.

Vanneste S, Plazier M, Van de Heyning P, De Ridder D (2011), Repetitive transcranial magnetic stimulation frequency dependent tinnitus improvement by

double cone coil prefrontal stimulation. J Neurol Neurosurg Psychiatry 82:1160-1164.

Vanneste S, van der Loo E, Plazier M, De Ridder D (2012), Parietal double-cone coil stimulation in tinnitus. Exp Brain Res 221:337-343.

Vassiliadis P, Grandjean J, Derosiere G, de Wilde Y, Quemener L, Duque J (2018), Using a Double-Coil TMS Protocol to Assess Preparatory Inhibition Bilaterally. Front Neurosci 12:139.

Vincent JL, Snyder AZ, Fox MD, Shannon BJ, Andrews JR, Raichle ME, Buckner RL (2006), Coherent spontaneous activity identifies a hippocampal-parietal memory network. J Neurophysiol 96:3517-3531.

Wall PD, Woolf CJ (1984), Muscle but not cutaneous C-afferent input produces prolonged increases in the excitability of the flexion reflex in the rat. J Physiol 356:443-458.

Wang, Arima T, Arendt-Nielsen L, Svensson P (2000), EMG-force relationships are influenced by experimental jaw-muscle pain. J Oral Rehabil 27:394-402.

Wang, Toro C, Zeffiro TA, Hallett M (1994), Head surface digitization and registration: a method for mapping positions on the head onto magnetic resonance images. Brain Topogr 6:185-192.

Wasan AD, Loggia ML, Chen LQ, Napadow V, Kong J, Gollub RL (2011), Neural correlates of chronic low back pain measured by arterial spin labeling. Anesthesiology 115:364-374.

Wassermann EM, McShane LM, Hallett M, Cohen LG (1992), Noninvasive mapping of muscle representations in human motor cortex. Electroencephalogr Clin Neurophysiol 85:1-8.

Wassermann EM, Wang B, Zeffiro TA, Sadato N, Pascual-Leone A, Toro C, Hallett M (1996), Locating the motor cortex on the MRI with transcranial magnetic stimulation and PET. NeuroImage 3:1-9.

Weiskopf N, Josephs O, Ruff CC, Blankenburg F, Featherstone E, Thomas A, Bestmann S, Driver J, et al. (2009), Image artifacts in concurrent transcranial magnetic stimulation (TMS) and fMRI caused by leakage currents: modeling and compensation. J Magn Reson Imaging 29:1211-1217.

Weng HR, Schouenborg J (1996), Cutaneous inhibitory receptive fields of withdrawal reflexes in the decerebrate spinal rat. J Physiol 493 (Pt 1):253-265.

Wiesenfeld-Hallin Z, Hallin RG, Persson A (1984), Do large diameter cutaneous afferents have a role in the transmission of nociceptive messages? Brain Res 311:375-379.

Wilkins DE, Hallett M, Wess MM (1986), Audiogenic startle reflex of man and its relationship to startle syndromes. A review. Brain 109 (Pt 3):561-573.

Willer JC (1977), Comparative study of perceived pain and nociceptive flexion reflex in man. Pain 3:69-80.

Willer JC, Boureau F, Berny J (1979), Nociceptive flexion reflexes elicited by noxious laser radiant heat in man. Pain 7:15-20.

Willer JC, Roby A, Le Bars D (1984), Psychophysical and electrophysiological approaches to the pain-relieving effects of heterotopic nociceptive stimuli. Brain 107 (Pt 4):1095-1112.

Wilson SA, Thickbroom GW, Mastaglia FL (1993), Transcranial magnetic stimulation mapping of the motor cortex in normal subjects. The representation of two intrinsic hand muscles. J Neurol Sci 118:134-144.

Witting N, Svensson P, Gottrup H, Arendt-Nielsen L, Jensen TS (2000), Intramuscular and intradermal injection of capsaicin: a comparison of local and referred pain. Pain 84:407-412.

Woolf CJ (1983), Evidence for a central component of post-injury pain hypersensitivity. Nature 306:686-688.

Woolf CJ (1984), Long term alterations in the excitability of the flexion reflex produced by peripheral tissue injury in the chronic decerebrate rat. Pain 18:325-343.

Woolf CJ, McMahon SB (1985), Injury-induced plasticity of the flexor reflex in chronic decerebrate rats. Neuroscience 16:395-404.

Woolf CJ, Salter MW (2000), Neuronal plasticity: increasing the gain in pain. Science 288:1765-1769.

Woolf CJ, Thompson SW (1991), The induction and maintenance of central sensitization is dependent on N-methyl-D-aspartic acid receptor activation; implications for the treatment of post-injury pain hypersensitivity states. Pain 44:293-299.

Woolf CJ, Wall PD (1986), Relative effectiveness of C primary afferent fibers of different origins in evoking a prolonged facilitation of the flexor reflex in the rat. J Neurosci 6:1433-1442.

Wooten M, Weng HJ, Hartke TV, Borzan J, Klein AH, Turnquist B, Dong X, Meyer RA, et al. (2014), Three functionally distinct classes of C-fibre nociceptors in primates. Nature communications 5:4122.

Wynford-Thomas R, Powell R (2017), Navigating the Island of Reil: how to understand the insular cortex. Pract Neurol 17:122-126.

Xu X, Kanda M, Shindo K, Fujiwara N, Nagamine T, Ikeda A, Honda M, Tachibana N, et al. (1995), Pain-related somatosensory evoked potentials following CO2 laser stimulation of foot in man. Electroencephalogr Clin Neurophysiol 96:12-23.

Yau JM, Hua J, Liao DA, Desmond JE (2013), Efficient and robust identification of cortical targets in concurrent TMS-fMRI experiments. NeuroImage 76:134-144.

Yau JM, Jalinous R, Cantarero GL, Desmond JE (2014), Static field influences on transcranial magnetic stimulation: considerations for TMS in the scanner environment. Brain stimulation 7:388-393.

Yi P, Pryzbylkowski P (2015), Opioid Induced Hyperalgesia. Pain Med 16 Suppl 1:S32-36.

Yousry TA, Schmid UD, Alkadhi H, Schmidt D, Peraud A, Buettner A, Winkler P (1997), Localization of the motor hand area to a knob on the precentral gyrus. A new landmark. Brain 120 (Pt 1):141-157.

Yu, Gollub RL, Spaeth R, Napadow V, Wasan A, Kong J (2014), Disrupted functional connectivity of the periaqueductal gray in chronic low back pain. NeuroImage Clinical 6:100-108.

Yu, Sessle BJ, Hu JW (1993), Differential effects of cutaneous and deep application of inflammatory irritant on mechanoreceptive field properties of trigeminal brain stem nociceptive neurons. J Neurophysiol 70:1704-1707.

Zhang ZG, Hu L, Hung YS, Mouraux A, Iannetti GD (2012), Gamma-band oscillations in the primary somatosensory cortex--a direct and obligatory correlate of subjective pain intensity. J Neurosci 32:7429-7438.

Ziegler EA, Magerl W, Meyer RA, Treede RD (1999), Secondary hyperalgesia to punctate mechanical stimuli. Central sensitization to A-fibre nociceptor input. Brain 122 (Pt 12):2245-2257.

Ziemann U, Chen R, Cohen LG, Hallett M (1998), Dextromethorphan decreases the excitability of the human motor cortex. Neurology 51:1320-1324.

Ziemann U, Rothwell JC, Ridding MC (1996), Interaction between intracortical inhibition and facilitation in human motor cortex. J Physiol 496 (Pt 3):873-881.